Quantum Cosmology and the Wavefunction of the Universe

Explorations in minisuperspace, eternal inflation, and topological defects

A dissertation submitted by

Georgios Fanaras

in partial fulfillment of the requirements

for the degree of

Doctor of Philosophy in Physics

Tufts University

February 2026

Advisor: Alexander Vilenkin

Committee members: Mark P. Hertzberg, Lawrence Ford, Krzysztof Sliwa, Jaume Garriga Torres, Soubhik Kumar

Abstract

In this thesis we study quantum cosmology with a primary focus on the wavefunction of the universe and the boundary conditions for the gravitational path integral. The main motivation is to advance our understanding of quantum gravity through applications to the universe, the only laboratory available for such theories. We begin by providing a thorough introduction into the standard cosmological model, the inflationary mechanism and the fundamentals of quantum cosmology. We proceed by studying the dynamics of eternal inflation within the framework of quantum cosmology, motivated by the swampland conjectures. Our analysis reveals a sharp transition when the curvature of the inflaton potential becomes large, signaling the end of eternal inflation and the onset of inhomogeneous domain wall formation. In the next chapters we explore the anisotropic Kantowski-Sachs (KS) model with spatial topology $S^1 \times S^2$ and a positive cosmological constant $\Lambda > 0$. To obtain a probability distribution for the initial state of this topology we calculated the gravitational path integral with appropriate boundary conditions utilizing Picard–Lefschetz theory. The results indicate that under Hartle–Hawking (HH) conditions, the prediction is an ensemble of classical universes with highly anisotropic spatial sections, even locally. In contrast, the tunneling approach favors global anisotropies that are smoothed out on local scales by inflation. Continuing in this direction, we construct a "1–1" mapping of the KS model to the 2D Jackiw–Teitelboim (JT) gravity toy model and obtain a normalizable probability distribution for the HH state. Finally, we investigate the nucleation of global strings via quantum tunneling. The instantons describing the process are characterized by the string core thickness and its gravitational backreaction. We find solutions across a wide range of these parameters, providing a complete treatment of global string nucleation in line with previous results on topological defects.

To my family,

who has always had my back.

Οἱ οὐρανοί διηγοῦνται δόξαν Θεοῦ, ποίησιν δὲ χειρῶν αὐτοῦ ἀναγγέλλει τὸ στερέωμα.

Ψαλμός ιθ ·1

The heavens declare the glory of God, the skies display his craftsmanship.

Psalm 19:1

Acknowledgements

The completion of this dissertation would not be possible without the support of my colleagues and mentors.

First, I want to thank my advisor, A. Vilenkin, for believing in me from day one and for treating me like a collaborator, not just a mentee. His pure passion for physics and relentless drive to finish projects set an example for me. His humility—despite his accomplished background—is something I hope to emulate. I am deeply grateful for the opportunity to work with Alex and I will always cherish the moments of our collaboration.

I am also deeply grateful to the members and affiliates of the Cosmology Institute at Tufts and their support throughout these years. K. D. Olum, M. P. Hertzberg, J. J. Blanco-Pillado, for guiding me during the last years of my PhD, being patient with me when my progress was slow and always being available when I needed them. They are all brilliant scientists in their own unique way. L. Ford for offering his expertise during the preparation of my qualifying exam. A. Lopez-Eiguren and O. Pujolas for the fruitful conversations during my work on cosmic strings. Furthermore, I am grateful for our informal discussions during cosmology lunches and for having the opportunity to connect with different members on a personal level.

I am also thankful to the teaching faculty at Tufts, H. Gallagher, T. Atherton, W. A. Mann, K. Sliwa. They played a big role in shaping me into a (decent) instructor by mentoring me in the discipline of physics education, and most importantly, by leading through their example.

My colleagues at Tufts, I. J. Allali, A. Cassem, D. Jiménez-Aguilar, A. Karis, Z. Bayat, A. Sucsuzer and H. Scholz, for keeping me good company, helping me with revisions of papers and job applications and for our informal and pressure-free physics discussions.

I also want to thank my close friends and fellow physicists outside of Tufts, N. Sioulas, M. Karydas and G. Papachatzakis for being there for me during this journey.

Finally, I want to thank the members of MIT cosmology group, A. H. Guth, D. I. Kaiser and T. Steingasser. I enjoyed our stimulating conversations during the joint seminars and our friendly interactions during lunches and dinners.

Contents

Chapter 1

Introduction

Cosmology, from the ancient Greek cosmos ("world") and logia ("study"), is the branch of physics devoted to understanding the origin, structure, evolution, and ultimate fate of the universe. In many ways, it can be considered the oldest of all sciences, deeply intertwined with metaphysics, religion, and philosophy. From the earliest moments of human consciousness, we have been driven by an inherent need to understand our place in the cosmos. Did the universe have a beginning? If so, how did the universe come to be? Why does the universe look the way it does today, and how did it evolve to this point? How large is it? Is it finite or infinite? Will it one day come to an end? These and many other timeless questions have captured the human imagination for millennia. And while such inquiries were once considered the domain of pure speculation, modern cosmology offers a rigorous scientific framework capable of addressing many of them. In this introduction, we will lay the groundwork for exploring these fundamental questions. Our goal is to provide a comprehensive picture of how the universe came to be, how it evolved into its current state, and what its future might hold. We hope that the story that follows will offer either a sense of clarity—or perhaps awaken an even deeper restlessness—in anyone with an inquisitive spirit drawn to the great questions of the universe.

1.1 Big-Bang cosmology

1.1.1 Basic facts about our universe

We live in the golden age of cosmology. Most of our understanding of the universe has been established over the past century, and our knowledge continues to grow due to the rapid technological advances of modern observations. A recurring theme has been that the more we learn, the less central or special we appear in the grand scheme of the cosmos. This perspective started with N. Copernicus in the 16th century proposed that the Earth orbits the Sun, challenging the long-held belief that we were at the center of the universe. In time, it became clear that the Sun itself is just one of countless stars in the Milky Way. In 1912, H. Leavitt discovered a relationship between the brightness and variability of certain stars, enabling astronomers to measure vast cosmic distances and establishing a *cosmic ladder*. Building on her work, E. Hubble found in 1923 that the Andromeda nebula was far beyond the Milky Way, revealing it to be a separate galaxy. This discovery showed that our galaxy is just one among billions in an expanding universe with each galaxy containing billions of stars.

Shortly after the discovery that other galaxies lie beyond the Milky Way, E. Hubble demonstrated in 1929 that galaxies are receding from us at speeds proportional to their distances [1]. As a result, the further a galaxy is from us the more redshifted it appears in our telescopes, due to the Doppler effect. This empirical relationship, now known as *Hubble's law*, provided the first evidence that the universe is expanding and plays a

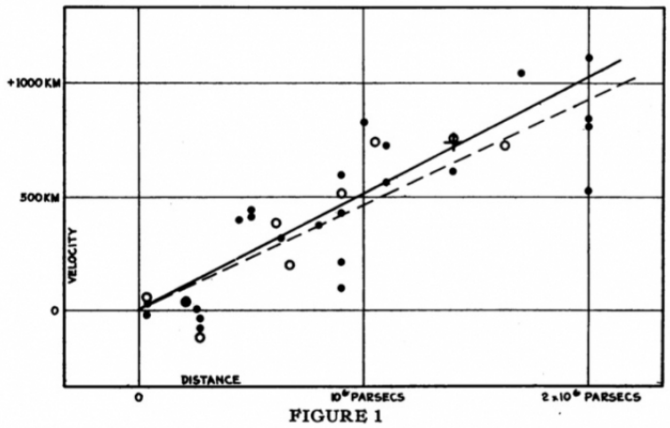

FIGURE 1
Velocity-Distance Relation among Extra-Galactic Nebulae.

Figure 1.1: E. Hubble's plot of the velocity-distance relationship for galaxies

fundamental role in establishing the Big-Bang theory.

A few decades later, in 1965, A. Penzias and R. Wilson detected a persistent, isotropic noise in their radio telescope. This signal was soon identified as the cosmic microwave background (CMB)—the relic radiation from the early universe [2]. Today, it appears as an almost perfectly uniform glow with a temperature of approximately 2.7 Kelvin. Its discovery offered compelling evidence that the universe was once in a much hotter and denser state, as predicted by the Big Bang theory.

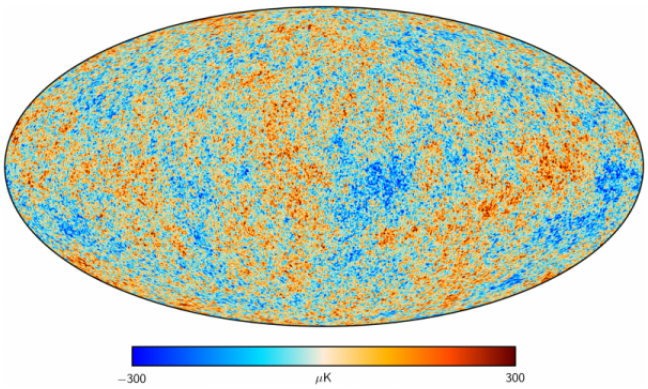

Figure 1.2: Map of the CMB temperature fluctuations measured by Planck. (Image credit: ESA and the Planck Collaboration.)

Subsequent observations in the 1970s by V. Rubin and W. Ford of galactic rotation curves revealed that stars in the outer regions of galaxies orbit at unexpectedly high velocities, suggesting the presence of unseen mass [3]. Around the same time, studies of gravitational lensing and large-scale structure formation further supported the existence of a non-luminous component—now known as *dark matter*—that does not emit or absorb light but dominates the matter content of the universe.

In the late 1990s, two independent teams—the Supernova Cosmology Project and the High-Z Supernova Search Team—measured the brightness of distant Type Ia supernovae and found that the expansion of the universe is accelerating [4, 5]. This surprising result pointed to a previously unknown energy component, now referred to as *dark energy*, which constitutes the majority of the energy density of the universe and drives its late-time accelerated expansion.

These observations form the foundation of modern cosmology and define the standard cosmological model. In this framework, the universe began in a hot, thermal state—the Big Bang—is homogeneous and isotropic on large scales, is currently undergoing acceler-

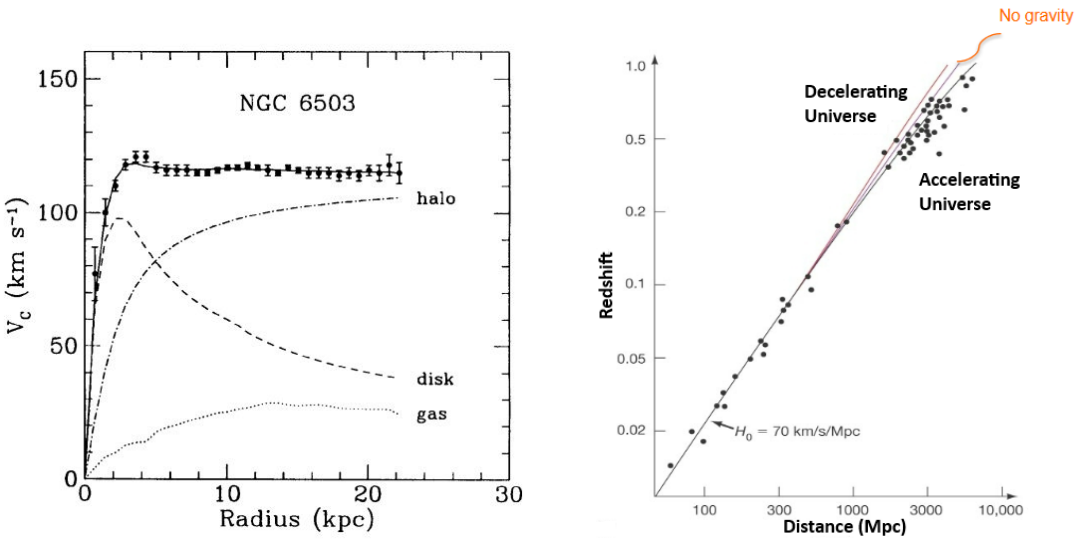

(a) Galactic rotation curve for NGC 6503 showing disk and gas contribution plus the dark matter halo contribution needed to match the data.

(b) Redshift–distance relation from Type Ia supernovae. Data lie below the decelerating universe curve, indicating accelerated expansion due to dark energy.

Figure 1.3: Dark matter and dark energy observational evidence.

ated expansion due to dark energy, and contains a dominant component of unseen matter known as dark matter. This model is commonly referred to as ΛCDM, where Λ represents the cosmological constant associated with dark energy, and CDM stands for "cold dark matter", highlighting its non-relativistic nature.

1.1.2 Thermal history of the universe

The expansion of the universe and the detection of the CMB naturally lead to the conclusion that our universe originated from a hot and dense thermal state—what we now call the Big Bang. As it expanded, it cooled, allowing for the formation of structure and matter as we observe it today. Starting from the initial moment, around 13.8 billion years ago, we outline the thermal history of our universe up to the present:

- **Quark–Gluon Plasma Epoch ($t \lesssim 10^{-6}$ s, $T \gtrsim 10^{12}$ K):** The universe was filled with a hot, dense plasma of free quarks and gluons. The energy was too high for quarks to bind into hadrons.

- **Hadron Epoch (10^{-6} s $\lesssim t \lesssim 1$ s, $T \sim 10^{12} - 10^{10}$ K):** Quarks combined into hadrons—mainly protons and neutrons—as the universe cooled. Most matter-

antimatter pairs annihilated, leaving a small matter excess.

- **Lepton Epoch ($1\ \mathbf{s} \lesssim t \lesssim 10\ \mathbf{s}$, $T \sim 10^{10} - 10^{9}\ \mathbf{K}$):** Leptons, such as electrons and neutrinos, dominated the energy density. Neutrinos decoupled around $t \sim 1$ second, forming the cosmic neutrino background.

- **Big Bang Nucleosynthesis ($t \sim 3$ minutes, $T \sim 10^{9}\ \mathbf{K}$):** Protons and neutrons fused to form light nuclei, primarily helium-4 and deuterium. This phase lasted a few minutes and fixed the primordial element abundances.

- **Photon Epoch ($10\ \mathbf{s} \lesssim t \lesssim 3.8 \times 10^{5}\ \mathbf{yr}$, $T \sim 10^{9} - 3000\ \mathbf{K}$):** The universe remained a hot plasma of nuclei, electrons, and photons. Photons constantly scattered off electrons, making the universe opaque.

- **Recombination ($t \sim 3.8 \times 10^{5}\ \mathbf{yr}$, $T \sim 3000\ \mathbf{K}$):** Electrons and nuclei combined into neutral atoms, and photons decoupled, forming the Cosmic Microwave Background (CMB), which we still observe today.

- **Dark Ages ($3.8 \times 10^{5}\ \mathbf{yr} \lesssim t \lesssim 10^{8}\ \mathbf{yr}$):** With no stars yet formed, the universe was dark and neutral. Matter clumped under gravity, preparing for the birth of the first luminous objects.

- **Structure Formation ($t \sim 10^{8}\ \mathbf{yr} \lesssim t \lesssim 10^{9}\ \mathbf{yr}$):** The first stars, galaxies, and black holes formed in growing dark matter halos. These luminous objects began shaping the universe gravitationally and chemically.

- **Reionization ($t \sim 10^{8}\ \mathbf{yr} \lesssim t \lesssim 10^{9}\ \mathbf{yr}$):** Radiation from the first stars, galaxies, and quasars reionized the intergalactic medium, breaking atoms back into free protons and electrons.

- **Cosmic Web Growth ($t \gtrsim 10^{9}\ \mathbf{yr}$):** Galaxies and galaxy clusters evolved through gravitational collapse and mergers, forming the large-scale cosmic web we observe today.

- **Dark Energy Domination ($t \gtrsim 8.8 \times 10^{9}\ \mathbf{yr}$, $T \sim 2.7\ \mathbf{K}$):** About 5 billion years ago, the expansion of the universe began accelerating due to dark energy. The universe today is 13.8 billion years old, with a CMB temperature of 2.725 K.

Before the quark–gluon plasma epoch, the universe was in an even hotter and denser state where known physics breaks down. This earliest period, often referred to as the *Planck era* ($t \lesssim 10^{-43}$ s, $T \gtrsim 10^{32}$ K), lies beyond the reach of our current theories, as quantum effects of gravity are expected to dominate. Without a complete theory of quantum gravity, the behavior of spacetime and matter during this era remains speculative. It is generally assumed that during this phase all fundamental forces may have been unified, and a classical description of spacetime loses meaning due to the domination of quantum fluctuations.

1.1.3 Friedmann cosmology

The standard model of cosmology is based on the assumption that the universe is homogeneous and isotropic on large scales. This is the *cosmological principle* and holds to great accuracy on scales of order $\sim 100 Mpc$. There are only three types of homogeneous and isotropic spaces: flat Euclidean space, spherical space and hyperbolic space. They are encoded in the Friedmann–Lemaître–Robertson–Walker (FLRW) metric which also takes into account the spatial expansion:

$$ds^2 = -dt^2 + a(t)^2 \left(\frac{dr^2}{1 - kr^2} + r^2 {d\Omega_2}^2 \right) \tag{1.1.1}$$

Here, $a(t)$ is the scale factor describing the expansion of the universe, k is the spatial curvature constant (with $k = 0, \pm 1$ for flat, closed, and open universes, respectively), and $d\Omega_2^2$ is the metric on the unit two-sphere. The coordinate r is called comoving distance and corresponds to the distance measured when we factor out the expansion.

We note that throughout this manuscript we will set the speed of light c, Planck's constant $\hbar$ and the Boltzmann constant k to the dimensionless value 1. This convention implies that time and length have equivalent units, while energy, mass, momentum, and temperature share the same units, inverse to those of time and length.

The expansion of the universe is described by the Hubble parameter:

$$H = \frac{\dot{a}}{a} \tag{1.1.2}$$

where $\dot{a}$ is the derivative of the scale factor in terms of the cosmic time t. From the

Hubble parameter it is straightforward to derive Hubble's law. Taking into account that physical distances d are related to comoving, r, by $d(t) = a(t)r$ we can write:

$$u = Hd \tag{1.1.3}$$

where u is the radial receding velocity of an object (e.g. a galaxy) at a distance d from us.

As previously mentioned, the farther away a galaxy is, the faster it is receding from us due to the expansion of the universe. This causes its light to appear redshifted when observed. The redshift factor z provides a useful way to measure distances in the universe and is defined by:

$$1 + z = \frac{\lambda_{\text{obs}}}{\lambda_{\text{emit}}} = \frac{a(t_0)}{a(t)} \tag{1.1.4}$$

where λ_{obs} and λ_{emit} are the observed and emitted wavelengths, corresponding to the scale factor at the time of observation t_0 and the time of emission t, respectively. Since looking farther into space means looking further back in time, redshift also serves as a proxy for cosmic time and is widely used by astronomers to study the universe's past.

Moving forward, we are interested in tracking the evolution of an FRW universe. This can be achieved by applying Einstein's field equations to the FRW metric. The result is the Friedmann equations, which play a fundamental law in cosmology:

$$\left(\frac{\dot{a}}{a}\right)^2 = \frac{8\pi G}{3}\rho - \frac{k}{a^2} + \frac{\Lambda}{3} \tag{1.1.5}$$

$$\ddot{a} = -\frac{4\pi G}{3}(\rho + 3p) + \frac{\Lambda}{3} \tag{1.1.6}$$

The first equation relates the expansion rate to the energy density of spacetime ρ and the spatial curvature k. The second Friedmann equation relates the acceleration in the expansion (or contraction) to the energy ρ and pressure p of matter. It is important to note that the quantity $\rho + 3p$ measures the gravitational effect of matter and the presence of the pressure is a purely General Relativistic artifact. For ordinary matter whose gravitational field is attractive, the expansion decelerates and when it is repulsive, it accelerates. This will be instrumental in the discussion of the inflationary scenario

in the following sections, but also on the current accelerated expansion of our universe which can be accounted for by the cosmological constant Λ.

Friedmann's equations can be uniquely solved once the matter content is specified. This is achieved using the continuity equation:

$$\dot{\rho} + 3H(\rho + p) = 0 \tag{1.1.7}$$

This equation governs how the energy density evolves as the universe expands, depending on the equation of state $p = p(\rho)$ of the cosmic fluid. We can also define the equation of state parameter $w = p/\rho$, which is useful to identify different types of matter. From (1.1.7) we can solve for the dust, radiation and vacuum dominated eras:

$$\rho(a) = \begin{cases} \rho_d \propto a^{-3}, & w = 0 \quad \text{(dust or cold matter)} \\ \rho_r \propto a^{-4}, & w = 1/3 \quad \text{(radiation or relativistic matter)} \\ \rho_\Lambda = \text{const}, & w = -1 \quad \text{(vacuum energy or cosmological constant)} \end{cases}$$

Inserting the above in the Friedmann equations we can solve for the evolution of the scale factor $a(t)$ for each of these epochs:

$$a(t) \propto \begin{cases} t^{2/3}\,, & w = 0 \\ t^{1/2}\,, & w = 1/3 \\ e^{Ht}\,, & w = -1 \end{cases}$$

In reality, the above evolution formulas do not fully capture the dynamics of the universe at a given epoch. That's because at any moment throughout the evolution the matter density is comprised of both relativistic and non-relativistic matter along with a vacuum energy. Thus we can write for the total energy density as the sum of these components: The total energy density is often modeled as a sum of these components:

$$\rho(t) = \rho_r + \rho_d + \rho_\Lambda \tag{1.1.8}$$

Where each component might dominate at different epochs in cosmic history, but all

are present to some extent at all times. In order to track how much each component contributes to the total energy budget of the universe we define the dimensionless density parameter:

$$\Omega = \frac{\rho}{\rho_c} = \Omega_d + \Omega_r + \Omega_\Lambda \tag{1.1.9}$$

for each component. The quantity ρ_c is called the critical density and is defined as:

$$\rho_c(t) = \frac{3H^2}{8\pi G} \tag{1.1.10}$$

It's significance will become clear shortly. Using the density parameters we can re-write the first Friedmann equation in order to relate the Hubble constant $H = H(a)$ in terms of the present values $\rho_{c,0}$, Ω_0 and H_0:

$$H^2(a) = H_0^2 \left[\Omega_{r,0} a^{-4} + \Omega_{d,0} a^{-3} + \Omega_{k,0} a^{-2} + \Omega_{\Lambda,0}\right] \tag{1.1.11}$$

Here, the present-day values $\Omega_{i,0}$ represent the fractional energy densities of radiation, matter, curvature, and dark energy, respectively. The above formula is of major significance in tracking the evolution of the universe throughout its history depending on the composition of the matter content in each era.
With the ansatz (1.1.9) the first Friedmann equation can be re-arranged in the form:

$$\frac{k}{a^2} = \frac{8\pi G}{3} \rho_c \left(\Omega - 1\right) \tag{1.1.12}$$

The above allows us to determine the curvature of spacetime depending on the density parameter Ω. In particular we have:

$$\begin{cases} \Omega > 1 & \Rightarrow k = +1 \quad \text{(closed)} \\ \Omega = 1 & \Rightarrow k = 0 \quad \text{(flat)} \\ \Omega < 1 & \Rightarrow k = -1 \quad \text{(open)} \end{cases}$$

Another way to interpret the above results is to compare the energy density ρ to the critical value ρ_c. If $\rho > \rho_c$ the universe is closed, if $\rho < \rho_c$ it is open and at the marginal value $\rho = \rho_c$ the universe is flat. The current value of the curvature is very close to 1 indicating that our universe is nearly flat. Present values of the density parameters and

Parameter	Description	Present Value
H_0	Hubble constant	$70\ \mathrm{km\,s^{-1}\,Mpc^{-1}}$
ρ_c	Critical density	$\sim 9.2 \times 10^{-30}\ \mathrm{g/cm^3}$
$\Omega_{r,0}$	Radiation density parameter	$\sim 9 \times 10^{-5}$
$\Omega_{b,0}$	Baryonic matter density parameter	~ 0.05
$\Omega_{DM,0}$	Dark matter density parameter	~ 0.27
$\Omega_{\Lambda,0}$	Dark energy density parameter	~ 0.68
Ω	Total density parameter	~ 1

Table 1.1: Present-day values of key cosmological parameters. We note that we use a fiducial value for H_0 which also affects the critical density ρ_c.

the Hubble constant are given in Table 1.1. It is worth noting, however, that the precise value of the Hubble constant H_0 is still under debate: local distance ladder measurements (e.g., Cepheid-calibrated supernovae) give $H_0 \sim 73\ \mathrm{km\,s^{-1}\,Mpc^{-1}}$ [6], while early-universe inferences from Planck CMB data yield a lower value of $H_0 \sim 67\ \mathrm{km\,s^{-1}\,Mpc^{-1}}$ [7]. This discrepancy, known as the "Hubble tension," remains one of the major open issues in modern cosmology.

Finally, to close this section we will briefly discuss the Big-Bang singularity. The second Friedmann equation expressed in terms of the Hubble parameter takes the form:

$$\dot{H} + H^2 = -\frac{4\pi G}{3}(\rho + 3p) \leq 0 \tag{1.1.13}$$

where we neglected the cosmological constant since it does not play an important role in the early universe. The right-hand side inequality arises from the fact that we are dealing with ordinary matter that has an attractive gravitational field. Applying the inequality to the left side of the equation and integrating we have:

$$\frac{1}{H} - \frac{1}{H_0} \geq t - t_0 \geq 0 \tag{1.1.14}$$

If we reverse the evolution, going backward in time we can set $H_0 < 0$ at a given time t_0. Then it can be shown that $H \to -\infty$ within a finite time interval $\Delta t = -H_0^{-1}$ indicating that the scale factor $a(t) \to 0$ and the energy density $\rho \to \infty$. This signals the existence of a curvature singularity in the past—what we call the Big-Bang singularity—marking the breakdown of classical general relativity and the necessity of a quantum theory of gravity for its description.

1.1.4 Problems with the standard cosmological model

Despite its successes the standard cosmological model suffers from fine-tuning problems at the Big-Bang and is not sufficient in explaining the current observations. We list the most notable problems that will be later addressed by the inflationary mechanism.

- **The flatness problem:** Our observable universe has a nearly flat, Euclidean, geometry according to observations. This is problematic because if we trace back the history of the universe all the way to the Big-Bang the curvature diminishes even more. A key question that arises is why was the initial curvature of the universe so fine-tuned near zero? We can easily demonstrate the problem by utilizing Friedmann's equation:

$$\Omega - 1 = \frac{k}{H^2 a^2} = \frac{k}{\dot{a}^2} \tag{1.1.15}$$

  Denoting with subscripts 0 and i for the end of the radiation era and the Big-Bang, respectively we can write:

$$\frac{\Omega_0 - 1}{\Omega_i - 1} = \left(\frac{\dot{a}_i}{\dot{a}_0}\right)^2 \gg 1 \tag{1.1.16}$$

  where the right hand side comes from the fact that the universe undergoes decellerated expansion. From the above, it is clear that if the current curvature is close to one, the past values are even more so. A rough estimate for the radiation era, taking into account that $\dot{a} \propto T$ and $T_i \approx 10^{16}\ GeV$, $T_0 \approx 10^{-9}\ GeV$ yields:

$$|\Omega_i - 1| < 10^{-50} \tag{1.1.17}$$

  The initial curvature was fine-tuned to zero at least one part in 10^{50}!

- **The horizon problem:** The nearly homogeneity and isotropy of the CMB spectrum with temperature variations of the order $\delta T/T \sim 10^{-5}$ strongly suggest that widely separated regions were once in causal contact. However, tracing the evolution of these regions back in time reveals that, although their physical separation was smaller than it is today, their causal horizons were even smaller. As a result, there was insufficient time for these regions to exchange information and equilibrate, posing a fundamental challenge to understanding their high correlation. A simple demonstration of the horizon problem goes as follows: The present size of

our horizon is $d_0 \approx 10^{28}\ cm$. The size of this region in the distant past $t_i \ll t_0$ was:

$$l_i = \left(\frac{a_i}{a_0}\right) d_0 \tag{1.1.18}$$

and the size of the causal horizon at that time was $d_i \sim t_i$. Their ratio is thus:

$$r = \frac{l_i}{d_i} = \left(\frac{a_i}{a_0}\right)\left(\frac{t_0}{t_i}\right) \approx \frac{\dot{a}_i}{\dot{a}_0} \gg 1 \tag{1.1.19}$$

where we used the fact that for a power law expansion $a/t \sim \dot{a}$ and the inequality due to the fact that we have decelerated expansion. It is clear that the physical size of that region was much greater than each causal horizon. For GUT energy scale $T_i \approx 10^{16}\ GeV$ and $t_i \approx 10^6 t_p$ we obtain the estimate:

$$r \approx 10^{25} \tag{1.1.20}$$

Thus, our region contains roughly 10^{75} causally disconnected patches, with temperature variations of 10^{-5}!

- **The large scale structure problem:** The universe today exhibits rich structure on a variety of scales — galaxies, clusters, and superclusters — which must have originated from tiny initial perturbations. However, in the standard Big Bang scenario, there is no compelling mechanism to generate these primordial fluctuations with the observed nearly scale-invariant spectrum. The formation of structure requires initial density perturbations with amplitude $\delta\rho/\rho \sim 10^{-5}$, as observed in the CMB. Without a theory for the origin of these seeds, the standard cosmology cannot fully explain the large-scale structure of the universe.

- **The monopole problem:** Grand Unified Theories (GUTs) predict the existence of heavy, stable magnetic monopoles produced during symmetry-breaking phase transitions in the early universe. These monopoles are expected to be extremely massive, with masses of order 10^{16} GeV, and would dominate the mass density of the universe if produced in even modest abundances. Observationally, however, no such relic monopoles have been detected, suggesting that their density must be exceedingly small. This discrepancy between theoretical expectation and observation

constitutes the monopole problem.

1.2 Cosmic inflation

1.2.1 Inflationary mechanism

In light of the fine-tuning problems facing standard Big-Bang cosmology, Alan Guth in 1980 proposed a mechanism of accelerated expansion during the early universe, called inflation [8]. The intuition behind his proposal stems from the fact that the horizon and flatness problems can be traced to the decelerated expansion of the universe. Thus, if a period of rapid expansion existed in the past, both problems will be remedied[1].

In order to achieve accelerated expansion, the Friedmann equation suggests that one must have gravitationally repulsive matter $\rho + 3p < 0$. Guth postulated that this can be done if our universe was the result of a bubble nucleation event in the past. In particular, if a first order phase transition occurred via quantum tunneling between a false and true vacuum [10] the universe would initially expand exponentially driven by the false vacuum energy. Eventually, bubbles of true vacuum will be formed and through their collisions the energy will be dissipated creating a hot Big-Bang. A key problem with this scenario, admitted by Guth himself, is that the necessary expansion rate to solve the flatness and horizon problems is too severe to allow for the subsequent bubble collisions. Thus, the universe ends up looking grossly inhomogeneous and inflation does not terminate. This unattractive feature was coined as *the graceful exit* problem of inflation.

The graceful exit problem was successfully addressed in 1981 independently by A. Linde [11] and A. Albrecht, P. Steinhardt [12]. They proposed a mechanism of inflation based on a 2nd order phase transition in which the scalar field *rolls slowly* from a high energy state and eventually reaches the true vacuum where it thermalizes. The thermalization of the field creates a hot fireball of standard model particles, the familiar Big-Bang of standard cosmology. The key ingredient of the new proposal is that the universe exits the inflationary phase smoothly, resulting in a nearly homogeneous and isotropic universe, after a period of exponential expansion.

[1] A similar proposal was put forward by A. Starobinsky in which he included higher curvature corrections to the Einstein-Hilbert action [9]

Before we go into a brief demonstration of the inflationary dynamics it is important to note the main characteristic of the inflationary scenario. The fundamental idea is that the universe undergoes a period of accelerated expansion in which the scale factor evolves approximately as:

$$a(t) \propto \exp(Ht) \tag{1.2.1}$$

driven by the repulsive vacuum energy from a scalar field with equation of state:

$$\rho \approx -p \tag{1.2.2}$$

called the inflaton. The dynamics of the inflationary mechanism can be studied by considering a scalar field ϕ in a flat (for simplicity) FRW spacetime with metric:

$$ds^2 = -dt^2 + a(t)^2 d\mathbf{x}^2 \tag{1.2.3}$$

The equations of motion for the scalar field ϕ along with the Friedmann equation (1.1.5) take the form:

$$\ddot{\phi} + 3\frac{\dot{a}}{a}\dot{\phi} - \frac{1}{a^2}\nabla^2\phi + \frac{\partial V}{\partial \phi} = 0 \tag{1.2.4}$$

and

$$H^2 = \frac{8\pi}{3}\left(\frac{1}{2}\dot{\phi}^2 + V(\phi)\right) \tag{1.2.5}$$

During the slow-roll inflationary phase the gradient term in the first equation becomes negligible as the scale factor grows. Furthermore, the conditions that $\dot{\phi}$ varies slowly and that the slope of the potential is small are respectively:

$$\ddot{\phi} \ll H\dot{\phi}\ , \quad \dot{\phi}^2 \ll V(\phi) \tag{1.2.6}$$

Thus, during the inflationary phase the dynamics of the inflaton are described by:

$$3H\dot{\phi} = \frac{\partial V}{\partial \phi}\ , \quad H^2 = \frac{8\pi}{3}V(\phi) \tag{1.2.7}$$

The above equations are sufficient to describe the inflationary dynamics of ϕ. They provide a quantitative description of the fact that the potential $V(\phi)$ is directly responsible for the expansion rate H and that (classical) rolling velocity of the field is proportional

to the slope of the potential.

Once the field exits the slow-roll regime, it settles into a minimum of the potential, where it undergoes oscillations. Because the inflaton is coupled to known forms of matter, these oscillations transfer energy into the production of a hot plasma of Standard Model particles. This final stage, during which the inflaton field thermalizes, is known as reheating, and it plays a crucial role in connecting the inflationary phase to the standard Big Bang cosmology. [2]

We note that there is a plethora of proposed inflationary mechanisms with different potentials $V(\phi)$ [3]. At the moment, it is not clear how the inflaton field can arise from a particle physics model and its fundamental origin is unknown. However, inflation is widely accepted by cosmologists as a mechanism that occurred in the early universe and it is considered as a key ingredient of the modern cosmological picture [4].

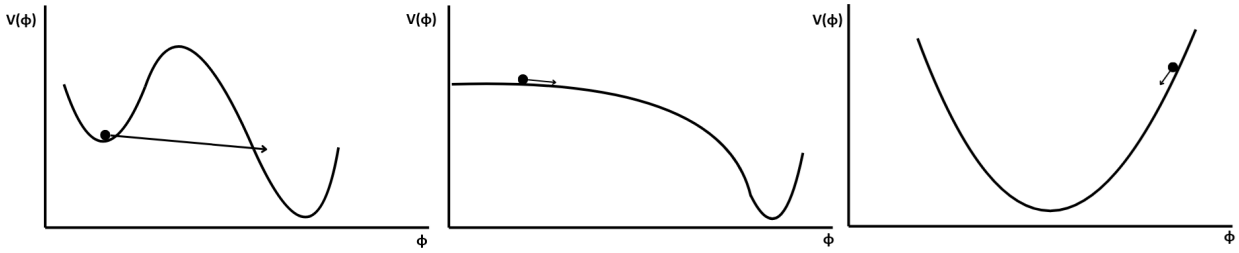

Figure 1.4: The potential $V(\phi)$ of the inflaton for the models of the old, new and chaotic inflationary scenarios respectively.

1.2.2 Successes of inflation

- **The flatness problem:** We will demonstrate how a period of inflationary expansion in the early universe flattens the curvature to miniscule values. Utilizing expression () and applying it to the begining and end of inflation we have:

$$\frac{\Omega_{in}-1}{\Omega_{end}-1}=\left(\frac{\dot{a}_{end}}{\dot{a}_{in}}\right)\approx\exp\left(2H\Delta t\right)\gg 1 \tag{1.2.8}$$

[2] In the inflationary framework, the Big Bang is typically identified with the reheating phase, when the inflaton thermalizes. This contrasts with the beginning of inflation, when the universe is cold and devoid of ordinary matter.

[3] A prominent example is A. Linde's chaotic inflation model [13]. For additional proposals that may include multiple scalar fields the reader is referred to [14, 15]

[4] For a simple overview of the inflationary scenario see [16]

where we assume an approximate exponential expansion () during this period. In order to achieve $\Omega_{end} - 1 < 10^{-50}$ we need an expansion of at least the order:

$$e^{2H\Delta t} \gtrsim 10^{50} \rightarrow \frac{a_{end}}{a_{in}} \approx 10^{25} \approx e^{58} \tag{1.2.9}$$

Thus, the solution to the flatness problem can be achieved with at least ~ 60 e-folds of inflation. In the early universe, space expanded so rapidly during inflation that any initial curvature was effectively flattened out. This is much like how we can't perceive the Earth's curvature from the ground—our limited field of view makes it appear flat.

- **The horizon problem:** Consider a small region of space in the early universe with physical size l_{in}, initially within causal contact. During inflation, this region is stretched exponentially due to the rapid expansion of space, while the causal horizon grows much more slowly—only linearly with time:

$$l_{end} = \frac{a_{end}}{a_{in}} l_{in} \approx e^{60} l_{in} \gg c t_{end} \tag{1.2.10}$$

Thus, the initially tiny patch of causally connected regions acquires an "astronomical" length after inflation. As the universe transitions to the standard radiation- and matter-dominated phases, the causal horizon begins to grow faster, eventually allowing regions that were pushed beyond it during inflation to re-enter. Despite the growth of the causal horizon, the original patch has become much larger than our current observable universe. This provides a natural explanation for the remarkable homogeneity and isotropy of the cosmic microwave background (CMB) we observe today.

- **The large-scale structure:** Inflation provides a mechanism for generating the primordial density perturbations that seeded the formation of galaxies and large-scale structure in the universe. During inflation, quantum fluctuations in the inflaton field are stretched to super-horizon scales and become effectively "frozen" as classical perturbations in the curvature of spacetime. These fluctuations have a nearly scale-invariant spectrum, in agreement with observations of the cosmic microwave

background (CMB) anisotropies and the distribution of galaxies. After inflation ends, these perturbations re-enter the horizon and grow via gravitational instability, eventually leading to the formation of the cosmic web we observe today. Thus, inflation not only explains the origin of these fluctuations but also provides their statistical properties, which have been confirmed to remarkable precision by experiments such as WMAP and Planck. The first to show how inflation can provide the seeds for structure formation were V. Mukhanov and G. Chibisov in 1981 [17]. Further developments were carried out in [18, 19, 20].

- **Magnetic monopole problem:** Inflation solves the monopole problem by stretching the universe so rapidly that any magnetic monopoles produced during an earlier GUT phase transition are diluted to an undetectable density. Although such monopoles are expected to be produced abundantly, a period of exponential expansion following their formation increases the volume of the universe by an enormous factor causing the monopole density to drop effectively to zero within our observable patch. This explains why we see no monopoles today, despite their robust theoretical prediction.

1.2.3 Eternal inflation

A key characteristic of inflationary models is that once the inflationary mechanism has began it will continue indefinitely into the future creating new inflating domains. In this sense, inflation ended in our local universe about 14 billion years ago, but is continuing in distant regions outside our horizon. The eternal nature of new inflationary models was first discovered by Steinhardt [21] and it was later proven by Vilenkin that new-inflationary models are generically eternal to the future [22]. Linde also showed that models of chaotic inflation are generically eternal [23].

The key ingredient in understanding the eternal nature of inflation lies in the quantum fluctuations experienced by the inflaton field in a false vacuum. The decay of the field to its true vacuum is closely analogous to the decay of radioactive material, which is an exponential process with a rate inversely proportional to the mean lifetime of the state . The exponential nature of the decay means that at late times the false vacuum should disappear, signaling the end of inflation [24]. However, a key distinction from typical

radioactive processes is that the false vacuum expansion rate competes with the decay rate. As a result, even though the field decays there is a continuous creation of new false vacuum domains that replenish the thermalized volume. In fact, in generic inflationary models the expansion rate of the false vacuum exceeds its decay leading to the eternal creation of new inflationary regions. Thus, once inflation begins, it never ends on a global scale, only locally in regions where the field has thermalized. We are inhabitants of one of these regions[5].

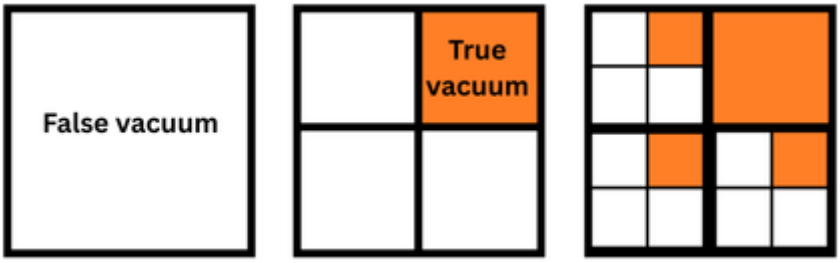

Figure 1.5: A schematic description of the expansion and decay process of the false vacuum. In each time step a quarter of the false vacuum decays, while the remaining regions quadruple. As a result the false vacuum grows by a factor of 3 in each iteration and never fully disappears. The expansion of each false vacuum region is factored out for illustrative convenience.

The dynamics of eternal inflation can be modeled by considering a scalar field ϕ at the false vacuum of a slowly varying potential $V(\phi)$. The end of inflation (locally) occurs when the field rolls down the potential and reaches its true vacuum state. Since the slope of the potential is substantially small, allowing a large amount of e-folds, the evolution of ϕ depends not only on the classical drift due to $V(\phi)$, but also on quantum fluctuations. We can describe the changes in ϕ in a time interval Δt by:

$$\Delta\phi = \Delta\phi_{cl} + \Delta\phi_q \tag{1.2.11}$$

where $\Delta\phi_{cl}$ is the changes due to the classical drift of the potential and $\Delta\phi_q$ are the quantum fluctuations. In the slow-roll regime we have from (1.2.7) that:

$$\dot{\phi}_{cl} = -\frac{V'}{3H} \tag{1.2.12}$$

[5]For a simple overview of eternal inflation and its implications see [25]

On the other hand, we can describe the quantum fluctuations by considering the quantum field theory of a light scalar field in deSitter. It can be readily shown that the variance of the field averaged over a Hubble size H^{-1} is given by [26, 27, 28]:

$$\langle \phi^2 \rangle = \frac{H^3}{4\pi^2} \Delta t \tag{1.2.13}$$

Thus on timescales of order $\Delta t = H^{-1}$ the field fluctuates by:

$$\Delta \phi_q = \frac{H}{2\pi} \tag{1.2.14}$$

and its diffusion velocity is:

$$\dot{\phi}_q \approx \frac{\Delta \phi_q}{\Delta t} = \frac{H^2}{2\pi} \tag{1.2.15}$$

Comparing (1.2.12) and (1.2.15) it is clear that quantum fluctuations dominate over the classical drift when:

$$\dot{\phi}_q > \dot{\phi}_{cl} \rightarrow \frac{V'}{H^3} < 1 \tag{1.2.16}$$

The region for which the above condition is satisfied is called the quantum diffusion regime and the evolution of the scalar field mimics that of a random walk. For new inflationary models it can be shown that the quantum diffusion regime $\phi < \phi_q$ must exist if the slow-roll conditions are satisfied. In particular if $\phi < \phi_I$ marks the region of slow-roll inflation then $\phi_q \ll \phi_I$ and there exists a part of the potential in which the evolution of the field is stochastic (Fig.1.6).

The stochastic nature of the new inflationary scenario leads to the continuous creation on new inflating domains and thermalized regions, the so-called pocket universes. A similar picture occurs in models that involve bubble nucleation. In these scenarios, when the underlying theory contains multiple vacuum states, such as the landscape of string theory, the global structure of spacetime will contain an infinite amount of bubble universes with varying vacuum energy. As a result, the mechanism of eternal inflation along with the vast landscape of states predicted by string theory results in the picture of the multiverse [29, 30]. The former is responsible for populating the vacuum states and the latter for creating bubble universes with varying physical properties (constants of nature, cosmological constant, etc).

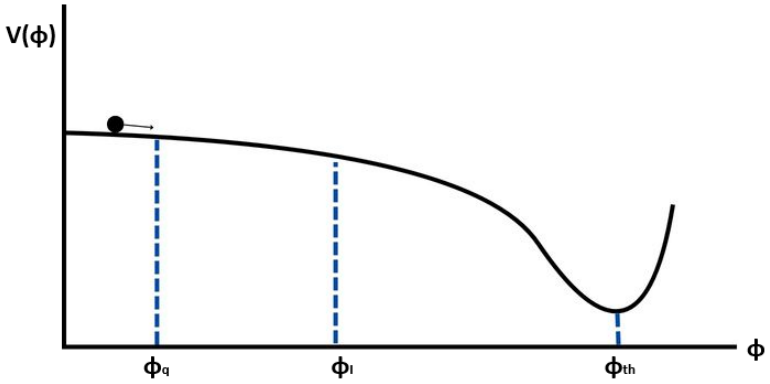

Figure 1.6: The scalar field in the new-inflationary scenario. The top of the potential $\phi < \phi_q$ is sufficientlly flat to allow quantum fluctuations to dominate over the classical roll. After, the random walk phase the fields evolution is captured by the classical velocity and it eventually reaches the minimum ϕ_{th} in which it oscillates.

The eternal creation of new and diverse bubble universes makes it necessary to quantify the probability of our existence in our local region [31, 32, 33]. Extracting predictions in this arena is by far a straightforward task since one has to figure out a way to regularize the infinities that arise by counting different states. This can only be achieved by providing an appropriate *probability measure*. The problem of measuring probabilities in an eternally inflating multiverse is called the *measure problem* of cosmology and is of paramount importance for extracting cosmological predictions. To this day, a satisfactory prescription for a measure has not been obtained. A main guiding principle is the avoidance of a number of cosmological paradoxes that arise from ill-defined measures such as the Boltzmann Brain Paradox and the Youngness Paradox [34]. For a comprehensive list of the different proposals for a measure the reader is referred to [35, 36, 37, 38, 39].

1.2.4 Did the universe have a beginning?

Under generic conditions the inflationary scenario results in the continuous creation of inflating domains and thermalized regions. The comoving volume of the former tends to zero at late times, since the inflaton gradually decays to its true vacuum. However, the physical volume grows exponentially due to the false vacuum expansion rate. As such, the universe is eternal to the future with an infinity of new Big-Bangs occurring outside of our local region. The eternal nature of the future raises the question of whether our universe is also eternal to the past. If so, the universe always existed and we avoid the

problem of initial conditions in the case of a beginning.

The Big-Bang singularity demonstrated in (1.1.14) relied on the core assumption of the strong energy condition $R_{ab}u^a u^b > 0$ in the case of timelike geodesics. This condition is violated during inflation, since the gravitational energy of the inflaton satisfies $\rho + 3p < 0$ and, as such, one might expect that inflationary spacetimes are singularity-free. However, a closer examination by A. Vilenkin and A. Borde refuted this claim by demonstrating that spacetimes satisfying the weak energy condition $G_{ab}u^a u^b > 0$ are indeed geodesically incomplete [40, 41]. Thus, the problem of an initial singularity did not seem to be remedied by inflation. In a follow-up paper, by the same authors, this picture was again overturned. It was shown that quantum fluctuations during inflation are bound to create violations of the weak energy condition [42]. This is typical in the case of an eternally inflating scenario, such as chaotic inflation, in which the Hubble parameter undergoes upward fluctuations. As a result, there was, yet again, a hope that one can construct singularity-free inflationary spacetimes.

The common theme in the above singularity theorems is the assumption of a particular energy condition. While the conditions gradually weakened and the theorems applied to a wider array of spacetimes there were still viable cosmological scenarios that violated them. This is where things stood until A. Borde, A. Guth and A. Vilenkin introduced a singularity theorem that is purely kinematic in nature and is not restricted by any assumption of the matter content of spacetime [43]. The theorem makes the following statement:

Theorem

If the average expansion rate H_{av} is positive along a timelike or null geodesic, the geodesic is past-incomplete.

Since the average expansion rate of geodesics in an inflationary spacetime satisfies this condition they arrived at the general conclusion that:

Lemma

Inflationary spacetimes are past-geodesically incomplete.

We will demonstrate the proof of the theorem by following the original paper [43].

Consider an observer following a geodesic $\mathcal{O}$ and a spacetime filled with comoving test particles that follow the expansion (or contraction) of spacetime. The 4-velocity of the observer is $v^\mu = \frac{dx^\mu}{d\tau}$ where τ is his/her proper time. We also denote as u^μ the 4-velocity of a test particle that passes by the observer at time τ. The gamma factor for the two reference frames is defined as $\gamma = u^\mu v_\mu$ and recasts to the familiar Lorentz factor for a flat spacetime.

At τ_1 the observer detects a test particle A and at τ_2 a test particle B. The relative velocity of the test particles as measured by $\mathcal{O}$ is:

$$\Delta u^\mu = -\frac{Du^\mu}{D\tau}\Delta\tau \tag{1.2.17}$$

where we applied parallel transport of the 4-velocity of particle A from τ_1 to τ_2 along the geodesic $\mathcal{O}$. Furthermore, we denote the relative distance of the test particles as measured by $\mathcal{O}$ at τ_2 as Δr^μ. Simple geometric considerations (see Fig.1.7) yield the expression:

$$\Delta r^\mu = \left(-v^\mu + \gamma u^\mu\right)\Delta\tau. \tag{1.2.18}$$

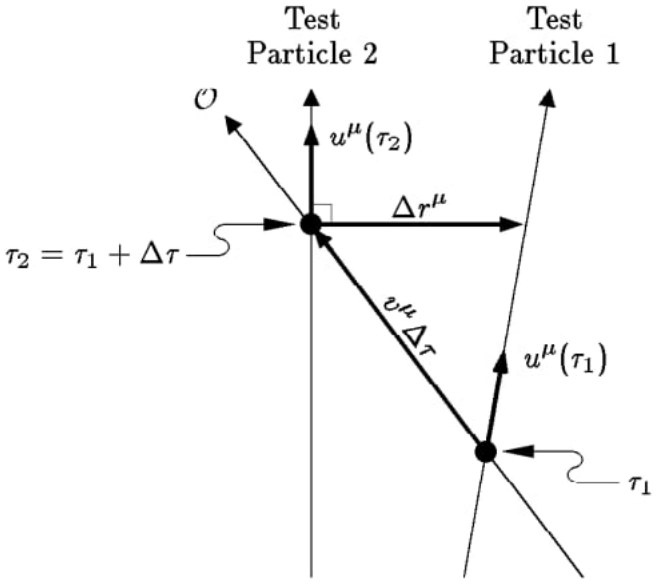

Figure 1.7: The separation of the comoving test particles Δr^μ is related to the displacement of the observer along the geodesic and the parallel transport of the particle velocity along $\mathcal{O}$. Image taken from [43].

The norm of the relative distance 4-vector can be readily calculated as:

$$\Delta r = \sqrt{\gamma^2 - \kappa}\ \Delta\tau \tag{1.2.19}$$

where $\kappa = u^\mu u_\mu$ and can be either 1 or 0 depending on whether we are considering a timelike or null geodesic, respectively. The Hubble expansion rate inferred by the observer is defined as the relative radial velocity of the test particles scaled over their separation:

$$H = \frac{\Delta u^r}{\Delta r} = \frac{\Delta u^\mu \Delta r_\mu}{(\Delta r)^2} \tag{1.2.20}$$

where we used the projection $\Delta u^r = \Delta u^\mu \Delta r_\mu / \Delta r$. Inserting Eqs. () the Hubble expansion rate takes the simple form:

$$H = -\frac{d\gamma/d\tau}{\gamma^2 - \kappa} = \frac{dF(\gamma)}{d\tau} \tag{1.2.21}$$

and the function $F(\gamma)$ is given by:

$$F(\gamma) = \begin{cases} \frac{1}{\gamma}\ , & \kappa = 0 \\ \frac{1}{2}\ln\frac{\gamma+1}{\gamma-1}\ , & \kappa = 1 \end{cases}$$

The final step is to compute the average expansion rate along the geodesic. Having all the necessary ingredients we write:

$$H_{av} = \frac{1}{\Delta\tau}\int_{\tau_1}^{\tau_2} H d\tau = \frac{1}{\Delta\tau}\left(F(\gamma_2) - F(\gamma_1)\right) \leq \frac{F(\gamma_2)}{\Delta\tau} \tag{1.2.22}$$

Thus, under the assumption of $H_{av} > 0$ the proper time along the geodesic is bounded from above:

$$\Delta\tau \leq \frac{F(\gamma_2)}{H_{av}} \tag{1.2.23}$$

As a result, the geodesic cannot be continued infinitely into the past and the space-time is past-incomplete. Applied to the inflationary scenario, the BVG theorem demonstrates that almost all geodesics, when extended to the past, are bound to terminate at a boundary of the inflationary region. The description of the universe beyond this boundary requires the introduction of new physics. From a physical perspective, the theorem strongly implies that the history of the universe is finite and inflation alone is

not sufficient in providing a full description of early universe cosmology[6].

1.3 Quantum cosmology

While the inflationary scenario successfully resolves several fine-tuning problems of the Big Bang model, it does not eliminate the need for specific initial conditions—it merely shifts the question further back in time. A more complete picture emerges within the framework of quantum cosmology, which aims to make probabilistic predictions about the universe's initial state by treating it as a quantum system described by a wavefunction. In this chapter, we outline the main formalism and show how a closed universe can arise naturally from "nothing", avoiding any initial singularities. [7]

1.3.1 Canonical quantization

We consider classical Einstein gravity with the Lagrangian corresponding to the Einstein-Hilbert action[8]:

$$L = \frac{1}{2}\int d^3x\sqrt{-g}R \tag{1.3.1}$$

In the canonical formulation of General Relativity we decompose the metric following the Arnowitt-Deser-Misner ADM formalism [49]. This is a general ansatz that foliates spacetime into a family of spatial hypersurfaces and encodes all the necessary information to transition from one slice to another. Explicitly it takes the form:

$$ds^2 = -N^2dt^2 + h_{ij}(dx^i + N^i dt)(dx^j + N^j dt) \tag{1.3.2}$$

where N is the lapse function and controls the rate of proper time flow between spatial hypersurfaces. N^i is the shift vector, which describes how the spatial coordinates shift from one hypersurface to the next. Finally, h_{ij} is the induced 3-metric on the spatial hypersurface of $t = \text{const}$.

In this ansatz the Einstein-Hilbert Lagrangian can be rewritten, up to boundary terms

[6] For criticism of the BVG theorem and its implications see [44, 45]
[7] For reviews of quantum cosmology, see [46, 47, 48].
[8] From here on, we are using the reduced Planck units $8\pi G = 1$.

as:

$$L = \frac{1}{2}\int d^3x\, N\sqrt{h}\left(R^{(3)} - K^2 + K_{ij}K^{ij}\right), \tag{1.3.3}$$

where h is the determinant of the spatial metric h_{ij}, $R^{(3)}$ is the Ricci scalar of the corresponding spatial slice and K_{ij} is the extrinsic curvature. The latter describes the curvature of the 3 manifold as viewed from the 4-dimensional spacetime in which it is embedded and $K = K^{ij}\gamma_{ij}$ is its trace. The conjugate momenta for the lapse N and the shift N^i are identically zero[9]:

$$\pi = \frac{\partial L}{\partial \dot{N}} = 0\ , \quad \pi^i = \frac{\partial L}{\partial \dot{N}_i} = 0 \tag{1.3.4}$$

They are called primary constraints and express the simple fact that derivatives of the lapse and shift are absent in the Lagrangian. This is expected, since these quantities are merely Lagrange multipliers that fix the spacetime gauge. On the other hand, the momentum conjugate to the 3-metric h_{ij} is non-trivial:

$$\pi^{ij} = \frac{\delta \mathcal{L}}{\delta \dot{h}_{ij}} = \frac{1}{2}\sqrt{h}\left(K^{ij} - h^{ij}K\right) \tag{1.3.5}$$

We now have the necessary ingredients to proceed with the Hamiltonian formalism of General Relativity [50, 51]. By definition we write:

$$H = \int \left(\pi\dot{N} + \pi^i\dot{N}_i + \pi^{ij}\dot{h_{ij}}\right) d^3x - L \tag{1.3.6}$$

Ignoring the primary constraints and after some lengthy calculation and reshuffling of terms one can arrive at the following expression for the Hamiltonian:

$$H = \int d^3x \left(N\mathcal{H} + N^i\mathcal{H}_i\right) \tag{1.3.7}$$

Taking into account that the primary constraints hold at all times and evaluating their Poisson brackets with the Hamiltonian, we are able to deduce the secondary, dynamical

[9] We have not shown it explicitly here, but the extrinsic curvature tensor K_{ij} depends only on spatial derivatives of the shift and not on $\dot{N}^i$.

constraints[10]. The first is the momentum constraint:

$$\mathcal{H}^i = -2\nabla_j \pi^{ij} = 0 \tag{1.3.8}$$

and the second is the Hamiltonian constraint:

$$\mathcal{H} = G_{ijkl}\pi^{ij}\pi^{kl} - \sqrt{h}R^{(3)} = 0 \tag{1.3.9}$$

where the tensor G_{ijkl} is called the superspace metric tensor (not related to supersymmetry) and is given by:

$$G_{ijkl} = \frac{1}{2}h^{-1/2}\left(h_{ik}h_{jl} + h_{il}h_{jk} - h_{ij}h_{kl}\right). \tag{1.3.10}$$

Equations (1.3.8) and (1.3.9) correspond respectively to the time-space and time-time components of Einstein's field equations and as such the two descriptions are equivalent. In the Hamiltonian formalism the arena in which the classical dynamics take place is called superspace [53]. It is the infinite dimensional space of all possible three metrics h_{ij}, modulo diffeomorphisms and matter field configurations $\Phi(\mathbf{x})$. It will play a central role in the description of the wavefunction of quantum gravity to follow.

The above discussion concludes the Hamiltonian description of General Relativity. The next step is to quantize the theory. We proceed with the Dirac quantization procedure in which the conjugate momenta are promoted to quantum mechanical operators acting on a state vector Ψ. In the metric representation of the state this corresponds to setting:

$$\hat{\pi}^{ij} \to -i\hbar\frac{\delta}{\delta h_{ij}} \tag{1.3.11}$$

The operators will act on the state vector $\Psi[\gamma]$ which is a functional of all possible three geometries h_{ij}. The wavefunctional Ψ is called the wavefunction of the universe and is of central importance for deriving predictions for the initial state of the universe.

In the quantized version of the theory the momentum constraints takes the form:

$$2i\hbar\nabla_j\left(\frac{\delta\Psi\left[h\right]}{\delta h_{ij}}\right) = 0 \tag{1.3.12}$$

[10]For a review of primary and secondary constraints see [52]

This is statement about the independence of the state vector on general coordinate transformations. In other words, Ψ depends only on the geometry of 3-space and not on its parametrizations.

Moreover, the Hamiltonian constraint takes the form:

$$\mathcal{H}\Psi = 0 \rightarrow \left(G_{ijkl} \frac{\delta}{\delta h_{ij}} \frac{\delta}{\delta h_{kl}} + p_{ij} \frac{\delta}{\delta h_{ij}} - \sqrt{h} R^{(3)} \right) \Psi[h] = 0 \tag{1.3.13}$$

This is the famous Wheeler-deWitt equation [54]. It is the analog of Schrodinger's equation for cosmology and can be expressed as a Klein-Gordon equation:

$$\left(\nabla^2 + U \right) \Psi = 0 \tag{1.3.14}$$

where the derivative operators are contracted with the superspace metric G_{ijkl} which has signature $(- + ++)$ for positive definite metrics h_{ij}, and the superspace potential $U = -\sqrt{h} R^{(3)}$. The tensor p_{ij} accounts for the ambiguity in the factor ordering of the operators and is usually neglected in simple applications. In order to obtain solutions to the Wheeler-deWitt equation, a prescription for the boundary conditions of Ψ should be imposed. This is an ongoing subject of research that we will dive into the following sections.

Since the infinite degrees of freedom of superspace are intractable we approach the WDW equation by coarse graining the geometry and considering a simplified subspace of the possible geometries. This subspace is referred to as minisuperspace and our approach in quantum cosmology will be mostly restrictred in that arena.

Finally, it is important to note that, just as in the Klein-Gordon case, we can now construct a conserved current:

$$J = \frac{i}{2} \left(\Psi^* \nabla \Psi - \Psi \nabla \Psi^* \right) \ , \quad \nabla J = 0 \tag{1.3.15}$$

The Wheeler-deWitt conserved current will play a crucial role in extracting well-defined probability distributions from the wavefunction Ψ. We will demonstrate this in the following Chapters.

1.3.2 Gravitational path integral

An alternative to the canonical quantization procedure is to define the state vector via Feynman's path integral [55]. In this approach the wavefunction is computed as a sum over all histories from which the system can evolve from an initial to a final state. Each path in the integral carries a weight dictated by the exponential of its action $\exp(iS)$, and as such, paths that extremize the action give the dominant contributions.

In the context of quantum cosmology, the wavefunction of the universe is defined as the sum over all possible 4-geometries g and matter field configurations ϕ that interpolate between fixed boundaries $\mathcal{B}$ of specified 3-metrics [56, 57, 58] (See Fig.1.8). Symbolically we can write:

$$\Psi[\gamma_{ij}, \phi] = \int \mathcal{D}g\mathcal{D}\phi \; e^{-S_E} \tag{1.3.16}$$

where as a matter of convention we defined the gravitational path integral in the Euclidean framework $\tau = it$. As it stands, the functional integral is not well-defined and one needs to specify a contour of integration that ensures its convergence. It is a known issue in quantum cosmology that the Euclidean action is unbounded from below and thus a purely Euclidean contour is problematic [59]. In practice one will have to explore contours that span the complex plane in order to arrive at well-behaved results and since the possible choices are infinite a clear prescription for the integration is necessary [60]. In this regard, the class of paths that are included in the summation and the contour that is specified are analogous to selecting boundary conditions for the Wheeler-deWitt equation. We note that the two approaches for the wavefunction are equivalent and solutions obtained via the path integral must satisfy the Wheeler-deWitt equation [61].

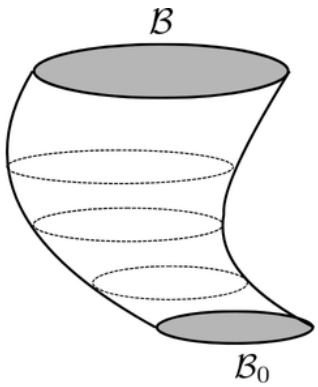

Figure 1.8: A sum over 4-geometries g following a path from an initial configuration $\mathcal{B}_0$ to a final $\mathcal{B}$.

We will try to obtain an approximate formula to evaluate (1.3.16). Our approach is based on the "saddle-point approximation" in which we pick up contributions from the dominant histories in the path integral [62, 63, 64]. The saddles are solutions to the classical equations of motion and extremize the action. Once we identify these configurations we can write:

$$\Psi \approx \sum_k e^{-S_k} \tag{1.3.17}$$

where k is the number of saddle points. Generally, not all saddles will contribute to the path integral since this depends crucially on the specified contour of integration. It is clear that different proposals for the wavefunction of the universe will select different solutions and as such provide distinct predictions about the initial state.

Carrying on with our approximation we will restrict our attention to minisuperspace cosmologies in which the lapse N is homogeneous, $N^i = 0$ and we have a finite number of degrees of freedom q^a. The transition amplitude from an initial state $q^{a''}$ to a final state $q^{a'}$ can now be expressed as an integral over the lapse and a functional integral over the minisuperspace degrees of freedom:

$$G(q^{a''}|q^{a'}) = \int dN \int \mathcal{D}q^a \exp\left(-S_E\right) \tag{1.3.18}$$

The above expression can be better understood by denoting the propagator:

$$\langle q^{a''}, N|q^{a'}, 0\rangle = \int \mathcal{D}q^a \exp\left(-S_E\right) \tag{1.3.19}$$

and rewritting the transition amplitude as:

$$G(q^{a''}|q^{a'}) = \int dN \langle q^{a''}, N|q^{a'}, 0\rangle \tag{1.3.20}$$

The propagator represents the quantum mechanical amplitude for the universe to evolve from $q^{a''}$ to $q^{a'}$ in a proper time N. The integral over the lapse function indicates that we should consider paths of every proper duration N as specified by our integration contour [65].

We proceed with the calculation of the propagator (1.3.19) by expanding around the

instanton solutions $\bar{q}^a$:

$$q^a(\tau) = \bar{q}^a(\tau) + Q^a(\tau) \tag{1.3.21}$$

where Q^a are fluctuations about the solutions and they vanish at the endpoints of the integral. Inserting into the Euclidean action we expand up to second order in the fluctuations. The first order terms vanish since these are extrema of the action. Overall, we can rewrite the transition amplitude as:

$$G(q^{a''}|q^{a'}) \approx \int dN \exp\left(-I_0\right) \int \mathcal{D}Q^a \exp\left(-I_2\right) \tag{1.3.22}$$

where S_0 is the instanton action and I_2 the action of the fluctuations. The functional integral over Q^a is straightforward to compute since it is a Gaussian. The result is a pre-exponential factor μ.

$$G(q^{a''}|q^{a'}) \approx \int \mu(q^{a''}, q^{a'}, N) \exp\left[-S_{E0}(q^{a''}, N|q^{a'})\right] \; dN \tag{1.3.23}$$

This is the final expression for the transition amplitude from an inital state $q^{a''}$ to a final state $q^{a'}$. It is an integral over the lapse N and will generally not be convergent for a purely Euclidean contour. Our approach in calculating it will be based on the method of steepest descent- Picard-Lefschetz- in which one distorts the initial integration contour so that it passes through some of the saddle-point geometries following paths in the complex plane that guarantee its convergence. This methodology is thoroughly explained in Apendix B and demonstrated in the following chapters.

1.3.3 Boundary conditions

So far we have discussed the two main formalisms that define the wavefunction of the universe: the Wheeler-DeWitt equation and the gravitational path integral. However, we have made no mention of their possible solutions and relevant predictions for cosmology. The key ingredient necessary for this discussion is the specification of appropriate boundary conditions. In the canonical formalism this corresponds to selecting boundary conditions for the Wheeler-deWitt equation, while for the path integral it consists of defining an integration contour that specifies the class of paths included. We note that

in the framework of quantum cosmology the boundary conditions cannot be inferred in the same manner as in standard quantum mechanics. In the latter case, the boundary conditions are determined by the physical setup external to the system. In our case since there is nothing external to the universe the boundary conditions have to be postulated independently as a fundamental law of Nature. The most developed proposals for the wavefunction of the universe are the Hartle-Hawking "no boundary" state and Vilenkin's tunneling wavefunction. We will begin by defining the former.

The main goal of Hartle and Hawking was to define the ground state of the wavefunction of the universe. Since the energy of a closed universe is identically zero, such state cannot be interpreted as the lowest energy state. However, the ground state can be defined as the state of the minimum possible excitation of the gravitational field. This corresponds to spacetimes of the highest possible symmetries and least degrees of freedom. Motivated by the successes of the Euclidean path integral in quantum field theory Hartle and Hawking made the following proposal [66]:

No boundary state

The no boundary state is defined as the Euclidean path integral summing over compact, regular four-geometries g and regular matter field configurations ϕ with a single boundary $\mathcal{B} = \{h_b, \phi_b\}$.

The above statement is expressed formally as:

$$\Psi_{HH}\left[h_b, \phi_b\right] = \int^{\mathcal{B}} \mathcal{D}g\mathcal{D}\phi \; e^{-S_E(g,\phi)} \tag{1.3.24}$$

It is essentially a topological statement about which 4-geometries to include in the path integral. The name "no-boundary" arises from the fact that the geometry of the initial state is taken to have a vanishing 3-geometry $h \to 0$ and close-off smoothly[11], like the South pole of a sphere. As a result the initial state has no topological boundary and there is no need to specify its initial conditions.

As it stands, the definition of the Hartle-Hawking state is vague and ill-defined. A key problem is that the integration is assumed to include only regular metrics and matter field configurations. This statement needs further clarification and constraints since

[11] Smooth closure of the geometry is a statement about the derivatives of the 3-metric, $\dot{h}$.

generally most of configurations contributing to the sum are not continuous, let alone differentiable. Another, more central issue, is that the path integral over Euclidean 4-geometries is divergent and one must specify a complex contour of integration to ensure its convergence. Generally, there is a plethora of contours that satisfy the definition of the Hartle-Hawking state and a clear prescription on which one to select is missing. This is a crucial ingredient, since as we mentioned in the previous section, the contour of integration picks which saddle point geometries contribute to the wavefunction and effectively determine its predictions. As a result, the uniqueness of the "no-boundary" state is questionable and further work is needed to constrain the configurations included in its path integral.

The second most developed proposal for the wavefunction of the universe is Vilenkin's tunneling wavefunction. Its name stems from the attempt of Vilenkin to describe the nucleation of the universe as a quantum mechanical tunneling event. Originally it was defined by imposing a boundary condition in superspace [67]. The formal statement reads:

Tunneling wavefunction

The tunneling wavefunction includes only outgoing modes at singular boundaries of superspace, carrying flux out of superspace.

The division of the superspace boundary into regular and singular parts has not been specified in the general case; here is a somewhat heuristic prescription. The boundary of superspace can be thought of as consisting of singular configurations which have some regions of infinite 3-curvature or infinite matter density, as well as configurations of infinite 3-volume and infinite values of matter fields. The regular part of the boundary includes singular 3-geometries which can be obtained by slicing regular Euclidean 4-geometries. For example, if a 4-sphere embedded in a $5D$ Euclidean space is sliced by parallel planes, one gets 3-spheres of vanishing radius and infinite curvature at the two poles, even though the 4-geometry is perfectly regular there. The outgoing wave[12] boundary condition is sometimes supplemented by requiring that the wave function is normalizable or that its

[12]The definition of outgoing modes in quantum cosmology is discussed in Ref.[68].

modulus is bounded from above.

$$|\Psi_T| < \infty \tag{1.3.25}$$

Physically, the outgoing modes condition can be thought as a requirement that the state predicts only expanding classical universes, in contrast with the Hartle-Hawking state which is usually assumed to conserve CPT symmetry.

An alternative definition of the tunneling wave function has also been given in terms of a path integral [68]. The formal statement is:

Tunneling wavefunction

The tunneling wavefunction is given by a path integral over Lorentzian histories interpolating between a 3-geometry of vanishing size and a given configuration g, with the lapse integration taken over the positive range $0 < N < \infty$.

Mathematically the statement is translated to:

$$\Psi_T\left[h_b, \phi_b\right] = \int_{\emptyset}^{g_b} \mathcal{D}g\mathcal{D}\phi \; e^{iS(g,\phi)} \tag{1.3.26}$$

As discussed in [69], a lapse integral over a half-infinite range gives a Green's function of the WDW equation. But in this case the source term has support only at geometries of vanishing size, which are at the boundary of superspace. Hence one can expect that Ψ_T is a solution of the WDW equation everywhere in the bulk of superspace. The positive lapse condition can be thought of as a causality requirement [69]: the histories included in the path integral are to the future of the origin event of "nothing". The equivalence of the two definitions is an open open problem and has only been demonstrated in the simple model of spherical S^3 spatial sections.

1.3.4 Creation of the universe from nothing

The implication of the BGV theorem is that an inflationary spacetime has a past boundary and as such raises the question of a beginning. In this section, we will demonstrate that the beginning of the universe can be explained by a quantum tunneling event in which the universe is created out of "nothing". In this context "nothing" corresponds to a state of no classical space-time and no energy. The idea of the quantum creation of the

universe was first put forward by E. Tryon [70] and A. Vilenkin was the first to formalize it mathematically.

First, we will show that the total energy of a closed universe—i.e., a universe without a boundary, such as a 3-sphere or a 3-torus—is zero. Since energy is not a generally well-defined concept in General Relativity, one typically defines it through surface integrals at spatial infinity in asymptotically flat spacetimes. However, a closed universe has no boundary, so such definitions do not apply. Instead, any calculation must be done in the bulk. If we choose a general foliation of spacetime and compute the energy as the volume integral of the bulk Hamiltonian, we have:

$$E = \int_{\mathcal{B}} \mathcal{H} d^4x + \int_{\partial\mathcal{B}} H d^3x \tag{1.3.27}$$

The first term corresponding to the bulk is identically zero since the Hamiltonian constraint imposes $\mathcal{H} = 0$ everywhere in the bulk. The boundary term vanishes for a closed spacetime and we are left with the result:

$$E_{closed} = 0 \tag{1.3.28}$$

Note that this result is independent of the time foliation used.

Since the total energy of a closed universe is zero, its creation from nothing does not violate any conservation laws. In quantum mechanics, processes that obey conservation laws between initial and final states are bound to occur with non-zero probability. In order to demonstrate this event for the entire universe we will start with the FRW metric for a closed spherical universe with spatial sections S^3:

$$ds^2 = -N^2 dt^2 + a^2(t) d{\Omega_3}^2 \tag{1.3.29}$$

The Einstein-Hilbert action for this spacetime with a positive cosmological constant reads:

$$S = 6\pi^2 \int_0^1 dt \left[-\frac{a\dot{a}^2}{N} + Na(1 - H^2 a^2) \right] \tag{1.3.30}$$

where $H^2 = \Lambda/3$ is the cosmological constant. Varying with respect to the scale factor a we obtain the equation of motion and varying with respect to the lapse we have the

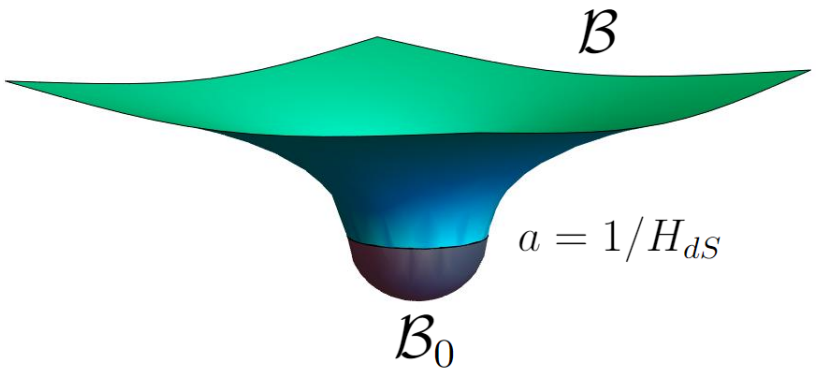

Figure 1.9: Nucleation of a de Sitter universe. Half of de Sitter space is matched to Euclidean hemisphere at the bounce radius $a = 1/H_{dS}$.

Hamiltonian constraint:

$$\dot{a}^2 + 2a\ddot{a} + N^2\left(1 - 3H^2a^2\right) = 0 \tag{1.3.31}$$

$$\dot{a}^2 + N^2\left(1 - H^2a^2\right) = 0 \tag{1.3.32}$$

In the gauge $N = 1$ we obtain the solution:

$$Ha = \cosh Ht \tag{1.3.33}$$

which corresponds to a deSiter space-time with minimum size H^{-1}, expanding exponentially. If we analytically continue the solution to Euclidean time $\tau = it$ we have:

$$Ha = \cos H\tau \tag{1.3.34}$$

and the metric (1.3.29) becomes the Euclidean deSitter 4-sphere S^4, with τ ranging from zero to π. At this point there is a strong hint that one can start with the Euclidean solution and match it to the Lorentzian one at $Ha = 1$. When we analytically continue to Lorentzian time one obtains equations for a classical universe. This description mimicks a quantum tunneling process Fig. 1.9.

We can now proceed with the quantization of the model. We promote our classical variable a to an operator in the Dirac formalism:

$$p_a \to -i\frac{\partial}{\partial a}\ , \quad a \to \hat{a} \tag{1.3.35}$$

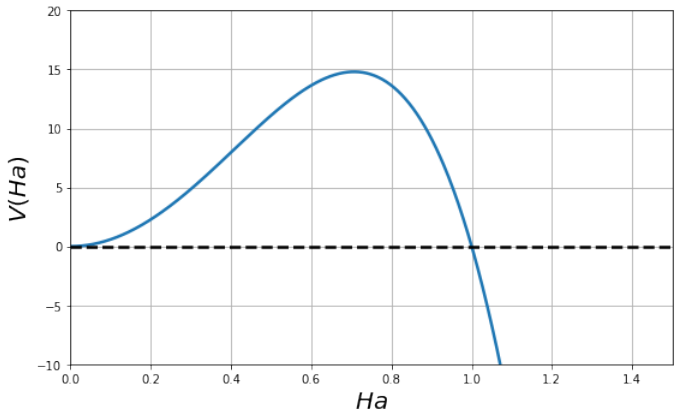

Figure 1.10: The minisuperspace potential $V(a)$ defines a potential barrier with a turning point at $Ha = 1$ and well-defined quantum and classical regimes.

Inserting in the Hamiltonian constraint we obtain the Wheeler-deWitt equation for the wavefunctional Ψ:

$$\left[-\frac{1}{24\pi^2}a^{-p}\frac{\partial}{\partial a}a^{p}\frac{\partial}{\partial a}+6\pi^2a^2\left(1-H^2a^2\right)\right]\Psi(a)=0 \tag{1.3.36}$$

where the parameter p depends on the choice of factor ordering and will not be important in the analysis to follow.

The above corresponds to the motion of a particle with coordinate $a(t)$ and zero energy moving in the potential $V(a) = 6\pi^2a^2\left(1 - H^2a^2\right)$. The classically allowed trajectories are restricted to $Ha > 1$ and the classically forbidden at $Ha < 1$, with $Ha = 1$ being the turning point. From Fig.1.10 it is clear that there are two possible trajectories. One can start from ∞ contract to the deSitter radius, bounce off the barrier and re-expand. Another trajectory begins at $a = 0$ in the quantum region and through quantum mechanical tunneling penetrates the barrier all the way to $Ha = 1$ and begins expanding exponentially. This is the trajectory we are most interested in. The tunneling probability for such event depends on the nature of the boundary conditions imposed on Ψ and different proposals yield different results. In the following section we will go over the two most established proposals for the wavefunction of the universe, the Hartle-Hawking state and Vilenkin's tunneling solution.

Equation (1.3.36) can be solved in the semiclassical approximation with the WKB

method. In the classically allowed region $Ha > 1$ we have two branches:

$$\Psi(Ha > 1) \propto \exp\left[\pm\frac{4i\pi^2}{H^2}\left(H^2a^2 - 1\right)^{3/2} \pm \frac{i\pi}{4}\right] \tag{1.3.37}$$

where the terms $\pm i\pi/4$ arise due to the WKB connection formulas at the turning point H^{-1}. In the forbidden region we have an exponentially growing and decaying branch:

$$\Psi(Ha < 1) \propto \exp\left[\pm\frac{4\pi^2}{H^2}\left(1 - H^2a^2\right)^{3/2}\right] \tag{1.3.38}$$

Vilenkin's tunneling proposal selects the outgoing wave at the classically allowed region and continuity at the turning point yields the under the barrier solution as a superposition of growing and decaying branches. Overall, the solution is of the form:

$$\Psi_T(a) = \begin{cases} \Psi^1_+(a), & Ha > 1 \\ \Psi^2_+(a) + \frac{i}{2}\Psi^2_-(a), & Ha < 1 \end{cases}$$

Except in the vicinity of H^{-1} the growing branch is subdominant and as such Vilenkin's solution is exponentially decreasing as we approach the turning point. This characteristic is analogous to a quantum tunneling and hence the name of Vilenkin's solution.

On the other hand, the Hartle-Hawking state is time symmetric and real in the classical region and, as such, has only the growing branch in the classically forbidden region:

$$\Psi_{HH}(a) = \begin{cases} \Psi^1_+(a) + \Psi^1_-(a), & Ha > 1 \\ \Psi^2_+(a), & Ha < 1 \end{cases}$$

The nucleation probability P for a spherical universe can be computed by evaluating the amplitude for the transition $a = 0 \to a = H^{-1}$. We have [13]:

$$P \propto \frac{\Psi(H^{-1})}{\Psi(0)} \tag{1.3.39}$$

[13] A formal calculation of probabilities in quantum cosmology is achieved by utilizing the WDW probability current. This will be shown explicitly in the following chapters. For details the reader is referred to [71]

For the tunneling wavefunction this yields:

$$P_T \propto \exp\left(-\frac{4\pi^2}{H^2}\right) \tag{1.3.40}$$

The above distribution is peaked at large values of $H \gg 1$. The interpretation is that the tunneling wavefunction describes the nucleation of a spherical universe with the maximum vacuum energy. The newly formed classical universe is created with a small size $\sim H^{-3}$ and follows rapid exponential expansion.

On the other hand, the Hartle-Hawking state yields the opposite weight:

$$P_{HH} \propto \exp\left(+\frac{4\pi^2}{H^2}\right) \tag{1.3.41}$$

This distribution is peaked at small values of H and the newly formed universe has a large size H^{-3} and a slow expansion rate.

These results represent some of the earliest and most notable predictions of quantum cosmology. When the vacuum energy is modeled as a slowly varying potential of a scalar field—the inflaton—the tunneling wavefunction favors initial conditions where the field starts near the maximum of the potential, while the Hartle–Hawking wavefunction prefers the minimum. Within the inflationary framework, this strongly supports the tunneling proposal, as it naturally leads to sufficient e-folds of inflation.

1.4 Overview

In the preceding sections, we presented a comprehensive overview of the framework of modern cosmology. Beginning with the standard cosmological model, we reviewed current observational evidence supporting a homogeneous and isotropic universe undergoing accelerated expansion, with dark matter as its dominant matter component. We provided an accurate account of its history, from the Big Bang singularity to the present epoch. The limitations of the Big Bang model are naturally addressed within the framework of inflationary cosmology. Moreover, inflation broadens our perspective by suggesting a finite past and an eternal future evolution of the universe. Nevertheless, inflation alone does not offer a complete cosmological picture and is subject to its own fine-tuning prob-

lems. A more complete framework is found in quantum cosmology, through the concept of the wavefunction of the universe. In this picture, a closed universe can spontaneously nucleate from "nothing" and begin inflating, providing a natural and singularity-free entrance into the inflationary phase. Predictions about the universe's initial state arise from competing proposals for its wavefunction—most notably the Hartle–Hawking no-boundary proposal and Vilenkin's tunneling wavefunction. In the following chapters we will delve into a detailed exploration of quantum cosmology and relevant gravitational instantons.

In Chapter 2, we explore quantum cosmology and eternal inflation beyond the slow-roll regime [72]. Recent insights from string theory suggest that many effective field theories may be incompatible with a consistent theory of quantum gravity, relegating them to the so-called "swampland." This casts doubt on the general validity of eternal inflation and motivates a study beyond the slow-roll approximation. We consider tunneling boundary conditions in quantum cosmology for a closed, spherical universe, describing its nucleation with the inflaton field near the top of its potential. By relaxing the slow-roll assumption, we identify a critical instability beyond which eternal inflation breaks down. Our analysis reveals that both the nucleation and subsequent inflationary dynamics undergo a sharp transition, resulting in the formation of domain-wall–like structures—inhomogeneous configurations that warrant further investigation.

In Chapters 3 and 4, we shift focus from spherical geometries to spacetimes with nontrivial topology. While the simplest wavefunction proposals have traditionally been studied in closed, isotropic models, a richer structure emerges when considering anisotropic cosmologies. One particularly interesting model is the Kantowski–Sachs (KS) universe, with spatial topology $S^1 \times S^2$. In such a setting, it is natural to investigate appropriate boundary conditions for the wavefunction of the universe and examine the physical predictions that follow.

In Chapter 3, we analyze the Hartle–Hawking (HH) wavefunction within the KS framework [73]. Rather than assuming a vanishing cosmological constant ($\Lambda = 0$), we consider the more physically relevant case of $\Lambda > 0$, which introduces significant complexity. We evaluate the semiclassical wavefunction by performing the Euclidean path integral using complex contour integration with suitable boundary conditions. This allows us to define

the HH state in the KS model. Our results indicate that the HH wavefunction exponentially favors large anisotropies—an outcome that is difficult to reconcile with present-day observational data.

In Chapter 4, we turn to the tunneling wavefunction in the same KS model and employ similar techniques to we extract cosmological predictions [74]. We find that the tunneling wavefunction favors a globally anisotropic but locally isotropic inflating universe. Remarkably, this implies that any primordial anisotropy would be unobservable at late times. Moreover, we find that the nucleation probability for a universe with $S^1 \times S^2$ topology is exponentially higher than for a standard de Sitter universe, suggesting that such configurations may play a significant role in the quantum origin of the universe.

In Chapter 5, we study a two-dimensional reduction of the KS cosmology via a mapping to the (1+1)-dimensional model introduced by Jackiw and Teitelboim (JT) [73]. The JT model provides a tractable framework that captures key aspects of quantum gravity in a lower-dimensional setting and can be viewed as a quantum theory of a one-dimensional closed universe. Our motivation is primarily theoretical: to gain insight into features of four-dimensional quantum gravity by examining a simpler toy model. Through the mapping, we find that the resulting wavefunction in the JT model is normalizable, enabling the construction of a well-defined probability distribution and offering a clearer probabilistic interpretation of quantum cosmological dynamics in lower dimensions.

In Chapter 6, we examine the formation of gravitating global strings via quantum tunneling [75]. The instantons describing this process are characterized by the string core thickness and its gravitational backreaction. Using numerical shooting methods, we obtain solutions across a broad parameter range and find qualitative agreement with prior results on topological defect nucleation. In particular, we identify a transition to homogeneous configurations reminiscent of Hawking–Moss solutions. Upon analytic continuation to Lorentzian signature, the resulting spacetime exhibits anisotropic expansion, providing further insight into the role of topological defects in quantum cosmology.

We summarize our results and discuss future research directions in Chapter 7.

Chapter 2

Quantum cosmology, eternal inflation and swampland conjectures

*Based on work with A. Vilenkin published in JCAP **04**, 034 (2023)*

In light of the recent swampland conjectures, we explore quantum cosmology and eternal inflation beyond the slow roll regime. We consider a model of a closed universe with a scalar field ϕ in the framework of tunneling approach to quantum cosmology. The scalar field potential is assumed to have a maximum at $\phi = 0$ and can be approximated in its vicinity as $V(\phi) \approx 3H^2 - \frac{1}{2}m^2\phi^2$. Using the instanton method, we find that for $m < 2H$ the dominant nucleation channel for the universe is tunneling to a homogeneous, spherical de Sitter space. For larger values of m/H, the most probable tunneling is to an inhomogeneous closed universe with a domain wall wrapped around its equator. We determine the quantum state of the field ϕ in the nucleated universe by solving the Wheeler-DeWitt equation with tunneling boundary conditions. Our results agree with earlier work which assumed a slow-roll regime $m \ll H$. We finally show that spherical universes nucleating with $m < 2H$ undergo stochastic eternal inflation with inflating regions forming a fractal of dimension $d > 2$. For larger values of m the field ϕ is unstable with respect to formation of domain walls and cannot be described by a perturbative stochastic approach.

2.1 Motivation

It is a widely held view that in order to understand how the universe originated we should treat the universe quantum mechanically and describe it by a wave function Ψ rather than by a classical spacetime. The picture that has emerged from this approach is that a small closed universe can spontaneously nucleate out of nothing, where 'nothing' refers to a state with no classical space and time[76, 66, 77, 78, 79, 80]. The cosmological wave function Ψ can be used to calculate the probability distribution for the initial states in the ensemble of nucleating universes. At least some of these universes are expected to go through a period of inflation, driven by the potential energy $V(\phi)$ of the inflaton field ϕ. This energy is eventually thermalized, inflation ends, and from then on the universe follows the standard hot cosmological scenario. Inflation is a necessary ingredient in this kind of scheme, since it provides the only way to get from a tiny nucleated universe to the large universe we live in today.

The wave function of the universe Ψ satisfies the Wheeler-DeWitt (WDW) equation

$$\mathcal{H}\Psi = 0, \tag{2.1.1}$$

where $\mathcal{H}$ is the Hamiltonian operator. To solve this equation, one has to choose some boundary conditions for Ψ. The most developed proposals for this choice are the Hartle-Hawking [66] and the tunneling [67, 81] boundary conditions. The predictions resulting from the two proposals have mostly been studied assuming a slowly varying potential $V(\phi)$,[1]

$$|V'|/V \ll 1, \quad |V''|/V \ll 1 \tag{2.1.2}$$

in reduced Planck units ($8\pi G = 1$). Then the Hartle-Hawking wave function predicts that the universe is most likely to nucleate with the lowest (positive) value of $V(\phi)$ and thus disfavors inflation. The tunneling wave function, on the other hand, predicts nucleation with ϕ near the maximum of $V(\phi)$, which is a favorable initial condition for (hilltop) inflation. Here we shall adopt the tunneling proposal.

With this choice, and assuming that the conditions (2.1.2) are satisfied, most of the universes nucleate with ϕ close to the maximum of $V(\phi)$ and immediately enter the regime of stochastic eternal inflation [22, 82, 83]. The dynamics of the field ϕ near the top of the potential is dominated by quantum fluctuations and is well approximated by a random walk. In any horizon

[1] We assume for simplicity that the potential depends on a single scalar field ϕ. An extension to multiple fields is briefly discussed in Section 2.

region the field gradually drifts away from the top and eventually rolls down to the minimum of $V(\phi)$, but in different regions this happens at different times, and at any time there are parts of the universe that are still inflating with ϕ near the top. The inflating regions form a self-similar fractal [84], with their total volume growing exponentially with time.

This scenario, however, is now being seriously questioned. There is growing evidence that a wide class of quantum field theories do not admit a UV completion within the theory of quantum gravity, even though they look perfectly consistent otherwise. Such theories are said to belong to the swampland, as opposed to the landscape. A number of different criteria that the landscape potential $V(\phi)$ should satisfy have recently been suggested [85, 86]. One of them is the so-called refined swampland conjecture [87, 88], which asserts that at any value of ϕ with $V(\phi) > 0$ one of the two conditions has to be satisfied:

$$|V'| \geq cV, \quad \text{or} \quad V'' \leq -\tilde{c}V, \tag{2.1.3}$$

where c and $\tilde{c}$ are positive constants of order one. This conjecture is clearly incompatible with the conditions (2.1.2). It is also in considerable tension with the inflationary scenario, which usually requires a slowly varying potential $V(\phi)$.

The swampland conjecture (2.1.3) as it stands may or may not be true. We take an agnostic attitude to this issue, but the above discussion motivates us to reconsider quantum cosmology and eternal inflation in the regime where the slow variation conditions (2.1.2) are not satisfied. This is our goal in the present paper. We start with quantum cosmology in Section 2. The tunneling wave function is expected to be peaked near the maximum of the potential, where $V(\phi)$ can be approximated as

$$V(\phi) \approx V_0 - \frac{1}{2}m^2\phi^2. \tag{2.1.4}$$

We have $|V''|/V(0) = m^2/3H^2$, where $H = (V_0/3)^{1/2}$ is the expansion rate of a de Sitter universe of vacuum energy density V_0. The slow variation condition (2.1.2) is then $m \ll H$. Here we are mostly interested in the regime $m \gtrsim H$.

We start in Section 2 by discussing nucleation of the universe using the instanton method. For sufficiently small values of the mass parameter, $\mu \equiv m/H < 2$, we find that nucleation is described by the homogeneous de Sitter instanton having the geometry of a 4-sphere. The initial state is then a spherical universe with $\phi = 0$, as usually assumed. On the other hand, for $\mu > 2$ the dominant instanton describes nucleation of a "domain wall universe". In this case the initial state still has the topology of a 3-sphere, but is inhomogeneous, having a domain

wall centered on a 2-sphere (the 'equator') where $\phi = 0$. We briefly discuss possible scenarios of subsequent evolution of a domain wall universe, referring to appropriate literature for more detail.

Focusing on the spherical initial configuration, we then discuss the quantum state of the nucleated universe in Sec.3. We expand the scalar field $\phi(\mathbf{x}, t)$ in spherical modes on a 3-sphere and solve the WDW equation for the wave function $\Psi(a, \phi_n)$, where a is the scale factor and ϕ_n are the mode amplitudes. Of special interest is the homogeneous mode $n = 1$. We find that the probability distribution for ϕ_1 is fully consistent with the instanton analysis. For small values of μ the wave function is peaked at $\phi_1 = 0$, while for $\mu > 2$ this behavior is modified and the top of the potential becomes a local minimum of $|\Psi|$. We argue that this marks a transition to a domain wall universe. For inhomogeneous modes, $n > 1$, the quantum state is an analytic continuation of the standard Bunch-Davies vacuum to a tachyonic field (with a possible exception of the dipole mode $n = 2$).

We finally discuss under what conditions nucleation of the universe is followed by stochastic inflation. One expects that there is some value μ_{max} above which stochastic inflation is not possible. Several attempts have been made to determine this threshold value in the literature with different results [89, 90, 91], so the question is still open at this time. We address this issue in Sec.4, with the conclusion that $\mu_{max} = 2$ – that is, stochastic inflation occurs for all values of μ that allow nucleation of a spherical universe.

Our conclusions are summarized and discussed in Sec.5.

2.2 Instanton analysis

We consider a model of a scalar field ϕ minimally coupled to gravity. The action of the model is

$$S = \int \sqrt{-g} d^4x \left(\frac{R}{2} - \frac{1}{2}(\nabla\phi)^2 - V(\phi) \right). \tag{2.2.1}$$

We assume that the potential $V(\phi)$ has a maximum at $\phi = 0$, where it can be approximated as in Eq.(5.3.8):

$$V(\phi) = 3H^2 \left(1 - \frac{1}{6}\mu^2\phi^2 \right), \tag{2.2.2}$$

where $\mu = m/H$.

In the leading order of semiclassical approximation, nucleation of the universe can be described using the instanton method. According to the tunneling prescription, the nucleation

probability is then given by

$$P_{nuc} \propto e^{-|S_E|}, \tag{2.2.3}$$

where S_E is the action of the Euclidean instanton solution. The dominant instanton is the one with the smallest magnitude of the action $|S_E|$. It is usually assumed [76, 66, 77, 78, 79] that this is the homogeneous de Sitter instanton with $\phi = 0$ and the geometry of a 4-sphere of radius H^{-1}. The corresponding Euclidean action is

$$S_E^{(dS)} = -\frac{8\pi^2}{H^2}. \tag{2.2.4}$$

We will now argue that this assumption is valid only for sufficiently small values of the mass parameter: $\mu < 2$. For larger values of μ the dominant instanton is an inhomogeneous domain wall instanton.

Domain wall instantons were first discussed in Refs.[92, 93] in the context of domain wall nucleation in the inflationary universe. They generally have $O(3) \times Z_2$ symmetry and the topology of a 4-sphere. Here we will mostly be interested in the regime of $\mu \approx 2$, corresponding to the transition between de Sitter and domain wall instantons. In this case the instanton solution covers only a small range of ϕ near $\phi = 0$, so we can use the approximate form of the potential (2.2.2) and the geometry is accurately described by the Euclideanized de Sitter metric

$$ds^2 = H^{-2}\{d\zeta^2 + \cos^2\zeta[d\chi^2 + \sin^2\chi(d\theta^2 + \sin^2\theta d\phi^2)]\}. \tag{2.2.5}$$

The domain wall instanton can be found with the ansatz $\phi = \phi(\zeta)$. The field equation for ϕ is then

$$\phi'' - 3\tan\zeta\phi' + \mu^2\phi = 0 \tag{2.2.6}$$

with boundary conditions $\phi'(-\pi/2) = \phi'(\pi/2) = 0$. With $\mu \approx 2$, this equation has two solutions: $\phi = 0$ and

$$\phi(\zeta) \approx A\sin\zeta \tag{2.2.7}$$

with $A = \text{const}$. The first solution corresponds to de Sitter instanton and the second to domain wall instanton.

The constant A depends on the nonlinear terms in the potential $V(\phi)$ [93]. Its particular value will not be important for our discussion, but as an illustrative example let us include in

the potential (2.2.2) an additional quartic term:

$$V(\phi) = 3H^2 - \frac{1}{2}H^2\mu^2\phi^2 + \lambda\phi^4. \tag{2.2.8}$$

Substituting this and the solution (2.2.7) into the Euclidean action

$$S_E = 2\pi^2 H^{-4} \int_0^\pi d\zeta \cos^3\zeta \left[\frac{1}{2}(\phi')^2 + V(\phi)\right], \tag{2.2.9}$$

we find

$$S_E = \frac{2\pi^2}{H^2}\left[3H^2 - \frac{2}{15}H^2(\mu^2-4)A^2 + \frac{4}{35}\lambda A^4\right]. \tag{2.2.10}$$

This action is minimized by

$$A^2 = \frac{7}{12\lambda}(\mu^2 - 4) \tag{2.2.11}$$

for $\mu > 2$ and by $A = 0$ for $\mu < 2$. Note that the domain wall instanton solution (2.2.7), (2.2.11) does not exist for $\mu < 2$. Note also that this threshold value depends only on μ and is not sensitive to the nonlinear part of the potential. A numerical calculation in Ref.[93] confirms that $|S_E^{(wall)}| < |S_E^{(dS)}|$ for all $\mu > 2$.[2]

Negative modes of the de Sitter instanton have been discussed in the Appendix of Ref.[93]. It shows that a homogeneous negative mode $\phi = \text{const}$ is always present for $\mu^2 > 0$, as it should be in a tunneling instanton. There are no other negative modes for $\mu < 2$, but for $\mu > 2$ additional, dipole negative modes of the form (2.2.7) appear. They signal that the de Sitter instanton is no longer dominant and that the leading instanton has a domain wall structure.

We conclude that the dominant nucleation channel in models with $\mu > 2$ is to a domain wall universe. Possible scenarios for subsequent evolution of such a universe depend on the shape of the potential $V(\phi)$ away from $\phi = 0$; they have been discussed in Ref.[97]. A few characteristic examples are illustrated in Fig.6.3.

In Fig.6.4a the potential is a double well with a maximum at $\phi = 0$ sandwiched between two symmetric de Sitter minima. Then at late times we have an approximately spherical expanding de Sitter universe with a domain wall on its equator. An important point is that domain walls of a fixed physical thickness exist in de Sitter space only for $\mu > 2$ [98, 99]. In the opposite case, wall-like configurations like Eq.(2.2.7) are smeared by the expansion of the universe, evolving towards a homogeneous $\phi = 0$ solution. In Fig.6.4b the minima of the

[2]This is similar to Coleman-de Luccia instanton [94] describing bubble nucleation in false vacuum. This instanton solution is dominant when it exists, but it disappears and is replaced by the Hawking-Moss instanton [95] when the tunneling barrier becomes sufficiently flat near the top [96].

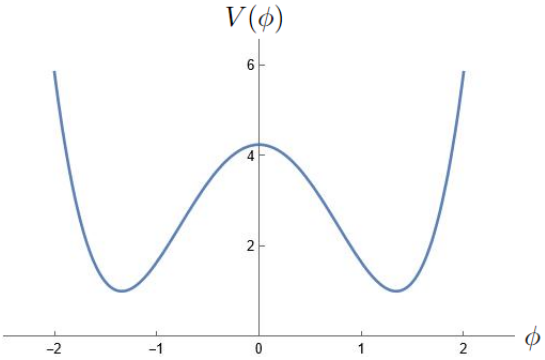

(a) Two de-Sitter vacua symmetric about $\phi = 0$.

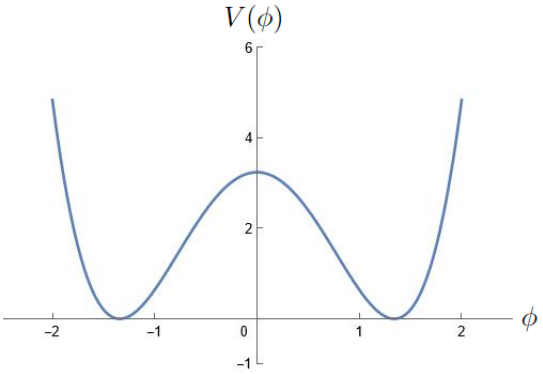

(b) Two Minkowski vacua symmetric about $\phi = 0$.

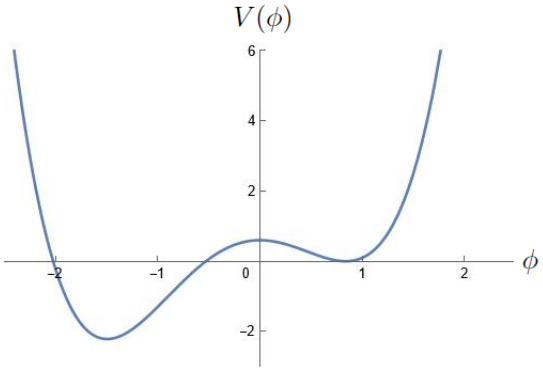

(c) An anti de-Sitter vacuum at $\phi < 0$ and a Minkowski vacuum at $\phi > 0$.

Figure 2.1: A plot of $V(\phi)$ with $\mu > 2$ and a local maximum at $\phi = 0$ in between two local minima.

potential are at $V = 0$. The universe then evolves to an inflating domain wall solution with two asymptotically Minkowski regions bounded by an expanding domain wall [100]. More precisely, the regions on the two sides of the wall have the geometry of open ($k = -1$) FRW universes. The minima of $V(\phi)$ do not have to be symmetric; an example is shown in Fig.6.4c. Once again, the wall separates two regions containing open FRW universes evolving with $\phi > 0$ and $\phi < 0$ branches of the potential. With a suitable choice of parameters, the potential can have a flat portion which can lead to a long inflationary period; an example is discussed in [97]. The potential minimum at $\phi < 0$ in Fig.6.4c is at $V < 0$. As a result the FRW universe on that side of the wall develops a big crunch singularity [101].

We finally briefly discuss multi-field models where the potential can be approximated near its maxima as

$$V(\phi) = 3H^2 - \frac{1}{2}\sum_{i=1}^{N} m_i^2 \phi_i^2. \tag{2.2.12}$$

Instanton solutions for such models in the de Sitter background have been discussed in [93]

assuming that the potential has an $O(N)$ symmetry, so that all mass parameters m_i^2 are equal to one another. For $N = 2$ the de Sitter instanton dominates if $m_i < 2H$. Otherwise, the dominant nucleation channel is to a 'global string universe', having a global string wrapped around its equator. Similarly, for $N = 3$ with $m_i > 2H$, the dominant tunneling is to a 'global monopole universe', having a global monopole and anti-monopole at its opposite poles. For models with lower symmetry the nucleated universe would have a more complicated defect structure. For example, in an $N = 2$ model with $Z_2 \times Z_2$ symmetry we would have $m_1 \neq m_2$ and the global string would be attached to four walls.

2.3 Quantum state of the universe

2.4 General formalism

We shall first review the standard minisuperspace analysis of the tunneling wave function. It was originally performed in the slow-roll regime $\mu \ll 1$ (e.g., [102, 103]). Here we will extend this analysis, but we will keep $\mu^2\phi^2 \ll 1$, so that the expansion about the maximum of the potential is justified.

The metric is assumed to be homogeneous, isotropic and compact:

$$ds^2 = a(\eta)^2 \left(-d\eta^2 + d\Omega_3^2\right) \tag{2.4.1}$$

where $a(\eta)$ is the scale factor, η is the conformal time and $d\Omega_3$ is the metric on a unit 3-sphere.

We expand our field ϕ in spherical harmonics Q:

$$\phi = (2\pi^2)^{1/2} \sum_{n,l,m} \phi_{nlm}(t) Q^n_{lm}(\mathbf{x}), \tag{2.4.2}$$

where $(2\pi^2)^{1/2}$ is a normalization factor and $n,\ l,\ m$ are harmonic numbers on a 3-sphere. For further convenience we will denote all harmonic numbers as n.

The Wheeler-DeWitt (WDW) equation for the model is obtained through the quantization of the Hamiltonian constraint. In this case it recasts to

$$\left[\frac{1}{24\pi^2}\frac{\partial^2}{\partial a^2} - 6\pi^2 V(a) - \sum_n \mathcal{H}_n\right] \Psi(a, \phi_n) = 0, \tag{2.4.3}$$

where we have neglected the factor ordering ambiguity and

$$V(a) = a^2\left(1 - H^2a^2\right), \tag{2.4.4}$$

$$\mathcal{H}_n = \frac{1}{2a^2}\frac{\partial^2}{\partial\phi_n^2} - \frac{1}{2a^2}\omega_n^2\phi_n^2, \tag{2.4.5}$$

$$\omega_n^2 = (n^2-1)a^4 - m^2a^6, \tag{2.4.6}$$

where $n \in \{1, 2, 3...\}$.

The next step is to solve the WDW equation. We will treat the scalar field modes ϕ_n as small perturbations. Then a solution to (2.4.3) can be obtained with the ansantz

$$\Psi \propto \exp\left[-12\pi^2 S_0(a) - \frac{1}{2}R_n(a)\phi_n^2\right]. \tag{2.4.7}$$

Substituting the above to (2.4.3) and neglecting subdominant terms in the WKB expansion along with terms of order $\sim \phi_n^4$, we have

$$\left(\frac{dS_0}{da}\right)^2 - V(a) = 0 \tag{2.4.8}$$

and

$$a^2\left(\frac{dS_0}{da}\right)\left(\frac{dR_n}{da}\right) - R_n^2 + \omega_n^2 = 0. \tag{2.4.9}$$

The solution to (2.4.8) is straightforward and given by

$$\frac{dS_0^{\pm}}{da} = \pm\sqrt{V(a)} \longrightarrow S_0^{\pm}(a) = \mp\frac{\left(1 - H^2a^2\right)^{3/2}}{3H^2} \tag{2.4.10}$$

where $S_0^{\pm}(a)$ correspond respectively to the decreasing and growing branches in the under-barrier region $Ha < 1$. In the classically allowed region $Ha > 1$ they are the contracting and expanding branches.

We now turn our attention to (2.4.9). We make a change of variables

$$\frac{da}{d\tau} = \begin{cases} \sqrt{V(a)} & \tau < 0 \\ -\sqrt{V(a)} & \tau > 0 \end{cases} \tag{2.4.11}$$

where τ is the Euclidean conformal time related to η through $\eta = i\tau$ and

$$a = \frac{1}{H\cosh(\tau)}. \tag{2.4.12}$$

With this change (2.4.9) becomes

$$a^2 \frac{dR_n^{\pm}}{d\tau} - R_n^{\pm 2} + \omega_n^2 = 0. \tag{2.4.13}$$

This is a Riccati equation and can be linearized via the transformation

$$R_n^{\pm}(\tau) = -\frac{a^2}{\nu_n}\frac{d\nu_n}{d\tau}. \tag{2.4.14}$$

The resulting ODE recasts to

$$\ddot{\nu}_n + 2\frac{\dot{a}}{a}\dot{\nu}_n - \left(n^2 - 1 - m^2 a^2\right)\nu_n = 0, \tag{2.4.15}$$

where we substituted the explicit form of ω_n.

The solutions to the above can be expressed in terms of the associated Legendre functions:

$$\nu_n(\tau) = A_n \cosh\tau \; P^n_{\gamma+1}(\tanh\tau) + B_n \cosh\tau \; Q^n_{\gamma+1}(\tanh\tau), \tag{2.4.16}$$

where

$$\gamma = \left(\frac{9}{4} + \frac{m^2}{H^2}\right)^{1/2} - \frac{3}{2} \tag{2.4.17}$$

and $A_n,\ B_n$ are constant coefficients. The functions ν_n correspond to the mode functions of a tachyonic field $\hat{\phi}$ of mass im in the de-Sitter background geometry. Selecting the integration constants in (2.4.16) is equivalent to selecting the quantum state of the scalar field $\hat{\phi}$.

The tunneling boundary conditions yield a total of three branches: growing and decaying under the barrier and expanding in the allowed region. The under the barrier components Ψ_+ and Ψ_- are to be evaluated for $\tau < 0$ and $\tau > 0$ respectively. The expanding branch in the Lorentzian region can be found by analytically continuing Ψ_- to imaginary conformal time $\eta = i\tau$. The coefficients multiplying the exponentials in Eq.(2.4.7) can then be determined by matching at the turning point $\tau = \eta = 0$ [102].

2.4.1 Regularity conditions

In order to specify the tunneling wave function we will need to determine the arbitrary coefficients $A_n,\ B_n$ in Eq.(2.4.16). This can be done by requiring that the wave functions for the

mode amplitudes ϕ_n in (2.4.7) for all three branches are Gaussian rather than inverse Gaussian:

$$R_n^{\pm}(a) \geq 0 \ , \quad Re\{R_n(a)\} \geq 0. \tag{2.4.18}$$

Here, R_n^+ and R_n^- are for the decaying and growing branches respectively and R_n is for the expanding branch. (Note that $R_n^{\pm}$ are real.) Following earlier literature, we will call Eq.(2.4.18) the regularity condition. It ensures that the wave function is peaked at $\phi_n = 0$, so that field fluctuations are suppressed.

We begin by examining the behavior of the growing branch well inside the Euclidean region, $Ha \ll 1$.[3] In the limit $\tau \to +\infty$ the mode functions ν_n behave as[4]

$$\nu_n(\tau) \approx \tilde{A}_n \ e^{(1-n)\tau} + \tilde{B}_n \ e^{(n+1)\tau} \tag{2.4.19}$$

where we have absorbed numerical factors in $\tilde{A}_n$ and $\tilde{B}_n$. For $B_n \neq 0$, the dominant term is the second one, so that $\nu_n \propto e^{(n+1)\tau}$. This would give

$$R_n^-(a) = -a^2 \frac{d \ln \nu_n}{d\tau} \approx -(n+1)a^2 < 0. \tag{2.4.20}$$

The regularity condition can be satisfied if we set $B_n = 0$; then

$$R_n^-(a) \approx (n-1)a^2 \geq 0. \tag{2.4.21}$$

This suggests that we set

$$\nu_n(\tau) = \cosh\tau \ P_{\gamma+1}^n(\tanh\tau). \tag{2.4.22}$$

We next check regularity at the turning point ($a = H^{-1}, \ \tau = 0$). Continuity of the wave function at this point requires that

$$\lim_{\tau\to 0^+} R_n^-(\tau) = \lim_{\tau\to 0^-} R_n^+(\tau) = \lim_{\eta\to 0^+} R_n(\eta) \tag{2.4.23}$$

The Legendre functions and their derivatives are continuous at the origin. This implies that the constants A_n and B_n ought to be identical and the values of $R_n(\tau = 0)$ should be the same for all three branches.

It is shown in Ref.[104] that with the mode functions (2.4.22) the regularity condition at

[3]Here we follow the analysis in Ref.[104].

[4]This expansion along with additional properties of Legendre functions which will be used throughout the paper can be found in DLMF or obtained with Mathematica.

the turning point is satisfied for all inhomogeneous modes ($n > 1$) with $\mu < 2$. Furthermore, it is shown in Ref.[105] that the regularity condition is satisfied in the entire classically allowed range $Ha > 1$ if it is satisfied at the turning point. However, the homogeneous mode $n = 1$ has $R_1(a = H^{-1}) < 0$ for all $\mu^2 > 0$. At smaller values of a it also develops a singularity on the dominant branch: $R_1^+(a \to a_1) \to -\infty$ at some point a_1 in the range $0 < a_1 < H^{-1}$. This mode therefore requires a special treatment.

To find the mode function suitable for the homogeneous mode, we shall use the results of Refs.[67, 103] for slow-roll potentials as a guide. They suggest that in the regime $Ha \ll 1$ and $\mu\phi_1 \ll 1$, the relevant part of the decaying branch should behave as

$$\Psi_+(Ha \ll 1) \propto \exp\left[-6\pi^2 a^2 - \frac{\pi^2 H^2 a^4}{4}\mu^2\phi_1^2\right], \tag{2.4.24}$$

where we kept the leading terms in a and ϕ_1. Comparing this with (2.4.7) we have

$$S_0^+(Ha \ll 1) \approx \frac{a^2}{2} \quad , \quad R_1^+(Ha \ll 1) \approx \frac{\pi^2 H^2 a^4}{2}\mu^2, \tag{2.4.25}$$

where the second expression is valid for $\mu \ll 1$.

On the other hand, the homogeneous mode function at $\tau \to -\infty$ (or $Ha \ll 1$) will generally behave as

$$\nu_1(\tau \to -\infty) \propto (2A_1 \sin\gamma\pi + B_1\pi\cos\gamma\pi)\ e^{-2\tau} = C_1 e^{-2\tau}, \tag{2.4.26}$$

where we defined

$$C_1 = 2A_1 \sin\gamma\pi + B_1\pi\cos\gamma\pi. \tag{2.4.27}$$

For $C_1 \neq 0$ this gives

$$R_1^+(Ha \ll 1) = -a^2\frac{d\ln\nu_1}{d\tau} \approx 2a^2, \tag{2.4.28}$$

which disagrees with (2.4.25). An agreement is achieved only if we set

$$B_1 = -A_1\frac{2}{\pi}\tan(\gamma\pi), \tag{2.4.29}$$

so that $C_1 = 0$.

The value of $R_1^+(0)$ for the above choice of the homogeneous mode is plotted as a function of μ in Fig.6.4. We see that regularity is satisfied for $\mu < 2$ and violated in some range above $\mu = 2$. This violation of regularity first occurs precisely at $\mu = 2$, when the de Sitter instanton becomes subdominant. At still larger values of μ, $R_1^+(0)$ becomes positive in some subregions.

However, inhomogeneous modes with $n > 1$ follow regularity patterns that interfere with the pockets of regularity of the homogeneous mode. This becomes clear from Fig.6.5 where we plot $R_n(0)$ for a number of leading inhomogeneous modes. When the mode $n = 1$ becomes regular at $\mu > 2$, higher order modes violate regularity.

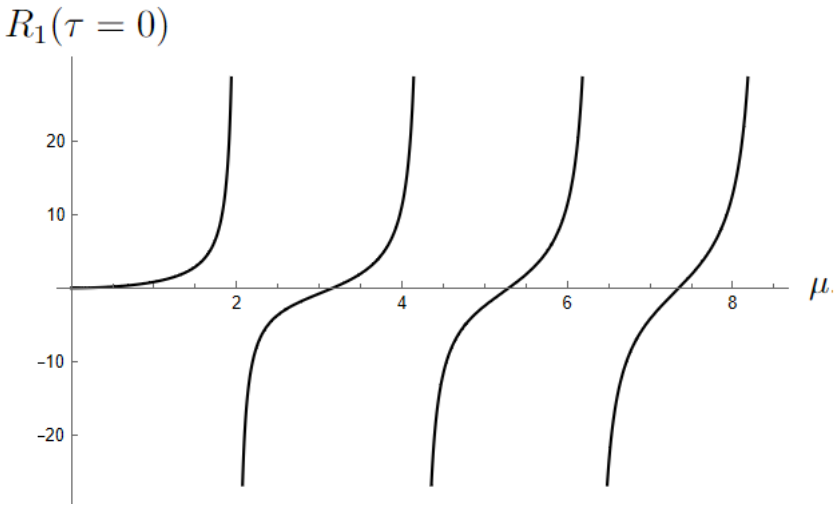

Figure 2.2: A plot of $R_1(\tau = 0)$ with respect to μ. For $\mu < 2$ regularity holds. As larger values of μ it still holds for some subregions.

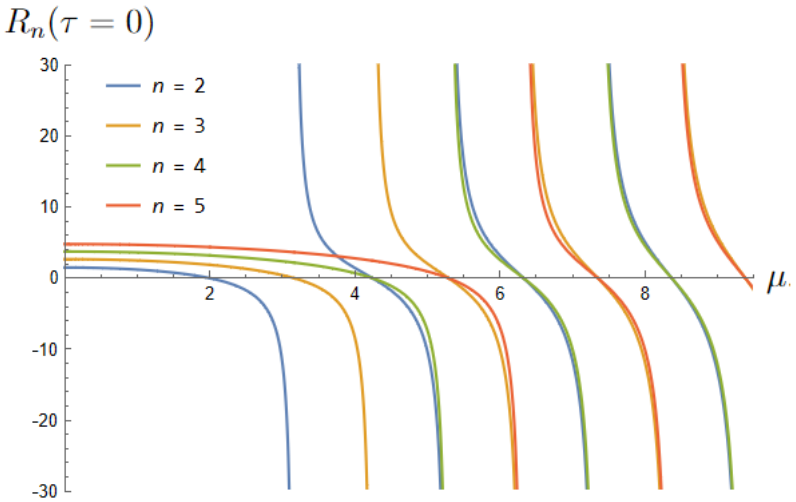

Figure 2.3: A plot of $R_n(\tau = 0)$ vs. μ for the modes $n = 2, 3, 4, 5$. Higher order modes violate regularity at larger values of μ. This leads to a pattern of interference in the pockets of regularity after $\mu > 2$.

So far we have only verified the regularity condition at $a \to 0$ and $a \geq H^{-1}$. By sampling different values of μ numerically, we convinced ourselves that regularity holds at $\mu < 2$ on both growing and decaying branches in the entire classically forbidden range $0 \leq a \leq H^{-1}$. There are however two exceptions to this rule.

The first exception is the homogeneous mode $n = 1$ on the growing branch, which has $R_1^-(a) < 0$ in a range of a adjacent to $a = 0$ for all $\mu^2 > 0$. The other exception is the dipole mode $n = 2$, which violates regularity on the decaying branch for $1.9 \lesssim \mu < 2$. These regularity violations are discussed in Appendix A, where we argue that they are not necessarily dangerous.

Overall, our analysis suggests the following choice of the mode functions:

$$\nu_n(\tau) = \begin{cases} \cosh\tau \ \left[P^1_{\gamma+1}(\tanh\tau) - \frac{2}{\pi}\tan(\gamma\pi)\ Q^1_{\gamma+1}(\tanh\tau)\right] & n = 1 \\ \cosh\tau \ P^n_{\gamma+1}(\tanh\tau) & n > 1 \end{cases} \tag{2.4.30}$$

We note that inhomogeneous modes follow the usual Bunch-Davies prescription, the only difference being that we are now dealing with a tachyonic field. As a result the modes with $n > 1$ will be regular even if we analytically continue to a field with a positive mass ($\mu^2 < 0$). The same does not hold for the homogeneous mode which would yield

$$R_1^+(Ha \ll 1) \approx -\frac{\pi^2 H^2 a^4}{2}|\mu^2|. \tag{2.4.31}$$

This is a clear characteristic of the tunneling wave function, for which the probability density is maximized at the maxima and minimized at the minima of the scalar potential.[5]

On the other hand, the appropriate choice for the Hartle-Hawking state is to select the Bunch-Davies modes (2.4.22) for all n. This gives a regular wave function for $\mu^2 < 0$ – that is, for an ordinary (non-tachyonic) massive field. Note that the difference between the tunneling and Hartle-Hawking approaches is limited only to the behavior of the homogeneous mode, and thus they predict the same quantum state for scalar field perturbations.

2.5 Condition for eternal inflation

Suppose now that the universe nucleates with ϕ near the top of the potential, where $V(\phi)$ is well approximated by Eq.(2.2.2) with $\mu < 2$, and has initial geometry close to de Sitter. We want to determine the conditions under which the universe will then undergo stochastic eternal inflation.

[5]Note that this conclusion differs from that in Ref.[106] which discussed a free massive scalar field ($\mu^2 < 0$) model using the Bunch-Davies mode function for the homogeneous mode. This mode function is regular for a non-tachyonic field discussed in that paper, but would exhibit pathological behavior in more general models that would include tachyonic fields at the maxima of the potential.

2.5.1 From Fokker-Planck equation

We shall first review the case of a small mass, $\mu \ll 1$, which has been extensively studied in the literature. The scalar field dynamics in this case is accurately described by the Fokker-Planck equation [83]

$$\frac{\partial \rho}{\partial t} = \frac{H^3}{8\pi^2}\frac{\partial^2 \rho}{\partial \phi^2} + \frac{1}{3H}\frac{\partial}{\partial \phi}\left(\rho \frac{\partial V}{\partial \phi}\right). \tag{2.5.1}$$

The field ϕ here should be understood as its average over a horizon volume $\sim H^{-3}$, and the quantity $\rho(\phi, t)d\phi$ has the meaning of the probability for ϕ to be in the range $[\phi, \phi + d\phi]$ at time t. The first term on the right-hand side of (2.5.1) accounts for quantum diffusion of the field and the second term for the classical drift due to the potential. Comparing the two terms and using $V(\phi)$ from Eq.(2.2.2) and 'naive' estimates like $\partial V/\partial \phi \sim V/\phi$, we find that quantum fluctuations dominate at

$$|\phi| \ll \phi_q \equiv H^2/m. \tag{2.5.2}$$

The eternally inflating region (EIR) of spacetime can be defined as the region where ϕ is in this range. We note that for such values of ϕ

$$\frac{m^2\phi^2}{V_0} \ll H^2 \ll 1, \tag{2.5.3}$$

where the last inequality assumes that the potential energy density at the top of the potential is small compared to Planck density. It follows from Eq.(2.5.3) that the geometry of EIR is well approximated by de Sitter space of energy density V_0.

Outside of EIR scalar field dynamics is nearly classical, so ϕ rolls down from the top of the potential and the geometry significantly deviates from de Sitter. However, this exterior region can affect the geometry of EIR only within a small distance $\sim H^{-1}$ from its boundary. The 3-volume of EIR at a late time t can be estimated as

$$\mathcal{V}_{EIR}(t) \sim \mathcal{V}_0 \exp(3Ht) \int_{-\kappa\phi_q}^{\kappa\phi_q} \rho(\phi, t)d\phi, \tag{2.5.4}$$

where $\kappa \gg 1$, $\mathcal{V}_0 = 2\pi^2 H^{-3}$ is the initial volume at nucleation and $\exp(3Ht)$ is the volume expansion factor of inflating regions. The parameter κ depends on our definition of EIR; its precise value is not important for our discussion here, while the condition $\kappa \gg 1$ ensures that the integration range in (2.5.4) covers the region where quantum fluctuations of ϕ are non-negligible.

With initial condition $\rho(\phi, 0) = \delta(\phi)$, the solution of the Fokker-Planck equation is given by

a Gaussian distribution

$$\rho(\phi,t) = (2\pi)^{-1/2}\sigma^{-1}(t)\exp[-\phi^2/2\sigma^2(t)]. \tag{2.5.5}$$

with [84]

$$\sigma^2(t) = \frac{3H^2}{8\pi^2\mu^2}\left[\exp\left(\frac{2}{3}\mu^2 Ht\right) - 1\right]. \tag{2.5.6}$$

In the limit of large t it approaches a ϕ-independent form

$$\rho = \text{const}\cdot\exp(-\mu^2 Ht/3) \tag{2.5.7}$$

and Eq.(2.5.4) gives

$$\mathcal{V}_{EIR}(t) \propto \exp(dHt), \tag{2.5.8}$$

where

$$d = 3 - \mu^2/3. \tag{2.5.9}$$

It was shown in Ref.[84] that the eternally inflating region in this case is a self-similar fractal of fractal dimension d.

The solution (2.5.5), (2.5.6) was used by Rudelius [89] to determine the condition for eternal inflation (see also references in [89] for earlier attempts in this direction). Requiring that the inflating volume grows with time, he found from Eq.(2.5.8) the condition $\mu < 3$. We note however that the Fokker-Planck equation on which the above solution is based is applicable only for slowly varying potentials satisfying the conditions (2.1.2), which in our case correspond to $\mu \ll 1$. Here we need to explore the regime of $\mu \sim 1$, so we cannot rely on the Fokker-Planck approximation.

2.5.2 From quantum cosmology

Our approach will be based on quantum cosmology. The wave function of the universe in the classically allowed region $Ha > 1$ is given by Eq.(2.4.7)

$$\Psi \propto \exp\left[-12\pi^2 S_0(a) - \frac{1}{2}R_n(a)\phi_n^2\right] \tag{2.5.10}$$

with

$$R_n(\eta) = -\frac{a^2}{\nu_n}\frac{d\nu_n}{d\eta}, \tag{2.5.11}$$

where $a(\eta) = -1/H\eta$ and the mode functions $\nu_n(\eta)$ are obtained by analytic continuation $\tau \to i\eta$ from Eq.(2.4.16). In this section it will be more convenient to use the proper time $t = -H^{-1}\ln(-H\eta)$ instead of the conformal time η.

The mode amplitudes ϕ_n behave as independent Gaussian variables; hence the probability distribution for ϕ_n can be written as

$$dP(\{\phi_n\}, t) = \prod_n d\phi_n \rho_n(\phi_n), \tag{2.5.12}$$

where

$$\rho_n(\phi_n, t) = (2\pi)^{-1/2}\sigma_n^{-1}(t)\exp[-\phi_n^2/2\sigma_n^2(t)]. \tag{2.5.13}$$

From Eq.(2.5.10) it is clear that the variances $\sigma_n(t)$ are given by

$$\sigma_n^2(t) = \frac{1}{2Re(R_n(t))} \tag{2.5.14}$$

The mode variances σ_n are calculated in Appendix B.

The total field ϕ, comprising all the modes, depends linearly on the mode amplitudes; hence its probability distribution is also Gaussian:

$$dP(\phi, t) = \rho(\phi, t)d\phi = (2\pi)^{-1/2}\sigma^{-1}(t)\exp[-\phi^2/2\sigma^2(t)]d\phi, \tag{2.5.15}$$

where

$$\sigma^2 = \langle\phi^2\rangle = \sum_n n^2\sigma_n^2 \tag{2.5.16}$$

and n^2 is the mode degeneracy factor.

As it stands, the sum in Eq.(2.5.16) is divergent at large n. This is not surprising: quantum fluctuations of ϕ on scale l grow as l is decreased, so a calculation of the expectation value of ϕ^2 at a point always gives a divergent result. This divergence can be regulated by smoothing the field operator $\hat{\phi}(\mathbf{x}, t)$ over horizon-size regions ($l \sim H^{-1}$). We can do this using a Gaussian window function, or more conveniently by cutting off the summation over n in (2.5.16) at some $n_* \sim e^{Ht}$.

The probability distribution for a smoothed field is still given by the Gaussian distribution (2.5.15). To analyze the regime of eternal inflation, we will be interested in this distribution in the limit of $t \to \infty$. We found in Appendix B that in this limit the time dependence of σ_n is the same for all n:

$$\sigma_n^2 \propto \exp(2\gamma Ht), \tag{2.5.17}$$

where

$$\gamma = \left(\frac{9}{4} + \mu^2\right)^{1/2} - \frac{3}{2}, \tag{2.5.18}$$

as before. Hence

$$\sigma^2 = \sum_{n=1}^{n_*} n^2 \sigma_n^2 = CH^2 \exp(2\gamma H t). \tag{2.5.19}$$

The dimensionless constant C is estimated in Appendix B:

$$C \approx \frac{2^{1+2\gamma}}{\sin(\gamma\pi)} \frac{\left[\Gamma\left(\gamma + \frac{3}{2}\right)\right]^2}{\Gamma(\gamma+1)\,\Gamma(\gamma+3)}. \tag{2.5.20}$$

In principle, C should depend on the cutoff n_*. However, we show in Appendix B that large-n terms in Eq.(2.5.16) make a negligible contribution to the series, making C effectively independent of n_*. This indicates that σ^2 is not sensitive to the size of the smoothing region. We note that C is divergent at $\gamma = 1$ ($\mu = 2$) when the modes become unstable. Another divergence is observed in the massless limit $\gamma \to 0$ ($\mu \to 0$) which corresponds to the infrared singularity in de-Sitter space (see [28, 26, 27]).

We can now estimate the volume of EIR in the same way as we did in the preceding subsection:

$$\mathcal{V}_{EIR} \sim \mathcal{V}_0 \int_{-\kappa\phi_q}^{\kappa\phi_q} \rho(\phi, t) d\phi = \mathcal{V}_0 \frac{2\kappa\phi_q}{H\sqrt{C}} e^{-\gamma H t}. \tag{2.5.21}$$

The result depends on the definition of EIR (parameter κ), but the fractal dimension d of the inflating region depends only on the time dependence of the inflating volume:

$$\mathcal{V}_{EIR} \propto e^{(3-\gamma)Ht} \equiv e^{dHt}. \tag{2.5.22}$$

This gives

$$d = 3 - \gamma = \frac{9}{2} - \left(\frac{9}{4} + \mu^2\right)^{1/2}. \tag{2.5.23}$$

It follows that for $\mu < 2$ we have stochastic inflation with fractal dimension $d > 2$. As μ approaches 2 from below, the fractal dimension approaches that of a domain wall, $d = 2$. And as we discussed in Sec.2, for $\mu > 2$ the dominant instanton describes nucleation of a domain wall universe.

We derived the fractal dimension (2.5.23) assuming that the universe originated by quantum nucleation from nothing. This result, however, is more general; it is not sensitive to the assumption about the initial state. For example, Guth and Pi [24] calculated the scalar field variance in de Sitter space with flat spatial sections assuming a thermal initial state. They

found the same asymptotic time dependence of $\langle\phi^2\rangle$ as in (2.5.19), and this would give the same fractal dimension of EIR as in (2.5.23).[6] This conclusion would formally also apply for $\mu > 2$, suggesting $d < 2$. However, in this case de Sitter space admits stable domain wall solutions, so fluctuations of the field ϕ are unstable with respect to formation of domain walls. These are nonlinear structures; they inflate along the wall surfaces and keep a fixed thickness in the transverse direction. Thus a description in terms of stochastic inflation is appropriate only for $\mu < 2$.

2.6 Conclusions

In this paper we studied quantum cosmology and eternal inflation in the regime where the slow-roll conditions are violated. Our approach was based on the wave function of the universe with tunneling boundary conditions. We considered a model of a closed universe with a scalar field ϕ, focusing on the range of ϕ near the top of its potential, where the potential can be approximated as $V(\phi) \approx 3H^2 - (1/2)m^2\phi^2$. We were mostly interested in the regime $m \gtrsim H$. Our analysis shows that the physics of both nucleation of the universe and eternal inflation undergo a sharp transition at the critical value of $m = 2H$.

We first used the instanton method in Section 2 to study nucleation of the universe from nothing. For small values of the steepness parameter $\mu = m/H$ we find that the dominant nucleation channel is to a spherical de Sitter universe with the scalar field at the top of the potential, $\phi = 0$. As the value of μ increases and reaches the threshold $\mu = 2$, another possible nucleation channel appears – to an inhomogeneous domain wall universe having a domain wall wrapped around its equator. This channel, when it exists, always dominates the nucleation probability. These conclusions are largely based on the work [93] in the context of domain wall nucleation in de Sitter space (which is described by the same instanton as nucleation of a domain wall universe). This earlier work, however, did not make a connection to quantum cosmology. The subsequent evolution of a domain wall universe depends on the nature of the vacua separated by the wall (which are generally different). We discussed possible scenarios for the cases of (A)dS and Minkowski vacua, following earlier discussion in Ref.[97].

The quantum state of a nucleated spherical universe is discussed in Section 3, where we extend earlier treatments which assumed a slow-roll potential. To this end, we expand the field

[6] We note that $\mu < 2$ was also suggested as the condition for topological inflation in which inflation takes place inside the cores of domain walls [107, 108]. For numerical simulations of the fractal structure of such models see [109].

in spherical harmonics and solve the Wheeler-DeWitt equation for the wave function of the universe $\Psi(a, \phi_n)$ with tunneling boundary conditions. The tunneling prescription instructs us to impose the regularity condition, ensuring that $|\Psi|$ decreases as the mode amplitudes ϕ_n are increased. We find a regular quantum state for $\mu < 2$, while for larger values of μ such states do not exist. These results are consistent with the instanton approach.

A caveat in the above analysis is the behavior of the dipole mode which violates regularity in the narrow range $2 > \mu \gtrsim 1.9$. This feature is discussed in Appendix A, where we argue that it is not necessarily problematic. We note that the origin of this behavior remains enigmatic for us and it should, perhaps, be further investigated.

Eternal inflation in the nucleated universe is discussed in Section 4. The standard treatment using the Fokker-Planck equation is not applicable beyond the slow-roll regime. Our approach here is based on quantum cosmology and does not suffer from this limitation. The wave function of the universe provides Gaussian probability distributions for individual modes ϕ_n. We use this to find the distribution for the total field ϕ (comprising all the modes) smoothed over horizon regions, and then use it in turn to estimate the volume of the eternally inflating region (EIR). We find that for $\mu < 2$ this volume grows exponentially with time, indicating that eternal inflation does occur in this range of μ. The rate of volume growth is related to the fractal dimension d of EIR, and we find that $d > 2$ and that $d \to 2$ from above as $\mu \to 2$ from below. For $\mu > 2$ stable domain wall solutions exist in de Sitter space, and fluctuations of the field ϕ are unstable with respect to formation of walls. A description in terms of stochastic inflation is not appropriate in this regime.

Acknowledgments

We are grateful to Gia Dvali for a stimulating discussion and to Jose Blanco-Pillado and Jaume Garriga for useful comments on the initial draft of the paper. This work was supported in part by the National Science Foundation under grant No. 2110466.

Chapter 3

The Hartle-Hawking state in Kantowski-Sachs quantum cosmology

*Based on work with A. Vilenkin published in JCAP **03**, no.03, 056 (2022)*

We explore quantum cosmology of the anisotropic Kantowski-Sachs (KS) model of spatial sections $S^1 \times S^2$ with a positive cosmological constant $\Lambda > 0$ and define the Hartle-Hawking (HH) state with the path integral formalism. Considering a range of possible boundary conditions,, we conclude that the most suitable is the one corresponding to a vanishing radius of S^1 supplemented with an appropriate regularity condition. We carry out the sum over regular geometries following Picard–Lefschetz theory and the saddle-point approximation. In the absence of a clear prescription for the path integration, the selection of the contour is decided based on general criteria that the HH state satisfies. The semiclassical HH state is obtained along with its probability distribution. Our analysis shows that the HH state predicts an ensemble of classical universes with pronounced local anisotropy—specifically, Nariai-type spacetimes, in which the S^2 radius is compactified to a de Sitter-like form while the S^1 radius undergoes inflation.

3.1 Motivation

In quantum cosmology the entire universe is treated quantum mechanically and is described by a wave function, rather than by a classical spacetime. The wave function $\Psi(g, \phi)$ is defined on the space of all 3-geometries (g) and matter field configurations (ϕ), called superspace. It can be found by solving the Wheeler-DeWitt (WDW) equation

$$\mathcal{H}\Psi = 0, \tag{3.1.1}$$

where $\mathcal{H}$ is the Hamiltonian operator. Alternatively, one can consider the transition amplitude from the initial state (g', ϕ') to the final state (g, ϕ), which can be expressed as a path integral,

$$G(g, \phi | g', \phi') = \int_{(g', \phi')}^{(g, \phi)} e^{iS}, \tag{3.1.2}$$

where S is the action and the integration is over the histories interpolating between the initial and final configurations. In general, G is a Green's function of the WDW equation [69]. But if (g', ϕ') is at the boundary of superspace, or if the geometries that are being integrated over have a single boundary at g, then G is a solution of the WDW equation and the path integral (4.1.2) may be used to define a wave function of the universe.

The choice of the boundary conditions for the WDW equation and of the class of paths included in the path integral representation of Ψ has been a subject of ongoing debate. The most developed proposals in this regard are the Hartle-Hawking [66] and the tunneling [103, 68] wave functions.[1] The intuition behind both of these proposals is that the universe originates 'out of nothing' in a non-singular way. But despite a large amount of work, a consensus on the precise definition of these wave functions has not yet been reached. In fact, the two wave functions are often confused with one another.

The Hartle-Hawking (HH) wave function is usually defined in terms of a Euclidean path integral,

$$\Psi_{HH}(g, \phi) = \int^{(g, \phi)} e^{-S_E}, \tag{3.1.3}$$

where S_E is the Euclidean action and the integration is over regular compact geometries with a single boundary on which the boundary values (g, ϕ) are specified. The tunneling wave function is defined either by an outgoing-wave boundary condition in superspace or by a path integral over Lorentzian histories interpolating between a vanishing 3-geometry and the configuration

[1] For early work closely related to HH and tunneling proposals, see Refs. [76] and [77, 78, 79, 80] respectively.

(g, ϕ). Here we will focus on the HH wave function; the tunneling wave function will be discussed in a separate publication.

In Section 3 we review the quantum cosmology of the Kantowski-Sachs (KS) model, following largely the treatment of Halliwell and Louko (HL) [64].

The semiclassical HH wave function for the KS model is discussed in Section 4. HL studied this wave function only for a vanishing cosmological constant, $\Lambda = 0$. Here we will need to extend their analysis to the case of $\Lambda > 0$, which is significantly more complicated. We impose the boundary conditions of smooth closure in the limit of small universes and follow standard methods to reduce the problem to evaluation of a lapse (N) integral over some contour $\mathcal{C}$ in the complex N plane. The choice of the contour $\mathcal{C}$ is restricted by the requirements that the HH wave function is expected to satisfy. We argue that there is only a single acceptable choice, with all other acceptable choices equivalent to it.

In the semiclassical limit the dominant contribution to the integral is given by saddle points of the action. We find these saddle points, as well as the steepest descent and ascent lines, and use the Picard-Lefschetz prescription to deform the contour so that the integral becomes absolutely convergent. The integral is then evaluated in the WKB approximation, including the prefactor.

Our results are summarized and discussed in Section 7. Some technical details are relegated to the Appendix.

3.2 Kantowski-Sachs model

3.2.1 Classical dynamics

As already mentioned, our focus in this paper will be on minisuperspace models. Here we are focusing on the homogeneous version of the Kantowski-Sachs (KS) model [110] that describes a homogeneous universe with spatial sections of the $S^1 \times S^2$ topology. Following Halliwell and Louko [64], we represent the metric of the KS model as

$$ds^2 = -\frac{N^2}{a^2} d\tau^2 + a^2 dx^2 + b^2 d\Omega^2, \tag{3.2.1}$$

where N, a and b are functions of time τ, which we can choose to vary in the range $0 < \tau < 1$ and $x \sim x + 2\pi$. After substituting this in the Lorentzian Einstein-Hilbert action with a cosmological

constant $\Lambda \equiv H^2$ and integrating over x and over the angular variables, the action reduces to

$$S = -\pi \int_0^1 d\tau \left[\frac{\dot{b}\dot{c}}{N} + N(H^2 b^2 - 1) \right], \tag{3.2.2}$$

where we have introduced a new variable $c = a^2 b$.

The factor $1/a^2$ is added in the first term of (4.2.12) in order to simplify the equations of motion, which take the form

$$\ddot{b} = 0, \tag{3.2.3}$$

$$\frac{\ddot{c}}{N^2} - 2H^2 b = 0, \tag{3.2.4}$$

where overdots stand for derivatives with respect to τ. The constraint equation is obtained by varying the action with respect to N:

$$\frac{\dot{b}\dot{c}}{N} - N(H^2 b^2 - 1) = 0. \tag{3.2.5}$$

An important solution of these equations is obtained by setting $\dot{b} = 0$. Then Eq.(4.2.14) tells us that $b = H^{-1}$ and Eq.(3.2.4), expressed in terms of the proper time variable $t = \int d\tau / a(\tau)$, becomes

$$\frac{d^2 a}{dt^2} = H^2 a, \tag{3.2.6}$$

which has a solution

$$a(t) = H^{-1} \cosh(Ht), \tag{3.2.7}$$

where we have set $N = 1$. This is the Nariai solution, which is a product of a $2D$ de Sitter space and a 2-sphere of radius H^{-1} [111].

It follows from Eq.(3.2.3) that $\dot{b}$ cannot change sign, indicating that the Nariai solution is unstable. If we perturb it by giving the radius of the sphere b a slight velocity, the sphere will collapse if $\dot{b} < 0$ and will expand to infinite size if $\dot{b} > 0$.

The Euclidean continuation of the Nariai solution is a product of two spheres of radius H^{-1}. It is often referred to as the Nariai instanton and describes nucleation of extremal black holes in de Sitter space [112, 113].

3.2.2 WDW equation

The quantum cosmology of the KS model has been studied by a number of authors [114, 64, 115, 116, 117]. Some exact solutions of the WDW equation have been found and semiclassical

methods have been used to study more general solutions. Here we will follow the method of Halliwell and Louko (HL) [64] which allows one not only to find the saddle points of the action, but also helps to determine which saddle points contribute to the semiclassical wave function. This method will also be useful for interpreting the solution (5.2.29) found by IKTV.

The momenta conjugate to the variables b and c are

$$p_b = -\pi\dot{c}/N, \qquad p_c = -\pi\dot{b}/N. \tag{3.2.8}$$

Using this in the constraint equation (4.2.14) and replacing $p_b \to -i\partial/\partial b$, $p_c \to -i\partial/\partial c$, we obtain the WDW equation

$$\pi\mathcal{H}\Psi = \left[\partial_b\partial_c + \pi^2(H^2b^2 - 1)\right]\Psi = 0. \tag{3.2.9}$$

This equation can be simplified by introducing a new variable ξ, which is related to b as $d\xi = \pi^2(H^2b^2 - 1)db$. Choosing the integration constant so that $\xi(Hb = 1) = 0$, we have

$$\xi = \frac{\pi^2}{3H}(H^3b^3 - 3Hb + 2) = \frac{\pi^2}{3H}(Hb - 1)^2(Hb + 2). \tag{3.2.10}$$

We also introduce the variable $\rho = c - H^{-3}$; then the WDW equation becomes

$$(\partial_\xi\partial_\rho + 1)\Psi = 0. \tag{3.2.11}$$

The general solutions of the above are given by:

$$\Psi_m = \left(\frac{\rho}{\xi}\right)^{m/2} H_m^{(2)}(2\sqrt{\xi\rho}). \tag{3.2.12}$$

where H_m is the Hankel function, a particular Bessel function. In practice, any Bessel function is an acceptable solution in the place of the Hankel function. The reason we present this solution will become clear in the following sections/chapters.

3.2.3 Transition amplitude

We now consider the transition amplitude from the initial state $\{b', c'\}$ to the final state $\{b, c\}$. We will be particularly interested in the initial state

$$\{b', c'\} = \{H^{-1}, H^{-3}\} \tag{3.2.13}$$

corresponding to the bounce point of the Nariai solution. We shall refer to it as 'Nariai initial conditions'.

The general framework for calculating transition amplitudes has been discussed by HL [64]. For a general minisuperspace model described by the Hamiltonian

$$\mathcal{H} = \frac{1}{2} f^{\alpha\beta}(q) p_\alpha p_\beta + V(q), \tag{3.2.14}$$

where q^α are the generalized coordinates and p_α their conjugate momenta, the transition amplitude between q' and q is

$$G(q|q') = \int_0^\infty dN \int \mathcal{D}p\mathcal{D}q e^{iS} = \int_0^\infty dN \langle q, N|q', 0\rangle. \tag{3.2.15}$$

Here N is the lapse parameter, the action is

$$S = \int_0^1 d\tau \left(p_\alpha \dot{q}^\alpha - N\mathcal{H}\right) \tag{3.2.16}$$

and the path integral is over histories interpolating between q' and q.

HL show that the amplitude (3.2.15) satisfies

$$\mathcal{H}G(q|q') = -i\langle q, 0|q', 0\rangle = -i\delta(q, q'), \tag{3.2.17}$$

where

$$\mathcal{H} = -\frac{1}{2}\nabla^2 + \zeta R + V \tag{3.2.18}$$

is the Hamiltonian operator, ∇^2 and R are the Laplacian and the curvature scalar in the metric $f_{\alpha\beta}$, and ζ is the conformal coupling. The magnitude of ζ depends on the dimension of superspace and vanishes in the case of $2D$, which is of interest to us here. We see from Eq.(3.2.17) that G is a Green's function of the WDW equation.

For the KS model the Hamiltonian is quadratic and the path integral in (3.2.15) can be performed exactly. Then, up to an overall multiplicative constant, HL found that the amplitude reduces to

$$G(b, c|b', c') = \int_0^\infty \frac{dN}{N} \exp\left[\frac{i}{2}\left(\alpha N - \frac{\beta}{N}\right)\right], \tag{3.2.19}$$

where

$$\alpha = 1 - \frac{H^2}{3}(b^2 + bb' + b'^2), \quad \beta = (2\pi)^2(c - c')(b - b'). \tag{3.2.20}$$

This amplitude should satisfy

$$\mathcal{H}G(b,c|b',c') \propto -i\delta(b-b')\delta(c-c'). \tag{3.2.21}$$

The integral over N in (4.4.1) can be expressed in terms of Bessel functions [64]. With Nariai initial conditions (3.2.13) we have

$$\alpha = -\frac{1}{3}(Hb-1)(Hb+2), \quad \beta = \left(\frac{2\pi}{H^2}\right)^2 (H^3c-1)(Hb-1) \tag{3.2.22}$$

and

$$G = -i\pi H_0^{(2)}\left(\sqrt{-\alpha\beta}\right) \qquad (H^3c > 1) \tag{3.2.23}$$

$$G = 2K_0\left(\sqrt{\alpha\beta}\right) \qquad (H^3c < 1) \tag{3.2.24}$$

Thus the transition amplitude between states of fixed scale factors can be analytically computed and is given by the above expressions.

3.3 Hartle-Hawking wave function

In the original Hartle & Hawling paper [**?**] the HH wave function is defined as

$$\Psi(g_b) = \int^{g_b} \mathcal{D}g e^{-S_E(g)}, \tag{3.3.1}$$

where the integration is over "regular" $4D$ Euclidean geometries g, having a single boundary $\mathcal{B}$ with a 3-metric g_b. For simplicity we specialize to models without any matter fields. As it stands, this definition is rather problematic. The Euclidean action S_E is unbounded from below, so the integral in (3.3.1) is divergent. This can often be dealt with by a suitable analytic continuation of the integration variables. Another problem is that the metrics contributing to the path integral are generally rather irregular, even non-differentiable. So the notion of integrating over regular geometries needs to be defined. The same problem arises in JT gravity.

IKTV attempted to get around this issue by focusing on the upper limit of integration in (3.3.1), with the hope that the regularity condition would somehow take care of itself. They allowed the boundary curve of the $2D$ geometry to fluctuate and required that the asymptotic form of the wave function agrees with the semiclassical pre-exponential factor resulting from these fluctuations. Another approach that they used was to calculate the path integral (3.3.1) for JT gravity with $\Lambda < 0$, where it is better defined, and then analytically continue to $\Lambda > 0$.

IKTV find that the two approaches agree and yield the wave function (5.2.29). Our analysis shows, however, that this wave function is unsatisfactory, as it is not a solution of the WDW equation. Instead, it is related to the transition amplitude from a Nariai initial state with $a = H^{-1}$ and $\phi = 0$. The path integral (3.2.15) for this amplitude is over geometries with two boundaries – one with the specified values of a and ϕ and the other with the 'Nariai' values. This does not square well with the intuitive idea of quantum creation of the universe from nothing.

We therefore need to revisit the question of how the path integral over regular Euclidean geometries has to be defined. In the context of minisuperspace KS model, this issue has been discussed in detail by HL [64], whose approach we largely follow.

3.3.1 Boundary conditions

To discuss the boundary conditions for the no-boundary path integral, it is more convenient to represent the Euclideanized KS metric as

$$ds_E^2 = N^2 dt^2 + a^2(t) dx^2 + b^2(t) d\Omega^2. \tag{3.3.2}$$

The Euclidean action is then [64]

$$S_E = \pi \int_0^1 dt \left[-\frac{1}{N}\left(a\dot{b}^2 + 2b\dot{a}\dot{b} \right) + Na(H^2 b^2 - 1) \right] + S_b, \tag{3.3.3}$$

where S_b is the boundary term[2]

$$S_b = -\left[\frac{\pi}{N} \frac{d}{dt}(ab^2) \right]_{t=0}. \tag{3.3.4}$$

The time variable t is defined so that $0 < t < 1$ with $t = 1$ corresponding to the boundary $\mathcal{B}$ and $t = 0$ corresponding to the "bottom" $\mathcal{B}_0$ of the 4-geometry g.

The boundary conditions at $t = 1$ fix the values of $\{a, b\}$, while the boundary conditions at $t = 0$ should be chosen so that the geometry closes smoothly at $\mathcal{B}_0$. HL show that for a classical 4-geometry(3.3.2) there are two choices:

$$a(0) = 0, \quad \frac{1}{N}\dot{a}(0) = \pm 1, \quad \frac{1}{N}\dot{b}(0) = 0 \tag{3.3.5}$$

[2]The Gibbons-Hawking boundary terms in the gravitational action cancel out after integration by parts if the geometry has two boundaries – at $t = 0$ and $t = 1$. But for a compact geometry with a single boundary at $t = 1$, the boundary term at $t = 0$ has to be kept [64].

and

$$b(0) = 0, \quad \frac{1}{N}\dot{b}(0) = \pm 1, \quad \frac{1}{N}\dot{a}(0) = 0, \tag{3.3.6}$$

where overdots now stand for derivatives with respect to t.

The time derivatives $\dot{a}$ and $\dot{b}$ are related to the (Euclidean) momenta conjugate to a and b:

$$p_a = -\frac{2\pi}{N}b\dot{b}, \quad p_b = -\frac{2\pi}{N}(a\dot{b} + b\dot{a}), \tag{3.3.7}$$

so these boundary conditions correspond to fixing $\{a, p_a, p_b\}$ or $\{b, p_a, p_b\}$ at $\mathcal{B}_0$. It is however inconsistent in quantum theory to fix a coordinate and its conjugate momentum. Hence the best one can do is to impose two out of the three conditions, for example

$$a(0) = 0, \quad p_b(0) = \mp 2\pi b(0) \tag{3.3.8}$$

or

$$b(0) = 0, \quad p_a(0) = 0. \tag{3.3.9}$$

HL note that if classical field equations hold, then with either of these choices all three conditions in (4.5.1) or (4.5.2) are satisfied. One can therefore expect that in the semiclassical regime the path integral will be dominated by regular geometries. Since we are interested in dimensional reduction of KS model with the S^2 part integrated out, we will focus on the boundary conditions (6.3.14), which correspond to fixing a and $\dot{a}$ on $\mathcal{B}_0$.

HL suggest that a better choice of variables, suitable for the boundary conditions (6.3.14), would be

$$A = 2\pi b^2, \quad B = 2\pi ab \tag{3.3.10}$$

with the conjugate momenta

$$P_A = -\frac{\dot{a}}{2N}, \quad P_B = -\frac{\dot{b}}{N}. \tag{3.3.11}$$

The boundary conditions (6.3.14) then take the form

$$B' = 0, \quad {P_A}' = \mp\frac{1}{2}, \tag{3.3.12}$$

where primes indicate the values at $t = 0$.

The HH wave function can now be expressed as [64]

$$\Psi_{NB}(A, B) = G(A, B|{P_A}', B') = \int dN \int \mathcal{D}Q^\alpha \mathcal{D}P_\alpha \exp(-S_E), \tag{3.3.13}$$

where the path integral is taken over histories with fixed $\{A, B\}$ and $\{{P_A}', B'\}$. Unlike the case of fixed initial values a' and b', this path integral cannot be evaluated exactly. We therefore use the WKB method to express Ψ_{HH} approximately as

$$\Psi_{HH}(Q^\alpha) = \int_C \mu\left(Q^\alpha, Z^\beta, N\right) \exp\left[-S_E(Q^\alpha; N|Z^\beta)\right] dN, \tag{3.3.14}$$

where $Q^\alpha = \{A, B\}$, $Z^\beta = \{{P_A}', B'\}$, μ is the semiclassical prefactor of the propagator and

$$S_E = \pi\left[\frac{H^2}{3}N(b^2 + bb' + {b'}^2) - N - \frac{1}{N}(b - b')\left(a^2 b - \frac{{B'}^2}{b'}\right) + 2{b'}^2{P_A}' + 2B'P_{B'}\right] \tag{3.3.15}$$

is the Euclidean action evaluated on a history satisfying the boundary conditions and the second order equations (3.2.3),(3.2.4) for a and b, but not the constraint equation (4.2.14). Note that the last term in (4.5.8) can be neglected since it does not contribute to the path integral and the semiclassical prefactor. The integration contour C in (3.3.14) is generally complex; we shall discuss the choice of this contour in Sec.4.4. The calculation of the prefactor is discussed in Sec. 4.3.

HL discussed the calculation of the HH wave functions for KS model only for the case of a vanishing cosmological constant, $H = 0$. Eqs.(3.3.14),(4.5.8) apply for arbitrary H, but from this point on we cannot directly use the results of HL and will have to extend their analysis to $H > 0$.

The initial value b' in Eq.(4.5.8) has to be expressed in terms of the boundary values A, B (or a, b), $B', {P_A}'$, and the lapse N. This can be done using the solutions $\bar{a}(\tau), \bar{b}(\tau)$ of the second order field equations (3.2.3),(3.2.4) (but not of the constraint equation). HL give these solutions in terms of the time variable τ, which is related to t as $d\tau = a(t)dt$:

$$\bar{b}(\tau) = (b - b')\tau + b' \tag{3.3.16}$$

$$\bar{a}^2(\tau)\bar{b}(\tau) = -\frac{H^2N^2}{3}(b - b')\tau^3 - H^2N^2b'\tau^2 + \left[a^2b - {a'}^2b' + \frac{H^2N^2}{3}(b + 2b')\right]\tau + {a'}^2b'. \tag{3.3.17}$$

Expressed in terms of τ, the boundary condition $(1/N)(da/dt) = \pm 1$ takes the form

$$\frac{\bar{a}}{N}\frac{d\bar{a}}{d\tau}(\tau = 0) = \mp 2{P_A}' = \pm 1. \tag{3.3.18}$$

To implement this boundary condition, we differentiate Eq.(6.4.13) with respect to τ and take

the limit $\tau \to 0$. This gives (after dividing by ${b'}^2$)

$$\frac{4N{P_A}'}{b}b' = -a^2 + \frac{{B'}^2}{{b'}^2} - \frac{H^2N^2}{3b}(b + 2b'). \tag{3.3.19}$$

where we have used $a' = B'/b'$.

We now have to solve Eq.(3.3.19) for b', substitute the result into the action (4.5.8), and use it to evaluate S_E and the pre-factor in (3.3.14) with the values of P'_A and B' specified by the boundary conditions (3.3.12). This calculation is significantly simplified if we note that the solution of Eq.(3.3.19) minimizes the action (with our boundary conditions), and thus $\partial S_E/\partial b' = 0$. It follows that when calculating the derivative of S_E with respect to B' in the determinantal prefactor in (3.3.14), we only need to account for an explicit dependence of S_E on this variable and can disregard the dependence through b'. This means that we can substitute the boundary value $B' = 0$ directly in Eq.(3.3.19). Then, instead of a cubic equation we get a linear equation for b', with the solution

$$b' = -\frac{b}{2N}\frac{a^2 + H^2N^2/3}{2{P_A}' + H^2N/3}. \tag{3.3.20}$$

Substituting this in the action (4.5.8) we find

$$S_E = \frac{\pi N}{3}(H^2b^2 - 3) - \frac{\pi}{N}a^2b^2 - \frac{\pi b^2}{4N^2}\frac{\left(a^2 + \frac{H^2N^2}{3}\right)^2}{2P'_A + \frac{H^2N}{3}} - \frac{\pi {B'}^2}{N}\frac{(a^2 + H^2N^2 + 4NP'_A)}{a^2 + H^2N^2/3}. \tag{3.3.21}$$

where we have not substituted the boundary values ${P_A}'$, B' yet, in order to calculate the prefactor.

3.3.2 Saddle points

Without making any approximations for the action, the saddle points cannot be found in closed form. Since we will be mostly interested in the regime where $b \approx H^{-1}$, we will first find the saddles for $b = H^{-1}$ and then treat deviations from these points as small perturbations.

We also have to decide on the choice of sign in the boundary condition (3.3.12) for P'_A. Here we will follow HL and pick $P'_A = -1/2$. Their justification is that for this choice the final boundary $\mathcal{B}$ is to the "future" of the initial boundary $\mathcal{B}_0$. In fact, there is a stronger argument: it can be shown that choosing the opposite sign in (3.3.12) does not yield convergent contours for the HH wave function. Furthermore, the characteristic exponential factor $\exp(\pi/H^2)$ can only be retrieved with the choice $P'_A = -1/2$.

Thus, setting $b = H^{-1}$, $B' = 0$ and $P'_A = -1/2$ we have

$$S_{E0} = -\frac{2\pi N}{3} - \frac{\pi a^2}{H^2 N} - \frac{\pi \left(3a^2 + H^2 N^2\right)^2}{12 H^2 N^2 \left(H^2 N - 3\right)}, \tag{3.3.22}$$

where the extra subscript "0" indicates that the action is evaluated at $Hb = 1$. Note the singularities at $N = 0$ and $N = 3/H^2$.

For the following analysis it will be convenient to introduce the rescaled variables

$$u = H^2 a^2 \quad , \quad \tilde{N} = H^2 N \quad , \quad \tilde{S_E} = \frac{H^2 S_E}{\pi} \tag{3.3.23}$$

The rescaled action (3.3.22) is given by

$$\tilde{S}_{E0} = -\frac{2\tilde{N}}{3} - \frac{u}{\tilde{N}} - \frac{\left(3u + \tilde{N}^2\right)^2}{12\tilde{N}^2\left(\tilde{N} - 3\right)} \tag{3.3.24}$$

In order to evaluate the integral (3.3.14) using the method of steepest descent, we first determine the extrema of the action $\tilde{S}_{E0}$. These are given by

$$\frac{\partial \tilde{S_{E0}}}{\partial \tilde{N}} = 0. \tag{3.3.25}$$

The resulting equation is quintic in $\tilde{N}$:

$$\left(\tilde{N}^2 - 2\tilde{N} + u\right)\left(\tilde{N}^3 - 4\tilde{N}^2 - 3\tilde{N}u + 6u\right) = 0 \tag{3.3.26}$$

Its solutions are

$$\tilde{N}_{1,2} = 1 \pm \sqrt{1 - u} \tag{3.3.27}$$

$$\tilde{N}_3 = \frac{4}{3} + \frac{16 + 9u}{3A} + \frac{A}{3} \tag{3.3.28}$$

$$\tilde{N}_{4,5} = \frac{4}{3} - \frac{\left(1 \mp i\sqrt{3}\right)(16 + 9u)}{6A} - \frac{\left(1 \pm i\sqrt{3}\right)A}{6} \tag{3.3.29}$$

where the quantity A is given by

$$A = (64 - 27u + 9\sqrt{-128u - 39u^2 - 9u^3})^{1/3} \tag{3.3.30}$$

The solutions $3, 4, 5$ are expressed here in a rather complicated form. Taking a closer look at the quantity A we can express it in a more convenient way with the Euler representation of

complex numbers. After some straightforward calculations we arrive at

$$A = \sqrt{16+9u}\; e^{i\frac{\theta}{3}}, \tag{3.3.31}$$

where θ is given by

$$\theta = \arctan\left[\frac{9\sqrt{9u^3+39u^2+128u}}{64-27u}\right] \tag{3.3.32}$$

The saddles $\tilde{N}_{3,4,5}$ are then simplified to:

$$\tilde{N}_3 = \frac{4}{3} + \frac{2\sqrt{16+9u}}{3}\cos\frac{\theta}{3} \tag{3.3.33}$$

$$\tilde{N}_{4,5} = \frac{4}{3} - \frac{2\sqrt{16+9u}}{3}\cos\left[\frac{\theta \pm \pi}{3}\right] \tag{3.3.34}$$

It is clear that the saddles $3, 4, 5$ are always real. $\tilde{N}_1$ and $\tilde{N}_2$ are also real for $u \leq 1$, while for $u > 1$ they form a complex conjugate pair.

3.3.3 Prefactor

The semiclassical prefactor for the propagator is given by [118]

$$\mu = f^{-1/4}\sqrt{D}f'^{-1/4} \tag{3.3.35}$$

where f' and f are the determinants of the minisuperspace metric $f_{\mu\nu}$ evaluated at $t = 0$ and $t = 1$ respectively and D is the Van Vleck-Morette determinant [119][120]. In the representation $A = 2\pi b^2$ and $B = 2\pi ab$ the Hamiltonian for the KS model takes the form [64]

$$\mathcal{H} = -P_B^2 - \frac{4AP_AP_B}{B} + 1 - \frac{H^2}{2\pi}A = \frac{1}{2}f^{\mu\nu}P_\mu P_\nu + V \tag{3.3.36}$$

where $V = 1 - AH^2/(2\pi)$. Thus the minisuperspace metric and its determinant are

$$f_{\mu\nu} = \begin{pmatrix} \frac{B^2}{8A^2} & -\frac{B}{4A} \\ -\frac{B}{4A} & 0 \end{pmatrix}, \qquad f \propto \frac{B^2}{A^2} \tag{3.3.37}$$

The action (4.5.10) expressed in variables $\{A, B\}$ is given by

$$S_E = \frac{\pi N}{3}\left(\frac{AH^2}{2\pi} - 3\right) - \frac{B^2}{4N\pi} - \frac{A}{8N^2}\frac{\left(\frac{B^2}{2\pi A} + \frac{H^2N^2}{3}\right)^2}{2P_A' + \frac{H^2N}{3}} - \frac{\pi B'^2}{N}\left(\frac{\frac{B^2}{2\pi A} + H^2N^2 + 4NP_A'}{\frac{B^2}{2\pi A} + \frac{H^2N^2}{3}}\right) \tag{3.3.38}$$

and the Van Vleck-Morette determinant D can be calculated as

$$D \equiv \det\left[-\frac{\partial^2 S_E}{\partial Q^\alpha \partial Z^\beta}\right] = \frac{3BB'}{AN^2\left(H^2N + 6P_A'\right)}, \tag{3.3.39}$$

where, as before, $Q^\alpha = \{A, B\}$, $Z^\beta = \{P_A{}', B'\}$. Inserting the above relations in Eq.(3.3.35) for the prefactor and switching back to variables $\{a, b\}$, we obtain[3]

$$\mu\left(a, b, N\right) \propto \frac{b'}{N\sqrt{H^2N - 3}}. \tag{3.3.40}$$

where b' is a function of a, b, N and is given by Eq.(4.5.9) and we have now inserted the boundary value of $P_A' = -1/2$.

The prefactor in Eq.(4.5.22) introduces a branch cut, which we can choose to lie at $N > 3/H^2$ along the real axis. From the analysis that follows, we will see that the choice of a suitable contour will not be affected significantly by this branch cut.

3.3.4 Integration contours

One of the key issues that remains to be addressed is the choice of the integration contour over N in Eq.(3.3.14). No general prescription for this choice has yet been given. Integration over real or pure imaginary values of N yields divergent integrals, so one has to look for a non-trivial contour in the complex plane that would make the integral convergent. The consensus view appears to be that the contour C should satisfy the following three criteria (see, e.g., [60]). (1) C should not have ends: it must be either infinite or closed. This guarantees that Ψ_{HH} is a solution of the WDW equation (rather than a Green's function). (2) The HH wave function should be real. This can be achieved by choosing a contour which is symmetric with respect to the real N axis. This requirement can be thought of as an expression of the CPT invariance of the HH state [121]. (3) The wave function should predict a classical spacetime when the universe is large. This means that in the appropriate limit Ψ_{HH} should be a superposition of

[3]We note that there is an error in the expression (6.5) for the prefactor in Ref.[64]. We are grateful to Jorma Louko for a discussion of this point.

rapidly oscillating terms of the form e^{iS}, where S is the classical action. We shall adopt these criteria as the defining properties of Ψ_{HH}.

Let us first consider infinite contours. From Eq.(3.3.22) we find that $S_E \sim -3N/8$ for $|N| \to \infty$. It follows that the integral over N can be convergent only if the asymptotic directions of the contour are at $|\arg N| > \pi/2$. Some inequivalent choices are illustrated in Fig.6.3. These contours are symmetric with respect to the real axis, so they define a real wave function. We will first consider the contour B which crosses the real axis at $0 < N < 3$ and will comment on the other choices at the end of this section. Note that the contour B may almost coincide with the imaginary axis. It could cross the real axis at $N = +\epsilon$ and asymptote to $\arg N = \pm(\pi/2 + \epsilon')$, where $\epsilon, \epsilon' \to +0$.

The integration contour B can be turned into a closed contour by adding to it an infinite arc $|N| = \text{const} \to \infty$. The integral over the arc vanishes in the limit, so the original integral remains unchanged. The resulting contour can be distorted into a finite closed contour which encircles the singularity at $N = 0$ but does not encircle the singularity at $N = 3$. Thus the infinite contours of type B are equivalent to this kind of closed contours. Following the Picard-Lefschetz prescription,[4] the closed contour can now be distorted so that it passes through saddle points following the steepest descent and ascent lines, making the integral absolutely convergent. Let us first consider the case of $a > H^{-1}$. The saddle points for this case are shown in Fig.6.4. The steepest descent and ascent lines are defined by $\text{Im } S_E = \text{const}$. The lines passing through

[4]For a simple review of Picard-Lefschetz theory see, e.g., Ref. [65].

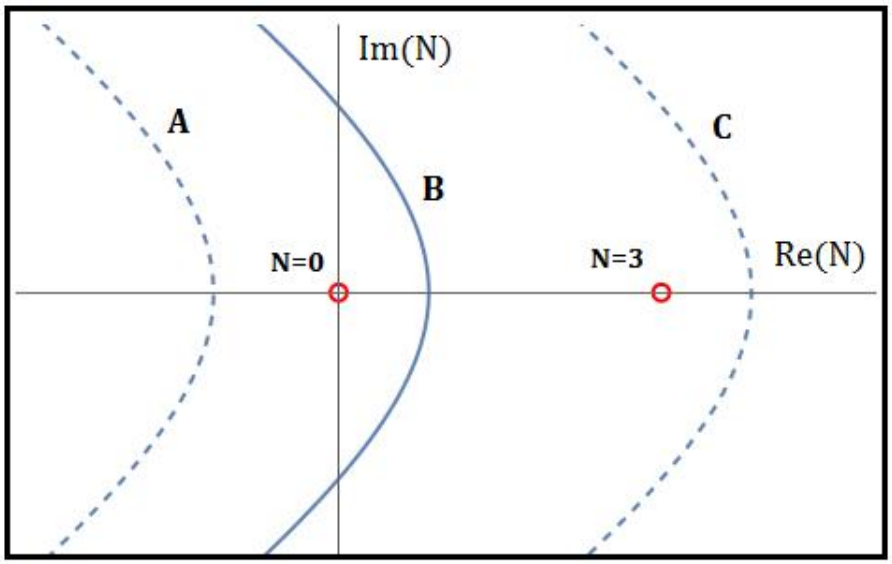

Figure 3.1: Examples of convergent infinite contours in the complex N plane. The singularities $N = \{0, 3\}$ are shown in circles.

the saddle points are also shown in the figure, with arrows indicating the direction in which $-\mathrm{Re}\ S_E$ is decreasing. The contour encircling the singularity at $N = 0$ can be distorted into the contour passing through the saddle points N_1, N_4, N_2 and N_5. This contour is dominated by the saddles at N_1 and N_2.

We now consider the case of $a < H^{-1}$, when all saddle points lie on the real axis. The steepest descent and ascent lines in this case are illustrated in Fig.6.5. The contour encircling $N = 0$ can now be deformed into the contour passing through N_4 and N_5. It is dominated by the saddle at N_4.

We finally comment on other possible choices of the integration contour. A contour of type A in Fig.1 crosses the real axis at $N < 0$. After it is closed by adding an infinite arc, this contour does not encircle any singularities, so it can be continuously shrunk to a point. The wave function defined by this contour is therefore identically zero.

Another possibility is to choose the branch cut to lie at $\tilde{N} < 3$ on the real axis and choose the contour that crosses the real axis at $\tilde{N} > 3$ (see contour C in Fig.1). For $a > H^{-1}$ such a contour can be deformed into a contour that runs along the steepest descent/ascent lines from N_3 to N_1, then takes a turn and goes to N_5, and from there runs above the branch cut along the real axis to $N \to -\infty$. This has to be supplemented by another half of the contour that runs symmetrically from N_3 through N_2 and N_5 to $-\infty$ in the lower half-plane. The resulting wave

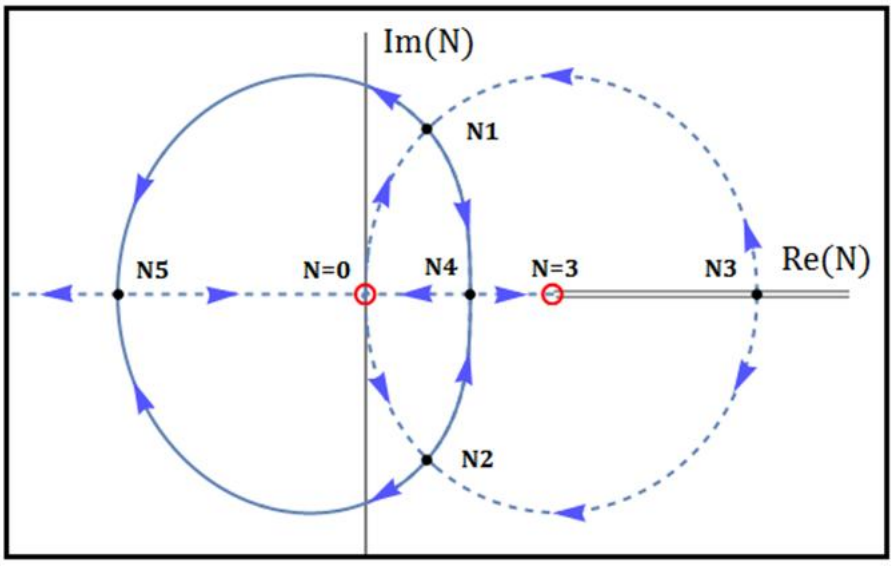

Figure 3.2: The steepest descent contours for $u > 1$ and $Hb = 1$. The arrowheads point to the direction where $Re(-\tilde{S}_E)$ decreases. The saddles $\tilde{N}_i$ are marked with solid dots and the singularities with circles. Note the branch cut at $\tilde{N} \in (3^+, +\infty)$. The HH contour corresponds to the solid curve encircling the singularity $N = 0$; it is dominated by saddles N_1, N_2.

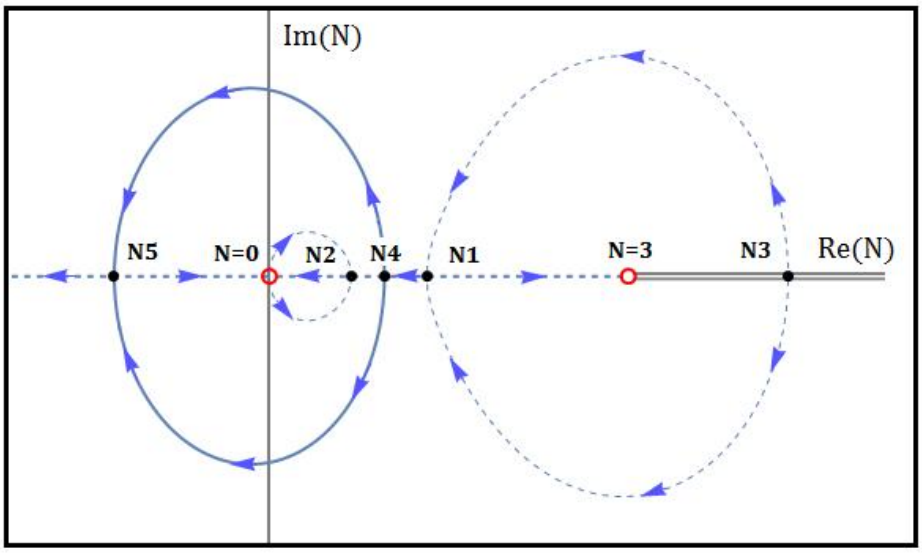

Figure 3.3: The steepest descent contours for $u < 1$ and $Hb = 1$. In this case, all the saddles are real. The HH contour corresponds to the solid curve encircling the singularity $N = 0$ and dominated by saddle N_4.

function is then non-oscillating, with the main contribution given by the real saddle point N_3. This is in conflict with the defining property (3) of the HH wave function. We thus conclude that the only acceptable choice of integration contour is an infinite contour of type B or equivalently a closed contour encircling the singularity at $N = 0$.

3.3.5 Perturbing the Saddle Points

To make a connection with JT gravity, we need to know the KS wave function for b very close but not equal to H^{-1}. The saddle points and the steepest descent/ascent lines will then be slightly different from those we found in the subsections B and D. For $a > H^{-1}$ we are interested in the complex saddle points $N_{1,2}$ which dominate the integral. Let us define the shift x of the saddle point $\tilde{N}_i$ as

$$\tilde{N} = \tilde{N}_i + x, \tag{3.3.41}$$

where $i = 1, 2$, $\tilde{N}_i$ are given by (4.5.25) and $|x| << 1$. We insert this into the action and expand to second order in x. This gives :

$$\tilde{S}_E \approx -1 \mp 2i(1 - Hb)\sqrt{u-1} - 2(1 - Hb)x + f(u)x^2 + O(x^3) \tag{3.3.42}$$

where the upper and lower signs are for N_1 and N_2 respectively and the function $f(u)$ is given in the Appendix.

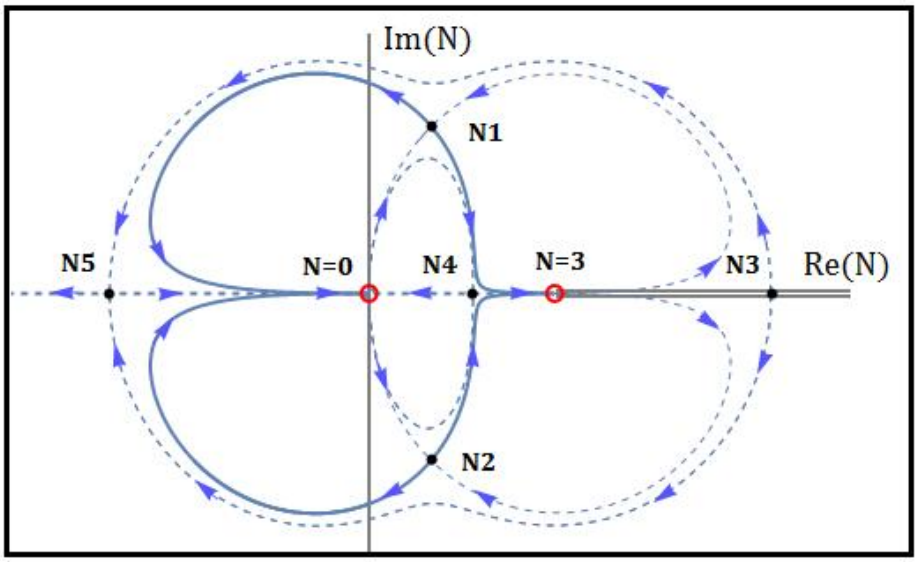

Figure 3.4: The perturbed steepest descent contours for $u > 1$ and $Hb > 1$. The HH contour does not pass through the saddles N_4 and N_5.

The action is extremized with

$$x = \frac{1 - Hb}{f(u)}. \tag{3.3.43}$$

Since x depends linearly on $(1 - Hb)$ the contribution of the x-dependent terms to the action is $\mathcal{O}[(1 - Hb)^2]$. Thus the action of the dominant saddle points is

$$S_E \approx -\frac{\pi}{H^2} \mp \frac{2i\pi}{H^2}(1 - Hb)\sqrt{H^2a^2 - 1} + \mathcal{O}[(1 - Hb)^2]. \tag{3.3.44}$$

The steepest descent/ascent lines can be calculated numerically for any values of a and b. For $Ha > 1$ the character of these lines changes when Hb is moved away from 1, even for an arbitrarily small amount. For $Hb > 1$, the steepest descent contour passing through N_1 follows nearly the same path as for $Hb = 1$, but short of reaching N_5 it makes a turn and runs along the real axis towards $N = 0$. Then it runs back, repeats the same path symmetrically in the lower half-plane and arrives at N_2. From there it runs towards N_4 following nearly the same path as for $Hb = 1$, but short of reaching N_4 it makes a turn and runs towards the singularity at $N = 3$. Finally it runs back symmetrically and returns to N_1. This contour is illustrated in Fig.3.4 . The only change compared to the original $Hb = 1$ contour is that small segments near N_4 and N_5 are now replaced by sharp spikes running towards the singularities and back. The integrals over the upper and lower halves of these spikes nearly cancel one another, so their combined contribution to the wave function is very small.

For $Hb < 1$ the situation is very similar, except now instead of shooting to the right the

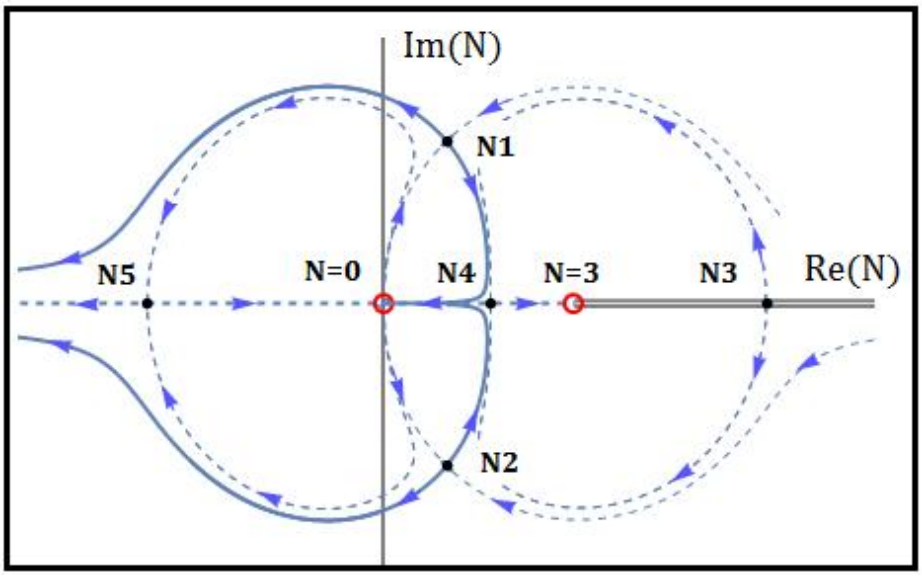

Figure 3.5: The perturbed steepest descent contours for $u > 1$ and $Hb < 1$. The HH contour does not pass through the saddles N_4 and N_5.

.

spikes shoot to the left. The spike originating near N_5 runs along the negative real axis to $-\infty$ and back, and the spike originating near N_4 runs to $N = 0$ and back (see Fig.3.5). As before, the contour is dominated by the saddles N_1 and N_2, with the spikes making a very small contribution.

For $Ha < 1$, small deviations of Hb from 1 do not change the character of the steepest descent lines. The contour is still dominated by the real saddle N_4, and the steepest descent line passing through this saddle also passes through N_5. At some critical value of $Hb > 1$ the saddles N_1 and N_4 merge, and at greater values they become a complex conjugate pair . A similar situation occurs for saddles N_2 and N_4 when $Hb < 1$. Generally, the saddle N_4 remains real in a range of $(Hb - 1)$ that depends on u. It can be shown that as u increases from 0 to 1, the range of $(Hb - 1)$ for which N_4 remain real shrinks from ~ 1 until it reaches zero at $u = 1$, where the saddles $N_{1,2,4}$ merge. For example, when $u \ll 1$ the contour behavior does not change qualitatively for $0 < Hb < \sqrt{3}$ and for $u = 0.9$ the range is $|1 - Hb| \sim 0.008$. It would be interesting to map the behavior of the contours and saddles for the full range of a and b, but we will not attempt this here.

3.3.6 The Hartle-Hawking wave function

We are now ready to calculate the semiclassical Hartle-Hawking wave function.

$Ha > 1$

For $Ha > 1$ we need to expand the action (3.3.22) up to quadratic order in $(N - N_i)$ at saddle points N_i $(i = 1, 2)$ and then do the Gaussian integrals. Up to an overall numerical factor, the corresponding contributions to the wave function are

$$\frac{b'(N_i)}{N_i\sqrt{3 - H^2 N_i}}\sqrt{\frac{1}{S_{NN}(N_i)}}e^{-S_E(N_i)}. \tag{3.3.45}$$

Here the factor $b'(N_i)/\left(N_i\sqrt{3 - H^2 N_i}\right)$ comes from Eq.(4.5.22), $S_E(N_i)$ from Eq.(4.5.30) and

$$S_{NN} = \frac{\partial^2 S_E}{(\partial N)^2}. \tag{3.3.46}$$

At $N = N_i$ we have

$$S_{NN}(N_{1,2}) = \frac{6\pi\left(H^2a^2 - 1\right)}{a^4H^2\left(H^2a^2 + 3\right)}\left[-2 \pm 2i\sqrt{H^2a^2 - 1} \pm iH^2a^2\sqrt{H^2a^2 - 1}\right] \tag{3.3.47}$$

and

$$b'(N_i)\left[N_i^2\left(3 - H^2N_i\right)S_{NN}(N_i)\right]^{-1/2} = \frac{H}{\sqrt{6\pi\left(H^2a^2 - 1\right)}}, \tag{3.3.48}$$

Combining the contributions of the two saddle points, we obtain an approximate semiclassical HH wave function. Up to an overall constant factor it is given by

$$\Psi_{HH}(Ha > 1) \propto \mathcal{A}\exp\left(\frac{\pi}{H^2}\right)\cos\left(\frac{2\pi}{H^2}(1 - Hb)\sqrt{H^2a^2 - 1}\right), \tag{3.3.49}$$

where

$$\mathcal{A} = \frac{1}{\sqrt{H^2a^2 - 1}}. \tag{3.3.50}$$

Note that we neglected corrections $\mathcal{O}(1 - Hb)$ in the prefactor, but kept them in the exponent, which includes a large factor H^{-2}. The WKB approximation is essentially an expansion in powers of H. It is easily verified that the wave function (3.3.49) satisfies the WDW equation to the leading order in H and $(Hb - 1)$.

As one might expect, Ψ_{HH} exhibits the characteristic WKB divergence at the turning point $a = 1/H$. This divergence is much milder than that in the IKTV solution. The WKB approximation breaks down near the turning point, and we expect the exact wave function to remain finite there.

$Ha < 1$

For $Ha < 1$ the integral over N is dominated by the saddle point N_4. This case is difficult to handle analytically, so we will only consider the limiting case $Ha \ll 1$. In this regime, we are able to go beyond the approximation $Hb \approx 1$, as long as the qualitative behavior of the contours and the respective saddles does not change (see section 4.5).

Let us first note that for $Ha \ll 1$ and $Hb \approx 1$, Eq.(3.3.34) gives

$$H^2 N_4 \approx \sqrt{\frac{3}{2}} Ha. \tag{3.3.51}$$

Let us further assume (to be verified shortly) that $H^2 N_4 = \mathcal{O}(Ha)$ in a wide range of $Hb \lesssim 1$. Then the action can be approximated by[5]

$$S_E \approx \frac{\pi N}{3}(H^2 b^2 - 3) - \frac{\pi}{N} a^2 b^2 \tag{3.3.52}$$

and the corresponding saddles are

$$N_{4,5} = \pm \frac{ab}{\sqrt{1 - H^2 b^2/3}}. \tag{3.3.53}$$

We note that Eq.(3.3.53) agrees with our assumption that $H^2 N_4 = \mathcal{O}(Ha)$ for $Hb \lesssim 1$, verifying that this assumption is consistent. Substituting (3.3.53) into the action we obtain

$$S_E \approx -\frac{2\pi ab}{\sqrt{3}} \sqrt{3 - H^2 b^2}. \tag{3.3.54}$$

The WKB prefactor in the regime $Ha \ll 1$ can be found along the same lines as for $Ha > 1$. To lowest order in Ha, it is proportional to $\sqrt{a}$. Thus, the wave function is given by

$$\Psi_{HH} \propto \sqrt{a} \exp\left(\frac{2\pi ab}{\sqrt{3}} \sqrt{3 - H^2 b^2} \right). \tag{3.3.55}$$

This approximation applies for $H \ll Ha \ll 1$, which is a wide range in the sub-Planckian regime $H \ll 1$. Also, we have to constrain the values of b to $Hb < \sqrt{3}$ in order for the saddles to remain real and the wavefunction to be non-oscillatory. (Note that our approximation breaks down at $Hb \approx \sqrt{3}$, where the lapse parameter N in Eq.(3.3.53) becomes large.)

Keeping the scale factor a fixed, the solution has a maximum at $Hb = \sqrt{3/2}$. This peak

[5]This can be seen from Eq.(A.1) for S_E in the Appendix by noticing that the first two terms in both of the big parentheses in that equation are $\mathcal{O}(Ha)$ while the last terms are $\mathcal{O}(H^2 a^2)$.

is not in the range $Hb \approx 1$ which is of most interest for dimensional reduction to JT. Note, however, that the maximum of the wave function (3.3.55) at a fixed $\tilde{a} = a\sqrt{Hb}$ is at $Hb = 1$. This is more relevant, since $\tilde{a}$ plays the role of the scale factor after dimensional reduction. A numerical WKB solution for Ψ_{HH} in the full range $a < 1/H$ with $Hb = 1$ is shown in Fig.A.1.

Finally, it can be verified that the wave function (3.3.55) satisfies the WDW equation to the leading order in H and that it grows exponentially with a, as expected.

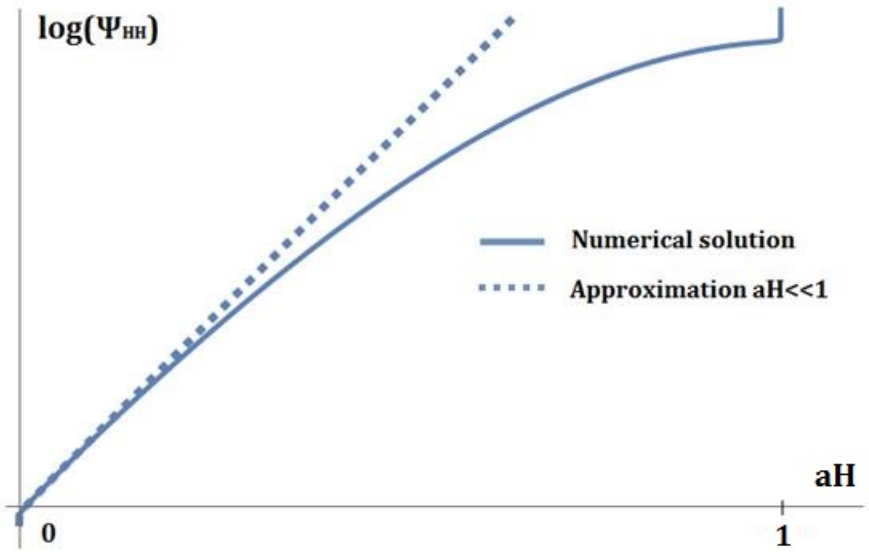

Figure 3.6: A graph of $(\log \Psi_{HH}, a)$ for $bH = 1$. A numerical WKB solution for the HH wavefunction is shown by the solid curve. It diverges abruptly at $aH = 1$, due to the WKB prefactor. The blue dashed line corresponds to the $aH << 1$ approximation. Note that both curves diverge to $-\infty$ at $a = 0$ due to the pre-exponential factor $\sqrt{a}$ in (3.3.55).

3.4 Probability distribution

Probability distributions in minisuperspace quantum cosmology can be expressed in terms of the conserved current density

$$j^{\alpha} = i\sqrt{-f} f^{\alpha\beta} \left(\Psi^* \partial_{\beta} \Psi - \Psi \partial_{\beta} \Psi^*\right), \tag{3.4.1}$$

$$\partial_{\alpha} j^{\alpha} = 0, \tag{3.4.2}$$

where $f^{\alpha\beta}$ is the minisuperspace metric and $f = \det(f_{\alpha\beta})$. In a d-dimensional minisuperspace one of the coordinates (or a combination of coordinates), call it T, can be designated as a "clock". Then the probability distribution for the other coordinates on surfaces of constant T

is given by

$$dP \propto j^{\alpha} d\Sigma_{\alpha}, \tag{3.4.3}$$

where $d\Sigma_{\alpha}$ is the $(d-1)$-dimensional surface element. If the clock variable T exhibits semi-classical behavior and its classical evolution is monotonic (which are the properties one can reasonably require from a good clock), then it can be shown that the probability defined by Eq.(3.4.3) is positive definite [71].

An obvious problem with the HH wave function is that it is real, so the current is identically zero. In the classically allowed range $Ha > 1$ this can be circumvented if we calculate the current using only the branch of the wave function describing expanding universes. Eq.(3.3.49) for Ψ_{HH} would then be replaced by

$$\Psi_{+}(Ha > 1) \propto \frac{1}{\sqrt{H^2a^2-1}} \exp\left[\frac{2\pi i}{H^2}(Hb-1)\sqrt{H^2a^2-1} + F(a)(Hb-1)^2 + \mathcal{O}\left((Hb-1)^3\right)\right], \tag{3.4.4}$$

where we have dropped the constant factor $\exp\left[\pi/H^2\right]$. We have also included a quadratic in $(Hb-1)$ correction in the exponential; we shall see that it plays an important role in the probability distribution. The coefficient function $F(a)$ is given in the Appendix.

In the KS model, a natural choice for the clock variable is the scale factor a (on the expanding branch of the wave function). Alternatively, we can use $c = a^2 b$, since we are working in the regime where $b \approx H^{-1} = \text{const}$. We shall adopt the latter choice, which is more convenient. It is also more appropriate for the dimensional reduction, since $c \propto \tilde{a}^2$, where $\tilde{a}$ is the scale factor of the JT model. Then the probability distribution for b, Eq.(3.4.3), takes the form[6]

$$dP \propto j^{c} db, \tag{3.4.5}$$

where

$$j^{c} \propto -i\left(\Psi^{*}\partial_{b}\Psi - \Psi\partial_{b}\Psi^{*}\right). \tag{3.4.6}$$

Substituting the wave function Ψ_{+} in j^{c} and setting $Hb = 1$ in the pre-exponential factor, we obtain

$$dP \propto \frac{db}{\sqrt{H^2a^2-1}} \exp\left[2(Hb-1)^2 \mathrm{Re}F(a)\right]. \tag{3.4.7}$$

[6]Note that with b and c used as minisuperspace coordinates, the metric is $f^{bc} = \text{const}$, $f^{bb} = f^{cc} = 0$, and its determinant is $f = -(f^{bc})^{-2} = \text{const}$

The real part of $F(a)$ is calculated in the Appendix:

$$\mathrm{Re}F(a) = -\frac{2\pi}{3H^2(H^2a^2-1)}. \tag{3.4.8}$$

Thus the probability distribution is

$$dP \propto \frac{db}{\sqrt{H^2a^2-1}} \exp\left[-\frac{4\pi(Hb-1)^2}{3H^2(H^2a^2-1)}\right]. \tag{3.4.9}$$

There are a few interesting things to note about this distribution. It is peaked at $b = H^{-1}$ with variance $\delta b \sim Ha$. Our approximations are accurate for $\delta b \ll H^{-1}$, that is for

$$H^{-1} \lesssim a \ll H^{-2}. \tag{3.4.10}$$

The distribution is obviously normalizable. Moreover, we note that

$$\int_{-\infty}^{\infty} \frac{dP}{db} db = \text{const}, \tag{3.4.11}$$

independent of a, so we can normalize the distribution to one. This is a direct consequence of conservation of j^α.

3.5 Conclusions

In this work, we have undertaken a detailed semiclassical analysis of the Hartle-Hawking (HH) wave function in the Kantowski-Sachs (KS) minisuperspace model with a positive cosmological constant. Building on and extending the approach of Halliwell and Louko, we have addressed several key challenges surrounding the definition and evaluation of the HH proposal in this context.

Our primary result is the construction of a well-defined semiclassical HH wave function that satisfies the Wheeler-DeWitt (WDW) equation and exhibits the expected physical properties. Specifically, we identified a unique integration contour in the complex lapse space, consistent with regularity at the no-boundary point, reality of the wave function, and classicality in the late universe. This contour, selected using Picard-Lefschetz theory, passes through a pair of complex conjugate saddle points in the classically allowed region and a single real saddle in the classically forbidden region. The resulting wave function exhibits the characteristic exponential enhancement $\exp(\pi/H^2)$ and correctly transitions from exponential to oscillatory behavior as

the scale factor crosses the classical turning point.

Importantly, we derived the HH wave function in the neighborhood of the Nariai geometry ($Hb = 1$), enabling a consistent comparison with the JT gravity limit via dimensional reduction. In this regime, the dominant saddle structure remains qualitatively unchanged for a wide range of b values around H^{-1}, allowing us to probe the transition amplitudes and wavefunction behavior near the quantum creation point. Our perturbative analysis of the saddles confirms the robustness of the contour prescription and highlights the suppressed contributions from subdominant directions.

We also constructed the associated conserved probability current and derived a peaked probability distribution for the spherical scale factor b, showing that it is sharply localized around the Nariai value with variance $\delta b \sim Ha$. This provides a natural probabilistic interpretation for the dimensional reduction and justifies the use of the JT limit in the corresponding 2D effective theory. The distribution is normalizable and exhibits the expected scaling behavior in the semiclassical regime $H^{-1} \lesssim a \ll H^{-2}$.

Our analysis also clarifies the relationship between the HH wave function and other proposals, such as the one derived by IKTV. We showed that the IKTV wave function corresponds to a transition amplitude from a Nariai-like initial condition and does not satisfy the WDW equation, highlighting its limitations as a genuine wave function of the universe. By contrast, our approach ensures consistency with the Hamiltonian constraint and the requirements of quantum cosmology.

In summary, our work provides a well-defined and physically consistent construction of the Hartle-Hawking wave function in a closed anisotropic universe with a positive cosmological constant. It clarifies several long-standing ambiguities in the literature and establishes a firm foundation for future investigations into the quantum origin of cosmological spacetimes.

Acknowledgments

We are grateful to Jose Blanco-Pillado, Jonathan Halliwell, Oliver Janssen, Jorma Louko, Juan Maldacena and Sandip Trivedi for very useful discussions and to Raymond Laflamme for sending us his 1986 thesis.

Chapter 4

The tunneling wavefunction in Kantowski-Sachs quantum cosmology

*Based on work with A. Vilenkin published in JCAP **08**, 069 (2022)*

We use a path-integral approach to study the tunneling wave function in quantum cosmology with spatial topology $S^1 \times S^2$ and positive cosmological constant (the Kantowski-Sachs model). If the initial scale factors of both S^1 and S^2 are set equal to zero, the wave function describes (semiclassically) a universe originating at a singularity. This may be interpreted as indicating that an $S^1 \times S^2$ universe cannot nucleate out of nothing in a non-singular way. Here we explore an alternative suggestion by Halliwell and Louko that creation from nothing corresponds in this model to setting the initial volume to zero. We find that the only acceptable version of this proposal is to fix the radius of S^1 to zero, supplementing this with the condition of smooth closure (absence of a conical singularity). The resulting wave function predicts an inflating universe of high anisotropy, which however becomes locally isotropic at late times. Unlike the de Sitter model, the total nucleation probability is not exponentially suppressed, unless a Gauss-Bonnet term is added to the action.

4.1 Motivation

In quantum cosmology the entire universe is treated quantum mechanically and is described by a wave function, rather than by a classical spacetime. The wave function $\Psi(g, \phi)$ is defined on the space of all 3-geometries (g) and matter field configurations (ϕ), called superspace. It can be found by solving the Wheeler-DeWitt (WDW) equation [54]

$$\mathcal{H}\Psi = 0, \tag{4.1.1}$$

where $\mathcal{H}$ is the Hamiltonian operator. Alternatively, one can consider the transition amplitude from the initial state (g', ϕ') to the final state (g, ϕ), which can be expressed as a path integral,

$$G(g, \phi | g', \phi') = \int_{(g', \phi')}^{(g, \phi)} \mathcal{D}g \; \mathcal{D}\phi \; e^{iS}, \tag{4.1.2}$$

where S is the action. In general, G is a Green's function of the WDW equation [69]. But if (g', ϕ') is at the boundary of superspace, then $G(g, \phi | g', \phi')$ is a solution of the WDW equation everywhere in the bulk of superspace, and the path integral (4.1.2) may be used to define a wave function of the universe.

The choice of the boundary conditions for the WDW equation and of the class of paths included in the path integral representation of Ψ has been a subject of ongoing debate. The most developed proposals in this regard are the Hartle-Hawking (HH) [66] and the tunneling [67, 103, 68] wave functions.[1] The intuition behind both of these proposals is that the universe originates 'out of nothing' in a nonsingular way. But despite a large amount of work, a consensus on the precise definition of these wave functions has not yet been reached.[2]

The two proposals have been thoroughly studied in the simple minisuperspace de Sitter model with S^3 spatial topology, where the only degree of freedom is the radius of the universe. A number of more complicated models with two or more degrees of freedom have also been considered. Among them is the Kantowski-Sachs (KS) model [110] which describes an anisotropic universe of spatial topology $S^1 \times S^2$ with different scale factors. We have recently presented a detailed analysis of the HH wave function in the KS model [123], and our goal in the present paper is to extend this analysis to the tunneling wave function.

We shall conclude this Introduction with some comments about prior work on this topic.[3]

[1] For early work closely related to the tunneling proposal, see Refs. [76, 77, 78, 79, 80].

[2] An interesting alternative is that the universe is in a mixed state and is described by a density matrix [122]

[3] For earlier work on KS quantum cosmology see [114, 124, 115, 125].

Conti and Hertog [117] considered the semiclassical wave function by studying complex Schwarzschild-de Sitter instantons of the model, imposing boundary conditions suitable for a smooth closure of the 4-geometry. An advantage of this approach is that it is straightforward to obtain approximate expressions for the saddles by algebraic means. On the other hand, it does not allow one to rigorously define a convergent path integral and select which of these saddles contribute to the wave function. Specifically, the divergence of the tunneling wave function found by CH can be attributed to the inclusion of saddle geometries that should not contribute.

Halliwell and Louko [64] used methods similar to Picard-Lefschetz theory in order to define a steepest descent contour that renders the path integral convergent. With this approach it is usually the case that not all extremum geometries contribute to the integral, since the lapse integration contour in the complex plane does not pass through all the saddles. In this paper we will follow this procedure, but we will have to extend the analysis to a non-vanishing cosmological constant, which makes the problem significantly more complicated.

This paper is organized as follows. In Section 2 we review the classical dynamics of the KS model and its canonical quantization. The definition of the tunneling wave function is discussed in Section 3, where we outline the approach based on the outgoing wave condition in superspace, as well as the path integral definition. In this paper we adopt the path integral approach and study alternative choices of boundary conditions for the path integral in Sections 4 and 5. In Sec.4 we fix the scale factors of S^1 and S^2 on both initial and final spacetime boundaries. The path integral in this case can be calculated exactly [64]. We find however that the resulting wave function is singular and thus is not an acceptable solution of the WDW equation.

Section 5 is the main part of this work. Here we investigate the choice of boundary conditions suggested by Halliwell and Louko [64]: we fix the two scale factors on the final boundary and require a smooth closure of the 4-geometry at the initial boundary. In this case the path integral cannot be computed exactly, so we employ the methods of Picard-Lefschetz theory in order to make the integral over the lapse N absolutely convergent. This is done by finding saddle points of the action in the complex plane and deforming the initial integration contour to a steepest descent path through the contributing saddles. The wave function is then found in the WKB approximation by carrying out the Gaussian integrals in the vicinity of the saddles. Since our analysis is approximate, we singled out three regimes of interest. Denoting the scale factors of S^1 and S^2 by a and b respectively and the cosmological constant by $\Lambda = H^2/3 \ll 1$ (in Planck units), we first looked into the case $b \approx 1/H$. This is the value at which the HH wave function gives a maximum probability [123]. We found that the tunneling wave function exhibits an opposite behavior: the probability grows away from this value. We continued by probing the

region of large S^2 and found that the wave function is peaked at high anisotropy: $a/b \lesssim H \ll 1$. We note that in this regime CH found a divergence in the tunneling solution which we do not observe. Finally, we obtained the wave function in the limit of $a \ll 1/H$. This wave function does not exhibit any exponential suppression as a function of b. Thus, the familiar picture of tunneling through a potential barrier does not hold in the KS model.

Our results are summarized and discussed in Section 6.

4.2 Kantowski-Sachs model

4.2.1 Classical dynamics

The Kantowski-Sachs (KS) model describing a homogeneous universe with spatial sections of $S^1 \times S^2$ topology is represented by a Lorentzian metric as

$$ds^2 = -N^2 dt^2 + a^2(t) dx^2 + b^2(t) d\Omega^2. \tag{4.2.1}$$

The Einstein-Hilbert action is then

$$S = -\pi \int dt \left[\frac{1}{N} \left(a\dot{b}^2 + 2b\dot{a}\dot{b} \right) + Na(H^2 b^2 - 1) \right] + S_b. \tag{4.2.2}$$

where the integration is carried out from the initial boundary $\mathcal{B}_0$ to the final boundary $\mathcal{B}$. The inclusion of the boundary term is needed if one chooses to impose Neumann conditions on one of the scale factors at $\mathcal{B}_0$ and is given by

$$S_b = -\left[\frac{\pi}{N} \frac{d}{dt}(ab^2) \right]_{\mathcal{B}_0}. \tag{4.2.3}$$

Varying the action with respect to the scale factors a, b we obtain the classical equations of motion in the gauge $N = 1$:

$$\ddot{a}b + a\ddot{b} + \dot{a}\dot{b} - H^2 ab = 0, \tag{4.2.4}$$

$$2b\ddot{b} + \dot{b}^2 + 1 - H^2 b^2 = 0, \tag{4.2.5}$$

and varying with respect to the lapse N we obtain the Hamiltonian constraint:

$$\dot{b}^2 + 2\frac{\dot{a}}{a}\dot{b}b + 1 - H^2 b^2 = 0. \tag{4.2.6}$$

Combining equations (4.2.5) and (4.2.6) we obtain

$$\dot{b} = \kappa a, \tag{4.2.7}$$

where κ is an integration constant. Plugging back into equation (4.2.5) and integrating we obtain

$$\kappa a = \dot{b} = \pm\sqrt{\frac{H^2 b^2}{3} - 1 + \frac{2M}{b}}, \tag{4.2.8}$$

where again M is an integration constant.

The above solution corresponds to a Euclidean Schwarzschild-deSitter black hole of mass M. In Euclidean time $t_E = it$ and in the gauge $N = 1$ the metric (4.2.1) becomes

$$ds_E^2 = \left(1 - \frac{2M}{b} - \frac{H^2 b^2}{3}\right) d\lambda^2 + \frac{db^2}{\left(1 - \frac{2M}{b} - \frac{H^2 b^2}{3}\right)} + b^2 d\Omega_2^2, \tag{4.2.9}$$

where $\lambda = \kappa x$. The black hole mass can be expressed in terms of the boundary data. Setting $a(t_E = 0) = a'$ and $b(t_E = 0) = b'$ we have

$$M = \frac{b'}{2}\left(1 - \frac{H^2 b'^2}{3} + \kappa^2 a'^2\right). \tag{4.2.10}$$

The limiting case in which $\kappa = 0$ corresponds to the Nariai solution [111] in which:

$$b = \frac{1}{H} \quad , \quad \ddot{a} = H^2 a \quad , \quad M = \frac{1}{3H} \ . \tag{4.2.11}$$

It describes a 4-geometry $dS_2 \times S^2$, where the characteristic radius of both dS_2 and S^2 is H^{-1}.

4.2.2 The WDW equation

The WDW equation of the KS model can be more conveniently realized by switching to time variable $d\tau = a(t)dt$. In this representation the metric is

$$ds^2 = -\frac{N^2}{a^2} d\tau^2 + a^2 dx^2 + b^2 d\Omega^2, \tag{4.2.12}$$

where N, a and b are functions of time τ, which we can choose to vary in the range $0 < \tau < 1$. After substituting this in the Lorentzian Einstein-Hilbert action and integrating over x and over

the angular variables, the action reduces to

$$S = -\pi \int_0^1 d\tau \left[\frac{\dot{b}\dot{c}}{N} + N(H^2 b^2 - 1) \right], \tag{4.2.13}$$

where we have introduced a new variable $c = a^2 b$.

The constraint equation is obtained by varying the action with respect to N:

$$\frac{\dot{b}\dot{c}}{N} - N(H^2 b^2 - 1) = 0, \tag{4.2.14}$$

where overdots stand for derivatives with respect to τ.

The momenta conjugate to the variables b and c are

$$p_b = -\pi \dot{c}/N, \qquad p_c = -\pi \dot{b}/N. \tag{4.2.15}$$

Using this in the constraint equation (4.2.14) and replacing $p_b \to -i\partial/\partial b$, $p_c \to -i\partial/\partial c$, we obtain the WDW equation

$$\pi \mathcal{H} \Psi = \left[\partial_b \partial_c + \pi^2 (H^2 b^2 - 1) \right] \Psi = 0. \tag{4.2.16}$$

This can be rewritten in the form of a Klein-Gordon (KG) equation,

$$\frac{1}{\sqrt{-f}} \partial_\alpha \left(\sqrt{-f} f^{\alpha\beta} \partial_\beta \Psi \right) + V\Psi = 0, \tag{4.2.17}$$

where the potential is $V = \pi^2(H^2 b^2 - 1)$, $f_{\alpha\beta}$ is the minisuperspace metric, and $f = \det(f_{\alpha\beta})$. With b and $c = a^2 b$ used as coordinates, the minisuperspace metric is given by $f_{bb} = f_{cc} = 0$, $f_{bc} = f_{cb} = 2$, and $\sqrt{-f} = 2$. The contravariant components of the metric are $f^{bb} = f^{cc} = 0$ and $f^{bc} = f^{cb} = 1/2$. The conserved current density corresponding to this KG equation is

$$j^\alpha = i\sqrt{-f} f^{\alpha\beta} (\Psi^* \partial_\beta \Psi - \Psi \partial_\beta \Psi^*). \tag{4.2.18}$$

It satisfies

$$\partial_\alpha j^\alpha = 0, \tag{4.2.19}$$

or

$$\frac{\partial j^b}{\partial b} + \frac{\partial j^c}{\partial c} = 0. \tag{4.2.20}$$

This suggests that

$$dP_b = j^c db \tag{4.2.21}$$

can be interpreted as the probability distribution for b at a fixed value of c; then c plays the role of a "clock" variable. Similarly,

$$dP_c = j^b dc \tag{4.2.22}$$

can be interpreted as the probability distribution for c at a fixed value of b, with b being the clock variable [71].

4.3 Tunneling wave function

In the simplest minisuperspace model, describing a de Sitter universe, the wave function depends only on the scale factor a and the superspace is a half-line, $0 \leq a < \infty$. The regular boundary in this case is at $a = 0$ and the singular boundary is at $a = \infty$. The general picture is that the probability flux is injected into superspace through the regular boundary and flows out through the singular boundary.

The origin of the universe in the de Sitter model can be pictured semiclassically as illustrated in Fig.6.3. The purple hyperboloid at the top is the classical de Sitter space and the blue hemisphere at the bottom is its Euclidean continuation. Such a continuation is necessary because Lorentzian geometries cannot close off at the bottom without a singularity. For this reason the regular boundary of superspace is specified in terms of Euclidean geometries.

The classical de Sitter model describes a universe contracting from infinite size, bouncing at the turnaround radius $a = 1/H_{dS}$, and re-expanding. (Here H_{dS} is the de Sitter expansion rate.) The tunneling wave function represents a universe that transits from $a = 0$ through the classically forbidden range $0 < a < 1/H_{dS}$ and expands from there. It is formally similar to a wave function describing quantum tunneling through a potential barrier.

It should be noted that the analogy between quantum cosmology and quantum tunneling often breaks down in models with more than one degree of freedom. Consider for example a model with coordinates q^α and conjugate momenta p_α, satisfying the Hamiltonian constraint $\mathcal{H} = K(q,p)+V(q) = 0$, where the kinetic energy K is a non-negative-definite quadratic form in momenta. Then classically we have $K \geq 0$, so the range $V(q) > 0$ is classically forbidden. On the other hand, in minisuperspace cosmology the quadratic form K is not generally positive-definite and not even bounded from below – not even at the classical level. Hence, in multi-dimensional models superspace cannot generally be divided into classically allowed and classically forbidden

regions.

In the case of de Sitter model the path integral is taken over the scale factor $a(t)$ with the boundary condition $a(0) = 0$. We note that this boundary condition, combined with the classical constraint equation $\dot{a}^2 + 1 = H_{dS}^2 a^2$ implies $\dot{a}(0) = \pm i$. After Euclidean continuation $t = i\tau$, this gives $da/d\tau = \pm 1$, which is the condition of a smooth closure (absence of a conical singularity) in the Euclidean geometry at $\tau = 0$. Thus the boundary condition $a = 0$ enforces the regularity condition at a semiclassical level. Alternatively, one could impose the regularity requirement $da/d\tau(0) = \pm 1$ as a boundary condition. Then the constraint equation would imply semiclassical closure, $a(0) = 0$. The Lorentzian path integral for the de Sitter model with both of these boundary conditions has been calculated in Refs.[62, 65]. In both cases the result coincides with the wave function obtained from the outgoing-wave boundary condition.

Turning now to the KS model, we first need to specify the class of histories included in the path integral. By analogy with the de Sitter model, one might consider histories originating from a configuration of vanishing 3-geometry, $a = b = 0$. However, it has been shown in Ref.[64] that Euclidean 4-geometries admitting $S^1 \times S^2$ slicing with radii a and b necessarily have a divergent 4-curvature in the limit $a, b \to 0$ and are therefore singular even at the semiclassical level.

The conclusion could be that a universe of topology $S^1 \times S^2$ cannot be created from nothing. In this paper we shall explore an alternative idea, suggested by Halliwell and Louko in Ref.[64]. We shall relax the condition $a = b = 0$ and require that only one of the two scale factors, a or b, is equal to zero. One possibility is then to fix the other scale factor at a nonzero value that is consistent with a non-singular geometry. Alternatively, we can leave the other scale factor unspecified and impose a regularity condition excluding conical singularities, as we mentioned for the de Sitter model. We shall discuss both of these approaches here.

4.4 Fixing initial scale factors

The transition amplitude from the initial state $\{a', b'\}$ to the final state $\{a, b\}$ in the KS model has been calculated by Halliwell and Louko in Ref.[64]. It is given by

$$G(a, b|a', b') = \int_0^\infty \frac{dN}{N} \exp\left[i\pi\left(\alpha N - \frac{\beta}{N}\right)\right], \tag{4.4.1}$$

where

$$\alpha = 1 - \frac{H^2}{3}(b^2 + bb' + b'^2), \quad \beta = (a^2 b - a'^2 b')(b - b'). \tag{4.4.2}$$

The contour of N-integration is generally complex; here we choose it to lie along the positive real axis, as required for the tunneling wave function.

The integral over N in (4.4.1) can be expressed in terms of Bessel functions [64]. The resulting wave function is

$$\Psi_T = -i\pi H_0^{(2)}(2\pi(-X)^{1/2}) \tag{4.4.3}$$

for $X < 0$ and

$$\Psi_T = 2K_0(2\pi(X)^{1/2}) \tag{4.4.4}$$

for $X > 0$, where $X = \alpha\beta$. If we set $a' = 0$, then

$$-X = a^2 b^2 \left(\frac{H^2 b^2}{3} - 1 + \frac{2M}{b}\right) \tag{4.4.5}$$

with M from Eq.(4.2.10), and if we set $b' = 0$, then $M = 0$ and X is independent of a',

$$-X = a^2 b^2 \left(\frac{H^2 b^2}{3} - 1\right). \tag{4.4.6}$$

We note that the same value of $M = 0$ is obtained for $a' = 0,\ b' = H^{-1}\sqrt{3}$; hence this choice of parameters gives the same wave function as $b' = 0$ with arbitrary a'.

Let us now consider the wave function with $M = 0$. For $Hb > \sqrt{3}$ it is given by

$$\Psi_T(Hb > \sqrt{3}) = -i\pi H_0^{(2)}\left(2\pi ab\sqrt{\frac{H^2 b^2}{3} - 1}\right). \tag{4.4.7}$$

To verify that this wave function satisfies the outgoing flux criterion, we first note its asymptotic form for large argument:

$$\Psi_T \propto \exp\left[-2i\pi ab\sqrt{\frac{H^2 b^2}{3} - 1}\right], \tag{4.4.8}$$

where we have ignored the pre-exponential factor. This gives a good approximation for the exponent, as long as b is not very close to $H^{-1}\sqrt{3}$. Acting with the momentum operators and using the gauge $N = 1$ we obtain:

$$\Pi_a \Psi_T = -i\frac{\partial \Psi_T}{\partial a} \longrightarrow \dot{b} = +\sqrt{\frac{H^2 b^2}{3} - 1} > 0 \tag{4.4.9}$$

$$\Pi_b \Psi_T = -i\frac{\partial \Psi_T}{\partial b} \longrightarrow \frac{\dot{a}}{a} = \frac{bH^2}{3\sqrt{\frac{H^2 b^2}{3} - 1}} > 0. \tag{4.4.10}$$

The solution of these equations for b and a is

$$b(t) = \frac{\sqrt{3}}{H}\cosh\left(\frac{Ht}{\sqrt{3}}\right), \quad a(t) = D\sinh\left(\frac{Ht}{\sqrt{3}}\right), \tag{4.4.11}$$

where $D > 0$ is a constant parameter.

In the semiclassical approximation, the wave function (4.4.7) describes a congruence of expanding classical trajectories (4.4.11) with different values of D. The trajectories start at $a' = 0$, $b' = H^{-1}\sqrt{3}$ and extend to $a, b \to \infty$. The trajectory with $D = H^{-1}\sqrt{3}$ describes a de Sitter space with expansion rate $H/\sqrt{3}$, while for other values of D the geometries (4.4.11) have conical singularities at $t = 0$. For large values of Ha and Hb all these geometries approach an expanding de Sitter space.

The wave function for $X > 0$ can be similarly analyzed. The resulting congruence of trajectories is a Euclidean continuation of (4.4.11):

$$b(\tau) = \frac{\sqrt{3}}{H}\cos\left(\frac{H\tau}{\sqrt{3}}\right), \quad a(\tau) = iD\sin\left(\frac{H\tau}{\sqrt{3}}\right), \tag{4.4.12}$$

where τ is the Euclidean time. It describes trajectories staring at $a' = 0$, $b' = H^{-1}\sqrt{3}$ and ending at $a = D$, $b = 0$. Once again, the trajectories with $D \neq H^{-1}\sqrt{3}$ have conical singularities at $\tau = 0$. We note that even though the wave function (4.4.7) is obtained for several choices of the initial values a', b', the congruence of trajectories that it describes corresponds to only one of these choices: $a' = 0,\ b' = H^{-1}\sqrt{3}$.

We can use the conserved current (4.2.18) to find the probability distribution for $c = a^2 b$ at a fixed value of b, with b playing the role of a clock. Using the Wronskian products of the Hankel functions, we find that the current is given by

$$j^\alpha = 4\pi\sqrt{-f}\, f^{\alpha\beta}\frac{\partial \ln(X)}{\partial y^\beta}, \tag{4.4.13}$$

where y^β are the superspace coordinates b, c and $X = 2\pi\sqrt{cb\left(\frac{H^2b^2}{3} - 1\right)}$. From Eq.(4.2.22) we obtain the probability distribution

$$dP_c \propto j^b dc \propto \frac{dc}{c}. \tag{4.4.14}$$

Since b is fixed, the distribution for a is $dP_a \propto da/a$. This distribution is not normalizable, but it admits a simple interpretation: values of a in each logarithmic interval are equally probable (at any given value of b).

The problem with the wave function (4.4.7) is that it exhibits a logarithmic singularity at $Hb = \sqrt{3}$. Hence it is not a solution of the WDW equation in the entire superspace, $0 \leq a, b < \infty$. Furthermore, the semiclassical geodesic congruence described by this wave function has conical singularities and thus does not correspond to a non-singular origin of the universe. The reason is that the boundary conditions that we used for initial scale factors do not enforce regular geometry even at the semiclassical level. Similar features are obtained for wave functions specified by a vanishing initial scale factor $a' = 0$ with an arbitrary value of b'. We therefore conclude that this class of wave functions is not a suitable choice for the tunneling wave function of the universe.

4.5 Smooth closure

We now consider the boundary condition of a smooth closure of Euclidean geometry with one of the scale factors vanishing. In the rest of the paper it will be more convenient to switch to Euclidean signature, by replacing $N \to -iN$.

It has been shown in [64] that in a classical Euclidean KS geometry a smooth closure can be achieved by one of the following two sets of boundary conditions:

$$a' = 0, \quad \frac{1}{N}\dot{a}' = \pm 1, \quad \frac{1}{N}\dot{b}' = 0, \tag{4.5.1}$$

$$b' = 0, \quad \frac{1}{N}\dot{b}' = \pm 1, \quad \frac{1}{N}\dot{a}' = 0, \tag{4.5.2}$$

where a prime indicates evaluation at the initial boundary and the Euclidean lapse parameter N is now real. The former set corresponds to a smooth closing of S^1, while the latter to a smooth closing of S^2.

Neither set of boundary conditions can be implemented in quantum theory. This becomes apparent if we introduce new variables

$$A = b^2, \quad B = ab \tag{4.5.3}$$

with conjugate momenta

$$P_A = -\frac{\dot{a}}{2N}, \quad P_B = -\frac{\dot{b}}{N}. \tag{4.5.4}$$

In this representation, the regularity conditions (4.5.1), (4.5.2) take the form

$$B' = 0, \quad {P_A}' = \mp\frac{1}{2}, \quad P'_B = 0 \tag{4.5.5}$$

and

$$A' = 0, \quad {P_A}' = 0, \quad P'_B = \mp 1. \tag{4.5.6}$$

Quantum mechanically, however, one is not allowed to impose these regularity conditions in their entirety, since that would violate the uncertainty principle: we cannot fix both a superspace variable and its conjugate momentum at the boundary. The best we can do is to enforce two of the three conditions. The third can then be inferred from the classical equations of motion, indicating that the semiclassical wave function would approximately describe a regular geometry. As we shall see in the next subsection, setting $b' = 0$ does not allow one to specify the momenta, since they appear in the action factored to b'. In fact, with $b' = 0$ one necessarily gets the same wave function (4.4.7) as we discussed in Sec 4, which we have concluded should be disqualified. We therefore focus on the boundary conditions

$$B' = 0, \quad {P_A}' = \mp\frac{1}{2}. \tag{4.5.7}$$

4.5.1 General formalism

The formalism for calculating the propagator with specified values of a and b at the future boundary $\mathcal{B}$ and boundary conditions (4.5.7) at the initial boundary $\mathcal{B}_0$ has been developed in [64, 123]. Here we will outline the approach for constructing the propagator; the details can be found in these references.

The fist step is to compute the action by integrating Eq.(4.2.2) while also evaluating the boundary term (4.2.3). After substituting $a' = 0$, the result is

$$S_E = \pi\left[\frac{H^2}{3}N(b^2 + bb' + {b'}^2) - N - \frac{a^2 b}{N}(b - b') + 2{b'}^2 {P_A}'\right]. \tag{4.5.8}$$

This is the action for $a(t)$ and $b(t)$ satisfying the classical equations of motion and boundary conditions, but not the constraint. The quantity b' in Eq.(4.5.8) has to be expressed in terms of the boundary data $\{a, b\}$, $\{P'_A\}$ and N using the equations of motion. This gives

$$b' = -\frac{b}{2N}\frac{a^2 + H^2N^2/3}{2{P_A}' + H^2N/3}. \tag{4.5.9}$$

Substituting this expression in the action (4.5.8) and simplifying, we have

$$S_E = \frac{\pi N}{3}(H^2b^2 - 3) - \frac{\pi}{N}a^2b^2 - \frac{\pi b^2}{4N^2}\frac{\left(a^2 + \frac{H^2N^2}{3}\right)^2}{2P'_A + \frac{H^2N}{3}} \tag{4.5.10}$$

The transition amplitude from the initial state $Z^\beta = \{B', P'_A\}$ to the final state $Q^\alpha = \{A, B\}$ can now be expressed as

$$\Psi_T(Q^\alpha) = \int_C \mu(Q^\alpha, Z^\beta, N) \exp\left[-S_E\left(Q^\alpha; N|Z^\beta\right)\right] dN \tag{4.5.11}$$

where μ is the semiclassical prefactor and C is a Lorentzian integration contour along the positive imaginary axis.

At this point the transition amplitude is not yet fully defined since we have not specified which of the values of $P'_A = \pm 1/2$ should be used. We make this choice by requiring that the integral (4.5.11) is convergent. Representing $N = iy$ with $0 < y < \infty$, let us examine the behavior of the integrand at $y \to 0$. In this limit the action (4.5.10) becomes

$$S_E \approx \left(\frac{\pi b^2 a^4}{8P'_A}\right)\frac{1}{y^2} \tag{4.5.12}$$

In order for the integral of $\exp(-S_E)$ to converge near the origin, the appropriate choice is $P'_A = +1/2$. This is opposite to the choice $P'_A = -1/2$ made in Refs.[123] for the Hartle-Hawking wave function.

In the limit $y \to +\infty$ the action becomes

$$S_E \approx i\pi(H^2b^2 - 4)\frac{y}{4}. \tag{4.5.13}$$

Thus the integral of $\exp(-S_E)$ will be convergent in the following cases:

$$\arg(y) \in (-\frac{\pi}{2}, 0) \quad , \quad Hb > 2 \tag{4.5.14}$$

or

$$\arg(y) \in (0, \frac{\pi}{2}) \quad , \quad Hb < 2. \tag{4.5.15}$$

So, depending on the sign of $(Hb - 2)$, the integration contour must be given an appropriate tilt in order to converge.

Unlike in the case of transition between fixed scale factors, the amplitude (4.5.11) cannot

be evaluated exactly. We shall therefore compute the integral following the methods of Picard-Lefschetz, namely distorting the integration contour C to a steepest descent/ascent path going through (at least) one of the saddle points of the action.

In order to simplify the analysis we will rescale our variables:

$$u = H^2 a^2 \quad , \quad v = H^2 b^2 \quad , \quad \tilde{N} = H^2 N \quad , \quad \tilde{S_E} = \frac{H^2 S_E}{\pi}. \tag{4.5.16}$$

In this representation the rescaled action becomes

$$\tilde{S}_E = \frac{\tilde{N}(v-3)}{3} - \frac{uv}{\tilde{N}} - \frac{v}{4\tilde{N}^2} \frac{\left(u + \frac{\tilde{N}^2}{3}\right)^2}{2P'_A + \frac{\tilde{N}}{3}}. \tag{4.5.17}$$

The saddle points of the action are found by solving the algebraic equation

$$\frac{\partial \tilde{S_E}}{\partial \tilde{N}} = 0. \tag{4.5.18}$$

This is a quintic equation for $\tilde{N}$ that cannot be solved exactly for all values of u, v, except in some limits.

Once the steepest descent contour has been specified, along with the contributing saddle points, the integral can be approximated by expanding the action about the extrema and carrying out a Gaussian approximation. Specifically, for each contributing saddle N_i the action can be expanded in the vicinity of N_i as

$$S_E(N - N_i) \approx S_E(N_i) + \frac{S_{NN}(N_i)}{2}(N - N_i)^2, \tag{4.5.19}$$

where $S_{NN} = \partial^2 S_E / \partial N^2$. Inserting in the integral (4.5.11) and integrating over $d(N - N_i)$ we can approximate the transition amplitude as

$$\Psi \propto \sum_i \frac{\mu(N_i)}{\sqrt{S_{NN}(N_i)}} \exp[-S_E(N_i)]. \tag{4.5.20}$$

Thus, the overall WKB pre-exponential factor for each contributing saddle will be given by

$$\tilde{\mu} = \frac{\mu}{\sqrt{S_{NN}}}. \tag{4.5.21}$$

The semiclassical prefactor μ for the propagator (4.5.11) has been derived in []. For the

choice of $P'_A = +1/2$ it is given by

$$\mu\,(a,b,N) \propto \frac{b'}{N\sqrt{H^2N+3}}, \tag{4.5.22}$$

where b' is the initial radius of S^2 defined in (4.5.9). The denominator of μ introduces a branch cut. For convenience, we can choose its orientation to be along the real axis at $H^2N < -3$, but as we will see this will not affect the calculation of the propagator, since any integration along the branch cut is exponentially suppressed.

4.5.2 S^2 of radius $Hb \approx 1$

The classical KS model has a Nariai solution (4.2.11), which describes a 4-geometry $dS_2 \times S^2$ with the radius of S^2 being $b = 1/H$. The dS_2 part of the geometry is a circle S^1 undergoing inflation with an expansion rate H. Our analysis of the Hartle-Hawking wave function Ψ_{HH} for this model [123] showed that it gives a probability distribution for b at fixed values of a which is peaked at $b = H^{-1}$. So this wave function predicts Nariai-type evolution as the most probable scenario. To compare this prediction with that of the tunneling wave function Ψ_T, we shall now study the behavior of Ψ_T in the regime $Hb \approx 1$.

Following the method of Ref.[123], we shall first find the saddle points for $Hb = 1$ and then consider small perturbations of those points. Using the rescaled variables (4.5.16) and setting $v = H^2b^2 = 1$, the action (4.5.17) becomes

$$\tilde{S}_{E0} = -\frac{2\tilde{N}}{3} - \frac{u}{\tilde{N}} - \frac{\left(3u+\tilde{N}^2\right)^2}{12\tilde{N}^2\left(\tilde{N}+3\right)}, \tag{4.5.23}$$

where the subscript 0 indicates zeroth order with respect to $(1-v)$. The saddle equation (4.5.18) for $v = 1$ is

$$\left(\tilde{N}^2+2\tilde{N}+u\right)\left(\tilde{N}^3+4\tilde{N}^2-3\tilde{N}u-6u\right) = 0. \tag{4.5.24}$$

It has two solutions,

$$\tilde{N}_{1,2} = -1 \pm \sqrt{1-u}, \tag{4.5.25}$$

which are real for $u \leq 1$ and form a complex conjugate pair for $u > 1$, along with three solutions $\tilde{N}_{3,4,5}$ which are real for all $u \geq 0$ and whose explicit form will not be needed.

The saddle points and steepest descent/ascent lines for $Ha > 1$ are shown in Fig.6.4 Our nearly Lorentzian contour can be distorted into a contour running from $N = 0$ along the arc

through the saddle N_1, all the way to N_5. Then it takes a turn and runs along the negative N axis to $N \to -\infty$. This contour is dominated by the saddle point at N_1.

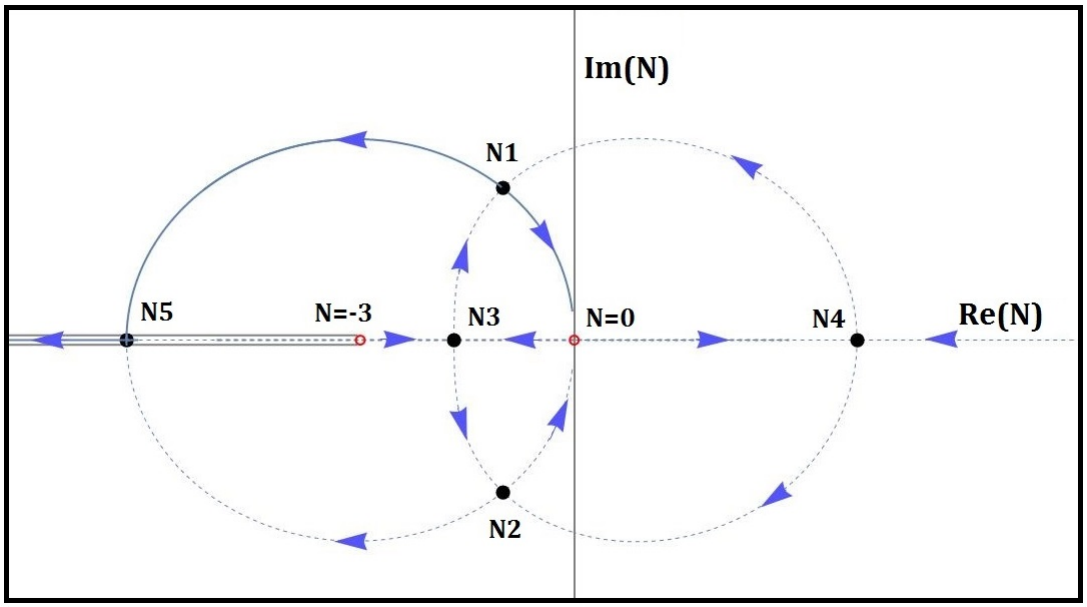

Figure 4.1: The steepest descent contours for $Ha > 1$ and $Hb = 1$. The arrowheads point to the direction where $Re(-\tilde{S}_E)$ decreases. The saddles $\tilde{N}_i$ are marked with solid dots and the singularities with circles. Note the branch cut at $\tilde{N} \in (-\infty, -3)$. Our nearly-Lorentzian contour corresponds to the solid curve starting from the singularity $N = 0$; it is dominated by the saddle N_1.

We now consider small deviations from $Hb = 1$. In the region $Ha > 1$ we have identified the saddle $\tilde{N}_1$ as the dominant one, so we will introduce a shift x defined by

$$\tilde{N} = \tilde{N}_1 + x, \tag{4.5.26}$$

where $\tilde{N}_1$ is given by (4.5.25) and $|x| << 1$. We insert this into the action (4.5.17) and expand to second order in x:

$$\tilde{S}_E \approx 1 - i(1-v)\sqrt{u-1} - (1-v)x + \frac{v}{f(u)}x^2 + O(x^3), \tag{4.5.27}$$

where

$$3f(u) = \left(2i + 2\sqrt{u-1} - iu - iu^2\right)(u-1)^{-3/2}. \tag{4.5.28}$$

The action is extremized with

$$x = \frac{1-v}{2v} f(u). \tag{4.5.29}$$

To lowest order in $(1 - Hb)$, we have $x \propto (1 - Hb)$, so the contribution of the x-dependent

terms to the action is $\mathcal{O}[(1-Hb)^2]$ and we can write

$$S_E \approx \frac{\pi}{H^2} - \frac{2i\pi}{H^2}(1-Hb)\sqrt{H^2a^2-1} + \mathcal{O}[(1-Hb)^2]. \tag{4.5.30}$$

The higher order correction term $\mathcal{O}[(1-Hb)^2]$ is proportional to $f(u)$ and will play an important role in the probability distribution that the tunneling wave function predicts.

We are now in a position to compute the WKB tunneling wave function in the region $Hb \approx 1$ and $Ha > 1$ following the prescription (4.5.20). The WKB prefactor $\tilde{\mu}$ defined in (4.5.21) can be computed for the saddle N_1 as:

$$\tilde{\mu} \propto \frac{1}{\sqrt{H^2a^2-1}} \tag{4.5.31}$$

Keeping only the lowest non-trivial orders of $(1-Hb)$ in the action (4.5.30), we arrive at an expression for the tunneling wave function:

$$\Psi_T(Ha>1) \propto \frac{1}{\sqrt{H^2a^2-1}} \exp\left(-\frac{\pi}{H^2}\right) \exp\left(\frac{2\pi i}{H^2}(1-Hb)\sqrt{H^2a^2-1}\right). \tag{4.5.32}$$

There are a few things to note about this solution. It exhibits a WKB-type divergence at the turning point $Ha = 1$, as expected. Additionally, the tunneling exponential suppression factor $\exp(-\pi/H^2)$ is present. This is a consequence of the choice $P'_A = +1/2$ for our boundary condition. Finally, it is easily verified that the wave function $\Psi_T(Ha > 1, Hb = 1)$ describes an outgoing wave at $Ha \gg 1$, and thus Ψ_T satisfies the outgoing wave boundary condition in the region $Hb \approx 1$.

In order to obtain a probability distribution for b in the region $Hb \approx 1$ we must include higher order corrections to the wave function (4.5.32). Making use of the perturbed action (4.5.27) and ignoring corrections to the prefactor, we arrive at

$$\Psi_T(Ha>1) \propto \frac{1}{\sqrt{H^2a^2-1}} \exp\left(-\frac{\pi}{H^2}\right) \exp\left[\frac{2\pi i}{H^2}(1-Hb)\sqrt{H^2a^2-1} + f(a)(Hb-1)^2\right], \tag{4.5.33}$$

where the function $f(a)$ is given by (4.5.28). Utilizing the methods of section 2.2, we calculate the current density:

$$dP_b \propto j^a db \propto \frac{db}{\sqrt{H^2a^2-1}} \exp\left[2(Hb-1)^2 \mathrm{Re} f(a)\right]. \tag{4.5.34}$$

This can be interpreted as the distribution for b on surfaces of constant a. The real part of $f(a)$

is given by:

$$\mathrm{Re}f(a) = \frac{2\pi}{3H^2(H^2a^2-1)}. \tag{4.5.35}$$

Thus the probability distribution can be written explicitly as:

$$dP \propto \frac{db}{\sqrt{H^2a^2-1}} \exp\left[\frac{4\pi(Hb-1)^2}{3H^2(H^2a^2-1)}\right]. \tag{4.5.36}$$

This distribution grows as we move away from $Hb = 1$, favoring large values of Hb. This is in contrast with the HH state for which the probability distribution is peaked at $Hb = 1$ [123].

4.5.3 Large S^2 region $Hb \gg 1$

Since the distribution (4.5.36) appears to favor large values of Hb, we shall now explore the behavior of the wave function at $Hb \gg 1$. In order to find the saddle points in this regime, we neglect the -3 term in the first parenthesis of (4.5.17). Then the saddle equation (4.5.18) can be factored:

$$\left(\tilde{N}^2 + 3u\right)\left(\tilde{N}^3 + 6\tilde{N}^2 + 12\tilde{N} + 3u\tilde{N} + 6u\right) = 0. \tag{4.5.37}$$

The corresponding solutions include two complex conjugate pairs and one real saddle. Two obvious solutions are

$$\tilde{N}_{1,2} = \pm i\sqrt{3u} \tag{4.5.38}$$

and we label the other pair as $\tilde{N}_{4,5}$ and the real saddle as $\tilde{N}_3$. We note that the numbering of saddle points here is not related to the one used in Section 5.2.

The steepest descent contours for this set of saddles are shown in Fig.6.5. A nearly Lorentzian contour can be distorted into a contour that follows the steepest ascent path from the origin $N = 0$ to the saddle N_1 and continues on the steepest descent path all the way to infinity in the first quadrant. The contour can be closed with an infinite arc at $N \to +i\infty$. The dominant contribution to the wave function comes from the saddle N_1.

To obtain a more accurate expression for the saddle point, we set $\tilde{N} = \tilde{N}_1 + x$ with $\tilde{N}_1$ from (4.5.38) and $x \ll \tilde{N}_1$. We then substitute it in the action (4.5.17), without neglecting the -3 term and expand the action to second order in x:

$$\tilde{S}_E \approx \frac{i\sqrt{u}(2v-3)}{\sqrt{3}} - x - \frac{vx^2}{3(u - i\sqrt{3u})} + \mathcal{O}(x^3). \tag{4.5.39}$$

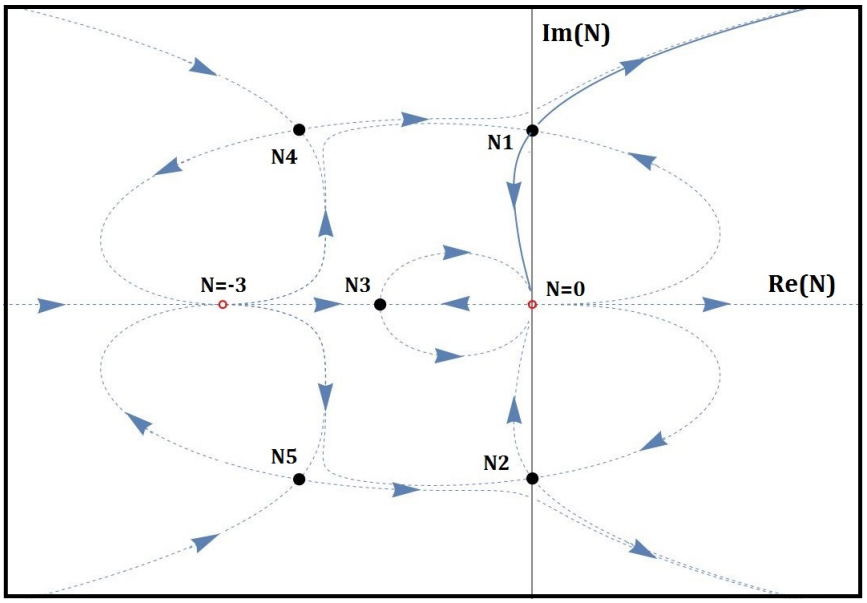

Figure 4.2: The steepest descent contours for $Hb \gg 1$. The tunneling contour corresponds to the solid curve starting from the singularity $N = 0$ and dominated by saddle N_1.

Extremizing with respect to x we find

$$x = \frac{3(i\sqrt{3u} - u)}{2v}. \tag{4.5.40}$$

This approximation is valid in the region of superspace where $v \gg 1$ and $u \ll v^2$ in order for the condition $\tilde{N}_1 \gg x$ to be satisfied. The x-dependent terms in the action introduce corrections $\mathcal{O}(v^{-1})$. Switching back to variables a and b, the perturbed action can be expressed as

$$S_E \approx \frac{2i\pi ab^2 H}{\sqrt{3}} - \frac{\sqrt{3}i\pi a}{H} - \frac{3\sqrt{3}i\pi a}{4H^3b^2} + \frac{3\pi a^2}{4H^2b^2} + \mathcal{O}\left(\frac{1}{H^3b^3}\right). \tag{4.5.41}$$

As with the case of $Hb \approx 1$, the higher order correction terms will be important for obtaining the probability distribution that the tunneling wave function predicts.

To lowest order in $(Hb)^{-1}$ the prefactor of the WKB wave function is:

$$\tilde{\mu} \propto \frac{\sqrt{a}}{b^2} e^{i\frac{\pi}{4}}. \tag{4.5.42}$$

Thus to the leading order of WKB approximation the tunneling wave function is given by

$$\Psi_T(Hb \gg 1) \propto \frac{\sqrt{a}}{b^2} \exp\left[-\frac{2i\pi ab^2 H}{\sqrt{3}}\right], \tag{4.5.43}$$

where we have kept only the dominant contribution in $Hb \gg 1$. It is straightforward to show

that the above solution describes expanding asymptotically de Sitter universes satisfying

$$\dot{b}/b \approx \dot{a}/a \approx H/\sqrt{3}, \tag{4.5.44}$$

just as in the case of fixed initial scale factors. Thus the outgoing wave criterion is satisfied.

To find the probability distribution for the scale factors, we have to include higher order corrections to the action, as given by Eq.(4.5.41). Ignoring corrections to the prefactor, we have

$$\Psi_T(Hb \gg 1) \propto \frac{\sqrt{a}}{b^2} \exp\left[-\frac{2i\pi a b^2 H}{\sqrt{3}} + \frac{\sqrt{3}i\pi a}{H} + \frac{3\sqrt{3}i\pi a}{4H^3 b^2} - \frac{3\pi a^2}{4H^2 b^2}.\right] \tag{4.5.45}$$

Noticing that the first three terms are the expansion of a square root, we can tidy this result to

$$\Psi_T(Hb \gg 1) \propto \frac{\sqrt{a}}{b^2} \exp\left[-2i\pi a b\sqrt{\frac{H^2 b^2}{3} - 1} - \frac{3\pi a^2}{4H^2 b^2}\right], \tag{4.5.46}$$

which is valid up to order $(Hb)^{-2}$. This wave function has the same asymptotic form as the transition amplitude (4.4.8) that we obtained for fixed initial scale factors, the only difference being its amplitude, which is controlled by the last term in the bracket. We will show that this term is responsible for the predictions of the tunneling wave function.

Following the formalism of Section 2.2 we calculate the probability current on surfaces of constant a. The calculation is simplified if we use the compact form (4.5.46), but take the limit $Hb \gg 1$ in the final step. The resulting expression is

$$dP \propto \frac{a^2}{b^3} \exp\left[-\frac{3\pi a^2}{2H^2 b^2}\right] db, \tag{4.5.47}$$

which is valid to lowest order in $(Hb)^{-1}$. Introducing a new variable l which characterizes the relative size of S^1 and S^2,

$$l = \frac{a}{b}, \tag{4.5.48}$$

we can express (4.5.47) as a distribution for l^2:

$$dP \propto \exp\left[-\frac{3\pi l^2}{2H^2}\right] dl^2. \tag{4.5.49}$$

This is a normalizable distribution with the average value

$$\bar{l}^2 = \frac{2H^2}{3\pi}. \tag{4.5.50}$$

Thus, in the regime of large a and b the tunneling wave function predicts an ensemble of classical de Sitter-like universes (4.5.44) with $a/b \lesssim H \ll 1$. This is in contrast with the HH state which gives a distribution peaked at the Nariai solution (4.2.11).

4.5.4 Small S^1 region $Ha \ll 1$

In the KS model there is no clear distinction between classically allowed and forbidden regions, except when $Hb \approx 1$. In this part of superspace the point $Ha = 1$ divides the classical and quantum regimes. On the contrary, the classical universes (4.4.11) do not have a well defined bounce point since $\dot{a}$ and $\dot{b}$ do not vanish simultaneously. Thus, we do not expect the wave function to bear much resemblance to the usual tunneling picture established in quantum cosmology. A related reason, mentioned in Sec.3, is that the WDW eq. is a hyperbolic equation, so the kinetic terms in the WDW operator have opposite signs. In this subsection we will try to obtain some insight into the behavior of the tunneling wave function close to the superspace boundary at $a = 0$, without assuming b to be small.

We are interested in finding the saddles in the region $u \ll 1$. Setting $u = 0$ in the action (4.5.17) and solving for the saddles through (4.5.18) we obtain

$$N_{1,2} \approx -3 \pm \sqrt{\frac{3v}{4-v}} \tag{4.5.51}$$

where we have dropped the tildes. This approximation is valid as long as $N^2 \gg 3u$ and v is not too close to 3. The first constraint justifies setting $u = 0$ in the parenthesis of the third term in the action. The second constraint is imposed so that the first term in the action is larger than the second, which justifies dropping it for $u \ll 1$.

The rest of the saddles can be approximately found by neglecting the third term in the action (4.5.17). Solving for the saddles yields

$$N_{3,4} \approx \pm\sqrt{\frac{3uv}{3-v}}. \tag{4.5.52}$$

This approximation is valid everywhere in the region $u \ll v$, apart from values of v that approach $v \approx 3$, for which N becomes large.

Finally, in order to find the 5th saddle we will use the insight obtained from numerical results. The 5 saddles in the region $u \ll 1$ and $v \sim 1$ have the following characteristics. Two of them are $\mathcal{O}(1)$, the other two are $\mathcal{O}(\sqrt{u})$, while the 5th is $\mathcal{O}(u)$. In fact, we observe that when

v is not too small, the 5th saddle is given approximately by

$$N_5 \approx -\frac{u}{2}, \tag{4.5.53}$$

which is in agreement with the lowest order expansion for $\tilde{N}_1$ given by Eq.(4.5.25). It is reassuring that all our saddle points can be matched in the appropriate limits in the different regions of KS superspace.

Overall, we expect the above saddles to be valid when $u \ll 1$, $u \ll v$, $v \neq \{3, 4\}$. We must also note that a consequence of these restrictions is that b is not allowed to approach zero.

The analytic expressions for the saddles in the region $u \ll 1$ suggest that there exist three qualitatively different steepest descent contour configurations depending on the value of v. In this subsection we are mostly interested in investigating the behavior of the wave function at small overall volume, so we will focus on the region $u \ll 1$ and $v < 3$.

In this case all five saddles are placed on the real-N axis. The steepest descent contours are similar to the ones in Fig.A.1. The only difference is that when $u \ll 1$, the loop surrounding the singularity $N = 0$ and the loop passing through $N = 0$ are shrunk to a very small size. These loops are defined by the saddles $\mathcal{O}(\sqrt{u})$ and $\mathcal{O}(u)$ respectively, $N_{3,4}$ and N_5. The loop encircling the singularity $N = -3$ does not shrink, since it is defined by the saddles of zero order in u, $N_{1,2}$.

The steepest descent/ascent lines for $u \ll 1$ and $v < 3$ are illustrated in Fig.A.1 . In this case the nearly Lorentzian contour can be distorted into a contour running from $N = 0$ along the upper arc to the saddle N_5, then along the real axis through the saddle N_4 until the saddle N_1. At that point it takes a turn and follows the upper arc to N_2, and runs from there to $N \to -\infty$. This contour is dominated by the saddle point N_4.

The WKB wave function corresponding to this saddle can be found along the same lines as previously demonstrated:

$$\Psi_T(Ha \ll 1, Hb < \sqrt{3}) \propto \exp\left(-2\pi ab\sqrt{1 - \frac{H^2b^2}{3}}\right), \tag{4.5.54}$$

where we have omitted the pre-exponential factor. This expression is valid in the region of superspace where $Ha \ll 1$ and $Ha \ll Hb \neq \sqrt{3}$. We notice that for a =const, Ψ_T is a decreasing function of Hb until it reaches a minimum at $Hb = \sqrt{3/2}$. For larger values of Hb the wave function increases until it approaches $Hb \approx \sqrt{3}$ where our approximation breaks down.

In the case of $4 > v > 3$, the saddles $N_{1,2}$ become a complex conjugate pair, while the

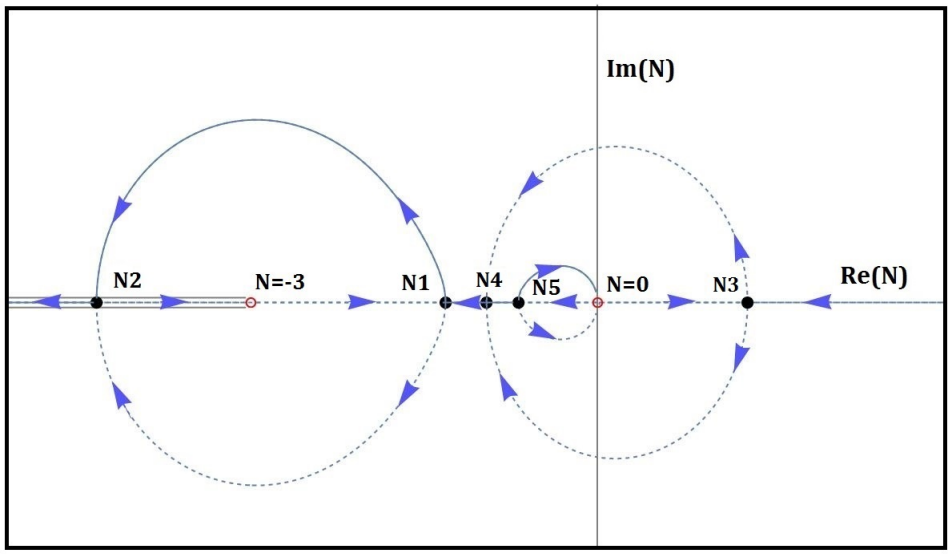

Figure 4.3: The steepest descent contours for $Ha \ll Hb < \sqrt{3}$. In this case, all the saddles are real. The tunneling contour corresponds to the solid curve starting from the singularity $N = 0$ and dominated by saddle N_4.

rest of the saddles remain real. Steepest descent analysis shows that the path integral receives dominant contributions from the saddles N_1 and N_5. Thus this region can be thought of as a transition from a fully quantum regime $v < 3$ to a hybrid one, in which classical trajectories do penetrate, however they are accompanied by Euclidean components.

Finally, the case for which $u \ll 1$, $v > 4$ is qualitatively similar to the region $v \gg 1$ discussed in section 5.3. So as long as $u \ll v$ the character of the steepest descent contours will not change and we are able to define a nearly-Lorentzian contour picking a contribution from the saddle N_1 as defined in Sec. 5.3 The WKB wavefunction will then be approximatelly given by the analytic continuation of (4.5.54) to $Hb > \sqrt{3}$ and will be valid for as long as $a \ll b$.

Overall, the behavior of Ψ_T that we have found is not in line with the familiar quantum tunneling through a barrier. We note especially that the nucleation of a universe with $b \gg a$ is not exponentially suppressed. This can be seen from

$$\left| \frac{\Psi_T(Hb \gg Ha \gg 1)}{\Psi_T(Ha \ll Hb < \sqrt{3})} \right| \sim 1. \tag{4.5.55}$$

On the other hand, exponential suppression is present in the narrow region $Hb \approx 1$, where there is a clear bounce point at $Ha = 1$ and

$$\left| \frac{\Psi_T(Ha > 1)}{\Psi_T(a \approx 0)} \right| \approx \exp(-\frac{\pi}{H^2}) \ll 1. \tag{4.5.56}$$

4.5.5 Total nucleation probability

The total nucleation probability of an $S^1 \times S^2$ universe can be found by integrating the distribution (4.5.49) over l^2. We obtain

$$P \propto H^2. \tag{4.5.57}$$

As in the de Sitter model, this probability is maximized at large values of H. But the dependence on H in (4.5.57) is a power law, while in de Sitter model it is exponential [103],

$$P_{dS} \sim \exp\left(-\frac{3\pi}{H^2}\right). \tag{4.5.58}$$

If one adopts a minisuperspace framework that allows both $S^1 \times S^2$ and S^3 topologies, then Eqs.(4.5.57),(4.5.58) suggest that for $H \ll 1$ nucleation of $S^1 \times S^2$ universes is exponentially favored. However, if different topologies are allowed, one can also consider adding a topological Gauss-Bonnet term to the action,

$$S_{GB} = \frac{\alpha}{16\pi}\int d^4x\sqrt{-g}\left(R_{\mu\nu\sigma\tau}R^{\mu\nu\sigma\tau} - 4R_{\mu\nu}R^{\mu\nu} + R^2\right) + S_{boundary}, \tag{4.5.59}$$

where α is a constant of dimension (length)^2 and $S_{boundary}$ is a boundary term which generalizes the Gibbons-Hawking term [126]. The addition of this term is necessary to make the boundary value problem well defined.

In $(3+1)$ dimensions the variation of the integrand in Eq.(4.5.59) is a total derivative, so the Gauss-Bonnet term has no effect on dynamics. This term is a topological invariant,

$$S_{GB} = -2\pi\alpha\chi, \tag{4.5.60}$$

where χ is the Euler character. It can nevertheless have physical implications (see, e.g., [127] and references therein). In the context of quantum cosmology, the extra term (4.5.59) adds only a constant factor to the wave function, $f_{GB} = \exp(-2\pi\alpha\chi)$, if the topology of the universe is fixed. But if the topology is allowed to vary, different topologies will be weighted with different factors. The Euler character is $\chi = 2$ for a de Sitter universe and $\chi = 4$ for the $S^1 \times S^2$ universe[4]. Hence the nucleation probabilities of such universes are

$$P_{dS} \sim \exp\left(-\frac{\pi}{H^2} - 4\pi\alpha\right), \tag{4.5.61}$$

[4]These are the Euler characters for S^4 and $S^2 \times S^2$ instantons, respectively.

$$P_{S^1\times S^2} \sim H^2 \exp\left(-8\pi\alpha\right). \tag{4.5.62}$$

This shows that de Sitter universes may dominate if α is sufficiently large,[5]

$$\alpha > 1/4H^2 \gg 1. \tag{4.5.63}$$

4.6 Conclusions

In this project we applied the tunneling proposal for the wave function of the universe to the Kantowski-Sachs (KS) minisuperspace model of spatial topology $S^1 \times S^2$. The path integral version of this proposal defines the wave function $\Psi_T(g)$ as a path integral over histories interpolating between a vanishing 3-geometry ("nothing") and a given configuration g, with the lapse integration taken over semi-infinite Lorentzian contour. It turns out, however, that all histories with vanishing initial radii of S^1 and S^2 in KS model necessarily have an initial curvature singularity, even after Euclidean continuation [64]. It follows that the wave function defined in this way does not describe a non-singular origin of the universe, even at the semiclassical level.

The conclusion could be that the tunneling wave function cannot be defined in the KS model. This could mean that a universe of topology $S^1 \times S^2$ cannot originate out of nothing – assuming that the tunneling approach to the wave function of the universe is on the right track.

Here we have explored an alternative possibility, introduced in Ref.[64] by Halliwell and Louko. They suggested that the boundary condition of vanishing 3-geometry should be replaced by the condition of a vanishing 3-volume. That is, only one of the initial scale factors should be set equal to zero. The interpretation of such a degenerate but non-vanishing 3-geometry as "nothing" may be found objectionable. On the other hand, such geometries can be obtained as limiting slices of regular Euclidean 4-geometries of topology $S^2 \times S^2$, which may be regarded as instantons describing a non-singular origin of the universe. We took an agnostic attitude to this issue and pursued the HL proposal in this paper, to see where it leads.

With one of the scale factors set to zero, the other one can be set at a nonzero value that is consistent with a non-singular 4-geometry. Alternatively, leaving the other scale factor unspecified one can impose a regularity condition excluding conical singularities. We have studied both of these approaches.

In the first approach, when the path integral is taken between fixed values of the scale factors

[5] A Gauss-Bonnet term (4.5.59) appears in the low-energy effective action of heterotic string theory [128], together with an infinite series of higher-order curvature corrections $\sim (\alpha R)^n$. However, the higher-order terms can be neglected only if $\alpha R \ll 1$ [127], which is in conflict with (4.5.63). Thus the Gauss-Bonnet term should have a different origin if it is to play a role in suppressing $S^1 \times S^2$ universes.

with one of them set to zero, we found that the resulting wave function diverges at a finite value of the radius of S^2, $b = H^{-1}\sqrt{3}$. Hence it is not a solution of the WDW equation in the entire superspace and is not a suitable choice for the tunneling wave function of the universe.

The main body of the paper is devoted to the second approach. Here we found that the choice of $b = 0$ cannot be supplemented by a regularity condition that would give an acceptable wave function. One always gets the same singular wave function that was obtained for fixed initial scale factors. The only option is then to set $a = 0$ and impose a regularity condition of smooth closure on S^1. We found that the resulting wave function is normalizable, with a probability distribution peaked at $b \gtrsim a/H \gg a$. It predicts a highly anisotropic initial universe. However, the universe expands exponentially in all directions, and after a large amount of inflation observers will see an isotropic local universe. In contrast, the Hartle-Hawking wave function gives a probability distribution peaked at Nariai-type universes with $b \approx 1/H$, which remain locally anisotropic until late times.

We have emphasized that the wave function we obtained here is rather different from wave functions describing tunneling in quantum mechanics. The reason is that the WDW equation of the KS model is a hyperbolic equation, with the two kinetic terms having opposite signs. There is therefore no clear division of superspace into classically allowed and forbidden regions. In particular, there is no exponential suppression of the probability distribution in the region of $b \gg a$.

We find that the total nucleation probability is $P \propto H^2$. As in de Sitter model, it is maximized at large values of H, but unlike de Sitter the dependence on H is a power law, not exponential. It follows that for $H \ll 1$ the nucleation probability is much higher for $S^1 \times S^2$ than for de Sitter universes. We noted that this situation can be reversed if the gravitational action is supplemented with a Gauss-Bonnet term with a sufficiently large coefficient.

Acknowledgments

We are grateful to Jorma Louko and Maulik Parikh for useful discussions. This work was supported in part by the National Science Foundation under grant No. 2110466.

Chapter 5

Jackiw-Teitelboim quantum cosmology

*Based on work with A. Vilenkin published in JCAP **03**, no.03, 056 (2022)*

We study quantum cosmology of the $2D$ Jackiw-Teitelboim (JT) gravity with $\Lambda > 0$ and calculate the Hartle-Hawking (HH) wave function for this model in the minisuperspace framework. Our approach is guided by the observation that the JT dynamics can be mapped exactly onto that of the Kantowski-Sachs (KS) model describing a homogeneous universe with spatial sections of $S^1 \times S^2$ topology. This allows us to establish a JT-KS correspondence between the wave functions of the models. The JT-KS connection formulas allow us to translate our results for the HH state in the KS model to JT gravity and obtain a probability distribution for the dilaton field.

5.1 Motivation

In the last few years there has been a renewed interest in quantum cosmology, inspired by recent work on the exactly soluble $(1+1)$-dimensional quantum gravity model – the Jackiw-Teitelboim (JT) gravity [129, 130]. This model can be thought of as a quantum theory of a one-dimensional closed universe. Apart from the scale factor a, it also includes an evolving scalar field ϕ – the dilaton, which makes a comparison with higher-dimensional models somewhat less informative. On the positive side, one can hope that exact solubility of the model may provide new insights into the nature of the wave function of the universe.[1]

The HH wave function for JT gravity has been recently discussed in the interesting paper by Maldacena, Turiaci and Yang (MTY) [132]. They calculated the wave function in the leading semiclassical order in the limit of large a and included the pre-exponential factor suggested by the Schwarzian analysis. In difference from the Hartle and Hawking approach, MTY focused on the outgoing branch of the wave function, describing expanding universes at large a. As a result the asymptotic behavior of Ψ is more consistent with the tunneling boundary conditions.

Another interesting recent work is the paper by Iliesiu, Kruthoff, Turiaci and Verlinde (IKTV) [133]. They presented an exact solution to the WDW equation of JT gravity, which they interpreted as the HH wave function, but their choice of boundary conditions was different from the earlier literature. Hartle & Hawking and most of the subsequent authors required that geometries included in the path integral close off smoothly in the limit of small universes. Instead, IKTV imposed a boundary condition in the opposite limit, requiring that the wave function exhibits Schwarzian behavior when the universe is large. The assumption of regularity and closure is implicit in their discussion, but these conditions are not explicitly enforced. The resulting wave function agrees with the semiclassical analysis of MTY in the appropriate limit. However, IKTV note an unexpected feature: the wave function develops a strong singularity at a finite value of the scale factor.

In the present paper we take a different approach to JT quantum cosmology. It is based on the observation of MTY that JT model can be obtained from $4D$ gravity by dimensional reduction. We shall use this connection between $2D$ and $4D$ theories as a guide to defining the cosmological HH wave function in the JT model. In their paper MTY discussed a dimensional reduction from a nearly extremal Schwarzschild-de Sitter solution, with the extra two dimensions compactified on a sphere (see also [136, 137] for earlier work). Since our emphasis is on the

[1] An exact quantization of JT model was first developed by Henneaux [131]. For recent discussions see Refs. [132, 133, 134, 135] and references therein.

cosmological aspects of the theory, we find it more useful to consider a cosmological $4D$ model describing a homogeneous universe with spatial sections having $S^1 \times S^2$ topology, known as the Kantowski-Sachs model. The main difference from the MTY and IKTV work is that we impose the boundary conditions in the small universe limit, requiring that the geometry closes off in a regular way.

We begin by reviewing JT gravity and its quantization, discussing in particular the semi-classical analysis of MTY and the exact solutions of IKTV. We argue that these solutions are not suitable to represent the HH wave function. We also discuss how JT model can be obtained by dimensional reduction from $4D$ gravity.

We establish an exact correspondence between the WDW equations for KS and JT models. Furthermore, we show that the transition amplitude between states with specified initial and final scale factors calculated by HL is closely related to the wave function found by IKTV. It follows from this analysis that their wave function satisfies an equation with a singular source and thus is not a solution of the WDW equation. This accounts for the divergence of the wave function pointed out by IKTV.

Finally, we use the correspondence between JT and KS models to define the HH wave function in JT gravity. We use this wave function to determine the probability distribution for the dilaton field ϕ, which we find to be normalizable. Our results are summarized and discussed in subsection 5.

5.2 JT gravity

5.2.1 The action

The action of the JT model is [129, 130]

$$S = \int d^2x\sqrt{-g}\phi(R - 2H^2) - 2\int_B \phi_b K, \tag{5.2.1}$$

where R is the $2D$ spacetime curvature, $H = \text{const}$, ϕ is the dilaton field, ϕ_b is its value at the boundary, and K is the extrinsic curvature of the boundary curve B. Throughout the paper we shall assume that $H > 0$. Variation with respect to ϕ yields $R = 2H^2$, telling us that the $2D$ spacetime is a de Sitter space with expansion rate H.

With the metric represented as

$$ds^2 = -N^2dt^2 + a^2dx^2, \tag{5.2.2}$$

where $0 < x < 2\pi$ and N is the lapse function, the state vector is a functional

$$\Psi[a(x), \phi(x)]. \tag{5.2.3}$$

We can choose the gauge so that $\phi_b = \text{const}$ at the boundary. Furthermore, we are going to adopt a minisuperspace picture, where $a = a(t)$, independent of x, and the boundary is a circle, $t = \text{const}$. Then Ψ is an ordinary function $\Psi(a, \phi)$. It has been shown in [133] that due to the simplicity of the model, the wave functional (5.2.3) can be recovered from the minisuperspace wave function $\Psi(a, \phi)$. Here, we shall restrict our analysis to the minisuperspace model with $a = a(t),\ \phi = \phi(t)$.

After integration by parts the action (5.2.1) can be represented as

$$S = -4\pi \int dt \left(\frac{\dot{a}\dot{\phi}}{N} + NH^2 a\phi \right), \tag{5.2.4}$$

where dots stand for derivatives with respect to t. We are going to use the gauge $N = \text{const}$. The momenta conjugate to a and ϕ are

$$\Pi_a = -\frac{4\pi}{N}\dot{\phi}, \qquad \Pi_\phi = -\frac{4\pi}{N}\dot{a}. \tag{5.2.5}$$

The equations of motion obtained by varying the action with respect to a and ϕ are

$$\ddot{a} - H^2 a = 0, \tag{5.2.6}$$

$$\ddot{\phi} - H^2 \phi = 0, \tag{5.2.7}$$

where we have set $N = 1$. The Hamiltonian constraint is obtained by varying with respect to N:

$$\dot{a}\dot{\phi} = H^2 a\phi, \tag{5.2.8}$$

or

$$\Pi_a \Pi_\phi = 16\pi^2 H^2 a\phi. \tag{5.2.9}$$

The classical solution of these equations is

$$a = a_0 \cosh(Ht), \qquad \phi = \phi_0 \sinh(Ht) \tag{5.2.10}$$

with $a_0, \phi_0 = \text{const}$. We shall set $a_0 = H^{-1}$, so that the metric covers the full de Sitter space

in a nonsingular way.

5.2.2 Semiclassical wave function

To lowest order in the WKB approximation, the wave function is given by

$$\Psi \sim e^{iS_{cl}}, \tag{5.2.11}$$

where S_{cl} is the classical action,

$$S_{cl} = -2\int_0^{2\pi} dx\ a\phi_b K = -4\pi a\phi_b K. \tag{5.2.12}$$

Here, we used the fact that $R = 2H^2$ in the classical solution, so only the surface terms make a contribution, and that ϕ and K are constant on the boundary. Following the no-boundary philosophy, we assume that the (Euclideanized) geometry closes off smoothly, so that there is no boundary contribution at $a = 0$.

In the classically allowed region ($a > H^{-1}$), the extrinsic curvature K is given by

$$K = \frac{\dot{a}}{a} = H\tanh(Ht) = a^{-1}\sqrt{H^2a^2 - 1}, \tag{5.2.13}$$

where we have used Eq. (5.2.10) with $a_0 = H^{-1}$. Substituting this in Eqs. (5.2.12) and (5.2.11), we obtain

$$\Psi \propto \exp\left(-4\pi i\phi_b\sqrt{H^2a^2 - 1}\right) \tag{5.2.14}$$

A linearly independent WKB wave function is a complex conjugate of (5.2.14). A general WKB solution is a linear combination of the two. The semiclassical approximation applies when the action is large, $\phi_b\sqrt{H^2a^2 - 1} \gg 1$.

The momentum operator Π_ϕ acting on Ψ gives

$$\Pi_\phi\Psi = -i\partial_\phi\Psi = -4\pi\sqrt{H^2a^2 - 1}\Psi. \tag{5.2.15}$$

The classical momentum is given by Eq. (5.2.5), so we get

$$\dot{a} = \sqrt{H^2a^2 - 1}. \tag{5.2.16}$$

This agrees with the expanding branch of the classical solution (5.2.10). The complex conjugate wave function describes a contracting universe.

5.2.3 Exact solutions of the WDW equation

The WDW equation corresponding to the Hamiltonian constraint (5.2.8) is

$$(\partial_a \partial_\phi + 16\pi^2 H^2 a\phi)\tilde{\Psi} = 0. \tag{5.2.17}$$

Here,

$$\tilde{\Psi} = \Psi/a \tag{5.2.18}$$

and the factor $1/a$ comes from the factor ordering indicated by the exact quantization of the JT model by Henneaux [131] (see IKTV [133] for a detailed explanation). Following MTY [132], we introduce new variables

$$u = \phi^2, \quad v = (2\pi)^2(H^2a^2 - 1). \tag{5.2.19}$$

Then the WDW equation becomes

$$(\partial_u \partial_v + 1)\tilde{\Psi} = 0. \tag{5.2.20}$$

Yet another change of variables

$$T = \sqrt{uv}, \quad \xi = \frac{1}{2}\ln\frac{v}{u} \tag{5.2.21}$$

brings the equation to a separable form

$$-\frac{1}{T}\partial_T(T\partial_T\tilde{\Psi}) + \frac{1}{T^2}\partial_\xi^2\tilde{\Psi} - 4\tilde{\Psi} = 0. \tag{5.2.22}$$

With the ansatz

$$\tilde{\Psi}_m = e^{m\xi} f_m(T) \tag{5.2.23}$$

we obtain an equation for $f_m(T)$:

$$f_m{}'' + \frac{1}{T}f_m{}' - \frac{m^2}{T^2}f_m + 4f_m = 0. \tag{5.2.24}$$

The solution is

$$f_m(T) = Z_m(2T), \tag{5.2.25}$$

where Z_m is a Bessel function.

Following MTY, IKTV required that the wave function should describe an expanding uni-

verse in the limit of large a. Then the appropriate choice of Bessel functions is $H_m^{(2)}(2T)$. The general solution of the WDW equation is then a linear combination of functions of the form (5.2.23):

$$\tilde{\Psi}_m = \left(\frac{v}{u}\right)^{m/2} H_m^{(2)}(2T). \tag{5.2.26}$$

In terms of the variables a and ϕ, the argument of the Bessel functions is

$$2T = 4\pi\phi\sqrt{H^2a^2 - 1}. \tag{5.2.27}$$

The asymptotic form of the Bessel functions at large T is $H_m^{(2)}(2T) \propto T^{-1/2}e^{-2iT}$; hence

$$\Psi_m(Ha\phi \gg 1) \propto \left(\frac{a}{\phi}\right)^{m+1/2} \exp\left(-4\pi i\phi\sqrt{H^2a^2 - 1}\right), \tag{5.2.28}$$

where we have accounted for the factor $1/a$ relating Ψ_m and $\tilde{\Psi}_m$. All these functions have the same asymptotic exponential factor as the WKB wave function (5.2.14). So in order to choose between them one has to determine the pre-exponential factor.

In the path integral formulation, the semiclassical pre-factor is determined by quantum fluctuations about the classical solution. In the JT model these are fluctuations in the shape of the boundary curve, which are described by the Schwarzian theory and yield a one-loop pre-factor $(\phi/a)^{3/2}$ at large a [138]. It is shown in [138] that this result is one-loop exact, so there are no further corrections. This pre-factor is obtained by setting $m = -2$ in (5.2.28). Then the exact wave function takes the form

$$\Psi(a, \phi) = \frac{a\phi^2}{H^2a^2 - 1} H_2^{(2)}\left(4\pi\phi\sqrt{H^2a^2 - 1}\right) \qquad (Ha > 1). \tag{5.2.29}$$

Analytic continuation of this wave function to $Ha < 1$ is not unique because of the singularity at $Ha = 1$. IKTV specify the wave function in the entire range of a by replacing the Hankel function in (5.2.29) with $K_2\left(i\sqrt{\phi^2(H^2a^2 - 1 - i\epsilon)}\right)$, which gives[2]

$$\Psi(a, \phi) = \frac{2i}{\pi} \frac{a\phi^2}{H^2a^2 - 1} K_2\left(4\pi\phi\sqrt{H^2a^2 - 1}\right) \qquad (Ha < 1). \tag{5.2.30}$$

IKTV identify the wave function (5.2.29),(5.2.30) with the HH wave function for JT gravity. There are however some problems with this identification. We first note that one of the defining properties of the HH wave function is that it is real. This can be interpreted as reflecting the

[2]The inclusion of the term $i\epsilon$ with $\epsilon \to +0$ is needed to make the solution well-defined on the branch cut.

CPT invariance of the HH state [121]. On the other hand, the tunneling wave function is specified by the outgoing wave boundary condition, which in the present context requires that the large a asymptotic of Ψ should only include terms corresponding to expanding universes. This seems to suggest that the wave function described by Eqs.(5.2.29),(5.2.30) is more appropriately interpreted as the tunneling wave function.

More importantly, the wave function (5.2.29) has a singularity at $a = H^{-1}$. It is actually not a solution of the WDW equation. We will show in the next Section that it satisfies

$$\mathcal{H}\Psi \propto \delta(\phi)\delta''(a - H^{-1}). \tag{5.2.31}$$

Hence it is not suitable for the role of HH or tunneling wave function.

IKTV have also proposed another candidate for the HH wave function:

$$\Psi(a,\phi) = \frac{a\phi^2}{H^2a^2 - 1} J_2\left(4\pi\phi\sqrt{H^2a^2 - 1}\right). \tag{5.2.32}$$

This wave function is real and non-singular. However, its behavior in the classically forbidden range $a < H^{-1}$ is very different from what is expected for the semiclassical HH wave function. We have

$$\Psi(a < H^{-1}) = \frac{a\phi^2}{1 - H^2a^2} I_2\left(4\pi\sqrt{\phi^2(1 - H^2a^2)}\right) \sim \frac{a\phi^{3/2}}{\sqrt{4\pi}(1 - H^2a^2)^{5/4}} \exp\left(4\pi|\phi|\sqrt{1 - H^2a^2}\right), \tag{5.2.33}$$

where the last expression is the asymptotic form of Ψ assuming that the argument of I_2 is large. As a varies from $a = 0$ to $a \sim H^{-1}$, the exponential factor in Ψ decreases, which is opposite to the expected behavior of the HH wave function.

5.3 JT-KS correspondance

5.3.1 Dimensional reduction

MTY discussed the relation between JT and Einstein $4D$ gravity using dimensional reduction from a nearly extremal Schwarzschild-de Sitter solution. Since our emphasis is on the cosmological aspects of the theory, we find it more useful to consider a cosmological $4D$ model describing a universe with spatial sections having $S^1 \times S^2$ topology and the metric

$$ds^2 = -dt^2 + a^2(x,t)dx^2 + b^2(x,t)d\Omega^2. \tag{5.3.1}$$

Here, $0 < x < 2\pi$ and $d\Omega^2$ is the metric on a unit sphere. Substituting this in the Einstein-Hilbert action (in Planck units)

$$S = \frac{1}{16\pi}\int d^4x\sqrt{-g^{(4)}}\left(R^{(4)} - 2\Lambda\right), \tag{5.3.2}$$

where Λ is the $4D$ cosmological constant, and integrating over the angular variables we obtain

$$S = \int d^2x\sqrt{-g}\left[\frac{b^2}{4}R + \frac{1}{2}(\nabla b)^2 + \frac{1}{2} - \frac{1}{2}\Lambda b^2\right]. \tag{5.3.3}$$

Here, R and g are respectively the $2D$ curvature scalar and the metric determinant and we have omitted the boundary term.

Following [139], we can remove the gradient term in the action by a conformal rescaling

$$\bar{g}_{\mu\nu} = \Omega^2(b)g_{\mu\nu} \tag{5.3.4}$$

with

$$\frac{d\ln\Omega}{d\ln b} = \frac{1}{2}. \tag{5.3.5}$$

This has the solution

$$\Omega = (b/2)^{1/2}, \tag{5.3.6}$$

where we have chosen the normalization factor for future convenience. The action then reduces to

$$S = \int d^2x\sqrt{-\bar{g}}\left[\bar{\phi}\bar{R} - V(\bar{\phi})\right], \tag{5.3.7}$$

where $\bar{\phi} = b^2/4$ and

$$V(\bar{\phi}) = 2\Lambda\sqrt{\bar{\phi}} - \frac{1}{2\sqrt{\bar{\phi}}}. \tag{5.3.8}$$

We define

$$\bar{\phi} = \phi_0 + \phi, \tag{5.3.9}$$

where $\phi_0 = 1/4\Lambda$, so that $V(\phi_0) = 0$. We shall assume that $\Lambda \ll 1$, so $\phi_0 \gg 1$. Then, for $|\phi| \ll \phi_0$ we can expand the potential (5.3.8) around $\phi = 0$. Neglecting quadratic and higher order terms in the expansion, we obtain an approximate JT action

$$S \approx \phi_0\int d^2x\sqrt{-\bar{g}}\bar{R} + \int d^2x\sqrt{-\bar{g}}\phi\left(\bar{R} - 2\bar{\Lambda}\right), \tag{5.3.10}$$

where $\bar{\Lambda} = 2\Lambda^{3/2}$.

Since the second term in (5.3.10) already includes a factor of ϕ, we can use

$$\bar{g}_{\mu\nu} \approx \frac{1}{2\sqrt{\Lambda}} g_{\mu\nu}, \quad \bar{R} \approx 2\sqrt{\Lambda} R. \tag{5.3.11}$$

Hence, in the same approximation we can rewrite the action in terms of the original metric $g_{\mu\nu}$ and the cosmological constant Λ as

$$S \approx \phi_0 \int d^2x\sqrt{-g}R + \int d^2x\sqrt{-g}\phi\,(R - 2\Lambda)\,, \tag{5.3.12}$$

The above analysis suggests that in the appropriate limit the dynamics of the $4D$ cosmological model (5.3.1) is well approximated by that of the JT gravity (5.2.1) with $\Lambda = H^2$. The radius of the sphere S^2 in this limit is $b \approx H^{-1}$. We will focus on this regime in most of the paper, but in the next section we will see that in the minisuperspace setting the two models are even more closely related and can be mapped onto one another for arbitrary values of the scale factors a and b.

5.3.2 Connection formulas

The WDW equation for the KS model Eq. (3.2.11) has the same form as Eq.(5.2.20) for the JT model. The difference is that Eq.(5.2.20) is for the function $\tilde{\Psi} = \Psi/a$, where the factor $1/a$ appeared due to a particular choice of the factor ordering. We mention, again, the solutions to the KS model:

$$\Psi_m = \left(\frac{\rho}{\xi}\right)^{m/2} H_m^{(2)}(2\sqrt{\xi\rho}). \tag{5.3.13}$$

The solution with $m = -2$ corresponds to the IKTV solution (5.2.29). We expect this solution to agree with (5.2.29) when $b \approx H^{-1}$. The argument of the Hankel function in (5.3.13) is

$$2\sqrt{\xi\rho} = \frac{2\pi}{H^2}\sqrt{\frac{Hb+2}{3}}(Hb-1)\sqrt{H^3a^2b-1} \approx \frac{2\pi}{H^2}(Hb-1)\sqrt{H^2a^2-1}. \tag{5.3.14}$$

Comparing this with the argument of the Hankel function in (5.2.29), we can identify

$$\frac{Hb-1}{H^2} \approx 2\phi. \tag{5.3.15}$$

It is interesting to note that the correspondence between the two wave function extends

beyond this approximation. If we define

$$\tilde{a} = (Hb)^{1/2} a, \qquad \phi = \frac{(Hb-1)}{2H^2}\sqrt{\frac{Hb+2}{3}}, \tag{5.3.16}$$

then $\tilde{a}\Psi(\tilde{a},\phi)$ exactly reproduces the wave function (5.2.29). More generally, the transformation (5.3.16) can be used to obtain a solution to the WDW equation of the JT model from that of the KS model and *vice versa*. Note also that $\tilde{a}$ and ϕ are simply related to the variables ξ and ρ:

$$\xi = 4\pi^2 H^3 \phi^2, \qquad \rho = H^{-3}(H^2\tilde{a}^2 - 1). \tag{5.3.17}$$

We thus see that JT and KS minisuperspace models are formally equivalent to one another. This equivalence, however, does not extend beyond minisuperspace. In the JT case, the minisuperspace wave function can be extended to a wave function in full superspace, but in the KS model the number of variables in the wave function and the pre-exponential factor depend on which perturbation modes are included in the minisuperspace truncation. Equivalence between the two models at the minisuperspace level will nevertheless be sufficient for our purposes here.

Finally, we close this section by discussing a problematic feature of the IKTV wavefunction and utilizing the transition amplitudes obtained in the KS model. The amplitude G in Eqs.(3.2.23),(3.2.24) is similar to the IKTV wave function (5.2.29),(5.2.30) with the only difference being the prefactor and the index of the Bessel functions. The two objects are closely related, as we will now show.

The Bessel functions appearing in Eqs.(3.2.23),(3.2.24) can be expressed as $Z_0(X)$, where

$$X = \sqrt{H^3 c - 1} f(b) = 4\pi\phi\sqrt{H^2\tilde{a}^2 - 1} \tag{5.3.18}$$

with

$$f(b) = \frac{2\pi}{H^2}(Hb-1)\sqrt{\frac{Hb+2}{3}} = 4\pi\phi, \tag{5.3.19}$$

where we have used the notation Z_ν for a Bessel function (of any kind) with index ν and Eqs.(5.3.16) relating a and b to $\tilde{a}$ and ϕ. Differentiating twice with respect to c, we obtain

$$\frac{\partial^2 Z_0}{\partial c^2} = \frac{H^6 f^2(b)}{4(H^3c-1)}\left[-Z_1' + \frac{1}{f(b)\sqrt{H^3c-1}}Z_1\right] = \frac{H^6 f^2(b)}{4(H^3c-1)}Z_2 = (2\pi H^3)^2\frac{\phi^2}{\tilde{a}^2-1}Z_2. \tag{5.3.20}$$

Here prime stands for a derivative with respect to the argument and we used an iteration formula for Bessel functions in the second step.

Now, the expression on the right-hand side of Eq.(5.3.20) has the same form as the wave function (5.2.29) of IKTV. We conclude that

$$\Psi_{IKTV} = C\frac{\partial^2}{\partial c^2}G(b,c|H^{-1},H^{-3}) \tag{5.3.21}$$

with $C = \text{const}$. Furthermore, it follows from Eq.(3.2.21) that[3]

$$\mathcal{H}\Psi_{IKTV} \propto -i\delta(b-H^{-1})\delta''(c-H^{-3}). \tag{5.3.22}$$

Hence Ψ_{IKTV} is not a solution of the WDW equation. It has a distributional source at $a = b = H^{-1}$, which is more singular than that of a Green's function.

5.4 Hartle-Hawking state

Once we have found the HH wave function $\Psi_{HH}^{(KS)}(a,b)$ for the KS model, we can *define* the HH wave function for JT gravity as the wave function obtained from $\Psi_{HH}^{(KS)}$ by dimensional reduction. This amounts to expressing the scale factors a, b in terms of the JT variables $\tilde{a}, \phi$ using the connection formulas (5.3.16) and adding an extra factor of $\tilde{a}$ to account for the difference between Ψ and $\tilde{\Psi}$ in the JT model.

An issue that needs to be addressed is that of the boundary conditions (3.3.12) that we used in the path integral for $\Psi_{HH}^{(KS)}$. These boundary conditions were imposed to ensure a smooth closure of the geometry at $t = 0$; they are equivalent to $a(0) = 0,\ \dot{a}(0)/N = 1$. However, after dimensional reduction the new scale factor is given by $\tilde{a} = a\sqrt{Hb}$, so the appropriate boundary conditions would now be

$$\tilde{a}(0) = 0,\ \dot{\tilde{a}}(0)/N = 1. \tag{5.4.1}$$

This is equivalent to (3.3.12) only if $Hb(0) = 1$. Requiring in addition that the dilaton is smooth at $t = 0$, we should add the condition

$$\dot{\phi}(0) = 0. \tag{5.4.2}$$

As we discussed, a smooth closure of a classical $S^1 \times S^2$ geometry requires three boundary conditions, while only two conditions can be consistently imposed in quantum theory. Classically, the three conditions are not independent and any two of them imply the third. In the present case the situation is similar: it follows from the boundary conditions (3.3.12) that

[3]Note that $\partial/\partial c$ commutes with $\mathcal{H}$.

$Hb(0) = 1$ if the constraint equation (4.2.14) is satisfied. Thus the boundary conditions that we used are equivalent to smooth closure conditions for JT model at the classical level. Quantum mechanically, different choices of two conditions out of three may be inequivalent, yielding wave functions satisfying WDW equations with different factor orderings. One can expect, however, that in the semiclassical regime these wave functions will be close to one another, differing perhaps only in the pre-exponential factor.[4]

For $Hb \approx 1$ the relations (5.3.16) become

$$Hb \approx 1 + 2\phi H^2 \quad , \quad a \approx \tilde{a}(1 - \phi H^2). \tag{5.4.3}$$

Then in the classically allowed range $Ha > 1$ the wave function (3.3.49) becomes

$$\Psi_{HH} \sim \frac{\tilde{a}}{\sqrt{H^2\tilde{a}^2 - 1}} \exp\left(\frac{\pi}{H^2}\right) \cos\left(4\pi\phi\sqrt{H^2\tilde{a}^2 - 1}\right), \tag{5.4.4}$$

were we have neglected H^2 corrections to the prefactor.

In the classically forbidden region we can use the small-Ha solution (3.3.55) to obtain the JT wave function for $H\tilde{a} \ll 1$. We find[5]

$$\Psi_{HH} \sim \tilde{a}^{3/2} \exp\left[\frac{4\tilde{a}\pi}{\sqrt{6}H}\sqrt{1 - 6\phi^2 H^4}\right], \tag{5.4.5}$$

where we have neglected corrections to the prefactor. This expression is valid for $\tilde{a}H \ll 1$ and $\phi^2 H^4 < 1/6$. The wave function peaks at $\phi = 0$ at a fixed $\tilde{a}$. It can be shown that it satisfies the WDW equation of JT gravity (5.2.17) to the leading order.

Similarly to the KS model, the expanding branch of the wave function (5.4.4) can be used to find the probability distribution for the dilaton field ϕ. The difference here is that now the conserved current is given by Eq.(4.2.18) with Ψ replaced by $\tilde{\Psi} = \Psi/a$. The reason is that the differential operator in Eq.(5.2.17) is not the covariant Laplacian, because of nonstandard factor ordering in Henneaux's quantization of the JT model. As a result the probability distribution is obtained by simply using the connection formulas (5.3.16) in Eq.(4.5.36) without any extra

[4]The semiclassical wave function for an FRW universe with a uniform scalar field ϕ was studied in Ref.[103] for different factor orderings in the WDW equation. A change of factor ordering had an effect on pre-exponential factor, but it did not affect the semiclassical probability distribution for ϕ. One can expect a similar situation to occur in the JT model. Since no particular choice appears to be preferred, we shall proceed to use our $\Psi_{HH}^{(KS)}$ for dimensional reduction.

[5]For this calculation, it is helpful to rearrange the relation of ϕ and b in the form: $\sqrt{\frac{2}{Hb}}\sqrt{1 - 6\phi^2 H^4} = \sqrt{3 - H^2 b^2}$.

factors of $\tilde{a}$:

$$dP \propto \frac{d\phi}{\sqrt{H^2\tilde{a}^2-1}} \exp\left[-\frac{16\pi H^2\phi^2}{3(H^2\tilde{a}^2-1)}\right]. \tag{5.4.6}$$

We expect this expression to be accurate for $\phi \lesssim H^{-1}\delta b \ll H^{-2}$ and $\tilde{a}$ satisfying the conditions (3.4.10).

We note that the classical solutions (5.2.10) of the JT model

$$a = H^{-1}\cosh(Ht), \qquad \phi = \phi_0 \sinh(Ht) \tag{5.4.7}$$

satisfy

$$\frac{\phi^2}{H^2a^2-1} = \phi_0^2 = \text{const.} \tag{5.4.8}$$

These solutions are parametrized by ϕ_0 and Eq.(5.4.6) gives a probability distribution for this parameter:

$$dP \propto d\phi_0 \exp\left(-\frac{16\pi H^2\phi_0^2}{3}\right). \tag{5.4.9}$$

This distribution can be interpreted as describing an ensemble of $(1+1)D$ universes that nucleate with $\tilde{a} \approx H^{-1}$, $\phi \approx 0$ and $\dot{\phi} \approx H\phi_0$ and then evolve according to Eqs.(5.4.7). Even though the approximations we used to derive the wave function break down at $\tilde{a} \gtrsim H^{-2}$, the classical solutions become increasingly accurate at large $\tilde{a}$ and we expect the distribution (5.4.9) to remain accurate as well.

5.5 Conclusions

Our main goal in this paper was to define and calculate the Hartle-Hawking wave function Ψ_{HH} in a $(1+1)$-dimensional minisuperspace JT model with a cosmological constant $\Lambda = H^2 > 0$. This model is closely related to that of a homogeneous $4D$ universe with the same cosmological constant and having spatial topology $S^1 \times S^2$ (the KS model). Our approach was first to find Ψ_{HH} for the KS model using its definition in terms of a Euclidean path integral and then to use the exact correspondence between the two models to define Ψ_{HH} for JT gravity. In our analysis of KS quantum cosmology we followed the work of Halliwell and Louko [64]. However, this work was mostly limited to the case of a vanishing Λ, so to implement our program we had to tackle the nontrivial task of extending it to $\Lambda > 0$.

The wave function that we found is normalizable, so we could obtain a normalized probability distribution for the dilaton in the JT model. Note, on the other hand, that the leading-order

semiclassical wave function found by Maldacena *et al* [132] is not normalizable, even after including a Schwarzian prefactor.

Our wave function is different from the exact WDW solution obtained earlier by Iliesiu *et al* [133]. This difference is due to a different choice of the boundary conditions. The HH wave function was originally defined as a path integral over smooth Euclidean geometries with a single boundary. We adopted this definition here and imposed the condition of smooth closure at $a = 0$, where a is the radius of S^1. On the other hand, Ref.[133] imposed boundary conditions at large a requiring that Ψ_{HH} has the asymptotic form suggested by Schwarzian theory, which accounts for quantum fluctuations of the boundary curve. Both boundary conditions seem to be reasonable, but it appears that they are not compatible with one another.

The wave function obtained in [133] using the Schwarzian boundary conditions has a strong singularity at $a = H^{-1}$.[6] We found that this wave function is not a solution of the WDW equation. Instead, it satisfies an equation with a singular source at $a = H^{-1}$. Furthermore, we showed that this wave function is closely related to the transition amplitude in the KS model from $a = b = H^{-1}$ to specified values of a and b at the boundary, where b is the radius of S^2. Since a state with $a = b = H^{-1}$ (which corresponds to $a = H^{-1}$, $\phi = 0$ in the JT model) can hardly be interpreted as "nothing", we believe that the wave functions discussed in [133] cannot be interpreted as the HH wave function. On the other hand, the wave function we found in the present paper satisfies the WDW equation and has only a mild singularity at $a = H^{-1}$, which one always expects in a WKB wave function at a classical turning point. It seems therefore that our choice of boundary conditions yields a more reasonable result for the HH wave function.

A possible reason why the Schwarzian boundary condition at large a fails to yield a suitable candidate for the HH wave function is that it leaves the geometry at small a completely unconstrained. It is assumed that the geometry closes off at $a = 0$ in a nonsingular way. However, this condition is not explicitly enforced, so one should not be surprised if geometries included in the path integral include conical singularities and even gaps.

Here is another problematic feature of the wavefunction specified in [133]. When imposing the boundary condition in the large a, ϕ limit IKTV identify the wavefunction with the gravitational partition function given by the Schwarzian theory. Thus, they pick the appropriate

[6] An alternative approach, suggested in Ref.[132], was to derive Ψ_{HH} by analytic continuation from JT gravity with a negative cosmological constant. A Euclidean dS metric (with $H = 1$) is $ds^2 = (1 - r^2)d\theta^2 + (1 - r^2)^{-1}dr^2$. With $r = \cosh\rho$, this becomes $ds^2 = -d\rho^2 - \sinh^2\rho d\theta^2$, which is minus Euclidean AdS metric. This method gives the same wave function as the Schwarzian boundary condition [133]. We note that the origin $\rho = 0$ in AdS analytically continues to the horizon ($r = 1$) in dS. This may explain why the transition amplitude from "nothing" ($\rho = 0$) to some $\rho > 0$ in AdS could be related to the transition amplitude from the horizon ($a = H^{-1}$) to some $a > H^{-1}$ in dS.

density of states to integrate over the expanding branch. It is not clear, however, whether the expression for the density of states is applicable away from the Schwarzian regime. This is investigated in [135] and three distinct regions depending on the boundary length are specified with their corresponding density of states. Once again, however, our results are not in agreement.

Chapter 6

Global string instantons

*Based on work with J. J. Blanco-Pillado and A. Vilenkin published in JCAP **07**, 087 (2025)*

We study the formation of gravitating global strings through quantum mechanical tunneling. The instantons that describe the nucleation process are characterized by two parameters: the string core thickness and its gravitational backreaction controlled by the string core energy density. We obtain solutions across a wide range of these parameters by carrying out numerical integration via multiple shooting methods. Our results are in agreement with previous findings on the nucleation of other topological defects; specifically, after reaching a certain threshold for the string core thickness or its gravitational backreaction, the configuration becomes homogeneous in a manner akin to Hawking-Moss solutions. Additionally, we analyze the global structure of the analytical continuation of the solutions to Lorentzian signature, revealing the emergence of a region of spacetime that describes an anisotropic universe. Finally, we also discuss the relevance of these instantons in the context of quantum cosmology.

6.1 Motivation

Inflation is widely regarded as the leading paradigm in early universe cosmology [8, 11]. According to this picture the universe underwent a period of exponential expansion driven by a scalar field, the inflaton. This mechanism is responsible for producing on large scales a nearly homogeneous, isotropic and flat universe and generating the seeds for structure formation[1]. One of the problems that the inflationary scenario also addresses is the absence of magnetic monopoles in our local universe. According to Grand Unified Theories (GUTs) [141, 142], magnetic monopoles should exist [143, 144] and be in abundance, arising as a result of phase transitions in the early universe [145, 146]. However, this conclusion would be dramatically altered if a period of inflation occurred after the phase transition that produced the monopoles. The exponential expansion during this inflationary phase would dilute the monopole density to negligible levels making them effectively irrelevant for cosmology.

Monopoles belong to a wide class of objects called topological defects like domain walls and cosmic strings [147, 148]. Similarly to the case of monopoles, many scenarios involving domain walls are stringently constrained by cosmological observations [149]. In contrast, cosmic string networks produced during phase transitions do not face such severe issues and have been extensively studied over the years in connection to their cosmological observables [150]. Most models explored in the literature consider the formation of these cosmic strings during a post-inflationary epoch, when the temperature of the universe is of the order of the energy scale characteristic of the objects being formed. This leads to the formation of a network of defects that subsequently evolves in an expanding universe. Owing to their topological stability, some of these objects could potentially survive until the present day. Even in cases where they decay, they may leave detectable imprints on certain cosmological observables, providing indirect evidence of their existence.

However, the formation of topological defects in a cosmological setting is not limited to post-inflationary mechanisms. It has been shown that monopole-antimonopole pairs, circular string loops, and spherical domain walls can also be produced during the inflationary stage through quantum mechanical tunneling [92, 93, 98]. The continuous production of such defects during inflation could lead to appreciable number densities in the present universe, provided their energy scale is not much higher than that of the expansion rate during inflation. The exponential expansion of the universe during inflation would stretch these defects to sizes that could extend well beyond the current horizon, depending on the time of their formation. In

[1]For a review of the predictions of inflation see, for example, [140].

general, such processes result in a distribution of objects with varying sizes, which, as in previous scenarios, could also produce observable effects.

One of the goals of this paper is to study the instanton solutions that describe the nucleation of global strings during inflation. The core ideas underlying the process of string nucleation have been already presented in the literature. In particular, here we will follow the analysis of thick topological defect instantons described in [93]. The case of domain walls is analyzed there numerically both in the case of a fixed spacetime background and also taking into account gravitational back-reaction. In the case of strings, the authors only studied the analytic case of a fixed spacetime background when the defect solution approaches a homogeneous configuration i.e. its core thickness approaches the size of the Hubble horizon. In this work, we aim to extend the previous analysis by conducting a comprehensive numerical investigation of nucleating global strings with different core sizes, incorporating the effects of gravitational backreaction on the geometry of spacetime.

Global strings have been studied in the context of post-inflationary formation scenarios for several decades now [151]. Their relevance has significantly increased in recent years, as they provide a mechanism for generating a cosmological density of axion-like particles, which are potential candidates for dark matter. In these models, a network of global (axionic) strings forms during the early universe following a symmetry-breaking phase transition the so-called Peccei-Quinn transition. One key distinction between global strings and their local counterparts is their coupling to the Goldstone mode, which results in significant radiation of those massless particles (the would be axions) as the strings undergo relativistic motion.

Axionic string networks have two significant implications: first, they create a background of axion particles, and second, they also lead to the production of a gravitational wave background. While certain details of these scenarios remain under debate, the hope of these investigations is to be able to put robust constraints on the scale of the new physics that leads to the formation of strings. Moreover, some models predict the formation of primordial black holes via the collapse of the string network, triggered by a subsequent phase transition that creates walls bounded by the strings, a scenario that is also under current investigation [152, 153].

In contrast, much less attention has been given to scenarios where topological defects are produced via quantum nucleation. Notable work has been done in this area for domain walls, particularly concerning the formation of primordial black holes and wormholes [154, 155, 156]. Our study marks a preliminary step in order to explore similar phenomena in the context of global strings. As we will discuss further, the spacetime structure induced by global string loops exhibits similarities to certain wormhole solutions found in previous studies of cosmological

domain walls.

Another interesting aspect of our solutions is their interpretation as instantons within the framework of quantum cosmology. The results presented in this paper suggest that these instantons can be used to understand the nucleation of compact universes with a global string embedded in their geometry. The presence of the global string alters the symmetry of the solution compared to the standard symmetric de Sitter instanton. By analytically continuing these instantons to a Lorentzian signature, they can be identified as a natural way to describe the creation of an anisotropic universe from nothing.

The rest of the paper is organized as follows. In Sec 2 we illustrate how cosmic strings can be nucleated in de Sitter space through quantum mechanical tunneling in the thin wall approximation. We proceed in Sec 3 by identifying a possible field theory description of these type of instantons in the context of global strings. In Sec 4 we obtain instanton solutions for a global string in a background spacetime with positive cosmological constant $\Lambda = H^2 > 0$, while also incorporating the gravitational deformations to the geometry. We numerically solve the instanton system of equations for different values of the string core thickness and the gravitational backreaction. In Sec 5 we describe the global structure of the solutions as well as their interpretation. In Sec 6. we evaluate the string instanton action and compare it with the corresponding homogeneous configuration. We finally discuss our results in Sec 7.

6.2 Quantum nucleation of thin cosmic strings

In this section, we will lay out a heuristic picture for the nucleation of strings in a fixed background spacetime with positive vacuum energy. Our main goal is to motivate the rigorous and complete analysis that will follow in the subsequent sections [2]. Therefore in order to simplify the problem we will restrict ourselves to the thin wall description of the string. Furthermore, we will also disregard for the time being any gravitational backreaction of any object present in our geometry and consider a fixed background given by the static representation of the de Sitter space metric, namely,

$$ds^2 = -f(r)dt^2 + \frac{dr^2}{f(r)} + r^2 d\Omega^2 \ , \tag{6.2.1}$$

where $f(r) = 1 - H^2 r^2$, $d\Omega^2$ is the metric on a unit 2-sphere and $\Lambda = H^2$ the positive cosmological constant.

[2] Here we follow closely the analysis presented in [92].

As we mentioned earlier, we begin by modeling the string using the Nambu-Goto action, which assumes the string can be effectively approximated by an infinitely thin relativistic object characterized solely by its tension, or energy per unit length. Namely we will consider the action,

$$S_{NG} = -\mu \int d^2\zeta \sqrt{-\gamma} \ , \tag{6.2.2}$$

where μ denotes the string tension and γ is the determinant of the two dimensional worldsheet metric parametrized by the coordinates ζ.

Taking these elements into consideration, we can now examine a circular loop of string of radius $r = R(t)$ in the de Sitter coordinate system presented in Eq. (6.2.1). Assuming this type of loop, we can see that the Nambu-Goto action for this configuration becomes,

$$S_{NG} = -2\pi\mu \int dt R \sqrt{f(R) - \frac{\dot{R}^2}{f(R)}} \ . \tag{6.2.3}$$

This reduced action defines a Lagrangian and a conjugate momentum p_R corresponding to the single degree of freedom in this simplified model, the radius $R(t)$. These quantities are defined as follows:

$$L = -2\pi\mu R \sqrt{f - \frac{\dot{R}^2}{f}} \quad , \quad p_R = \frac{2\pi\mu \dot{R} R}{f\sqrt{f - \frac{\dot{R}^2}{f}}} \ . \tag{6.2.4}$$

In order to study the loop dynamics it will be convenient to use the Hamiltonian constraint of the system:

$$E = p\dot{R} - L = \text{const.} \tag{6.2.5}$$

Inserting the expression for the momentum, the above conservation law recasts to:

$$\dot{R}^2 + V(R) = 0 \ , \tag{6.2.6}$$

where the effective potential is given by, $V(R) = -f(R)^2 + R^2 f(R)^3 \epsilon^{-2}$ and $\epsilon = E/(2\pi\mu)$ is the ratio of the string energy to its tension. This can be viewed as the equation describing the classical motion of a particle of zero energy moving in the potential V.

It can be shown that for $2H\epsilon < 1$, $V(R)$ forms a potential barrier and we can have bounded classical trajectories. The turning points of the potential can be readily found as the solutions to $V(R) = 0$:

$$R_{1,2} = \sqrt{\frac{1}{2H^2}\left(1 \pm \sqrt{1 - 4\epsilon^2 H^2}\right)} \ . \tag{6.2.7}$$

The trajectories of (6.2.6) can be classified as follows. The string loop can start from zero size

at $R = 0$ expand to $R = R_1$, bounce and recollapse. An alternative solution is a contracting loop that bounces at $R = R_2$ and then reexpands towards the horizon H^{-1}.

However, there is yet another possibility. Quantum mechanically, the loop can follow the first trajectory, penetrate the potential barrier from R_1 to R_2 and start expanding. The tunneling probability for this process can be estimated in the WKB approximation as:

$$P \sim e^{-B} \ , \tag{6.2.8}$$

where $B = 2 \int |p_R| dR$ integrating over the two turning points R_1 to R_2.

We can compute the tunneling probability explicitly with the help of (6.2.4) and (6.2.6):

$$P \sim \exp\left(-4\pi\mu \int_{R_1}^{R_2} \frac{dR}{f(R)} \sqrt{R^2 f(R) - \epsilon^2}\right) \ . \tag{6.2.9}$$

In this paper, we are mainly interested in the spontaneous nucleation of loops, meaning loops that tunnel from zero size and have zero energy. To calculate the tunneling rate for such process we take the limit $\epsilon \to 0$. The turning points in this case become, $R_1 = 0$ and $R_2 = H^{-1}$, while the nucleation rate acquires the finite, non zero value:

$$P \sim \exp\left(-\frac{4\pi\mu}{H^2}\right) \ . \tag{6.2.10}$$

This process describes the spontaneous nucleation of a loop of string of de Sitter radius with a nucleation rate given by (6.2.10). We note that our result is valid as long as the semiclassical approximation holds, that is, $\mu/H^2 \gg 1$ and as long as the string core thickness is much smaller than the de Sitter radius so we can use the thin wall approximation. Similar expressions for the nucleation rates of different objects in de Sitter space have been obtained for domain walls, monopoles [92] and black holes [157].

It is well known that quantum tunneling processes can be effectively described using instantons [158, 159]. The present scenario can similarly be examined from this perspective. In particular, the action derived previously indicates that the appropriate instanton representing the nucleation of a string in de Sitter space corresponds to the area of a two-dimensional Euclidean sphere representing the worldsheet of the string wrapping the equator of the four-dimensional sphere that characterizes Euclidean de Sitter space. It can be readily demonstrated that the equations of motion for the Nambu-Goto action in Euclidean space yield a solution consistent with this description.

This simplified form of the instanton will serve as a basis for identifying new deformed

solutions once we relax some of the assumptions employed to derive this straightforward solution. In our analysis, we aim to incorporate several factors that have been omitted thus far, which stem from the simplified approach used when describing our global string with the Nambu-Goto term.

In particular, it is clear that in certain regions of the parameter space, we cannot treat the string as thin, as its thickness, in a field theory description, becomes comparable to the other relevant scale in the problem, specifically the size of the horizon. Hence, at least for these cases we need to go beyond the simple description given here[3]. Furthermore, our instantons will also incorporate the effects of the global string's coupling to the Goldstone mode in relation to the instanton solutions and their corresponding action.

Lastly, we seek to understand the gravitational backreaction on the instantons associated with the global string. While this has been examined in the context of a thin local string in [92], it is well known that the coupling of global strings to the massless mode induces significant gravitational effects on the global string metric [160]. Therefore, we anticipate that this coupling will also play an important role in our solutions.

To account for all these effects in our analysis, we transition in the following section to a smooth description of the global string within the framework of a scalar field theory coupled to gravity. This approach requires numerical integration of the equations of motion, but wherever feasible, we will compare our solutions to the simplified ones presented here to better understand the origin of any deviations.

6.3 Quantum nucleation of field theory global strings

6.3.1 The model

To derive the instanton solutions representing the nucleation of global strings in de Sitter space within field theory, we must first define the specific model under consideration. The Euclidean action for the model we consider is expressed as follows:

$$S_E = \int \sqrt{g}\; d^4x \left(-\frac{R}{16\pi G} + \rho_v \right) + S_E^s \ , \tag{6.3.1}$$

[3]This effect has been considered in detail for domain walls in [93]. However, the string case was only discussed in the limiting scenario where the string thickness equals the de Sitter horizon. In this work, we will consider the full range of possible values of these parameters.

where we have included the gravitational Einstein-Hilbert term, a cosmological term and the string action given in terms of the complex scalar field, ϕ, namely:

$$S_E^s = \int d^4x \, \sqrt{g} \left[\partial^\mu \phi \, \partial_\mu \phi^* + V(\phi) \right] , \tag{6.3.2}$$

and where the vacuum energy ρ_v and string potential can be respectively given by,

$$\rho_v = \frac{3H^2}{8\pi G} \quad ; \quad V(\phi) = \lambda \left(|\phi|^2 - \eta^2 \right)^2 . \tag{6.3.3}$$

Our model posses three parameters, the de Sitter energy density ρ_v (or alternatively H) and the parameters that specify the string potential, λ and η. As we will show in the following, these parameters introduce three distinct scales, namely the de Sitter radius, the string core thickness and the induced spacetime horizon due to the gravitational interaction of the defect. We will comment more about each scale and their effect in our solutions as we proceed forward with our analysis.

The appropriate ansatz for the Euclidean metric of the instantons we are looking for should match the symmetries of the thin wall solution described. In other words our ansatz for the geometry should reduce itself to the simple instanton presented earlier in the thin wall limit. Therefore we are led to the following form of the metric,

$$ds_E^2 = dr^2 + a^2(r) \left(d\tau^2 + \sin^2 \tau \, d\chi^2 \right) + b(r)^2 d\theta^2 , \tag{6.3.4}$$

where $a(r)$ and $b(r)$ are scale factors and we take $0 \leq \tau \leq \pi$ and $0 \leq \chi, \theta \leq 2\pi$. We also parametrize the complex scalar field as:

$$\phi = \varphi(r) e^{i\theta} \tag{6.3.5}$$

where θ is the angle describing the S^1 part of the geometry in Eq. (6.3.4). Note that with this ansatz the string worldsheet is parametrized by the (τ, χ) coordinates and describes a S_2 sphere, as in the thin wall limit, while the (r, θ) part of the geometry represents the $2d$ manifold perpendicular to the string. Furthermore the scalar field ansatz is consistent with the presence of a vortex configuration around the region where $b(r) \to 0$ and its particular form assumes that the vortex winding number is one[4]. This is the position of the center of our global string.

[4]Here we will focus our discussion in the unit winding number. There is in principle no impediment to find similar solutions to higher winding numbers.

The Euclidean action can be calculated by inserting the ansantz (6.3.4) in (6.3.1). It is straightforward to show that action becomes,

$$S_E^G = -\frac{\pi}{G}\int dr\left[b\left(a'^2+1\right)+2aa'b'-3H^2a^2b\right]+S_b\ , \tag{6.3.6}$$

where we carried out the angular integration and also derived a boundary term as a result of the integration by parts:

$$S_b = \frac{\pi}{G}\left[\frac{d}{dr}\left(a^2b\right)\right]\ . \tag{6.3.7}$$

At this point we will not specify the integration bounds for the radial component r, but in the proceeding sections it will be explicitly defined as the string core up to the deformed de Sitter horizon. We proceed by evaluating the string Euclidean action in the same manner:

$$S_E^s = 8\pi^2\int dra^2b\left[\varphi'^2+\frac{\varphi^2}{b^2}+V(\varphi)\right]\ . \tag{6.3.8}$$

The action comprises of three terms, namely the kinetic energy of the massive (radial) mode of the scalar field, its potential and the gradient, which appears due to the coupling to the massless Goldstone. We note that the latter contributes logarithmically to the energy momentum tensor necessitating a physical cutoff for the computation of the string tension in asymptotically flat space [150].

The Euclidean equations of motion are derived by the varying the above expressions with respect to $a(r)$, $b(r)$ and $\varphi(r)$. The result of this procedure yields :

$$2aa''+a'^2-1+3H^2a^2=-8\pi Ga^2\left(\varphi'^2-\frac{\varphi^2}{b^2}+V(\varphi)\right)\ , \tag{6.3.9}$$

$$ab''+ba''+a'b'+3H^2ab=-8\pi Gab\left(\varphi'^2+\frac{\varphi^2}{b^2}+V(\varphi)\right)\ , \tag{6.3.10}$$

and

$$\varphi''+\left(\frac{b'}{b}+\frac{2a'}{a}\right)\varphi'=\frac{\varphi}{b^2}+\frac{1}{2}\left(\frac{\partial V}{\partial\varphi}\right)\ . \tag{6.3.11}$$

Finally, the Hamiltonian constraint equation reads:

$$a'^2+2aa'\frac{b'}{b}-1+3H^2a^2=8\pi Ga^2\left(\varphi'^2-\frac{\varphi^2}{b^2}-V(\varphi)\right) \tag{6.3.12}$$

Only three of the above equations are independent, as the constraint is essentially the integration of (6.3.9) and (6.3.10).

6.3.2 Boundary conditions

A key step in solving the equations given above is to impose appropriate boundary conditions that are consistent with the instantons we are looking for.

Let us first consider the $r = 0$ region with the following conditions,

$$a(0) = a_0 \ , \quad b(0) = 0 \ , \quad \phi(0) = 0 \ . \tag{6.3.13}$$

The fact that at $r = 0$ the function $b(r)$ vanishes and the field climbs to the top of the potential are clearly signaling that this region corresponds to the core of the global string. Additionally, the interpretation of the parameter a_0 becomes clear: it defines the size of the sphere representing the Euclidean worldsheet of the string span by the τ, χ coordinates.

On the other end of the range of the radial coordinate r, we impose

$$a(r_*) = 0 \ , \quad b(r_*) = b_* \ , \quad \varphi(r_*) = \varphi_* \ . \tag{6.3.14}$$

This choice is motivated by the case where the gravitational backreaction of the string is negligible. In this limit the manifold should be approximately given by de Sitter space. Indeed, there exists a simple vacuum solution with the same symmetry, which is essentially pure de Sitter space. In Appendix C.1, we provide a detailed discussion of this anisotropic formulation of de Sitter space and outline the corresponding boundary conditions for comparison with the current solution.

Finally we note that in order to ensure the absence of any singular behaviour of the metric we also need to impose

$$a'(r_*) = \pm 1 \ , \quad b'(r_*) = 0 \ , \quad a''(r_* = 0) \ \ , \tag{6.3.15}$$

as well as,

$$b'(0) = \pm 1 \ , \quad a'(0) = 0 \ , \quad b''(0) = 0 \ \ . \tag{6.3.16}$$

Furthermore, regularity of the equation of motion for ϕ imposes the condition:

$$\varphi'(r_*) = 0 \ . \tag{6.3.17}$$

Given these conditions, the regularity of the metric is guaranteed. In fact, one can show that the region $r = r_*$ is a horizon and the metric can be extended beyond this region in a smooth

way given these boundary conditions. We will comment on this fact later on in the paper.

6.4 Instanton solutions

The next step is to solve the above equations for different values of the parameters H, λ and η. In particular we plan to solve the following system of equations for the scale factors a, b and the field profile φ:

$$2aa'' + a'^2 - 1 + 3H^2a^2 = -8\pi Ga^2\left(\varphi'^2 - \frac{\varphi^2}{b^2} + \lambda\left(\varphi^2 - \eta^2\right)^2\right) , \tag{6.4.1}$$

$$\varphi'' + \left(\frac{b'}{b} + \frac{2a'}{a}\right)\varphi' = \frac{\varphi}{b^2} + \lambda\varphi\left(\varphi^2 - \eta^2\right) , \tag{6.4.2}$$

$$a'^2 + 2aa'\frac{b'}{b} - 1 + 3H^2a^2 = 8\pi Ga^2\left(\varphi'^2 - \frac{\varphi^2}{b^2} - \lambda\left(\varphi^2 - \eta^2\right)^2\right) . \tag{6.4.3}$$

For future reference, we will define the following dimensionless quantities that are related to our initial input parameters and possess straightforward physical interpretations. The classification of solutions will be based on the values of these parameters.

The first one is the squared of the ratio between the de Sitter horizon H^{-1} and the string core thickness $\delta = (\lambda\eta^2)^{-1/2}$,

$$C = \frac{\lambda\eta^2}{H^2} . \tag{6.4.4}$$

The other interesting quantity is a measure of the string's gravitational backreaction to the geometry, and is given by,

$$D = 8\pi G\eta^2 . \tag{6.4.5}$$

6.4.1 Nucleation in a flat background

As a first step, we study solutions of our system of equations for global strings in a flat background spacetime [5]. Accordingly, we set $H = 0$. For the sake of convenience we will rescale our variables in terms of the characteristic length scale, δ, and introduce the dimensionless description of the scalar field in terms of $y = \varphi/\eta$. This reduces the equations of motion to a

[5] We begin by studying these solutions to highlight the significant new gravitational effects that arise in the global string configurations. Additionally, as we will demonstrate later, these solutions can be interpreted as instantons in the context of quantum cosmology.

system dependent on a single parameter (D):

$$2aa'' + a'^2 - 1 = -Da^2\left(y'^2 - \frac{y^2}{b^2} + \left(y^2-1\right)^2\right) \tag{6.4.6}$$

$$y'' + \left(\frac{b'}{b} + \frac{2a'}{a}\right)y' = \frac{y}{b^2} + 2y\left(y^2-1\right) \tag{6.4.7}$$

$$a'^2 + 2aa'\frac{b'}{b} - 1 = Da^2\left(y'^2 - \frac{y^2}{b^2} - \left(y^2-1\right)^2\right) \tag{6.4.8}$$

where:

$$a \to \frac{a}{\delta}\ , \quad b \to \frac{b}{\delta}\ , \quad r \to \frac{r}{\delta} \tag{6.4.9}$$

It is important to note, that the above system does not differ qualitatively from the de Sitter case we will present later on. The backreaction of a global string to the geometry induces the presence of a horizon, even in the absence of a background positive cosmological constant. As such, we can proceed with numerically solving the system with the same boundary conditions as in the de Sitter case for the string core and horizon.

This effect has previously been identified in the Lorentzian formulation of spacetime surrounding a global string. In that context, it has been shown that the energy-momentum tensor associated with the winding mode around the string prevents the existence of a smooth, static, singularity-free spacetime [160]. This issue is resolved by allowing the induced metric on the global string to become time-dependent, specifically adopting a de Sitter-like form for the string worldsheet [161]. Our Euclidean configuration can be understood as the analytic continuation of such a solution, where the de Sitter-like configuration is mapped into a sphere representing the string's worldsheet in Euclidean space.

Although the mathematical structure of the solution is the same, our interpretation is quite different from the Lorentzian case. As we will discuss in detail, the flat-space solution can be understood as an instanton in quantum cosmology representing the nucleation of a universe from nothing with a global string—analogous to similar studies involving domain walls [162, 100, 163, 97, 72].

Before presenting the numerical solutions, we note that the current setup contains only two relevant length scales: the thickness of the string and the horizon distance induced by the string. It is therefore worthwhile to examine the behavior of the solutions as a function of these two scales.

In the limit where $D \to 0$, the horizon is pushed to infinity. This case can be interpreted as the regime where gravity is effectively decoupled, with the scalar field profile being localized in

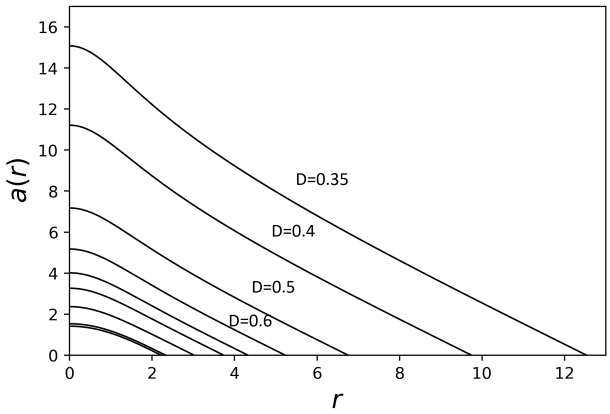

(a) Profiles $a(r)$ for different values of D

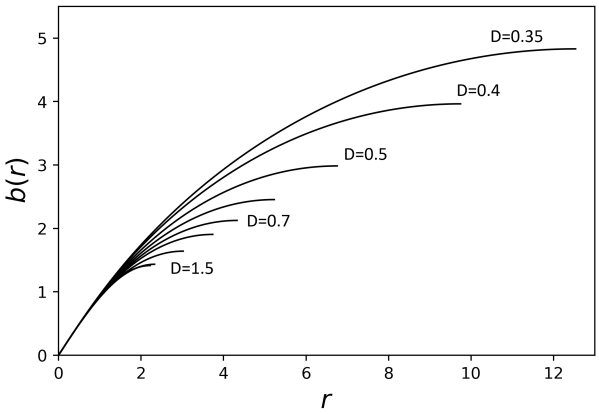

(b) Profiles $b(r)$ for different values of D

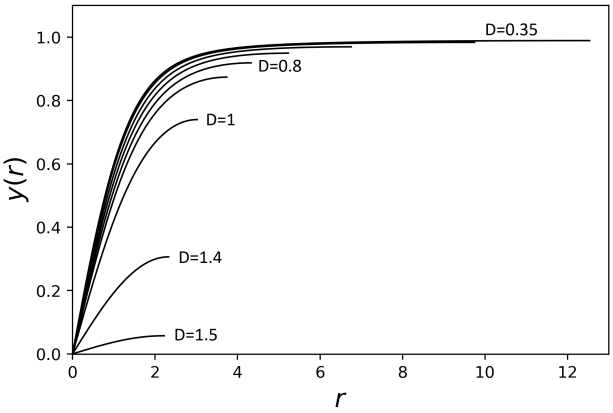

(c) Profiles $y(r)$ for different values of D

Figure 6.1: Plots of the profiles $a(r)$, $b(r)$ and $y(r)$ for varying D. We start with values of $D \to 3/2$ and decrease till $D \sim 0.1$. In the former case the geometry is equivalent to de Sitter and $y \approx 0$. As D decreases the horizon is pushed to larger and larger distances and the scalar field profile resembles the one in a fixed flat background.

a small region around the region $r \approx 0$. The horizon, being far removed, does not significantly influence the solution in this regime.

Conversely, in the limit where $D \sim \mathcal{O}(1)$, the horizon distance becomes comparable to the string thickness. In this region of the parameter space, the geometry is strongly distorted by the string, and the field profile approaches the top of the potential across the entire region. This leads to a solution of the Hawking-Moss type [**?**], corresponding to the regime of topological inflation, where the effective cosmological constant associated with the potential energy induces a horizon distance on the order of the string thickness [108, 109]. In this case, the field configuration becomes nearly homogeneous. We will discuss in detail and derive the condition for the appearance of the homogeneous instanton in Sec. 4.3 .

We begin by exploring the behavior of the geometry and the scalar field profile for different values of the coupling parameter D [6].The results are illustrated in Figs. 6.1 and 6.2.

For minimal backreaction, the scalar field approaches the solution obtained by solving the equations of motion in a fixed flat background. Specifically, the core region has $y \approx 0$, but the field eventually reaches its vacuum expectation value, $y \approx 1$, for most of the regime where $r > 1$. However, as expected, the gravitational effect of the coupling between the vortex and the long-range Goldstone mode still induces a cosmological horizon, although it is displaced far from the string core whenever $D \ll 1$.

[6]As previously mentioned, it is crucial to impose the correct boundary conditions to obtain the desired solutions. This necessitates the use of specific numerical methods to avoid potential numerical singularities. The detailed description of these methods is provided in Appendix C.2, while in the following sections we just focus on the description of the solutions obtained using those techniques.

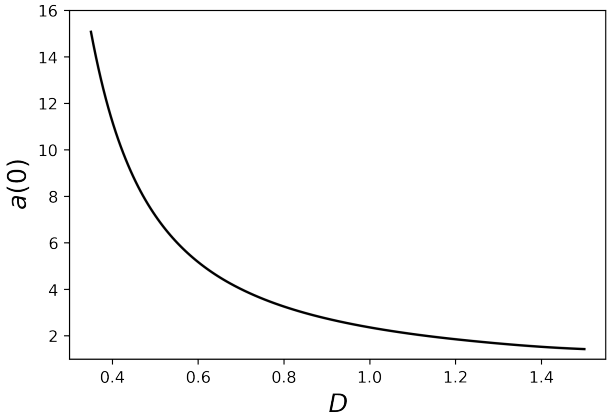

(a) Plot of $a(0)$ vs D

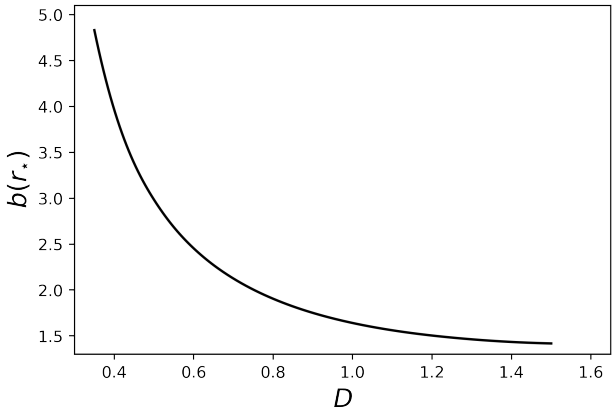

(b) Plot of $b(r^*)$ vs D

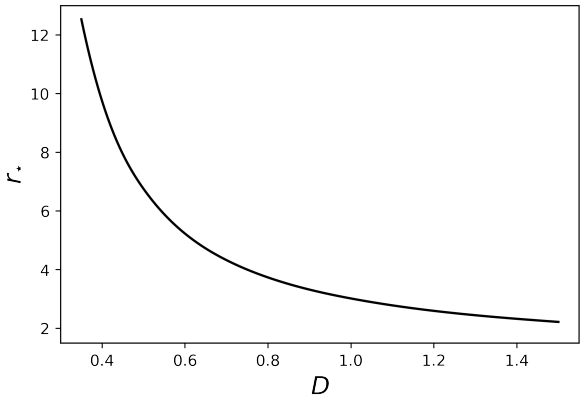

(c) Plot of r_* vs D

Figure 6.2: Plots of a_0, b_* and r_* in terms of D. As $D \to \frac{3}{2}$ we approach the Hawking-Moss configuration. For $D \sim 0.1$ the scale factors and the radial displacement grow since we approach the flat space solution.

When the coupling parameter D increases, the string distorts the geometry substantially rendering it effectively with the same structure as the anisotropic de Sitter discussed in Appendix C.1. In the marginal case where $D \approx 3/2$, the cosmological horizon is pushed inward, reaching the string core. As a result, the configuration becomes homogeneous, with $y \approx 0$ and a de Sitter background geometry.

Furthermore, we examine the geometrical distortions that the coupling D induces. As expected, for $D \to 0$ the range of a and b are much larger than the size of the defect. As the system couples more strongly to the background, and approaches its limiting case where $D = 3/2$, the geometry gradually compactifies with the radial displacement approaching the core of the vortex. See Figs. 6.2.

6.4.2 Nucleation in a de Sitter background

Let us now consider the instanton solutions representing the nucleation of global strings in an external de Sitter background. First, we rescale the variables again, this time by the following transformations,

$$a \to Ha \ , \quad b \to Hb \ , \quad r \to Hr \ , \tag{6.4.10}$$

essentially measuring the lengths in terms of de Sitter units. With this rescaling the system of equations takes the form:

$$2aa'' + a'^2 - 1 + 3a^2 = -Da^2 \left(y'^2 - \frac{y^2}{b^2} + C\left(y^2 - 1\right)^2 \right) \ , \tag{6.4.11}$$

$$y'' + \left(\frac{b'}{b} + \frac{2a'}{a} \right) y' = \frac{y}{b^2} + 2Cy\left(y^2 - 1\right) \ , \tag{6.4.12}$$

$$a'^2 + 2aa'\frac{b'}{b} - 1 + 3a^2 = Da^2 \left(y'^2 - \frac{y^2}{b^2} - C\left(y^2 - 1\right)^2 \right) \ , \tag{6.4.13}$$

The interesting point about these equations is the simultaneous presence of three distinct length scales: the two previously discussed—the string thickness and the induced horizon scale—and the de Sitter horizon scale associated with a non-zero H. In the following section, we present some of the numerical solutions obtained, which provide deeper insight into the qualitative behavior of these instanton solutions across different regions of the parameter space.

In this section we obtain the solutions for different values of the parameters C and D and find once more the profiles $a(r)$, $b(r)$ and $y(r)$. An example is shown in Figs. 6.3 where we kept

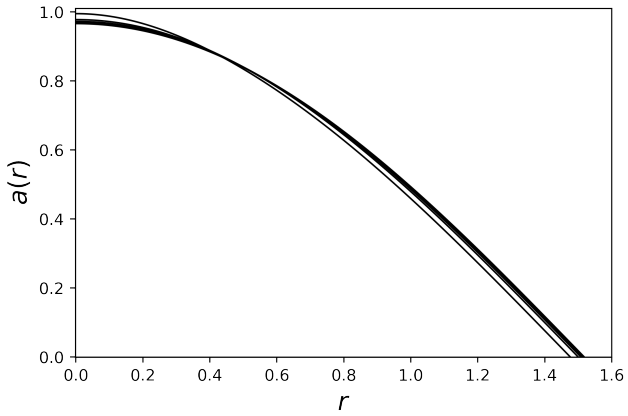

(a) Plot of $a(r)$ vs r for varying string thickness

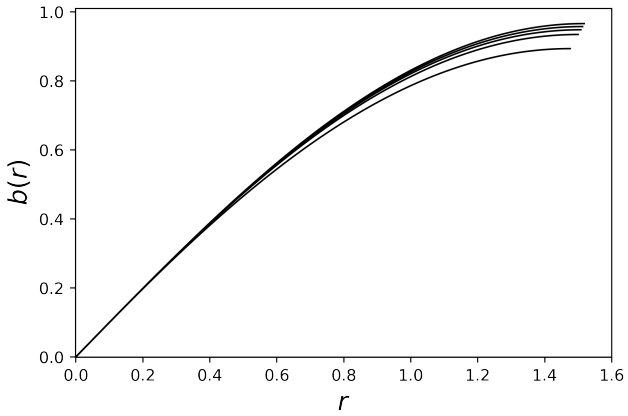

(b) Plot of $b(r)$ vs r for varying string thickness

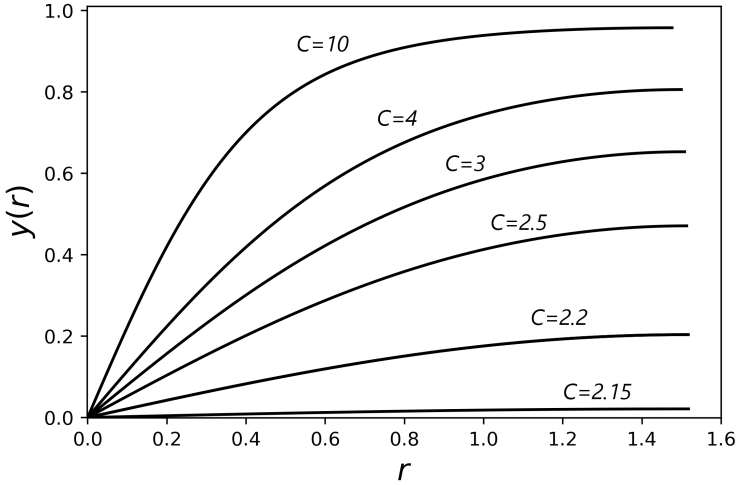

(c) Plot of the field profile $y(r)$ vs r for varying string thickness

Figure 6.3: Plots of the profiles $a(r)$, $b(r)$ and $y(r)$ for fixed backreaction $D = 0.1$ and varying thickness C^{-1}

the backreaction of the string to the geometry constant and relatively small, meaning we take $D = 0.1$, and varied the thickness of the vortex core relative to the Hubble scale. As expected, when the backreaction is minimal, the thickness does not significantly deform the geometry. This is evident by the fact that a_0 and b_* are relatively close to 1, the value corresponding to de Sitter geometry.

However, the field profile is substantially altered for varying string thickness. When the core is thin the field approaches rapidly the vacuum value $y \to 1$, while as the core thickens the field is closer to the maximum of the potential $y \approx 0$. There exists a threshold for the thickness after which the configuration is homogeneous with $y(r) \approx 0$. This occurs at a specific value of

the parameters C and D as we will show in the next subsection.

In order to probe the effect of the string backreaction to the geometry we kept the thickness fixed at $C = 10$ and varied the parameter D from zero, which corresponds to pure de Sitter, to $D = 1.2$ for which the homogeneous instanton appears. The distortion of the geometry is demonstrated in Fig. 6.4 where we plot the values a_0, b_* and r_* for the range of values of D. As expected, the scale factors acquire the maximum value at the de Sitter radius and shrink for increasing backreaction. The same is true for the range of the radial displacement r^*. Overall, the string gravity acts as to shrink the size of S^1 and S^2 parts of the metric.

Finally, we are interested in the value that the field acquires at the horizon $y(r^*)$ for different parameters C and D. As already illustrated, a thick defect results in the false vacuum covering most of Euclidean geometry inside the horizon. The same is true in the case of strong gravitational backreaction for which the location of the horizon is shifted closer to the core. In

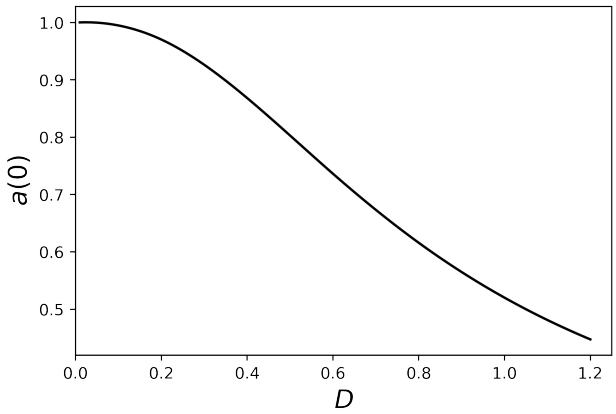

(a) Plot of $a(0)$ vs D

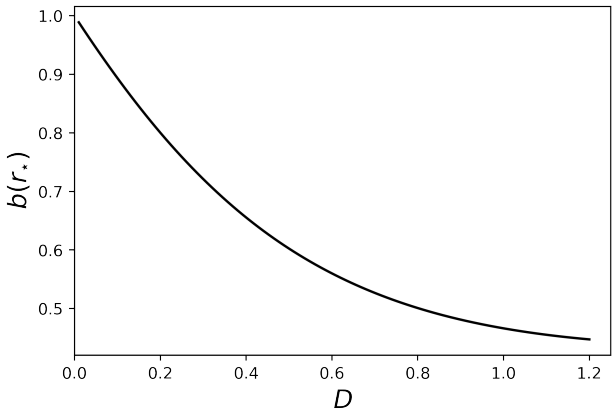

(b) Plot of $b(r^*)$ vs D

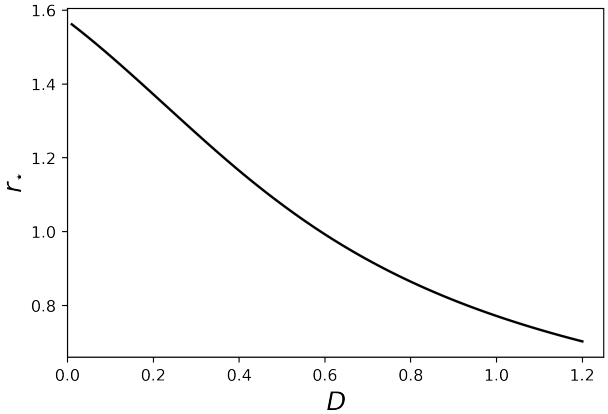

(c) Plot of r^* vs D

Figure 6.4: Plots of $a_0,\ b_*,\ r_*$ in terms of D. For no backreaction the geometry is pure de-Sitter while as D increases the instanton gets substatially distorted.

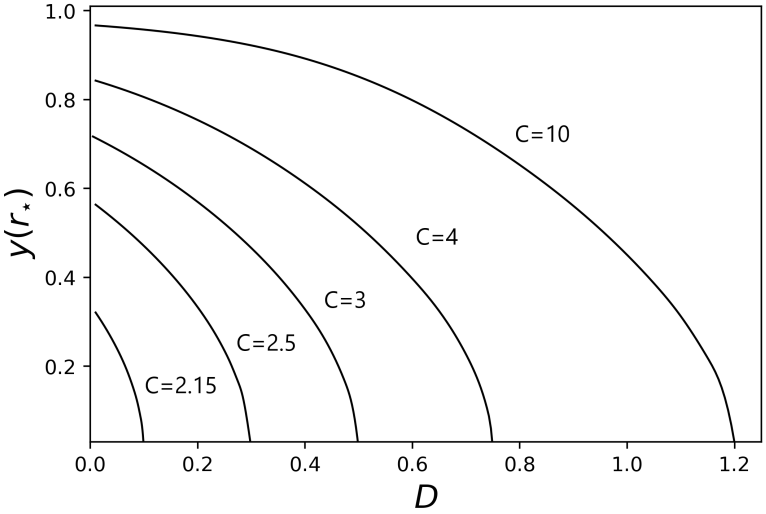

Figure 6.5: A plot of the field value at the horizon $y(r^*)$ with respect to D for different values of C.

.

both cases we expect $y(r^*)$ to be close to zero. On the other hand, in the absence of gravity and in the thin-defect limit $y(r^*)$ should be at the vacuum expectation value. The results are illustrated in Fig. 6.5

6.4.3 The homogeneous instanton

As shown in the previous examples there are some thresholds for the values for the parameters C and D for which the field is at the maximum $y = 0$ throughout the whole range of r. Here we will analytically study this regime and determine precisely the condition for the appearance of these homogeneous configurations. Let us start by taking equations (6.4.11) and (6.4.13) with the approximation $y \approx 0$ we have:

$$2aa'' + a'^2 - 1 + 3a^2\left(1 + \frac{CD}{3}\right) = 0 \ , \tag{6.4.14}$$

and

$$a'^2 + 2aa'\frac{b'}{b} - 1 + 3a^2\left(1 + \frac{CD}{3}\right) = 0 \ . \tag{6.4.15}$$

The above can be analytically solved for the scale factors a and b with the solutions being:

$$a = \frac{\cos\tilde{r}}{\sqrt{1+\frac{CD}{3}}} \ , \quad b = \frac{\sin\tilde{r}}{\sqrt{1+\frac{CD}{3}}} \ , \tag{6.4.16}$$

where $\tilde{r} = r\sqrt{1+\frac{CD}{3}}$ and its range is $\tilde{r} \in [0, \pi/2]$.

We now turn our attention to scalar field equation (6.4.12). Neglecting the quadratic term on the parenthesis of the right hand and inserting (6.4.16) we can arrive at:

$$\frac{d^2y}{d\tilde{r}^2} + \left(\frac{-2+3\cos^2\tilde{r}}{\cos\tilde{r}\sin\tilde{r}}\right)\frac{dy}{d\tilde{r}} - \left(\frac{1}{1-\cos^2\tilde{r}} - \frac{2C}{1+\frac{CD}{3}}\right)y = 0 \ . \tag{6.4.17}$$

Yet another change of variables $u = \cos^2\tilde{r}$ transforms the above the hypergeometric equation to the following form:

$$4u\,(1-u)\,\frac{d^2y}{du^2} + 2\,(3-5u)\,\frac{dy}{du} - \left(\frac{1}{1-u} - \frac{2c}{1+\frac{cd}{3}}\right)y = 0 \ . \tag{6.4.18}$$

The solution that satisfies the boundary condition at the horizon (6.3.17) is given up to a multiplicative factor by:

$$y(u) = {}_2F_1\,(\alpha, \beta, 3/2, u)\,\frac{1}{\sqrt{1-u}} \ , \tag{6.4.19}$$

where ${}_2F_1$ is the hypergeometric function and:

$$\alpha, \beta = \frac{1}{4}\left(1 \mp \sqrt{9 + \frac{8C}{1+CD/3}}\right) \ . \tag{6.4.20}$$

Making use of the hypergeometric identities, the solution (6.4.19) can be further expressed as:

$$y(u) \propto \frac{y_1(u) + y_2(u)}{\sqrt{1-u}} \ , \tag{6.4.21}$$

where:

$$y_1(u) = \frac{{}_2F_1(\alpha, \beta, 3/2, 1-u)}{\Gamma\left(\frac{3}{2}-\alpha\right)\Gamma\left(\frac{3}{2}-\beta\right)} \tag{6.4.22}$$

and

$$y_2(u) = \frac{\Gamma\left(\alpha+\beta-\frac{3}{2}\right)}{\Gamma(a)\Gamma(b)}\,(1-u)\,{}_2F_1(3/2-\alpha, 3/2-\beta, 2, 1-u) \ . \tag{6.4.23}$$

It is clear that in order for the solution to also satisfy the boundary condition $y(r=0) = 0$ at the core of the string, the first term should be absent[7]. This in turn means that either $3/2 - \alpha = -n$ or $3/2 - \beta = -n$ where $n = 0, 1, 2, 3....$ Selecting the lowest possible integer for

[7] One might worry that the coefficient in front of the second term diverges due to the factor $\Gamma(\alpha+\beta-\frac{3}{2})$, but this is not an issue because the final solution will be properly normalized.

which this is satisfied ($n = 0$) yields the constraint:

$$\frac{1}{C} + \frac{D}{3} = \frac{1}{2} \ . \tag{6.4.24}$$

This is precisely the condition for which homogeneous instanton appears. Neglecting gravity yields the familiar result $C = 2$. We note that for $C < 2$ there is no value of D that satisfies (6.4.24) and the same goes for $D > 3/2$. This is the parameter space for which the only acceptable solution is the homogeneous deSitter instanton.

The appearance of the homogeneous, Hawking-Moss like configuration can be given a simple physical interpetation. Let us consider the string thickness δ which in de-Sitter units is given by $\delta = 1/\sqrt{C}$. We expect the false vacuum of the core to cover all of space when the core size is similar to that of the horizon:

$$\delta \sim b_* \tag{6.4.25}$$

the expression for the horizon size b_* when we approach the homogeneous instanton is given by setting $\tilde{r} = \pi/2$ in (6.4.16). Inserting in (6.4.25) we obtain:

$$\frac{1}{\sqrt{C}} \sim \frac{1}{\sqrt{1 + \frac{CD}{3}}} \to \frac{1}{C} + \frac{D}{3} \sim 1 \tag{6.4.26}$$

which agrees with (6.4.24).

Thus, we can either increase the thickness C and expand the core all the way to the horizon, or increase the backreaction D and distort the geometry in a way that the horizon approaches the core.

6.5 Global structure and interpretation

6.5.1 Global structure of the geometry

As discussed previously, in certain regions of the parameter space of our model, the solutions are nearly indistinguishable from a pure de Sitter solution expressed in a specific slicing (see Appendix C.1 for details on the pure de Sitter solution in the relevant gauge for us.).

This observation suggests that, analogous to the procedure in pure de Sitter space, one can analytically continue the solution to a Lorentzian signature by taking the metric in the form:

$$ds_E^2 = dr^2 + a^2(r) \left(-dt^2 + \cosh^2 t \ d\chi^2 \right) + b(r)^2 d\theta^2 \ , \tag{6.5.1}$$

while the scalar field remains as in the Euclidean solution:

$$\phi = \varphi(r)e^{i\theta} \tag{6.5.2}$$

This analytic continuation does not alter the structure of the equations of motion, thus the numerical solutions presented earlier also apply to these Lorentzian configurations.

Furthermore, as in the pure de Sitter case, this solution can be extended beyond the horizon in a smooth manner by using a metric of the form:

$$ds^2 = H^{-2}\left[-dT^2 + \tilde{a}^2(T)\left(d\psi^2 + \sinh^2\psi\ d\chi^2\right) + \tilde{b}^2(T)d\theta^2\right]\ . \tag{6.5.3}$$

where the function $\tilde{a}^2(T)$ and $\tilde{b}^2(T)$ can be obtained from the equations of motion but their leading behaviour is fixed by imposing the smoothness of the horizon at $T \to 0$. This metric represents a cosmological spacetime with anisotropic spatial slices. Two of the dimensions correspond to an infinite open universe, while the angular coordinate θ parametrizes an S_1 component of the geometry. Moreover, the matter content in this universe is, once again, provided by a complex scalar field winding along the circle. Solutions of this type have been studied in the context of dimensional decompactification and anisotropic phases in the early universe [164].

It is important to note that this description of the spacetime remains valid even in the absence of a cosmological constant [161, 165]. As discussed earlier, the global spacetime structure of a global string in flat space is remarkably similar to the structure when a cosmological constant is included. The primary difference in these scenarios lies in the subsequent evolution of the spacetime.

In this work, we do not numerically evolve these configurations and instead just provide a brief discussion of the possible types of solutions. Depending on the parameter values in the model, a range of configurations can emerge, from pure flat space, which asymptotically approaches a Bianchi-type solution, to other solutions exhibiting a brief period of anisotropic inflation, and extending all the way to cases where eternal inflation occurs in the regime of topological inflation [108, 109].

6.5.2 Interpretation of the solutions

As discussed earlier, the solutions presented in this paper allow for a dual interpretation. On the one hand, they can be viewed as instantons describing the nucleation of global strings in

de Sitter space. In this context, these configurations and their subsequent evolution could be relevant to the early universe [154, 166].

Moreover, even in the absence of a cosmological constant, these configurations may have cosmological significance for a large value of D. For example, one could imagine a global string produced during inflation, which persists into later stages of the universe's evolution, when the energy density is much lower, making it effectively describable by solutions with $H = 0$ and obtained in Sec. 4.1 . The radial component of this metric resembles the solutions in the case of domain walls [156] so it is likely that a wormhole-like structure will develop in these situations as well. However, the angular component complicates this interpretation. We leave further exploration of this intriguing possibility for future work.

Alternatively, these solutions can be interpreted in the framework of quantum cosmology. In this context, the universe could be created from "nothing", a process that can be described using gravitational instantons. The classic example of such creation is pure de Sitter space, where the corresponding instanton is the round Euclidean 4-sphere. Its analytic continuation results in the formation of a closed de Sitter universe [22].

In a more general scenario, one might consider including some form of matter content in the universe's creation process, such as topological defects like domain walls or strings. For instance, a model described in [72, 97] considered the creation of the universe with a domain wall wrapping around its equator, referred to as a "domain wall universe". Here, we have explored the existence of instantons with global strings.

A particularly interesting aspect of these solutions is the interpretation of the flat-space case ($H = 0$) as a quantum cosmology instanton. The structure of this solution indicates that one could contemplate the creation of a universe from nothing, even in the absence of a cosmological constant. Depending on the parameters of the model, it is also possible for these models to exhibit a period of anisotropic inflation in the region beyond the horizon. In that regard, these type of solutions give a motivation for the somewhat unnatural initial conditions of the universe in these models.

6.6 The euclidean action

6.6.1 The bounce action

The tunneling rate (6.2.10) evaluated in Sec. 1 is valid so long the the string core is sufficiently thin compared to the horizon and the gravitational effects of the coupling of the string to

the Goldstone mode are negligible. A more complete treatment of the nucleation process is achieved through the evaluation of the Euclidean action (6.3.6). The nucleation rate is given by the expression [159]:

$$P \sim e^{-B} \ , \tag{6.6.1}$$

where:

$$B = S_E - S_E^{dS} \ , \tag{6.6.2}$$

is the bounce action and $S_E^{dS} = -\pi/(GH^2)$ is the Euclidean de Sitter action. The above rate can be understood as the probability to nucleate a global string characterized by the parameters C and D in a de Sitter background of cosmological constant H^2.

In order to evaluate the Euclidean string action, we proceed by inserting the equation of motion (6.3.9) in (6.3.6) and perform integration. We arrive at:

$$S_E = \frac{\pi}{G}\left[\frac{d}{dr}\left(a^2 b\right) - 2aba'\right]_0^{r_*} + 16\pi^2 \int_0^{r_*} dr \frac{a^2}{b}\varphi^2 \ , \tag{6.6.3}$$

which can be recast as,

$$S_E = -\frac{\pi a_0^2}{G} + 16\pi^2 \int_0^{r_*} dr \frac{a^2}{b}\varphi^2 \tag{6.6.4}$$

after imposing the instanton boundary conditions presented in subsection 3.1. Finally, in the scaled variables the expression for the action is:

$$\tilde{S}_E = -a_0^2 + 2D \int_0^{r_*} \frac{a^2 y^2}{b} dr \ , \tag{6.6.5}$$

where $\tilde{S}_E = GH^2 S_E/\pi$ and a_0 is described in terms of the Hubble scale units. We note the presence of two terms. A geometric component that captures the gravitational sector and a contribution from the field profile responsible for the string dynamics. We note that the latter is positive and, for the most part, subdominant to the gravitational contribution. The action for the homogeneous configuration can be readily found by using (6.4.16) to express a_0. Setting $y = 0$ one arrives at:

$$\tilde{S}_E^{HM} = -\frac{1}{1 + \frac{CD}{3}} \tag{6.6.6}$$

It is evident from the above expression that the effective cosmological constant-in deSitter units- is $1 + CD/3$.

Overall, we compute the bounce action:

$$\tilde{B} = 1 - a_0^2 + 2D \int_0^{r_*} \frac{a^2 y^2}{b} dr \ , \tag{6.6.7}$$

As expected, the geometric "Gibbons-Hawking" contributions cancel out in the limit of minimal gravitational distortions. Furthermore, since $a_0 \leq 1$ the bounce is always positive and as a result the nucleation process is exponentially suppressed. The expression of the homogeneous bounce can be readily found by using (6.6.6) and (6.6.2):

$$\tilde{B}^{HM} = \frac{1}{1 + \frac{3}{CD}} \tag{6.6.8}$$

We plot the bounce action for several values of the parameters C and D in Fig.A.3. It is clear that the nucleation rate is enhanced for thick strings with minimal backreaction.

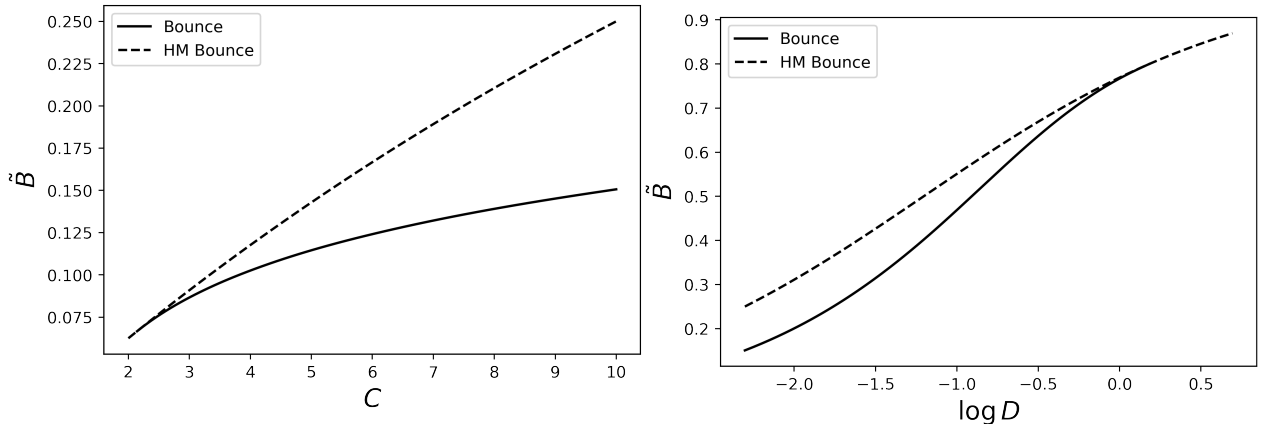

Figure 6.6: Plots of the bounce action, $\tilde{B}$, for different values of C and D, keeping $D = 0.1$ (Left) and $C = 10$ fixed (Right), respectively.

6.6.2 The creation of the global string universe from nothing

As discussed earlier, the instantons identified in this paper can also be interpreted within the framework of quantum cosmology. However, while the instantons themselves remain the same, the calculation of the probabilities for various processes depends on the specific prescription applied.

In this work, we adopt the tunneling wavefunction prescription to compare the creation of a homogeneous universe with that of a "global string universe". According to this approach, the nucleation probability is given by [79]:

$$P \sim e^{-|S_E|} \tag{6.6.9}$$

The computation of the Euclidean action suggests that the probability of forming a universe with a string may be lower than that of forming the homogeneous de Sitter universe at the top of the potential for the scalar field as shown in Fig.6.7. However, it will be preferred with respect to the formation of a pure de Sitter universe with scale H.

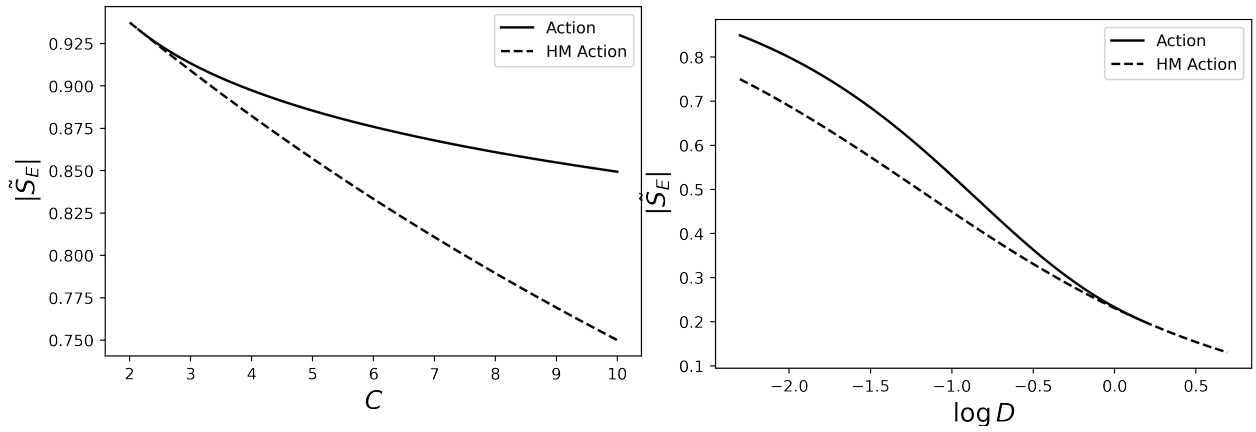

Figure 6.7: Plots of the Euclidean action for different values of C and D, keeping $D = 0.1$ and $C = 10$ fixed, respectively.

It is important to note, however, that this conclusion could be modified by a more detailed analysis of the quantum state of the scalar field in each of these scenarios. In particular, it was shown in [72] that the nucleation rate of a spherical universe with a scalar field governed by a hilltop potential undergoes a sharp transition when the curvature of the potential exceeds a certain threshold. This seems to suggest that the homogeneous instanton is not realized as a stable initial state for a certain regime of the parameter space $\{C, D\}$ and the inhomogeneous global string configuration is the only viable nucleation channel. We leave the exploration of this subtlety for future work.

6.7 Conclusions

In this work we provided a complete treatment of the global string instantons. Strings along with other topological defects can spontaneously nucleate at a continuous rate during the inflationary period and as such reach appreciable number densities in our local horizon. The nucleation process occurs as quantum mechanical tunneling of a defect into a horizon size object that

is later stretched by the expansion of the universe. The rate for such a process is governed by the defect instanton which is a two parameter function: the core thickness relative to the horizon, C^{-1}, and the gravitational backreaction on the de Sitter background geometry, D. The instanton analysis has been carried out in [92, 93] in the case of domain walls, while strings and monopoles were only studied in the analytically accessible limits. Here we continued this work and provide a complete treatment of the global string instantons for the whole range of relevant parameters C and D.

We initiate our analysis by considering a complex scalar field, ϕ, with a "Mexican hat" potential, representing a global string loop embedded in an Euclidean background spacetime. The instanton equations of motion, together with the Hamiltonian constraint, are derived for the field profile φ and the scale factors a and b that parametrize the metric. We then numerically solve this system across a wide range of parameters of the underlying model, ensuring regularity conditions that guarantee a smooth 4-geometry. The boundary conditions governing these solutions turns these equations into a boundary value problem, which can be addressed using multiple shooting methods.

We present results for the field profile $\varphi(r)$ and the scale factors $a(r)$ and $b(r)$ across different string core thicknesses. While the core size does not significantly alter the overall geometry, it does influence the range of values for the field profile φ. We also examine the impact of varying gravitational backreaction. When gravitational effects become significant, the resulting distortion of the geometry causes the horizon to shift closer to the string core. In both cases, we identify a regime in which the potential's maximum extends across the entire Euclidean space up to the horizon, resembling a homogeneous Hawking-Moss configuration.

We also discuss the analytic continuation of these solutions to Lorentzian signature. Our analysis reveals that the solutions describe global string loops expanding with an induced metric corresponding to a 2-dimensional de Sitter space. This result is in agreement with the nucleation process described in the thin wall approximation. Additionally, the global structure of these gravitational instantons can be extended beyond the horizon of the Euclidean geometry. Unlike the open universe geometries typical of Coleman-de Luccia (CdL) instantons, the creation of these global strings leads to the formation of a region with the structure of an anisotropic FRW universe. This anisotropy arises due to the reduced symmetry of the instanton caused by the presence of the string, resulting in distinct initial conditions. Beyond the horizon, the universe exhibits an open $2+1$ dimensional structure with an expanding compact dimension wound by the phase of the scalar field present in our model.

Finally, we also comment on the possible implications of the instantons described in this

work to Quantum Cosmology. Similar to the nucleation of strings in de Sitter space, these instantons also describe the creation of an anisotropic universe from nothing. This suggests a connection between the presence of the axionic Goldstone mode and the creation of anisotropic universes. In this context, the solutions provide a natural explanation for the specific initial conditions in these spacetimes, offering some insight into the origin of such anisotropies which otherwise may seem arbitrary.

Acknowledgments

We are grateful to Jaume Garriga, Asier Lopez-Eiguren, Ken D. Olum and Oriol Pujolas for stimulating discussion. G. F. acknowledges support from the Constantine and Patricia Mavroyannis fellowship and the John F. Burlingame fellowship. J.J.B.-P. has been supported in part by the PID2021-123703NB-C21 grant funded by MCIN/AEI/10.13039/501100011033/and by ERDF;“ A way of making Europe”; the Basque Government grant (IT-1628-22) and the Basque Foundation for Science (IKERBASQUE).

Chapter 7

Future directions

7.1 Eternal inflation and anthropic selection

Inflationary cosmology has impressive observational support and at this time there seem to be no viable alternatives. It seems reasonable therefore to assume that the swampland criteria, whatever their final form will be, must be consistent with slow-roll inflation. It is possible for example that the constants c, c' in Eq. (2.1.3) have somewhat smaller values, e.g., $\sim 0.1 - 0.01$ [167]. This would be compatible with slow-roll inflation, even though the possible form of the inflaton potential would be strongly restricted. Depending on the values of c and $\tilde{c}$, quantum random walk of the inflaton field and the associated eternal inflation may or may not be excluded [168, 169, 170]. Some authors have even suggested that regardless of the validity of any specific form of the swampland conjecture, eternal inflation may be forbidden by some fundamental principle [171, 172, 89]. As stated in the introduction we take an agnostic approach towards these views. However, let's assume for a moment that stochastic eternal inflation is forbidden. The most probable scenario is then a domain wall universe whose walls will inflate indefinitely spawning new inflationary regions [97]. It would be interesting to explore the issues related to anthropic selection and to the measure problem in this new kind of multiverse.

The spacetime structure of a domain wall universe is depicted in Fig. 7 of [97]. In that scenario, the inflaton is assumed to roll down to an AdS minimum after inflation. An alternative possibility is that it instead settles in a Minkowski vacuum. In either case, dark energy is expected to arise from a quintessence field. We are interested in models that include additional scalar fields beyond the inflaton. These extra fields will generally exhibit spatial variation on the thermalization surface—the spacelike hypersurface marking the end of inflation. Probabilities for such field configurations can be computed using the method developed in [38] and [173].

Notably, this approach avoids the need for a global time cutoff, thereby evading the standard measure problem. It also circumvents issues such as the overproduction of Boltzmann brains and paradoxes like those raised by Guth-Vanchurin and Olum [174]. However, a potential drawback is that the resulting probabilities scale with the amount of inflationary expansion, which grows exponentially with certain potential parameters. This can lead to runaway behavior, such as the so-called "Q-catastrophe" [175]. To study the probability distributions of dark energy and density fluctuations, one can consider simple two-field models. A minimal example involves an auxiliary field χ that influences only the post-inflationary quintessence dynamics. For further insights and related developments, see [35] and [86], as well as more recent literature.

7.2 Kantowski-Sachs quantum cosmology

In our work we applied the formalism of quantum cosmology to the anisotropic Kantowski-Sachs (KS) model with spatial topology $S^1 \times S^2$ and a positive cosmological constant. To obtain a probability distribution for the initial state of this topology we calculated the gravitational path integral with appropriate boundary conditions. Our methods were based on Picard–Lefschetz theory of complex contour integration. The results indicate that for Hartle-Hawking boundary conditions the prediction is an ensemble of classical universes with highly anisotropic spatial sections, even on a local scale. On the other hand, the tunneling approach to quantum cosmology favors global anisotropies that are smoothed on local scales due to inflation.

It would be interesting to extend our analysis by including a homogeneous scalar field ϕ, replacing the cosmological constant with a slowly varying potential $V(\phi)$. In the case of S^3 topology, the tunneling wave function is peaked at the highest maximum of the potential [103]. This is due to the exponential suppression in the classically forbidden region; hence in the KS model the situation is likely to be different. A similar extension of the de Sitter model resulted in a replacement of the nucleation probability (4.5.58) by a probability distribution for ϕ at nucleation:

$$dP(\phi) \propto F(\phi) d\phi, \tag{7.2.1}$$

where $F(\phi)$ is given by (4.5.58) with H^2 replaced by $8\pi V(\phi)$. This suggests that in the KS model such an extension would yield

$$dP(\phi) \sim V(\phi) d\phi. \tag{7.2.2}$$

A first investigation in this direction was carried out by Laflamme [114], but the probability

distribution for the inflaton field was not calculated and the analysis was restricted to the HH state.

Another interesting extension would be to study a "mini-superspace" model, including perturbatively an infinite number of inhomogeneous modes of a quantum field. In the de Sitter model one finds that the universe nucleates with the field in a de Sitter invariant Bunch-Davies state, and in a more realistic model this initial state may lead to a nearly scale-invariant spectrum of density fluctuations, in agreement with observations. On the other hand, in the KS model the initial quantum state will not have de Sitter, and not even rotational symmetry. It is possible however that the field will approach the Bunch-Davies state at late times in the course of inflation, due to the no-hair "theorem" (e.g., [176]). Furthermore, the inclusion of inhomogeneous modes could in principle "smooth-out" the logarithmic singularity of the wavefunction found in Chapter 4. It is also quite possible that the probability distribution (4.5.57) will be altered, since it depends strongly on the prefactor structure.

7.3 Jackiw-Teitelboim gravity

In chapter 5, we established a "1-1" mapping of the 4D KS model to the 2D Jackiw Teitelboim (JT) gravity toy-model. The latter has gathered the attention of theorists as a safe arena to study the gravitational path integral. Utilizing the "1-1" correspondence we were able to obtain a normalizable probability distribution for the wavefunction of the JT model. Notably, similar explorations in the literature are plagued by divergent distributions which warrant further examination.

It is perhaps not surprising that the wave function we found using the boundary condition of smooth closure does not exhibit Schwarzian asymptotic behavior. An obvious reason is that our analysis was restricted to minisuperspace, so the Schwarzian degrees of freedom were not included. On the other hand, Iliesiu *et al* [133] argued that the minisuperspace wave function is simply related to the wave functional of full JT gravity. This issue needs to be better understood. Another possibility is that the condition of smoothness (absence of a conical singularity) at $a = 0$ is too restrictive. We know that the metrics contributing to the path integral are generally rather irregular, so the Hartle-Hawking proposal of integrating over smooth metrics should not be taken too literally. Finally, the Schwarzian boundary condition was imposed in Ref.[133] assuming that the dynamics of the boundary curve at large a are completely decoupled from the geometry at small a. It is conceivable, however, that the decoupling is incomplete, so the conditions of closure and maybe smoothness modify the asymptotic behavior of Ψ_{HH}.

In this paper we utilized the familiar $4D$ minisuperspace framework in order to explore the closely related JT quantum cosmology and to define the corresponding HH wave function. Due to the simplicity of JT theory, one can hope that with better understanding the relation between the two models will be reversed and JT cosmology will provide important insights for the $4D$ case. Towards this goal, it would be interesting to do a path integral calculation of Ψ_{HH} directly in JT model, without a reference to KS and without using the minisuperspace truncation. This would help to understand the Schwarzian issue that we referred to above. It would also be interesting to define the tunneling wave function in the JT model. We hope to return to these problems in future work.

7.4 Instantons

In our final work, we explored the nucleation of global strings through quantum mechanical tunneling. The instantons that describe the nucleation process are characterized by two parameters: the string core thickness and its gravitational backreaction to the geometry. We obtained solutions across a wide range of these parameters by carrying out numerical integration via multiple shooting methods, a non-trivial computational technique.

The extension of these solutions beyond the horizon of the Euclidean geometry describe an anisotropic FRW universe. Interestingly, these solutions bear similarities to other configurations found in the literature, particularly in the context of extra dimensions [177, 178, 179]. Specifically, these instanton solutions can be seen as 4-dimensional analogs of the "Bubbles from Nothing" scenarios discussed in the framework of flux compactifications [180]. In those models, the solution terminates on an expanding brane, which in our case corresponds to the vortex core. Following this connection with higher dimensional solutions, it would be interesting to explore whether similar solutions exist in spacetimes with a negative cosmological constant that resemble the ones obtained already in the litearature (See for example [178] or [181]).

Furthermore, we comment on the instanton solutions obtained and their relevance in the context of quantum cosmology. The nucleation process describes the creation of loops of string in a background deSitter space. However, the same instanton describes the creation of a universe out of nothing with a closed global string in it. Here "nothing" is a state of no classical spacetime. It was shown in [72] that given a multifield potential with a maximum the homogeneous configuration will be the dominant nucleation channel as long as $V''/V < 2$. For larger values of steepness and depending on the number of field components of the underlying theory the nucleation process yields a domain wall universe ,for 1-field, a global string or a global

monopole. Thus, it seems that the fact the the string action is less then the homogeneous is irrelevant since the latter becomes unstable when the former channel appears. We plan to explore this ambiguity in the future.

Finally, we leave the case of nucleation of monopole-antimonopole pairs for future work, but we expect the qualitative analysis to follow that of domain wall and global string nucleation.

7.5 Final remarks

In this thesis, we tried to present a complete cosmological picture. The Universe is proposed to originate from "nothing", a state devoid of spacetime and energy, containing only the abstract framework of physical laws. As an analogy, one might think of preparing a full-course meal with no ingredients—only a recipe. In a similar spirit, A. Guth famously described inflation as the *"ultimate free lunch"*. Yet, despite the appeal of this scenario, the origin of the physical laws themselves remains a mystery. S. W. Hawking captured this puzzle by asking: *"What is it that breathes fire into the equations and makes a universe for them to describe?"* This question remains one of the deepest and most unresolved in theoretical physics.

Following its quantum birth, the Universe enters the inflationary stage and continues to expand eternally. In our local patch, inflation came to an end, giving rise to a hot Big Bang. The subsequent evolution is well described by the standard cosmological model, which reliably traces the Universe's history up to the present. Nevertheless, numerous puzzles remain, most notably the nature of dark matter and dark energy, which dominate the late-time dynamics.

Although much of our discussion has focused on advanced topics of interest to specialists, we emphasize that the core principles of physics are accessible and conceptually elegant. The real challenge lies in the details, which, though subtle and intricate, are essential for a full understanding. It is our hope that readers, regardless of their background, will come away with an appreciation for the fundamental picture we have outlined.

Appendix A

Appendix for Chapter 2

A.1 Anomalous behavior of $n = 1, 2$ modes

We noted at the end of Sec. 3.2 that the homogeneous mode $n = 1$ violates regularity on the growing branch and the dipole mode $n = 2$ violates regularity on the decaying branch. The latter violation occurs in an intermediate range of a for $1.9 \lesssim \mu < 2$ (see Fig.A.1). We will argue that these violations are not necessarily dangerous, after discussing a related issue below.

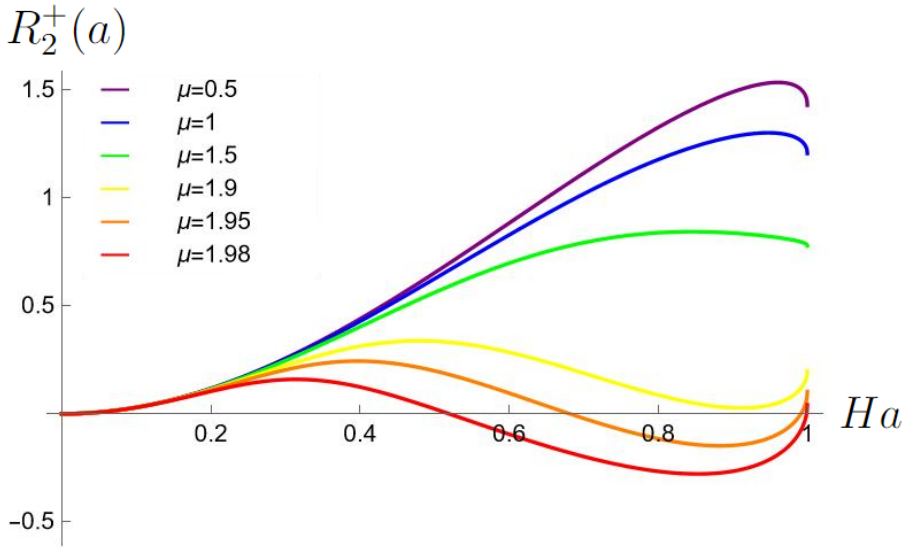

Figure A.1: A plot of $R_2^+(a)$ for several values of μ. Lower curves correspond to higher values of μ, with the yellow curve which nearly violates regularity corresponding to $\mu = 1.9$.

Our selection of the mode functions in Eq.(2.4.30) was partly based on the analysis of the growing branch of the wave function $\Psi_-(a, \phi_n)$. However, this branch is exponentially

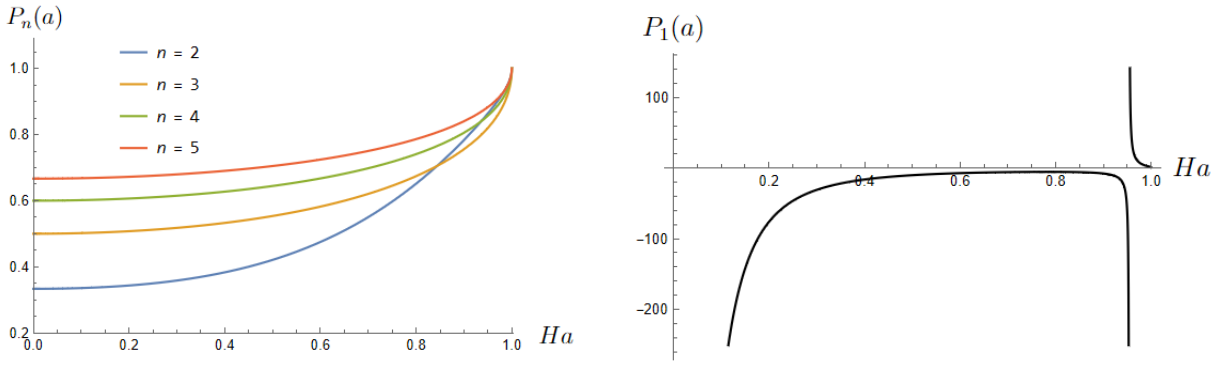

(a) (b)

Figure A.2: A plot of $P_n(a)$ in the entire Euclidean region for the modes $n = 1, 2, 3, 4, 5$ and $\mu = 3/2$.

suppressed compared to the decreasing branch (at $\phi_n = 0$), so keeping it while we neglect larger corrections to the WKB formula requires some justification. This issue was addressed in Refs.[102, 104] with the following argument. First note that the growing and decreasing branches have comparable magnitudes near the turning point, $Ha \sim 1$, so keeping the growing branch is justified in this range. Furthermore, it was argued in [104] that

$$P_n(a) \equiv \frac{R_n^-(a)}{R_n^+(a)} < 1 \tag{A.1.1}$$

in the entire classically forbidden region $Ha < 1$. This means that the function $\Psi_+(a, \phi_n)$ decreases with ϕ_n exponentially faster than $\Psi_-(a, \phi_n)$, and therefore Ψ_- dominates at sufficiently large ϕ_n. We thus have a continuous domain in the $\{a, \phi_n\}$ superspace, ranging from $a = H^{-1}$ to $a = 0$, where Ψ_- is non-negligible compared to Ψ_+. The inclusion of the growing branch can therefore be extended all the way to $a = 0$. The condition (A.1.1) was verified near the turning point in Ref.[104]. Here we used numerical methods to extend this analysis to the entire range $Ha < 1$.

To illustrate the characteristic behavior of the ratio $P_n(a)$, we plotted it in Fig.A.2a in the Euclidean region $Ha < 1$ for the leading inhomogeneous modes with $\mu = 3/2$. It is always less than 1, apart from the turning point $Ha = 1$, where $P_n(H^{-1}) = 1$. By sampling different values of μ, we found that his behavior holds in the entire range of $\mu \in (0, 2)$ for all modes, with the following two exceptions. One exception is the homogeneous mode $n = 1$ which exhibits a segment adjacent to the turning point where $P_1(a) > 1$ for all $\mu > 0$ (see Fig.A.2b). The other is the dipole mode $n = 2$ which exhibits similar behavior for $\mu \gtrsim 1.6$ (see Fig.A.3).

For modes violating the condition (A.1.1), we cannot trust their behavior on the growing

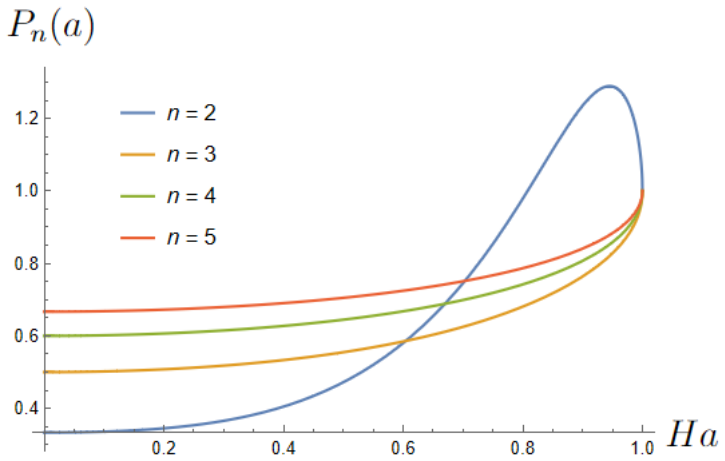

Figure A.3: A plot of $P_n(a)$ in the entire Euclidean region for the modes $n = 2, 3, 4, 5$ and $\mu = 1.75$.

branch in the classically forbidden region. For the homogeneous mode this means that violation of regularity by $R_1^-(a)$ may be spurious in this case. Note also that even if $R_1^-(a) < 0$ in some range of $a < H^{-1}$, this would not necessarily be a problem. The homogeneous mode on the growing branch behaves as the Hartle-Hawking wave function which has a minimum at the maximum of $V(\phi)$. This would not be problematic, as long as the growing branch remains subdominant.

For the dipole mode, violation of (A.1.1) implies that we could not have used regularity of $R_2^-(a)$ to select the mode function $\nu_2(a)$ for $\mu \gtrsim 1.6$. This suggests that in this range of μ a different dipole mode function could be selected which would satisfy the regularity condition. We have verified that this is indeed the case for mode functions (2.4.16) with a range of values of B_2/A_2. We note however that a specific value of B_2/A_2 is not selected in this case. The significance of the anomalous behavior of the dipole mode is not clear to us. This issue may require further study.

A.2 Field variance

In this section we will calculate the individual variances for each mode and the total variance of the field by determining the values of $Re(R_n(a))$. We will first consider the inhomogeneous modes $n > 1$. An explicit calculation yields:

$$Re(R_n(a)) = -\frac{Ha^3}{h_1 + h_2 + h_3} \tag{A.2.1}$$

where the functions h_i, $i = 1, 2, 3$ are given respectively by:

$$h_1 \sim (Ha)^{3+2\gamma} \frac{\Gamma(-1-\gamma+n)}{\Gamma(2+\gamma+n)}, \tag{A.2.2}$$

$$h_2 \sim 1, \tag{A.2.3}$$

$$h_3 \sim (Ha)^{-(3+2\gamma)} \frac{\Gamma(2+\gamma+n)}{\Gamma(-1-\gamma+n)}, \tag{A.2.4}$$

where we factored out $\mathcal{O}(1)$ terms independent of n and a.

For $n \gg 1$ we can use the asymptotics of Gamma functions to find

$$h_1 \sim \left(\frac{Ha}{n}\right)^{3+2\gamma}, \tag{A.2.5}$$

$$h_3 \sim \left(\frac{n}{Ha}\right)^{3+2\gamma}. \tag{A.2.6}$$

(Note that the range of interest for γ is $0 < \gamma < 1$.) It follows that for $n \ll n_* \sim Ha$ we have $h_1 \gg h_2, h_3$; hence we can drop h_2 and h_3 in Eq.(A.2.1). Then using Eqs.(2.5.14),(A.2.5) we obtain

$$\sigma_n^2 \sim H^2 n^{-3-2\gamma} (Ha)^{2\gamma}. \tag{A.2.7}$$

Since $\gamma > 0$, successive terms in the sum of Eq.(2.5.16) decrease faster than n^{-1}, and thus the sum is not sensitive to the cutoff n_*. For $n \sim n_*$, we have $h_1 \sim h_2 \sim h_3$, but this does not change the estimate (A.2.7) by order of magnitude. In any case, the estimate of σ_n at large n is unimportant, since the large-n terms give a negligible contribution to the sum.

Including now $O(1)$ factors, we find

$$\sigma_n^2 = \frac{\pi \Gamma(\gamma+2+n)}{4^{\gamma+1} |\Gamma(-\gamma-1+n)| \left[\Gamma\left(\gamma+\frac{3}{2}\right)\right]^2} \frac{(Ha)^{-2\gamma}}{H^2} \tag{A.2.8}$$

where the absolute value is necessary to include the homogeneous mode $n = 1$. To a good approximation we can extend the summation in Eq.(2.5.16) to $n \to \infty$. This gives

$$\sigma^2 \approx C H^2 (Ha)^{2\gamma}, \tag{A.2.9}$$

where

$$C = \frac{2^{1+2\gamma}}{\sin(\gamma\pi)} \frac{\left[\Gamma\left(\gamma+\frac{3}{2}\right)\right]^2}{\Gamma(\gamma+1)\Gamma(\gamma+3)} \tag{A.2.10}$$

Appendix B

Appendix for Chapter 3

B.1 Picard–Lefschetz theory

Picard-Lefschetz theory offers a systematic framework for evaluating oscillatory integrals of the form

$$I = \int_D dx\, e^{iS[x]/\hbar}, \tag{B.1.1}$$

where $S[x]$ is a real-valued function (the action), $\hbar$ is a small parameter, and D is a real domain of integration. These integrals arise naturally in the semiclassical analysis of quantum systems, particularly in quantum mechanics and cosmology. When $\hbar \to 0$, the integral becomes highly oscillatory, and naive numerical methods or saddle-point approximations can fail or become ambiguous. Picard-Lefschetz theory addresses this by deforming the original integration contour into the complex plane, where convergence and saddle-point contributions can be rigorously handled.

The key idea is to complexify the integration variable x and regard $S[x]$ as a holomorphic function on some domain in $\mathbb{C}$. By Cauchy's theorem, one is allowed to deform the original real contour D into a complex contour C, as long as the endpoints and singularities are appropriately handled. The goal is to deform the contour so that it passes through relevant *saddle points* of the action—points p_σ where $\partial_x S = 0$—along paths known as *Lefschetz thimbles* J_σ, where the integral is exponentially damped rather than oscillatory.

To make this precise, one rewrites the exponent $iS[x]/\hbar \equiv h + iH$ in terms of its real and imaginary parts. The function $h = \mathrm{Re}[iS/\hbar]$ acts as a *Morse function*, and the direction of

steepest descent is given by the gradient flow equations:

$$\frac{du^i}{d\lambda} = -g^{ij}\frac{\partial h}{\partial u^j}, \tag{B.1.2}$$

where u^i are real coordinates on the complexified space and g^{ij} is a Riemannian metric. Along this flow, h decreases monotonically while the imaginary part $H = \mathrm{Im}[iS/\hbar]$ remains conserved. This conservation implies that the integrand, originally a rapidly oscillating function on D, becomes exponentially suppressed along the flow lines. As a result, the integral over each thimble J_σ converges absolutely.

Each critical point also defines an *upward flow* (or dual cycle) K_σ, defined by reversing the gradient flow direction. The *intersection number* between J_σ and $K_{\sigma'}$ is topological and satisfies

$$\mathrm{Int}(J_\sigma, K_{\sigma'}) = \delta_{\sigma\sigma'}, \tag{B.1.3}$$

which establishes a duality between the thimbles and their upward flow counterparts. One can then express the deformed contour C as a linear combination of thimbles:

$$C = \sum_\sigma n_\sigma J_\sigma, \tag{B.1.4}$$

with integer coefficients $n_\sigma \in \{0, \pm 1\}$, determined by the intersection of the original contour D with K_σ. This means a given saddle contributes to the integral if its associated upward flow intersects the original real axis.

In one-dimensional integrals relevant for minisuperspace quantum cosmology, such as

$$I = \int_0^\infty \frac{dN}{\sqrt{N}} e^{if(N)/\hbar}, \tag{B.1.5}$$

the integrand often has singularities at $N = 0$ and $N = \infty$, and $f(N)$ is typically a holomorphic function. Using change-of-variable arguments and bounding the integrals along arcs near the singularities, one can show that the original contour along the real axis may be deformed into a combination of steepest descent contours. Specifically, the contributions from arcs at large N or small N vanish in the respective limits, ensuring that the original and deformed integrals agree.

Once the deformation is performed, the original oscillatory integral is expressed as a *sum*

over thimbles, each yielding an absolutely convergent integral:

$$I = \sum_{\sigma} n_\sigma \int_{J_\sigma} dx\, e^{iS[x]/\hbar}. \tag{B.1.6}$$

Each term can be expanded in $\hbar$ via the method of steepest descents, giving a semiclassical series:

$$\int_{J_\sigma} dx\, e^{iS[x]/\hbar} \approx e^{iS(p_\sigma)/\hbar} \left[A_\sigma + \mathcal{O}(\hbar)\right], \tag{B.1.7}$$

where A_σ is the leading-order Gaussian contribution near the saddle p_σ.

This decomposition makes precise how multiple saddle points can contribute to the Lorentzian path integral in quantum cosmology. It also clarifies why the Lorentzian contour—unlike the Euclidean one—typically picks up contributions from multiple complex saddles, with no exponential suppression. The Picard-Lefschetz framework thus provides a robust, non-perturbative foundation for interpreting semiclassical path integrals in gravitational theories.

B.2 Higher order corrections

The rescaled action of Eq.(4.5.10) can be split into two components. The first is $\tilde{S}_{E0} = \tilde{S}_E(bH = 1)$ and the second depends linearly on $(1 - H^2b^2)$. Specifically, using the definitions for $\tilde{S}_E, \tilde{N}, u$ and defining $v = H^2b^2$ we can decompose the action in the following way:

$$\tilde{S}_E = \left(-\frac{2\tilde{N}}{3} - \frac{u}{\tilde{N}} - \frac{(\tilde{N}^2+3u)^2}{12\tilde{N}^2(\tilde{N}-3)}\right) + \left(\frac{\tilde{N}}{3} - \frac{u}{\tilde{N}} - \frac{(\tilde{N}^2+3u)^2}{12\tilde{N}^2(\tilde{N}-3)}\right)(v-1) \tag{A.1}$$

Note that this expression is exact and not an expansion to first order in $(1 - H^2b^2)$.

Setting $v = 1$ in the action (A.1) and taking a derivative with respect to $\tilde{N}$, we obtain Eq.(4.5.24) for the saddles. These are the saddles of the zeroth order action $\tilde{S}_{E0}$. We will refer to the 5 solutions of this equation as $\tilde{N}_i$ with $i = \{1, 2, 3, 4, 5\}$.

It can be shown that if we introduce a perturbation x as in Eq.(3.3.41), $\tilde{N} = \tilde{N}_i + x$, the action is extremized for

$$x = \left(\frac{1-v}{2v}\right)\frac{1}{f(\tilde{N}_i, u)} + \frac{1}{v}h(\tilde{N}_i, u) \tag{A.2}$$

where the function h vanishes at all saddles $\tilde{N}_i$. Thus the perturbed saddles will be given by

$$\tilde{N}_i^\star = \tilde{N}_i + \left(\frac{1-v}{2v}\right)\frac{1}{f(\tilde{N}_i, u)} \tag{A.3}$$

Setting $\tilde{N} = \tilde{N}_i^\star$ in the action (A.1) and expanding to 2nd order in $(1 - v)$ we notice the

following. The 0-th order term does not depend on the function f, as expected. The 1st order term takes the form

$$\left[\left(\frac{\tilde{N}_i}{3}-\frac{u}{\tilde{N}_i}-\frac{(\tilde{N}_i^2+3u)^2}{12\tilde{N}_i^2(\tilde{N}_i-3)}\right)+\frac{3}{8f(\tilde{N}_i,u)}\frac{\left(\tilde{N}_i^2-2\tilde{N}_i+u\right)\left(\tilde{N}_i^3-4\tilde{N}_i^2-3\tilde{N}_iu+6u\right)}{(\tilde{N}_i-3)^2\tilde{N}_i^3}\right](v-1) \tag{A.4}$$

From (4.5.24) we see that the term depending on f vanishes. Thus, the action up to first order corrections is

$$\tilde{S}_E=\left(-\frac{2\tilde{N}_i}{3}-\frac{u}{\tilde{N}_i}-\frac{(\tilde{N}_i^2+3u)^2}{12\tilde{N}_i^2(\tilde{N}_i-3)}\right)+\left(\frac{\tilde{N}_i}{3}-\frac{u}{\tilde{N}_i}-\frac{(\tilde{N}_i^2+3u)^2}{12\tilde{N}_i^2(\tilde{N}_i-3)}\right)(v-1)+\mathcal{O}\left[(1-v)^2\right] \tag{A.5}$$

This equation is the same as Eq.(A.1) with $\tilde{N}=\tilde{N}_i$. This means that the 1st order corrections to the action are obtained by finding the saddles for $v=1$ and inserting them into the action for $v\neq 1$. The perturbed saddles contribute only to 2nd order and higher corrections to the action. Note that we did not make any specification for which saddle we are referring to. This analysis is true for all 5 saddles.

In the classically allowed region the contributing saddles for the Hartle-Hawking solution are N_1, N_2. In this regime the function $f(N_{1,2}, a)$ is given by

$$f(N_{1,2})=\frac{3(1-H^2a^2)}{2\pm 2i\sqrt{H^2a^2-1}\pm iH^2a^2\sqrt{H^2a^2-1}} \tag{A.6}$$

Thus, the first order correction to the saddles with respect to $(1-Hb)$ is given by

$$H^2N_{1,2}=1\pm i\sqrt{H^2a^2-1}-(1-Hb)\left(\frac{2\pm 2i\sqrt{H^2a^2-1}\pm iH^2a^2\sqrt{H^2a^2-1}}{3(H^2a^2-1)}\right) \tag{A.7}$$

and the action evaluated at $N_{1,2}$ up to second order corrections is

$$S_E(N_{1,2})\approx S_{E1}(N_{1,2})-\frac{\pi(1-Hb)^2}{3H^2}\left(\frac{2\pm 2i\sqrt{H^2a^2-1}\pm iH^2a^2\sqrt{H^2a^2-1}}{1-H^2a^2}\right) \tag{A.8}$$

where $S_{E1}(N_{1,2})$ is the action evaluated at $N_{1,2}$ up to first order corrections in $(1-Hb)$. From the above we can specify the coefficient function $F(a)$ in Eq. (3.4.4) as

$$F(a)=\frac{\pi}{3H^2}\left(\frac{2\pm 2i\sqrt{H^2a^2-1}\pm iH^2a^2\sqrt{H^2a^2-1}}{1-H^2a^2}\right) \tag{A.9}$$

Its real part is

$$\mathrm{Re}F(a) = \frac{2\pi}{3H^2(1-H^2a^2)} \tag{A.10}$$

Appendix C

Appendix for Chapter 6

C.1 Pure de Sitter space instanton

C.1.1 Euclidean de Sitter metric

In this Appendix we would like to describe the $4d$ Euclidean de Sitter space in a gauge which is particularly useful for the comparison with our instantons. As is well known 4d-Euclidean de Sitter space can be described as a $4d$ sphere of radius H^{-1} by embedding it in a 5-dimensional Euclidean space. Here we would like to do this by using the following coordinate system

$$t = H^{-1}\cos(r)\sin(\tau) \ , \tag{C.1.1}$$

$$w = H^{-1}\cos(r)\cos(\tau)\cos(\chi) \ , \tag{C.1.2}$$

$$z = H^{-1}\cos(r)\cos(\tau)\sin(\chi) \ , \tag{C.1.3}$$

$$x = H^{-1}\sin(r)\cos(\theta) \ , \tag{C.1.4}$$

$$y = H^{-1}\sin(r)\cos(\theta) \ , \tag{C.1.5}$$

which clearly satisfies the condition $t^2 + w^2 + x^2 + y^2 + z^2 = H^{-2}$. Therefore, this coordinate system represents a particular chart of a $4d$ Euclidean sphere with an induced metric of the form,

$$ds_E^2 = H^{-2}\left[dr^2 + \cos^2(r)\left(d\tau^2 + \sin^2\tau \ d\chi^2\right) + \sin^2(r)d\theta^2\right] \ . \tag{C.1.6}$$

We note that the form of this metric is consistent with the general ansatz we use to parametrize our instanton solution in Eq. (6.5.1). Moreover, as this metric corresponds to pure de Sitter space, it is manifestly regular, and the boundary conditions are fully consistent

with those imposed to ensure a smooth geometry in our general instanton solutions, as specified in Eqs. (6.3.14, 6.3.15, 6.3.16).

We adopt this slicing of de Sitter space as the reference metric for all global string instantons considered in this work. As demonstrated in the main text, there exist several distinct regions in the parameter space where the solutions closely approximate the pure de Sitter metric presented here. In other cases, while the geometry exhibits greater distortion, it retains its overall structure and satisfies the same boundary conditions.

C.1.2 Lorentzian continuation

We can analytically continue this metric to the Lorentzian signature to obtain a slicing of de Sitter space of the form,

$$ds^2 = H^{-2}\left[dr^2 + \cos^2(r)\left(-dt^2 + \cosh^2 t\ d\chi^2\right) + \sin^2(r)d\theta^2\right]\ . \tag{C.1.7}$$

This particular chart of de Sitter space exhibits a notable structure. If we momentarily disregard the angular part of the metric, the $d\theta$ part, it becomes apparent that the geometry closely resembles the Coleman-de Luccia (CdL) ansatz for a domain wall universe, but in a lower dimensional case, in 2+1 dimensions. Based on this, one might expect our $4d$ solution to exhibit two distinct horizons at the extremes of the radial coordinate as in the CdL geometry. However, in our 4-dimensional spacetime, this is not the case.

Specifically, while the geometry can indeed be extended beyond the region $r = \pi/2$ region, it terminates at the opposite end where the part of the geometry smoothly pinches off. This implies that our metric can only be extended beyond the horizon at $r = \pi/2$. The form of de Sitter space in this case can be written as

$$ds^2 = H^{-2}\left[-dT^2 + \sinh^2(T)\left(d\psi^2 + \sinh^2\psi\ d\chi^2\right) + \cosh^2(T)d\theta^2\right]\ . \tag{C.1.8}$$

which can be identify as cosmological but anisotropic slicing of de Sitter space [1]. As we discuss in the main part of the text, the instanton solutions we found in our field theory models with a global string have a similar global structure to the one explain here for the pure de Sitter space.

[1] One can recognize the Bianchi III form of this metric representing an initially anisotropic de Sitter space geometry. This type of geometry has been discussed in relation to anisotropic quantum tunneling in [164].

C.2 Numerical integration methods

The set of equations (6.4.1)-(6.4.3) will have to be integrated numerically for different values of the parameters C and D. Due to the nature of the boundary conditions the task belongs in the category of boundary value problems and a solution can be found via shooting methods. The general idea is to reduce the boundary value problem to an initial value one by guessing the values of the variables at one boundary, integrating and checking whether the boundary conditions at the other boundary are met. This procedure can be automated by utilizing optimization methods to determine the value of the shooting parameter for which the conditions at each boundary are satisfied.

A non-trivial characteristic of our system is the presence of two shooting parameters, a_0 and y_0', if we integrate from the core of the string, and b_* and y_* if we start from the horizon. Thus, we will have to resort to a multivariable optimization method such as Powell's hybrid method in order to determine the appropriate boundary values. We also note that since our system is autonomous we are free to integrate from either side while making the appropriate rescaling of the r-coordinate.

A further complication is the fact that both boundaries exhibit potential numerical singularities. Such singularities are not present analytically, but arise numerically at the boundaries of integration due to the presence of terms sensitive to large numerical cancelations. As a result shooting from one side is a highly unstable process. To better understand this obstacle consider that we pick the values of the shooting parameters at the horizon with a reasonably good precision and shoot towards the core. While the code runs it will gradually pick up computational error. Eventually, we want the integration to terminate once the boundary conditions are met. In particular this means once the condition $b_0 \to 0$ and $y \to 0$ is met with an acceptable accuracy. For equation (6.4.12) to yield consistent results we should expect a cancellation of the terms $b'y'/b - y/b^2$ which go symbolically as $\sim 1/0 - 1/0$. This is highly sensitive to the error accumulated during the calculation because even if b and y approach minuscule values, they might nevertheless differ by a few orders of magnitude. This results in the appearance of, at least, $\mathcal{O}(1)$ order terms which analytically should not be present. The same phenomenon is also present if we shoot from the core to the horizon. Thus, we need to figure a method that does not run into this issue.

Taking all this into consideration, we implemented a double shooting method which belongs in the broader category of multiple shooting [2]. The motivation behind multiple shooting is

[2]For a thorough analysis on multiple shooting methods in calculating tunneling rates see [182].

to split the integration interval in many sub-intervals so as to control the accumulation of error which depends exponentially on the amount of integration. The only compromise is that the shooting parameters multiply by the number of intervals we choose to split the initial range. In our case, we find it sufficient to shoot from both sides and match the solutions at an intermediate point. We first Taylor expand the equations near each boundary in order to deal with the singular behavior that arises in numerical integration. Using a Runge-Kutta method of order 8, denoted in Python as $DOP853$ we shoot towards one end and terminate once the scale factor a reaches ≈ 0.4, a value which is roughly half a_0 and sufficiently far away from each boundary. We then shoot from the latter boundary and terminate at the exact same point, which is not plagued by numerical singularities. The precision of our calculation is measured by taking the differences of all variables and their first and second derivatives at the meeting point. The shooting parameters at the core a_0, y_0' and at the horizon b_*, y_* are then determined by solving a 4×4 system at the midpoint using Powell's hybrid optimization method. Once the system has been solved, we are also able to obtain the location of the horizon r^*.

Bibliography

[1] E. Hubble, "A relation between distance and radial velocity among extra-galactic nebulae," Proc. Nat. Acad. Sci. **15**, 168-173 (1929)

[2] A. A. Penzias and R. W. Wilson, "A Measurement of excess antenna temperature at 4080-Mc/s," Astrophys. J. **142**, 419-421 (1965)

[3] V. C. Rubin and W. K. Ford, Jr., "Rotation of the Andromeda Nebula from a Spectroscopic Survey of Emission Regions," Astrophys. J. **159**, 379-403 (1970)

[4] A. G. Riess *et al.* [Supernova Search Team], "Observational evidence from supernovae for an accelerating universe and a cosmological constant," Astron. J. **116**, 1009-1038 (1998)

[5] S. Perlmutter *et al.* [Supernova Cosmology Project], "Measurements of Ω and Λ from 42 High Redshift Supernovae," Astrophys. J. **517**, 565-586 (1999)

[6] A. G. Riess, S. Casertano, W. Yuan, L. M. Macri and D. Scolnic, "Large Magellanic Cloud Cepheid Standards Provide a 1% Foundation for the Determination of the Hubble Constant and Stronger Evidence for Physics beyond ΛCDM," Astrophys. J. **876**, no.1, 85 (2019)

[7] N. Aghanim *et al.* [Planck], "Planck 2018 results. VI. Cosmological parameters," Astron. Astrophys. **641**, A6 (2020) [erratum: Astron. Astrophys. **652**, C4 (2021)]

[8] A. H. Guth, "The Inflationary Universe: A Possible Solution to the Horizon and Flatness Problems," Phys. Rev. D **23**, 347-356 (1981)

[9] A. A. Starobinsky, "A New Type of Isotropic Cosmological Models Without Singularity," Phys. Lett. B **91**, 99-102 (1980)

[10] S. R. Coleman, "The Fate of the False Vacuum. 1. Semiclassical Theory," Phys. Rev. D **15**, 2929-2936 (1977) [erratum: Phys. Rev. D **16**, 1248 (1977)]

[11] A. D. Linde, "A New Inflationary Universe Scenario: A Possible Solution of the Horizon, Flatness, Homogeneity, Isotropy and Primordial Monopole Problems," Phys. Lett. B **108**, 389-393 (1982)

[12] A. Albrecht and P. J. Steinhardt, "Cosmology for Grand Unified Theories with Radiatively Induced Symmetry Breaking," Phys. Rev. Lett. **48**, 1220-1223 (1982)

[13] A. D. Linde, "Chaotic Inflation," Phys. Lett. B **129**, 177-181 (1983)

[14] A. D. Linde, "Hybrid inflation," Phys. Rev. D **49**, 748-754 (1994)

[15] L. Randall, M. Soljacic and A. H. Guth, "Supernatural inflation," [arXiv:hep-ph/9601296 [hep-ph]]

[16] A. H. Guth, "Inflation and eternal inflation," Phys. Rept. **333**, 555-574 (2000)

[17] V. F. Mukhanov and G. V. Chibisov, "Quantum Fluctuations and a Nonsingular Universe," JETP Lett. **33**, 532-535 (1981)

[18] A. H. Guth and S. Y. Pi, "Fluctuations in the New Inflationary Universe," Phys. Rev. Lett. **49**, 1110-1113 (1982)

[19] J. M. Bardeen, P. J. Steinhardt and M. S. Turner, "Spontaneous Creation of Almost Scale - Free Density Perturbations in an Inflationary Universe," Phys. Rev. D **28**, 679 (1983)

[20] V. F. Mukhanov, H. A. Feldman and R. H. Brandenberger, "Theory of cosmological perturbations. Part 1. Classical perturbations. Part 2. Quantum theory of perturbations. Part 3. Extensions," Phys. Rept. **215**, 203-333 (1992)

[21] P. J. Steinhardt,"NATURAL INFLATION," UPR-0198T.

[22] A. Vilenkin, "The Birth of Inflationary Universes," Phys. Rev. D **27**, 2848 (1983)

[23] A. D. Linde, "ETERNALLY EXISTING SELFREPRODUCING INFLATIONARY UNIVERSE," Phys. Scripta T **15**, 169 (1987)

[24] A. H. Guth and S. Y. Pi, "The Quantum Mechanics of the Scalar Field in the New Inflationary Universe," Phys. Rev. D **32**, 1899-1920 (1985)

[25] A. H. Guth, "Eternal inflation and its implications," J. Phys. A **40**, 6811-6826 (2007)

[26] A. A. Starobinsky, "Dynamics of Phase Transition in the New Inflationary Universe Scenario and Generation of Perturbations," Phys. Lett. B **117**, 175-178 (1982)

[27] A. Vilenkin and L. H. Ford, "Gravitational Effects upon Cosmological Phase Transitions," Phys. Rev. D **26**, 1231 (1982)

[28] A. D. Linde, "Scalar Field Fluctuations in Expanding Universe and the New Inflationary Universe Scenario," Phys. Lett. B **116**, 335-339 (1982)

[29] B. Freivogel, M. Kleban, M. Rodriguez Martinez and L. Susskind, "Observational consequences of a landscape," JHEP **03**, 039 (2006)

[30] L. Susskind, "The Anthropic landscape of string theory," [arXiv:hep-th/0302219 [hep-th]]

[31] A. Vilenkin, "Predictions from quantum cosmology," Phys. Rev. Lett. **74**, 846-849 (1995) doi:10.1103/PhysRevLett.74.846

[32] V. Vanchurin, A. Vilenkin and S. Winitzki, "Predictability crisis in inflationary cosmology and its resolution," Phys. Rev. D **61**, 083507 (2000)

[33] A. Vilenkin, "Making predictions in eternally inflating universe," Phys. Rev. D **52**, 3365-3374 (1995)

[34] A. De Simone, A. H. Guth, A. D. Linde, M. Noorbala, M. P. Salem and A. Vilenkin, "Boltzmann brains and the scale-factor cutoff measure of the multiverse," Phys. Rev. D **82**, 063520 (2010)

[35] J. Garriga and A. Vilenkin, "On likely values of the cosmological constant," Phys. Rev. D **61**, 083502 (2000)

[36] J. Garriga, D. Schwartz-Perlov, A. Vilenkin and S. Winitzki, "Probabilities in the inflationary multiverse," JCAP **01**, 017 (2006)

[37] A. Vilenkin, "A Measure of the multiverse," J. Phys. A **40**, 6777 (2007)

[38] A. Vilenkin, "Unambiguous probabilities in an eternally inflating universe," Phys. Rev. Lett. **81**, 5501-5504 (1998)

[39] A. Linde and M. Noorbala, "Measure Problem for Eternal and Non-Eternal Inflation," JCAP **09**, 008 (2010)

[40] A. Borde and A. Vilenkin, "Eternal inflation and the initial singularity," Phys. Rev. Lett. **72**, 3305-3309 (1994)

[41] A. Borde, "Open and closed universes, initial singularities and inflation," Phys. Rev. D **50**, 3692-3702 (1994)

[42] A. Borde and A. Vilenkin, "Violations of the weak energy condition in inflating space-times," Phys. Rev. D **56**, 717-723 (1997)

[43] A. Borde, A. H. Guth and A. Vilenkin, "Inflationary space-times are incompletein past directions," Phys. Rev. Lett. **90**, 151301 (2003)

[44] S. M. Carroll,"In What Sense Is the Early Universe Fine-Tuned?," [arXiv:1406.3057 [astro-ph.CO]]

[45] S. M. Carroll,"Why Is There Something, Rather Than Nothing?," [arXiv:1802.02231 [physics.hist-ph]]

[46] J. J. Halliwell, "INTRODUCTORY LECTURES ON QUANTUM COSMOLOGY," [arXiv:0909.2566 [gr-qc]]

[47] J. B. Hartle, "Quantum cosmology: Problems for the 21st century," [arXiv:gr-qc/9701022 [gr-qc]]

[48] J. L. Lehners, "Review of the no-boundary wave function," Phys. Rept. **1022**, 1-82 (2023) doi:10.1016/j.physrep.2023.06.002

[49] R. L. Arnowitt, S. Deser and C. W. Misner, "Dynamical Structure and Definition of Energy in General Relativity," Phys. Rev. **116**, 1322-1330 (1959)

[50] P. A. M. Dirac, "The Theory of gravitation in Hamiltonian form," Proc. Roy. Soc. Lond. A **246**, 333-343 (1958)

[51] R. L. Arnowitt, S. Deser and C. W. Misner, "The Dynamics of general relativity," Gen. Rel. Grav. **40**, 1997-2027 (2008)

[52] P. A. M. Dirac, "Lectures on Quantum Mechanics," Belfer Graduate School of Science, Yeshiva University Press, New York (1964).

[53] J. A. Wheeler, "SUPERSPACE AND THE NATURE OF QUANTUM GEOMETRODYNAMICS," Adv. Ser. Astrophys. Cosmol. **3**, 27-92 (1987)

[54] B. S. DeWitt, "Quantum Theory of Gravity. 1. The Canonical Theory," Phys. Rev. **160**, 1113-1148 (1967)

[55] R. P. Feynman, "Space-time approach to non-relativistic quantum mechanics," Rev. Mod. Phys. **20**, 367–387 (1948).

[56] C. Teitelboim, "Quantum Mechanics of the Gravitational Field," Phys. Rev. D **25**, 3159 (1982)

[57] G. W. Gibbons and S. W. Hawking, "Action Integrals and Partition Functions in Quantum Gravity," Phys. Rev. D **15**, 2752-2756 (1977)

[58] S. W. Hawking, "THE PATH INTEGRAL APPROACH TO QUANTUM GRAVITY,"Part of General Relativity : An Einstein Centenary Survey, 746-789

[59] G. W. Gibbons, S. W. Hawking and M. J. Perry, "Path Integrals and the Indefiniteness of the Gravitational Action," Nucl. Phys. B **138**, 141-150 (1978)

[60] J. J. Halliwell and J. B. Hartle, "Integration Contours for the No Boundary Wave Function of the Universe," Phys. Rev. D **41**, 1815 (1990)

[61] J. J. Halliwell, "Derivation of the Wheeler-De Witt Equation from a Path Integral for Minisuperspace Models," Phys. Rev. D **38**, 2468 (1988)

[62] J. J. Halliwell and J. Louko, "Steepest Descent Contours in the Path Integral Approach to Quantum Cosmology. 1. The De Sitter Minisuperspace Model," Phys. Rev. D **39**, 2206 (1989)

[63] J. J. Halliwell and J. Louko, "Steepest Descent Contours in the Path Integral Approach to Quantum Cosmology. 2. Microsuperspace," Phys. Rev. D **40**, 1868 (1989)

[64] J. J. Halliwell and J. Louko, "Steepest Descent Contours in the Path Integral Approach to Quantum Cosmology. 3. A General Method With Applications to Anisotropic Minisuperspace Models," Phys. Rev. D **42**, 3997-4031 (1990)

[65] J. Feldbrugge, J. L. Lehners and N. Turok, "Lorentzian Quantum Cosmology," Phys. Rev. D **95**, no.10, 103508 (2017)

[66] J. B. Hartle and S. W. Hawking, "Wave Function of the Universe," Phys. Rev. D **28**, 2960-2975 (1983)

[67] A. Vilenkin, "Boundary Conditions in Quantum Cosmology,"Phys. Rev. D **33**, 3560 (1986)

[68] A. Vilenkin, "Approaches to quantum cosmology," Phys. Rev. D **50**, 2581-2594 (1994)

[69] C. Teitelboim, "Quantum mechanics of the gravitational field". Phys. Rev. D **25**, 3159–3179 (1982)

[70] E. P. Tryon, "Is the universe a vacuum fluctuation," Nature **246**, 396 (1973)

[71] A. Vilenkin, "The Interpretation of the Wave Function of the Universe," Phys. Rev. D **39**, 1116 (1989)

[72] G. Fanaras and A. Vilenkin, "Quantum cosmology, eternal inflation, and swampland conjectures,"JCAP **04**, 034 (2023)

[73] G. Fanaras and A. Vilenkin, "Jackiw-Teitelboim and Kantowski-Sachs quantum cosmology," JCAP **03**, no.03, 056 (2022)

[74] G. Fanaras and A. Vilenkin, "The tunneling wavefunction in Kantowski-Sachs quantum cosmology," JCAP **08**, 069 (2022)

[75] J. J. Blanco-Pillado, G. Fanaras and A. Vilenkin, "Global string instantons," JCAP **07**, 087 (2025)

[76] A. Vilenkin, "Creation of Universes from Nothing,"Phys. Lett. B **117**, 25-28 (1982)

[77] A. D. Linde, "Quantum Creation of the Inflationary Universe,"Lett. Nuovo Cim. **39**, 401-405 (1984)

[78] V. A. Rubakov, "Quantum Mechanics in the Tunneling Universe,"Phys. Lett. B **148**, 280-286 (1984)

[79] A. Vilenkin,"Quantum Creation of Universes,"Phys. Rev. D **30**, 509-511 (1984)

[80] Y. B. Zeldovich and A. A. Starobinsky, "Quantum creation of a universe in a nontrivial topology,"Sov. Astron. Lett. **10**, 135 (1984)

[81] A. Vilenkin and M. Yamada, "Tunneling wave function of the universe,"Phys. Rev. D **98**, no.6, 066003 (2018)

[82] A. D. Linde, "Eternally Existing Selfreproducing Chaotic Inflationary Universe,"Phys. Lett. B **175**, 395-400 (1986)

[83] A. A. Starobinsky, "STOCHASTIC DE SITTER (INFLATIONARY) STAGE IN THE EARLY UNIVERSE,"Lect. Notes Phys. **246**, 107-126 (1986) doi:10.1007/3-540-16452-9_6

[84] M. Aryal and A. Vilenkin,"The Fractal Dimension of Inflationary Universe,"Phys. Lett. B **199**, 351-357 (1987)

[85] G. Obied, H. Ooguri, L. Spodyneiko and C. Vafa,"De Sitter Space and the Swampland,"[arXiv:1806.08362 [hep-th]].

[86] P. Agrawal, G. Obied, P. J. Steinhardt and C. Vafa,"On the Cosmological Implications of the String Swampland,"Phys. Lett. B **784**, 271-276 (2018)

[87] S. K. Garg and C. Krishnan, "Bounds on Slow Roll and the de Sitter Swampland,"JHEP **11**, 075 (2019)

[88] H. Ooguri, E. Palti, G. Shiu and C. Vafa,"Distance and de Sitter Conjectures on the Swampland,"Phys. Lett. B **788**, 180-184 (2019)

[89] T. Rudelius, "Conditions for (No) Eternal Inflation,"JCAP **08**, 009 (2019)

[90] W. H. Kinney, "Eternal Inflation and the Refined Swampland Conjecture,"Phys. Rev. Lett. **122**, no.8, 081302 (2019)

[91] G. Barenboim, W. I. Park and W. H. Kinney,"Eternal Hilltop Inflation,"JCAP **05**, 030 (2016)

[92] R. Basu, A. H. Guth and A. Vilenkin, "Quantum creation of topological defects during inflation,"Phys. Rev. D **44**, 340-351 (1991)

[93] R. Basu and A. Vilenkin,"Nucleation of thick topological defects during inflation,"Phys. Rev. D **46**, 2345-2354 (1992)

[94] S. R. Coleman and F. De Luccia, "Gravitational Effects on and of Vacuum Decay,"Phys. Rev. D **21**, 3305 (1980)

[95] S. W. Hawking and I. G. Moss, "Supercooled Phase Transitions in the Very Early Universe,"Phys. Lett. B **110**, 35-38 (1982)

[96] D. A. Samuel and W. A. Hiscock, "Effect of gravity on false vacuum decay rates for O(4) symmetric bubble nucleation,"Phys. Rev. D **44**, 3052-3061 (1991)

[97] J. J. Blanco-Pillado, H. Deng and A. Vilenkin, "Eternal Inflation in Swampy Landscapes,"JCAP **05**, 014 (2020)

[98] R. Basu and A. Vilenkin, "Evolution of topological defects during inflation,"Phys. Rev. D **50**, 7150-7153 (1994)

[99] F. Bonjour, C. Charmousis and R. Gregory, "Thick domain wall universes," Class. Quant. Grav. **16**, 2427-2445 (1999)

[100] J. Ipser and P. Sikivie, "The Gravitationally Repulsive Domain Wall,"Phys. Rev. D **30**, 712 (1984)

[101] L. F. Abbott and S. R. Coleman, "The Collapse of an Anti-de Sitter Bubble,"Nucl. Phys. B **259**, 170-174 (1985)

[102] T. Vachaspati and A. Vilenkin, "On the Uniqueness of the Tunneling Wave Function of the Universe,"Phys. Rev. D **37**, 898 (1988)

[103] A. Vilenkin, "Quantum Cosmology and the Initial State of the Universe,"Phys. Rev. D **37**, 888 (1988)

[104] S. J. Wang, M. Yamada and A. Vilenkin, "Constraints on non-minimal coupling from quantum cosmology,"JCAP **08**, 025 (2019)

[105] T. Damour and A. Vilenkin, "Quantum instability of an oscillating universe,"Phys. Rev. D **100**, no.8, 083525 (2019)

[106] J. Garriga and A. Vilenkin, "In defense of the 'tunneling' wave function of the universe,"Phys. Rev. D **56**, 2464-2468 (1997)

[107] A. D. Linde,"Monopoles as big as a universe," Phys. Lett. B **327**, 208-213 (1994)

[108] A. Vilenkin,"Topological inflation," Phys. Rev. Lett. **72**, 3137-3140 (1994)

[109] A. D. Linde and D. A. Linde,"Topological defects as seeds for eternal inflation," Phys. Rev. D **50**, 2456-2468 (1994)

[110] R. Kantowski and R. K. Sachs, "Some spatially homogeneous anisotropic relativistic cosmological models," J. Math. Phys. **7**, 443 (1966)

[111] H. Nariai, "On a New Cosmological Solution of Einstein's Field Equations of Gravitation". General Relativity and Gravitation, **31(6)**, 963–971 (1999)

[112] P. H. Ginsparg and M. J. Perry, "Semiclassical Perdurance of de Sitter Space," Nucl. Phys. B **222**, 245-268 (1983)

[113] R. Bousso and S. W. Hawking, "Pair creation of black holes during inflation," Phys. Rev. D **54**, 6312-6322 (1996)

[114] R. Laflamme, "The wave function of a $S_1 \times S_2$ universe", Ph. D. Thesis, University of Cambridge (1986).

[115] H. D. Conradi, "Quantum cosmology of Kantowski-Sachs like models," Class. Quant. Grav. **12**, 2423-2440 (1995)

[116] D. Anninos, F. Denef and D. Harlow, "Wave function of Vasiliev's universe: A few slices thereof," Phys. Rev. D **88**, no.8, 084049 (2013)

[117] G. Conti and T. Hertog, "Two wave functions and dS/CFT on $S^1 \times S^2$," JHEP **06**, 101 (2015)

[118] Schulman, L. S. (2005). *Techniques and Applications of Path Integration* (Dover Books on Physics) (Illustrated ed.). Dover Publications.

[119] J. H. Van Vleck, "The Correspondence Principle in the Statistical Interpretation of Quantum Mechanics," Proc. Nat. Acad. Sci. **14**, 178-188 (1928)

[120] C. Morette, "On the Definition and Approximation of Feynman's Path Integrals," Phys. Rev. **81**, 848 (1951)

[121] J. J. Halliwell, J. B. Hartle and T. Hertog, "What is the No-Boundary Wave Function of the Universe?," Phys. Rev. D **99**, no.4, 043526 (2019)

[122] A. O. Barvinsky and A. Y. Kamenshchik, "Cosmological landscape from nothing: Some like it hot," JCAP **09**, 014 (2006)

[123] G. Fanaras and A. Vilenkin, "Jackiw-Teitelboim and Kantowski-Sachs quantum cosmology," JCAP **03**, no.03, 056 (2022)

[124] J. Louko, "Canonizing the Hartle-hawking Proposal," Phys. Lett. B **202**, 201-206 (1988)

[125] J. Louko and T. Vachaspati, "On the Vilenkin Boundary Condition Proposal in Anisotropic Universes," Phys. Lett. B **223**, 21-25 (1989)

[126] R. C. Myers, "Higher Derivative Gravity, Surface Terms and String Theory," Phys. Rev. D **36**, 392 (1987)

[127] S. Chatterjee and M. Parikh, "The second law in four-dimensional Einstein-Gauss-Bonnet gravity," Class. Quant. Grav. **31**, 155007 (2014).

[128] B. Zwiebach, "Curvature Squared Terms and String Theories," Phys. Lett. B **156**, 315-317 (1985)

[129] R. Jackiw, "Lower Dimensional Gravity," Nucl. Phys. B **252**, 343-356 (1985)

[130] C. Teitelboim, "Gravitation and Hamiltonian Structure in Two Space-Time Dimensions," Phys. Lett. B **126**, 41-45 (1983)

[131] M. Henneaux, "Quantum Gravity in Two-Dimensions: Exact Solution of the Jackiw Model" Phys. Rev. Lett. **54**, 959-962 (1985)

[132] J. Maldacena, G. J. Turiaci and Z. Yang, "Two dimensional Nearly de Sitter gravity," JHEP **01**, 139 (2021)

[133] L. V. Iliesiu, J. Kruthoff, G. J. Turiaci and H. Verlinde, "JT gravity at finite cutoff," SciPost Phys. **9**, 023 (2020)

[134] U. Moitra, S. K. Sake and S. P. Trivedi, "Jackiw-Teitelboim gravity in the second order formalism," JHEP **10**, 204 (2021)

[135] D. Stanford and Z. Yang, "Finite-cutoff JT gravity and self-avoiding loops," arXiv:2004.08005 [hep-th]

[136] A. Fabbri, D. J. Navarro and J. Navarro-Salas, "Quantum evolution of near extremal Reissner-Nordstrom black holes," Nucl. Phys. B **595**, 381-401 (2001)

[137] R. Bousso, "Quantum global structure of de Sitter space," Phys. Rev. D **60**, 063503 (1999)

[138] D. Stanford and E. Witten, "Fermionic Localization of the Schwarzian Theory," JHEP **10**, 008 (2017)

[139] D. Louis-Martinez, J. Gegenberg and G. Kunstatter, "Exact Dirac quantization of all 2-D dilaton gravity theories," Phys. Lett. B **321**, 193-198 (1994)

[140] M. Tegmark, "What does inflation really predict?," JCAP **04**, 001 (2005)

[141] H. Georgi and S. L. Glashow, "Unity of All Elementary Particle Forces,"Phys. Rev. Lett. **32**, 438-441 (1974)

[142] H. Georgi, H. R. Quinn and S. Weinberg, "Hierarchy of Interactions in Unified Gauge Theories,"Phys. Rev. Lett. **33**, 451-454 (1974)

[143] G. 't Hooft, "Magnetic Monopoles in Unified Gauge Theories,"Nucl. Phys. B **79**, 276-284 (1974)

[144] A. M. Polyakov, "Particle Spectrum in Quantum Field Theory,"JETP Lett. **20**, 194-195 (1974)

[145] Y. B. Zeldovich and M. Y. Khlopov, "On the Concentration of Relic Magnetic Monopoles in the Universe,"Phys. Lett. B **79**, 239-241 (1978)

[146] J. Preskill, "Cosmological Production of Superheavy Magnetic Monopoles," Phys. Rev. Lett. **43** (1979), 1365

[147] T. W. B. Kibble, "Topology of Cosmic Domains and Strings," J. Phys. A **9** (1976), 1387-1398

[148] A. Vilenkin, "Cosmic Strings and Domain Walls,"Phys. Rept. **121**, 263-315 (1985)

[149] Y. B. Zeldovich, I. Y. Kobzarev and L. B. Okun, "Cosmological Consequences of the Spontaneous Breakdown of Discrete Symmetry," Zh. Eksp. Teor. Fiz. **67**, 3-11 (1974) SLAC-TRANS-0165

[150] A. Vilenkin and E. P. S. Shellard, Cambridge University Press, 2000, ISBN 978-0-521-65476-0

[151] R. L. Davis, Phys. Lett. B **180**, 225-230 (1986); A. Vilenkin and T. Vachaspati, Phys. Rev. D **35**, 1138 (1987); R. A. Battye and E. P. S. Shellard, Nucl. Phys. B **423**, 260-304 (1994); M. Yamaguchi, M. Kawasaki and J. Yokoyama, Phys. Rev. Lett. **82**, 4578-4581 (1999); C. Hagmann, S. Chang and P. Sikivie, Phys. Rev. D **63**, 125018 (2001); L. Fleury and G. D. Moore, JCAP **01**, 004 (2016); M. Gorghetto, E. Hardy and G. Villadoro, JHEP **07**, 151 (2018); C. J. A. P. Martins, Phys. Lett. B **788**, 147-151 (2019); A. Saurabh, T. Vachaspati and L. Pogosian, Phys. Rev. D **101**, no.8, 083522 (2020); M. Gorghetto, E. Hardy and G. Villadoro, SciPost Phys. **10**, no.2, 050 (2021); M. Hindmarsh, J. Lizarraga, A. Lopez-Eiguren and J. Urrestilla, Phys. Rev. D **103**, no.10, 103534 (2021); M. Buschmann, J. W. Foster, A. Hook, A. Peterson, D. E. Willcox, W. Zhang and B. R. Safdi, Nature Commun. **13**, no.1, 1049 (2022); A. Drew and E. P. S. Shellard, Phys. Rev. D **105**, no.6, 063517 (2022); A. Drew and E. P. S. Shellard, Phys. Rev. D **107**, no.4, 043507 (2023); J. J. Blanco-Pillado,

D. Jiménez-Aguilar, J. M. Queiruga and J. Urrestilla, JCAP **05**, 011 (2023); J. Baeza-Ballesteros, E. J. Copeland, D. G. Figueroa and J. Lizarraga, Phys. Rev. D **110**, no.4, 043522 (2024); A. Drew, T. Kinowski and E. P. S. Shellard, Phys. Rev. D **110**, no.4, 043513 (2024); K. Saikawa, J. Redondo, A. Vaquero and M. Kaltschmidt, [arXiv:2401.17253 [hep-ph]].

[152] F. Ferrer, E. Masso, G. Panico, O. Pujolas and F. Rompineve, "Primordial Black Holes from the QCD axion," Phys. Rev. Lett. **122** (2019) no.10, 101301.

[153] D. I. Dunsky and M. Kongsore, "Primordial black holes from axion domain wall collapse," JHEP **06** (2024), 198

[154] J. Garriga and A. Vilenkin, "Black holes from nucleating strings," Phys. Rev. D **47**, 3265-3274 (1993)

[155] J. Garriga, A. Vilenkin and J. Zhang, "Black holes and the multiverse," JCAP **02**, 064 (2016)

[156] H. Deng, J. Garriga and A. Vilenkin, "Primordial black hole and wormhole formation by domain walls," JCAP **04**, 050 (2017)

[157] R. Bousso and S. W. Hawking, "Lorentzian condition in quantum gravity,"Phys. Rev. D **59**, 103501 (1999) [erratum: Phys. Rev. D **60**, 109903 (1999)]

[158] S. Coleman, "Aspects of Symmetry: Selected Erice Lectures,"Cambridge University Press, 1985, ISBN 978-0-521-31827-3

[159] S. R. Coleman and F. De Luccia, "Gravitational Effects on and of Vacuum Decay," Phys. Rev. D **21** (1980), 3305

[160] R. Gregory, "GLOBAL STRING SINGULARITIES," Phys. Lett. B **215**, 663-668 (1988); A. G. Cohen and D. B. Kaplan, "The Exact Metric About Global Cosmic Strings," Phys. Lett. B **215**, 67-72 (1988).

[161] R. Gregory, "Nonsingular global strings," Phys. Rev. D **54** (1996), 4955-4962

[162] A. Vilenkin, "Gravitational Field of Vacuum Domain Walls," Phys. Lett. B **133** (1983), 177-179

[163] J. Garriga and M. Sasaki, "Brane world creation and black holes," Phys. Rev. D **62**, 043523 (2000).

[164] J. J. Blanco-Pillado and M. P. Salem, "Observable effects of anisotropic bubble nucleation," JCAP **07** (2010), 007.

[165] R. Gregory and C. Santos, "Space-time structure of the global vortex,"Class. Quant. Grav. **20** (2003), 21-36

[166] J. P. Conlon, E. J. Copeland, E. Hardy and N. S. González, "Percolating Cosmic String Networks from Kination," arXiv:2406.12637 [hep-ph]

[167] W. H. Kinney, S. Vagnozzi and L. Visinelli, "The zoo plot meets the swampland: mutual (in)consistency of single-field inflation, string conjectures, and cosmological data,"Class. Quant. Grav. **36**, no.11, 117001 (2019)

[168] H. Matsui and F. Takahashi, "Eternal Inflation and Swampland Conjectures,"Phys. Rev. D **99**, no.2, 023533 (2019)

[169] S. Brahma and S. Shandera, "Stochastic eternal inflation is in the swampland,"JHEP **11**, 016 (2019)

[170] Z. Wang, R. Brandenberger and L. Heisenberg, "Eternal Inflation, Entropy Bounds and the Swampland,"Eur. Phys. J. C **80**, no.9, 864 (2020)

[171] G. Dvali and C. Gomez, "On Exclusion of Positive Cosmological Constant,"Fortsch. Phys. **67**, no.1-2, 1800092 (2019)

[172] G. Dvali, C. Gomez and S. Zell, "Quantum Breaking Bound on de Sitter and Swampland," Fortsch. Phys. **67**, no.1-2, 1800094 (2019)

[173] J. Garriga, T. Tanaka and A. Vilenkin, "The Density parameter and the anthropic principle," Phys. Rev. D **60**, 023501 (1999)

[174] K. D. Olum, "Is there any coherent measure for eternal inflation?," Phys. Rev. D **86**, 063509 (2012)

[175] J. Garriga and A. Vilenkin, "Anthropic prediction for Lambda and the Q catastrophe," Prog. Theor. Phys. Suppl. **163**, 245-257 (2006)

[176] N. Kaloper and J. Scargill, "Quantum Cosmic No-Hair Theorem and Inflation," Phys. Rev. D **99**, no.10, 103514 (2019).

[177] I. Olasagasti and A. Vilenkin, "Gravity of higher dimensional global defects," Phys. Rev. D **62** (2000), 044014

[178] R. Gregory, "Nonsingular global string compactifications," Phys. Rev. Lett. **84**, 2564-2567 (2000)

[179] I. Cho and A. Vilenkin, "Gravity of superheavy higher dimensional global defects," Phys. Rev. D **68** (2003), 025013

[180] J. J. Blanco-Pillado, H. S. Ramadhan and B. Shlaer, "Bubbles from Nothing," JCAP **01**, 045 (2012)

[181] J. J. Blanco-Pillado and B. Shlaer, "Bubbles of Nothing in Flux Compactifications," Phys. Rev. D **82**, 086015 (2010)

[182] A. Masoumi, K. D. Olum and B. Shlaer, "Efficient numerical solution to vacuum decay with many fields,"JCAP **01**, 051 (2017)